

# Some dissipative problems in celestial mechanics

PHD THESIS  
by  
MAURICIO MISQUERO



UNIVERSIDAD  
DE GRANADA



PhD co-supervisors:

Prof. Alessandra Celletti (Università degli Studi di Roma "Tor Vergata")  
and

Prof. Rafael Ortega (Universidad de Granada)

Dottorato di Ricerca in Matematica (Ciclo XXXII)

PhD Coordinator: Prof. Andrea Braides

and

Programa de doctorado en Física y Matemáticas

PhD Coordinator: Prof. Juan Soler

September 2020



The doctoral candidate Mr. Mauricio Paul Misquero Castro and the thesis supervisors Dr. Alessandra Celletti and Dr. Rafael Ortega Ríos:

Guarantee, by signing this doctoral thesis, that the work has been done by the doctoral candidate under the direction of the thesis supervisors and, as far as our knowledge reaches, in the performance of the work, the rights of other authors to be cited (when their results or publications have been used) have been respected.

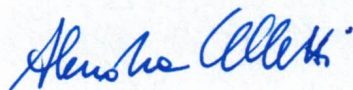
Likewise, we guarantee that, during his doctoral studies, the candidate has completed two research stays for a total period of five months (one + four) at the University of Lisbon (Portugal) under the supervision of Dr. Alessandro Margheri. The second stay (four months) was supported by the grant program Ibero-America Santander Research 2018-2019.

During the first three years (U. Granada), this doctoral thesis has been supported by the doctoral grant FPU15/02827, awarded by the Spanish Ministry of Education, Culture and Sport (MECD). The fourth year (U. of Rome Tor Vergata) was supported by the Marie Skłodowska-Curie Innovative Training Network Stardust-R, grant agreement 813644. The author also received partial support from the project MTM2014-52232-P, awarded by the Spanish Ministry of Economy, Industry and Competitiveness (MINECO).

Granada, September 29, 2020.

Thesis supervisor 1;

Thesis supervisor 2;



Signed



Signed

Doctoral candidate:



Signed



*Para Fabiola, Patricia y Ainhoa,  
por haber llenado mi vida de amor.*



# Agradecimientos

Me siento inmensamente afortunado por haber tenido la oportunidad de dedicar tanto tiempo a algo tan bello. La naturaleza es fascinante y es ciertamente un privilegio haber podido estudiarla usando las herramientas de la ciencia durante estos años. En este camino me ha acompañado mucha gente muy valiosa, a la que le debo, no solo esta tesis, sino todo un aprendizaje vital. Y aunque sé que no es posible, voy a intentar condensar en unas pocas palabras lo enormemente agradecido que estoy.

In the first place I want to thank both of my supervisors. From deep in my heart I always say that they are the best supervisors I could ever imagine. I owe them my love for this job. Rafael, las matemáticas se convierten en arte en tus manos. Siempre tendrás mi aprecio y mi más sincera admiración. Alessandra, your genuine curiosity and passion for research inspires me in my work every day. For me, you embody the purest side of science. I am greatly honoured to work by your side.

El lugar más especial de estos agradecimientos es para mi familia. Dedico esta tesis a Fabiola, mi abuela, a Patricia, mi madre, y a Ainhoa, mi hermana. Vuestro amor me da vida y me acompaña siempre. Vuestras vidas son para mí el mayor modelo de humanidad, sencillez y generosidad. Soy lo que habéis hecho de mí. No me olvido de mis abuelos, mis tíos y mis primos, por un apoyo y amor incondicional a pesar de la distancia. Nos reuniremos pronto y recuperaremos juntos todos esos recuerdos.

A mis amigas y amigos les agradezco el hueco que me han hecho en sus corazones. Desde allí la vida se llena de color y de magia. Gratitud especial a Paco, mi alma gemela. A Sara, una profunda parte de mí. A Sonia, un preciado tesoro. A Joana, mi amistad inextinguible. A Javi, compañero y referente. A mis maravillosos colegs, Salva, Víctor, Ana, Simona, Antonio, Guille, Gimmy, Sevilli, Cris, Manu, Pablo, David, Claudia, Lorena, Arturo y la Momo, por ese sabio azar que nos quiso juntar en Granada estos años. Sois cada uno un pequeño y apasionante universo. A todos mis amigos cuyos nombres no quedan escritos, esta tesis también es gracias a vosotros.

Quero expressar a minha gratidão e o meu afeto a Alessandro Margheri e

Carlota Rebelo. As calorosas boas-vindas durante a minha estadia em Lisboa mostraram-me o lado mais humano deste trabalho. Quero também recordar os momentos partilhados sob a luz de Lisboa com amigos como Marlo, Juned, Renata, Vicente, Carlos, Myriam, Annabelle, Edo e Max.

My warmest thanks to all my colleges of research. It has been a pleasure to learn from all of you and to share this passion for science. Empiezo por la Universidad de Granada, gente como Antonio Ureña, Pedro Torres, Juan Soler y Juan Calvo, que me han hecho sentir parte de esta profesión. Ringrazio anche il mio gruppo di ricerca dell'Università degli Studi di Roma Tor Vergata, Ugo, Giuseppe, Alfonso, Tudor, Sevi, Mara, Chiara, Marco e Joan, che sempre mi hanno mostrato un grande valore personale e scientifico. Also to the people involved in the Stardust-R network, especially to Christos, Giovanni, Catalin and the ESRs, particularly to the math team, Oscar, Marco, Edo, Irene and Roberto. And finally, to the uncountable people that I met in conferences, seminars and schools.

Quiero dedicar un agradecimiento muy especial a aquellos profesores que plantaron en mí la semilla de la curiosidad y del entusiasmo por el conocimiento. Aquí no puedo dejar de mencionar a Andrés Cassinello, Luis Garay, Artemio González, Jacobo Santamaría y Javier Gorgas. Del mismo modo, quiero agradecer a mis alumnos, por llenarme de esperanza en el futuro.

Por último, me gustaría recordar dos espacios que han entrado en mi vida en este tiempo y hoy son parte de mi identidad. En primer lugar, a toda la comunidad del swing: pronto volveremos a hacer temblar las pistas! Un caro saluto ai miei amici delle piste romane, Nello, Ana e del mercoledì al Swing and Soda, Valentina, Giamma e le mie follower, Giulia, Laura, Alessandra e Martina. Para terminar, un cariñoso abrazo para Fernando, María, Pilar, Emilio, Ainhoa y toda la familia que es la Resistencia de La Cafetera, con quienes comparto cada mañana un espacio de plena sintonía y de reflexión sobre los derechos humanos, el feminismo y la ecología. Gracias por estar ahí, por fin os he encontrado.







# Abstract

In this thesis we study the long term dynamics of some models of celestial mechanics including dissipative effects. Our objective is to characterize solutions with physical relevance from a theoretical point of view. We deal with three models derived from the Two-Body problem. First, we consider the Kepler problem with a biparametric family of dissipative forces, with a singularity at the origin. This family represents several physical phenomena. Here we give a fairly complete description of the qualitative asymptotic behavior of the solutions for a wide range of the parameters. Additionally, we discuss the existence of an asymptotic first integral in some cases. Second, we investigate the spin-orbit problem with a family of dissipative tidal torques. We do so using its full non-autonomous form and allowing large orbital eccentricities. Specifically, we are interested in the existence and asymptotic stability of a particular periodic solution that represents the capture into the synchronous spin-orbit resonance. Our quantitative results are in correspondence with real data of systems such as the Earth-Moon system. Third, we develop a planar version of the Full Two-Body Problem model that generalizes the dissipative spin-orbit model for two extended bodies with mutual spin interaction: the spin-spin model. Following the analogy, we characterize with analytical tools an asymptotically stable periodic solution that represents the double synchronous resonance. Likewise, our results are applied to real bodies such as the Pluto-Charon system and the binary asteroid 617 Patroclus. Our results are based upon analytical methods from dynamical systems, nonlinear analysis, theory of real analytic functions, etc., combined with numerical simulations to validate the results.



# Resumen

En esta tesis estudiamos la dinámica a largo plazo de algunos modelos de mecánica celeste que incluyen efectos disipativos. Nuestro objetivo es caracterizar soluciones con relevancia física desde un punto de vista teórico. Consideramos tres modelos derivados del problema de los dos cuerpos. En primer lugar, nos centramos en el problema de Kepler con una familia biparamétrica de fuerzas disipativas. Esta familia incluye distintos fenómenos físicos. Nuestros resultados dan una descripción bastante completa del comportamiento asintótico de las soluciones para un amplio rango de los parámetros del problema. Además, discutimos la existencia de una integral primera asintótica en algunos casos. En segundo lugar, analizamos el problema spin-orbit con una familia de torques disipativos causados por fuerzas de marea. Aquí estudiamos el modelo completamente no autónomo y consideramos órbitas con altas excentricidades. Concretamente, nos interesa la existencia y la estabilidad asintótica de una solución periódica particular que representa la captura en el estado de rotación sincrónica del sistema. Nuestros resultados cuantitativos son consistentes con medidas de casos reales, como el sistema Tierra-Luna. En tercer lugar, desarrollamos un modelo plano del problema completo de dos cuerpos: el modelo spin-spin. Este modelo generaliza el problema spin-orbit disipativo para dos cuerpos extensos cuyas rotaciones están en influencia mutua. Siguiendo la analogía, utilizamos herramientas analíticas para caracterizar una solución periódica asintóticamente estable que representa la rotación sincrónica doble. Asimismo, aplicamos nuestros resultados a sistemas reales como es el caso del sistema Plutón-Charonte y el asteroide binario 617 Patroclo. Nuestros resultados se basan en métodos analíticos de sistemas dinámicos, análisis no lineal, teoría de funciones analíticas, etc., en combinación con simulaciones numéricas para contrastar los resultados.



# Sintesi

In questa tesi studiamo le dinamiche a lungo termine di alcuni modelli di meccanica celeste che includono gli effetti dissipativi. Il nostro obiettivo è di caratterizzare da un punto teorico le soluzioni che hanno rilevanza fisica. Ci occupiamo di tre modelli derivati dal problema dei due corpi. In primo luogo, consideriamo il problema di Keplero con una famiglia bi-parametrica di forze dissipative e con una singolarità all'origine. Questa famiglia è rappresentativa di diversi fenomeni fisici. In questo lavoro forniamo una descrizione piuttosto completa del comportamento asintotico qualitativo delle soluzioni per un'ampia gamma di parametri. Inoltre, in alcuni casi discutiamo l'esistenza di un integrale primo asintotico. In secondo luogo, analizziamo il problema spin-orbita con una famiglia di coppie di marea dissipative. Per questo studio utilizziamo la forma non autonoma del modello e consentiamo elevate eccentricità orbitali. In particolare, siamo interessati all'esistenza e alla stabilità asintotica di una particolare soluzione periodica che rappresenta la cattura nella risonanza sincrona spin-orbita. I nostri risultati quantitativi sono in corrispondenza con dati reali di sistemi fisici come il sistema Terra-Luna. In terzo luogo, sviluppiamo una versione planare del modello "Full Two-Body Problem" che generalizza il modello dissipativo spin-orbita per due corpi estesi e che include l'interazione reciproca degli spin' ci riferiamo a questo caso come il modello spin-spin. Seguendo l'analogia con gli altri modelli, caratterizziamo con strumenti analitici una soluzione periodica asintoticamente stabile che rappresenta la doppia risonanza sincrona. I nostri risultati vengono poi applicati a corpi reali come il sistema Plutone-Charonte e l'asteroide binario 617 Patroclo. I risultati ottenuti si basano su metodi analitici derivati dalla teoria dei sistemi dinamici, analisi non lineare, teoria delle funzioni analitiche reali, ecc., combinati con simulazioni numeriche utilizzate per convalidare i risultati.





# Contents

Agradecimientos	v
Abstract	ix
Resumen	xi
Sintesi	xiii
<b>1 Introduction</b>	<b>1</b>
1.1 The scope of this thesis . . . . .	1
1.2 The context of this thesis . . . . .	4
1.2.1 Dissipation in celestial mechanics . . . . .	4
1.2.2 A selected historical review . . . . .	8
1.2.3 Preliminaries . . . . .	12
1.3 The content of this thesis . . . . .	20
1.3.1 The Kepler problem with singular drags . . . . .	20
1.3.2 Stability of the 1:1 spin-orbit resonance . . . . .	30
1.3.3 The spin-spin model . . . . .	43
<b>2 The Kepler problem with singular drags</b>	<b>59</b>
2.1 Some preliminaries . . . . .	59
2.2 Forward dynamics . . . . .	63
2.2.1 A threshold for the existence of escape orbits and non existence of oscillatory ones . . . . .	63
2.2.2 Non-rectilinear motions . . . . .	68
2.2.3 Rectilinear motions . . . . .	77
2.3 The asymptotic Runge-Lenz vector . . . . .	85
<b>3 Stability of the 1:1 spin-orbit resonance</b>	<b>91</b>
3.1 Linear stability . . . . .	91
3.1.1 Uniqueness of the odd $2\pi$ -periodic solution . . . . .	91
3.1.2 Upper and lower solutions . . . . .	100

3.2	Instability for high eccentricity . . . . .	102
3.3	Dissipative regime . . . . .	112
3.3.1	The dissipative function $D(t, e)$ . . . . .	124
3.3.2	Quantitative estimates for the linear MacDonald torque	125
<b>4</b>	<b>The spin-spin model</b>	<b>127</b>
4.1	Derivation of the conservative spin-spin model . . . . .	127
4.1.1	Potential of the Full Two-Body Problem . . . . .	127
4.1.2	Potential of the ellipsoidal spin-spin model . . . . .	131
4.1.3	The planar Lagrangian model . . . . .	135
4.1.4	The Keplerian assumption . . . . .	137
4.2	Linear stability . . . . .	139
4.2.1	Existence of the odd $2\pi$ -periodic solution . . . . .	139
4.2.2	Uniqueness of the solution . . . . .	141
4.2.3	Linear stability of the solution . . . . .	144
4.3	The synchronous resonance in the dissipative regime . . . . .	148
4.4	Applications . . . . .	152
4.4.1	Real systems . . . . .	152
4.4.2	Stability diagrams in the space of parameters . . . . .	154

# Chapter 1

## Introduction

### 1.1 The scope of this thesis

In this thesis we study the asymptotic dynamics of some low dimensional models related to the Two-Body problem involving a dissipative phenomenon. We consider three problems, that are described as follows.

In the first problem, a dissipative Kepler problem, developed in Chapter 2, we consider the orbital evolution of a particle in a Keplerian potential created by another particle fixed at the origin. The moving particle is affected by a large family of dissipative forces that are proportional to its velocity and have a singularity at the origin. These forces depend on two parameters whose values distinguish several physical phenomena, such as viscous friction and the Poynting-Robertson effect. Our results give a general theoretical description of the global asymptotic dynamics as time goes to infinity. Particularly, we analyse the changes in the qualitative asymptotic behavior when we vary the parameters of the dissipative force. Additionally, in some cases we discuss the existence and further properties of a first integral that is an asymptotic Runge-Lenz vector. This research is developed in the following paper.

A. MARGHERI AND M. MISQUERO, *A dissipative Kepler problem with a family of singular drags*. *Celest. Mech. Dyn. Astr.* **132**, 17 (2020). <https://doi.org/10.1007/s10569-020-9956-7>

In the second problem, the spin-orbit problem in Chapter 3, we study the spin evolution of an extended body, when it moves in a Keplerian potential created by a point mass. Here we include a family of dissipative tidal torques, generalizing the well-known MacDonald torque, [75]. We deal with the synchronous spin-orbit resonance of the problem, say, when the spin is  $T$ -periodic, where  $T$  is the orbital period. More precisely, we deal with the existence and asymptotic stability of a particular periodic solution of the

full non-autonomous problem, that has a complicated pendulum-like structure. This study includes large orbital eccentricities. Our results, both for the conservative and the dissipative problem, are rigorous and have a direct application to real systems. Particularly, our quantitative results on the dissipative mechanism are consistent with data from the Earth-Moon system. The corresponding article is the following.

M. MISQUERO AND R. ORTEGA, *Some Rigorous Results on the 1:1 Resonance of the Spin-orbit Problem*. SIAM J. Appl. Dyn. Syst. (In press) (2020). Preprint available at <https://www.ugr.es/~ecuadif/files/MisqueroOrtega.pdf>

In the last problem, the spin-spin problem in Chapter 4, we deal with two extended bodies orbiting around each other in Keplerian orbits. Here we are focused on the mutual spin interaction and consider only the MacDonald dissipative torque that they exert on each other. We develop the model in an analogous way as the spin-orbit model, and we study it following an outline similar to the one in Chapter 3. That is, we are interested in a particular solution with physical relevance, the double synchronous resonance: when both spins have the same period as the orbital one. We want to prove that such solution exists and it is asymptotically stable. The main difference with respect to the spin-orbit model is that now we deal with one more degree of freedom.

M. MISQUERO, *The spin-spin model and the capture into the double synchronous resonance* Submitted. Preprint available at <https://www.ugr.es/~ecuadif/files/Misquero.pdf>

The rest of the current introductory chapter is organized as follows.

Section 1.2 contextualizes the topics included in this thesis. It is of **optative reading** since it does not include original content, but it gives a general overview of three important aspects. First, Section 1.2.1 discusses the role of the dissipation in celestial mechanics, a discipline historically linked to the conservative point of view. Second, Section 1.2.2 reviews some remarkable previous works that have contributed to dissipative celestial mechanics, with special stress on theoretical studies. Third, Section 1.2.3 introduces some concepts used along the rest of the text and defines, from a physical perspective, the dissipative forces that this thesis is concerned with.

The reader interested in the results of the thesis can directly go to Section 1.3. Each of its subsections corresponds to each of the models and all of them have the same structure. In the first subsection we describe the model and cite some results existing in the literature. The second subsection is dedicated to enumerate specific objectives of our research dealing with the

presented model. The third subsection is devoted to make a general exposition of the results achieved in this thesis. The results are in correspondence with the mentioned objectives. The fourth subsection contains the most important specific methods that led us to our results. This can serve as a guide to follow the steps of the proofs given in the dedicated chapters: Chapter 2 - The Kepler problem with singular drags, Chapter 3 - Stability of the 1:1 spin-orbit resonance and Chapter 4 - The spin-spin model. In the last subsection there is a discussion of the results compared to the literature and we present some future work as a continuation of our research.

## 1.2 The context of this thesis

### 1.2.1 Dissipation in celestial mechanics

**Dissipation and its role.** This thesis is devoted to the study of the effect of certain dissipative forces in the motion of stars, planets, natural and artificial satellites, etc. This motion is primarily dictated by their mutual gravitational influence. However, the force of gravity alone is not enough to explain how celestial bodies move in the space as we observe today. In a few words we can say that, there are many physical processes beyond gravity that transform mechanical energy into heat (dissipation of energy). This heat is ultimately transferred from the hot parts of the system to the cold ones, leading to a balance of temperature. In this context, dissipative effects embody the fact behind the second law of thermodynamics: as time goes forward, nature tends to specific states of equilibrium. Or in other words, gravitation makes some motions possible, but dissipation chooses which ones become permanent.

**Celestial mechanics in the old times and today.** Celestial mechanics includes the mathematical methods that help us to understand how the celestial bodies move. It is indeed a very old discipline. In the search to explain the harmony of the heavens, Kepler discovered the laws that rule the motion of the planets. In this way we learned that their orbits were ellipses instead of perfect circles. Later, celestial mechanics was well established thanks to the Newtonian foundations of dynamics. In that moment we learned that the force that attracts everything to the ground was the same that moves the huge bodies up in the sky. Further developments of celestial mechanics have always been guided by the fact that the skies were not as ideal as we thought before. The timeless question of the stability of the solar system received an unexpected answer by Poincaré at the end of the 19th century. We learned then that the Three-Body problem is chaotic<sup>1</sup>, say, its behavior is almost impossible to predict. This is far from the ideally steady universe conceived by Kepler. Later, the actual observation of chaos in the solar system and the possibility of performing advanced numerical simulations confirmed us the vast complexity of the dynamics of the celestial bodies. At present, we have a particularly challenging situation due to the astonishing development of astronomy, astrophysics and space science, in general. In one hand, astrophysics has conceived very elaborated theories on the formation of stars, planetary systems, galaxies, etc. Such theories are well based on the classi-

---

<sup>1</sup>At least for some values of the masses.

fication of the huge variety of observed astronomical objects. On the other hand, the expansion of the aerospace industry of the last decades provide many practical problems involving the dynamics of artificial satellites and space mission design. In fact, we have to deal with new dynamical situations that were hardly imagined before, but are becoming real now. All this discussion confronts us with the need of developing new and powerful dynamical models adapted to the description of the evolving worlds of astronomy and the special circumstances of the space exploration. In this context, a huge computational power is necessary, but we also need to develop theoretical tools that optimize the available resources.

**Theoretical approach.** At this point, it is worth mentioning that, although the motivation is practical, the approach of this thesis is mainly theoretical. More specifically, we will deal with very simplified models and prove rigorous results with physical significance. This means that our intention is not to provide realistic answers, but to be precise in the mathematical formulation of some physical problems including dissipation and in the results. As a consequence, the applicability of this research relies on the fidelity of the models that we have chosen. Indeed, in this thesis not only the mathematical techniques have a central role, but also the models themselves. For example, in this thesis we will deal with a model (we call it spin-spin model) that has not been studied much so far, but we think it has great potential. This is an elementary model that helps us to understand the rotational dynamics of two extended bodies interacting gravitationally. Apart from this model, in line with classical models of celestial mechanics, we will put the emphasis on how the dissipation is integrated in the dynamics of the bodies.

**Conservative celestial mechanics.** The theory of Hamiltonian systems is nowadays the fundamental theoretical framework of celestial mechanics. This is a very rich mathematical field, widely used in the past, as well as in modern physics. Its predominant role in celestial mechanics was mainly due to the advances in perturbative techniques developed in the second half of the 20th century. Their suitability for numerical implementation have reinforced the relevance of these methods. Normal forms, KAM theory, Nekhoroshev's theory, Arnold diffusion, etc. have been the core of the theoretical methods used in celestial mechanics, see for example [23]. It is remarkable the application of KAM theory to the question of the stability of the solar system. Actually, many of these tools have entered into the language of astronomy and astrophysics. The book *Modern celestial mechanics* [94], by A. Morbidelli, has been an important contribution in this sense because it shows

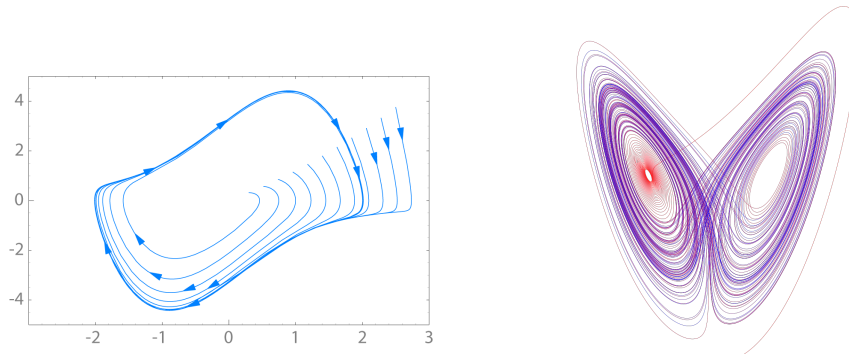


Figure 1.1: Remarkable attractors. Left: The Van der Pol limit cycle. Right: The Lorenz attractor. Source: Wikipedia.

the considerable applicability of the tools of celestial mechanics. Hamiltonian dynamics is a natural framework when we consider conservative systems, as those determined by gravity. However, more realistic systems require a more general treatment. For these kind of systems it is necessary to consider dissipative effects, that, although much smaller than the gravitational interaction, contribute to its long-term behavior.

**Dissipative dynamics.** Although the conservative approach in celestial mechanics is widely spread, here we want to remind that Poincaré developed the general methods of dynamical systems precisely motivated by celestial mechanics, [107]. Dissipative dynamics is a fruitful branch of dynamical systems whose central objects of study are called *attractors*. Later we will make a precise definition, but in a few words we can say that an attractor is the endpoint of the evolution of a dissipative system in the phase space. In some cases the attractor of a system is just an equilibrium point, meaning that the system does not change anymore once the equilibrium is reached. For example, the lower equilibrium of a pendulum with dissipation. In other cases the attractor is a periodic orbit, meaning that, the system will continue to evolve resembling a specific periodic motion more and more. This is the case of the limit cycles like that of the Van der Pool oscillator. There are more complicated attractors with intricate topologies, such as the celebrated Lorenz attractor, that is an example of the so-called strange attractors. See Figure 1.1. The following question arises in our context: Many of the objects that we see through a telescope have been exposed to dissipative forces and have evolved for a very long time. Can we identify them with physical representations of attractors of certain dissipative problems of celestial mechanics? There have been several attempts trying to explain the astronomical struc-



tures with attractors. For instance, planetary systems in [6], or the presence of spiral structure and bars in some galaxies [104].

### 1.2.2 A selected historical review

**Some old examples.** The consideration of non-conservative effects in celestial mechanics is not new at all. For example, in one of the lectures of Jacobi in 1842-43 [59], he considers the dynamics of a body orbiting around a center within a resistive medium. In 1884 H. Gylden considered time-variation in the mass of the Kepler problem, [55]. This is a time-dependent Hamiltonian model that was proposed to explain the secular acceleration of the Moon's longitude due to a mass increase. J. Mestschersky found out in 1902 [90] that the resulting orbit would be a spiral leading to a collision or to a distancing. The problem was addressed from a theoretical point of view by J. Littlewood in 1964 [74], he gave some results involving adiabatic invariants. Although it is questionable that the model is useful for the initial purpose, it has been used in different situations such as the evolution of comets, binary stars, pulsating stars, among others. See for example [64, 38], and the references therein. On the other hand, in 1904, J.H. Poynting described an interesting effect on small particles in the solar system arising from the solar radiation [108]. This is the so-called Poynting-Robertson effect and it acts as a dissipative force. Here Poynting studies this dissipative Kepler problem and concludes that the particle would fall in a spiral orbit and hit the Sun at some point. This effect was later addressed by H.C. Plummer [105] and H.P. Robertson [110]. These are just some interesting old examples among others, but it is not our intention to give a complete review.

**Hypotheses on the formation of the solar system.** The dissipative effects in celestial mechanics started to be relevant in the search of a theory of the formation of the solar system in consistence with the observations. The specific dynamical structure of the solar system has always intrigued scientists: The circularity and planarity of the orbits, the resonant structure appearing between the orbital and spin periods of many bodies and their particular distribution must have a dynamical explanation. In 1911, Poincaré published his *Leçons sur les hypothèses cosmogoniques*<sup>2</sup>, [106]. There, he summarizes several theories on the formation of the solar system available at that time and exposes them mathematically whenever possible. There is a very detailed discussion on the nebular hypothesis of Laplace. The hypothesis

---

<sup>2</sup>Unfortunately for non-French speakers, there is not an available translation of the book. Anyhow, an interesting discussion on the book, in contrast with modern theories, is given in a talk by A. Morbidelli in 2012, entitled *Leçons sur les hypothèses cosmogoniques: Poincaré's view of solar system formation. What remains valid today?*. It is available on the YouTube channel of the Institut Henri Poincaré <https://www.youtube.com/watch?v=FXNa00sqTL8>.

of R. du Ligondès is remarkably modern in some parts, such as the role of the dissipation and the gravitational instabilities in the formation of the Sun, the protoplanetary disk, the rings and the planets. The hypothesis of T.J.J. See that the planets were captured by the solar nebula is quite obsolete, but is used by Poincaré to illustrate that the friction with the viscous nebula leads to circularization and shrinking of the orbits of the planets. He explains this by arguing that the friction force is proportional to the velocity, then, its effect on the periapsis is stronger than in the apoapsis, resulting in orbits that are more and more circular. Besides, Poincaré pays special attention to the tidal theory of G.H. Darwin on the origin of the Moon and considers that tides should have a predominant role in the evolution of the whole solar system. Although all these theories have been widely surpassed by modern theories, the global intuitions of Poincaré exposed along the book are very valuable in our context so we can speak about dissipative celestial mechanics.

**Early dissipative celestial mechanics.** The decade of 1960's, in the midst of the so-called Space Race, was a stimulating period in the study of the space. As far as this thesis is concerned, there are two main topics that acquired much relevance at that time. In one hand, the motion of artificial satellites exposed to atmospheric drag, and on the other hand, the understanding of the role of dissipative tides in the phenomenon of capture into spin-orbit resonances. The effects of the atmospheric drag in the evolution of the orbital elements for different models of drags were addressed in [62, 15, 10]. How to model the atmospheric drag has been always a problem because it is desirable a high accuracy in the computation of orbits of real satellites. Particularly, in [10], V.V. Beletsky pays also special attention to the spacial orientation of the satellite in the orbit, including the spin-orbit interaction. He even proposes some ways to implement dissipative devices (involving viscous fluids or magnetic dampers) in artificial satellites to stabilize their orientation. He argues that dissipation would lead to asymptotically stable states of relative equilibrium, for circular orbits, and forced eccentricity oscillations, for eccentric orbits. The theory of tidal dissipation proposed by G.J.F. MacDonald [75], modifying the tidal theory of G.H. Darwin, had a great impact in the theory of the evolution of natural satellites. In [51], P. Goldreich and S.J. Peale investigate the capture into spin-orbit resonances due to the action of dissipative torques and derive the probabilities of such captures. Then, not only relative equilibria are stabilized by dissipation, but also more complicated motions such as the 3:2 spin-orbit resonance of Mercury (it completes three rotations every two orbital revolutions), considered as an orbiting body around the Sun. In fact, in 1970 [65], W.T. Kyner ex-

plains that the KAM tori structure of the conservative problem of Mercury is destroyed by the dissipation and convert some stable periodic orbits into attractors that are asymptotically stable periodic solutions. In this way, instead of using the concept of capture probability, he proposes the capture measure, i.e., the (relative) measure of the basin of attraction of the attractor. Although both concepts are intimately related, the second one deepens into the dissipative dynamics. A few more papers follow this line [97, 111]. On the other hand, there are some other studies dealing with the dissipative effects on orbit-orbit resonances in the solar system, such as [93, 54]. In [127], orbit-orbit and spin-orbit resonances are studied with a unified damped pendulum-like model. The need for a theoretical development of dissipative celestial mechanics following the previous papers is pointed out in [66]. It is worth mentioning that the Hamiltonian framework has been present in many of the studies above.

**Dissipative celestial mechanics: a practical approach.** The tidal interaction was the major dissipative phenomenon considered in celestial mechanics, but many other dissipative perturbations were also taken into account. See for example the following two papers with an ample view. In one hand, [123] focuses the effect of different friction forces in the solar nebula during the formation of the solar system. The size of the particle (from dust to protoplanets) is the main parameter for the type of motion it performs. On the other hand, in [17], there is an extensive study on forces produced by the Sun radiation acting on dust and small bodies. Among these forces we have the solar radiation pressure, the Poynting-Robertson effect, the differential Doppler effect and the so-called Yarkovsky effect. Thus, at this moment we consider more realistic situations. For example, the interaction between stable resonances and non-gravitational forces was investigated in [53], for large bodies affected by gas drag or collisions with small bodies, and [52], for small bodies for which the Poynting-Robertson effect is not negligible. At this point the numerical experiments acquire much relevance due to the immediate practical application to the theories that were consolidating. The commensurability of orbital periods has been constantly revisited with new models, see [103]. In particular, the capture into resonances in the solar system due to dissipation is studied in [8], for planetesimals, and [9], for dust. See also [78, 98, 73]. For a more analytical study see [70].

**The particular context of this thesis.** In the last decades there has been an increasing interest in the dissipative dynamics of celestial bodies. Advances have been produced both from the analytical and the numerical

points of view. The co-supervisors of this thesis are involved in this current development. A. Celletti and her collaborators have elaborated a series of articles considering weakly dissipative and nearly integrable Hamiltonian systems, [27, 20, 25, 22, 24, 26]. There are both numerical and theoretical works. These works characterize different kinds of attractors (periodic and quasi-periodic orbits, strange attractors). Their theoretical techniques include the theory of conformally symplectic system, dissipative versions of KAM results, normal forms, exponential stability estimates, among others. In these papers, the spin-orbit problem is taken as a paradigmatic dissipative model in celestial mechanics. On the other hand, R. Ortega and his collaborators have contributed with analytical studies of the dissipative Kepler problem and the dissipative Three-Body problem, [80, 81, 82, 83]. In these works they find results on the continuation of periodic orbits to the dissipative regime, characterization of the asymptotic behavior of solutions, existence of asymptotic first integrals, etc. Their techniques have a geometrical approach and come from the general qualitative theory of ordinary differential equations.

### 1.2.3 Preliminaries

In this thesis we will provide some theoretical results on ordinary differential equations given by celestial mechanics. They are of the type

$$\dot{\mathbf{x}} = \mathbf{f}(t, \mathbf{x}, \mathbf{p}), \quad (1.1)$$

where the dot indicates derivation with respect to  $t \in \mathbb{R}$ , the time variable,  $\mathbf{x} \in \mathbb{R}^n$ , and  $\mathbf{p} \in \mathbb{R}^d$  is a vector containing some parameters of the problem. The vector function  $\mathbf{f} : \mathbb{R} \times \mathbb{R}^n \times \mathbb{R}^d \rightarrow \mathbb{R}^n$  is usually an analytic function in all the entries.

In the next subsection we discuss when equation (1.1) is called dissipative.

#### The definition of dissipative systems

There are many definitions of what a dissipative system is, and not all of them are equivalent. The simplest definition in physics is the following. Let  $E_{mec}$  be the mechanical energy of the system,  $E_{mec} = E_{kin} + E_{pot}$ , where  $E_{kin}$  is the kinetic energy and  $E_{pot}$  is the potential energy. If  $E_{mec}$  is a constant of motion, then, the system is conservative, otherwise, it is non-conservative. Furthermore, if there is a loss of energy, i.e.,  $\dot{E}_{mec}(t) \leq 0$  for any  $t$ , then, the system is dissipative. Indeed, physics generally considers that, if we take into account all the degrees of freedom involved in a phenomenon, then, the system is always conservative. Thus, in non-conservative systems we are disregarding some of the degrees of freedom and make an *effective* description of them. For example, if we have a block moving on a surface, normally we describe the mutual friction as an effective external force exerted by the surface, instead of taking into account the transfer of energy between the atoms/molecules of the block and the surface. In mathematics we usually avoid the description of physical phenomenology and focus on rigorous definitions. The mathematical definitions of dissipative systems are varied as well and, again, there is not always a correspondence between them and with the physical definition. Let us cite some of them.

The first one is a simple definition for autonomous differential equations.

**Definition 1.1** (From Def. 13.9 in [57]). *An equation  $\dot{\mathbf{x}} = \mathbf{f}(\mathbf{x})$ ,  $\mathbf{x} \in \mathbb{R}^n$  is said to be dissipative if there exists a bounded subset  $B$  of  $\mathbb{R}^n$  such that, for any  $\mathbf{x}^0 \in \mathbb{R}^n$ , there is a time  $t_0$ , which depends on  $\mathbf{x}^0$  and  $B$ , so that the solution  $\mathbf{x} = \mathbf{x}(t)$  with  $\mathbf{x}^0 = \mathbf{x}(t_0)$  satisfies  $\mathbf{x}(t) \in B$  for all  $t \geq t_0$ .*

This means that any solution ends up entering in a bounded subset of the phase space at some moment. A consequence of this definition is stated in Theorem 13.10 in [57]. It says that there exists a set  $D \subseteq \mathbb{R}^n$  diffeomorphic

to a ball such that the vector field at the boundary of  $D$  points inside  $D$ . Note that for this definition it was not necessary the concept of energy. The following definition is based on the contraction/expansion of the phase space.

**Definition 1.2** (from [23]). *Let  $\mathbf{x}(t) = \phi(t; \mathbf{x}^0)$  be the solution (flow) of  $\dot{\mathbf{x}} = \mathbf{f}(\mathbf{x})$ ,  $\mathbf{x} \in \mathbb{R}^n$ , such that  $\mathbf{x}^0 = \mathbf{x}(0) = \phi(0; \mathbf{x}^0)$ . The equation is dissipative if  $|\det J_t| \neq 1$ , where the Jacobian matrix  $J_t \in \mathbb{R}^{n \times n}$  is given by  $J_t = \partial_{\mathbf{x}} \phi(t; \mathbf{x})$ . If  $|\det J_t| > 1$  for all  $t$ , it is called expansive. On the other hand, if  $|\det J_t| < 1$  for all  $t$ , it is called contractive.*

Here, the elements of the Jacobian matrix are  $\frac{\partial \phi_i}{\partial x_j}$ , where  $\phi_i$  are the components of  $\phi(t; \mathbf{x})$  and  $x_j$  are the components of  $\mathbf{x}$ . Definition 1.2 is quite general because all the systems that are not conservative ( $|\det J_t| = 1$  for all  $t$ ) are called dissipative. In [50] there is an example that is sometimes contractive and sometimes expansive.

There are other advanced definitions. To give some examples, see the concept of contraction of the phase space on average [72], or the entropy approach to dissipation [109], or conformally symplectic systems [20], that produce a uniform contraction of the phase space in all the directions.

Despite the different characterizations of dissipative systems, the related concepts of attractor and basin of attraction are quite standard. First we need to define positive invariance and the  $\omega$ -limit set associated to an initial condition.

**Definition 1.3.** *Let  $\dot{\mathbf{x}} = \mathbf{f}(\mathbf{x})$ ,  $\mathbf{x} \in \mathbb{R}^n$ , be an equation whose flow is given by  $\phi(t; \mathbf{x})$ .*

1. *We say that a set  $U \subseteq \mathbb{R}^n$  is a positively invariant set if, for all  $t \geq 0$  and  $\mathbf{x} \in U$ , we have that  $\phi(t; \mathbf{x}) \in U$ .*
2. *The  $\omega$ -limit set of  $\mathbf{x}^0 \in \mathbb{R}^n$  is given by*

$$\omega(\mathbf{x}^0) = \left\{ \mathbf{x} \in \mathbb{R}^n : \text{there exists a sequence } \{t_k\} \rightarrow \infty, k = 1, 2, \dots, \right. \\ \left. \text{such that } \phi(t_k; \mathbf{x}^0) \rightarrow \mathbf{x} \text{ as } k \rightarrow \infty \right\}.$$

An attractor is a positively invariant set that is the  $\omega$ -limit of some set of initial conditions. Attractors are sets of the phase space that attract the nearby solutions as time increases. The basin of attraction associated to some attractor is the union of all the possible initial conditions that it attracts. If the basin of attraction of some attractor is the whole phase space we will call global attractor. Thus, the global attractor of a dissipative system contains the most important information of the long-term behavior of it.

Attractors can have a very complicated topology. In general, we can associate a dimension to the attractor that can be non-integer (fractal dimension). In this thesis we will not enter into the existence of attractors with fractal dimension (strange attractors), but rather, on simpler ones. The following definition characterizes asymptotically stable solutions (local attractors). Let  $\|\cdot\|$  be any norm in  $\mathbb{R}^n$ .

**Definition 1.4** (From [56]). *Assume that  $\mathbf{x}^* \in \mathbb{R}^n$  is an equilibrium point of  $\dot{\mathbf{x}} = \mathbf{f}(\mathbf{x})$ , whose flow is given by  $\phi(t; \mathbf{x})$ . We will call  $\mathbf{x}^*$  asymptotically stable if it is Lyapunov stable and there exists  $b > 0$  such that  $\|\mathbf{x}^0 - \mathbf{x}^*\| < b$  implies that  $\|\phi(t; \mathbf{x}^0)\| \rightarrow \mathbf{x}^*$  as  $t \rightarrow \infty$ .*

The same definition can be extended to a more general solution of the equation instead of an equilibrium point. In this thesis we deal particularly with asymptotically stable periodic solutions.

### Dissipative forces

In this section we introduce, from a physical point of view, the dissipative forces that are relevant for the models of this thesis. For a more general and detailed discussion we refer to the book *Dissipative forces in celestial mechanics* by S. Ferraz-Mello et al. [47].

**Fluid drag.** A body that moves in a viscous fluid is influenced by a friction force that points in the opposite direction to its velocity<sup>3</sup>. This force can be modelled as

$$\mathbf{F} = -k_D \|\mathbf{v}\|^{m-1} \mathbf{v}, \quad (1.2)$$

where  $\mathbf{v} \in \mathbb{R}^3$  is the velocity vector of the body and  $\|\cdot\|$  is the Euclidean norm in  $\mathbb{R}^3$ . It implies  $\|\mathbf{F}\| \propto \|\mathbf{v}\|^m$ . The parameter  $k_D > 0$  takes into account different types of behavior between the fluid and the body depending on the density, the size and the shape of the body. This is an empirical law and the value of  $m$  is associated to a specific range of velocities. For example, according to [96], experiments have shown that, for a satellite moving in the Earth's atmosphere, we can take  $m = 1$  for velocities  $\|\mathbf{v}\| < 3\text{m/s}$ ,  $m = 2$  if  $3\text{m/s} < \|\mathbf{v}\| < 300\text{m/s}$ , and approximately  $m = 3$  if  $\|\mathbf{v}\| > 300\text{m/s}$ . For the case of an atmosphere whose density that decays with the altitude we can include a factor  $\exp[-\alpha_0 h]$ , where  $\alpha_0 > 0$  is a parameter and  $h > 0$  is the altitude, [15]. This atmosphere model has been corrected in later works

---

<sup>3</sup>There are also other components acting in the perpendicular direction with respect to the velocity. For instance, the lift force appearing in an airplane wing.



including oblateness of the body with the atmosphere, periodic variations, rotation, etc. See [121].

According to [123], we can distinguish between two models depending on the size of the moving body with respect to the mean free path  $\bar{\lambda}$  of the particles of the fluid. These models describe the motion of bodies of all sizes, from dust particles to protoplanets. Let us consider that the moving body is spherical with radius  $s$  and is moving in a fluid with density  $\rho$ .

1. Gas regime:  $s \ll \bar{\lambda}$ . It is applicable to a dust particle that moves in a gaseous medium and the force takes the form

$$\mathbf{F} = -\frac{4}{3}\pi s^2 \rho \bar{v}_T \mathbf{v} \quad (\text{Epstein law}), \quad (1.3)$$

where  $\bar{v}_T$  is the mean thermal velocity of the gas particles.

2. Fluid regime:  $s \gg \bar{\lambda}$ . We have a law

$$\mathbf{F} = -\frac{1}{2}C_D \pi s^2 \rho \|\mathbf{v}\| \mathbf{v}, \quad (1.4)$$

where  $C_D$  is the drag coefficient that depends on the Reynolds number  $R_e$ , defined by

$$R_e = \frac{\text{inertial force}}{\text{drag force}} = \frac{2s\rho\|\mathbf{v}\|}{\eta},$$

here  $\eta = \rho \bar{v}_T \bar{\lambda}/3$  is the dynamic viscosity of the fluid. It is usual to take  $C_D$  proportional to a power of  $R_e$ . For  $R_e < 1$  we take  $C_D \approx 24R_e^{-1}$ , which reproduces the Stokes law  $\mathbf{F} = -6\pi\eta s\mathbf{v}$ . If  $1 < R_e < 800$  we take  $C_D \approx 24R_e^{-3/5}$ , whereas for  $R_e > 800$  we take  $C_D \approx 0.44$ . The Stokes law and the Epstein law coincide when  $\bar{\lambda}/s = 7/9$ , that is defined as the transition point between the two of them.

The cited article [123] studies the motion of several bodies in the solar nebula. The nebula is considered as an ideal gas with a pressure gradient and a temperature gradient. It takes simple laws for the pressure  $P \propto r^{-a}$ , and for the temperature  $T \propto r^{-b}$ , where  $r$  is the distance to the Sun and  $a, b > 0$ . With these laws, the pressure of the gas has a conservative effect on the dynamics.

The effect of the drag force on the motion of the particle depends on its size. For small bodies, tangential velocity decreases rapidly and they are dragged by the rotating nebula and fall to the Sun gradually. Larger objects

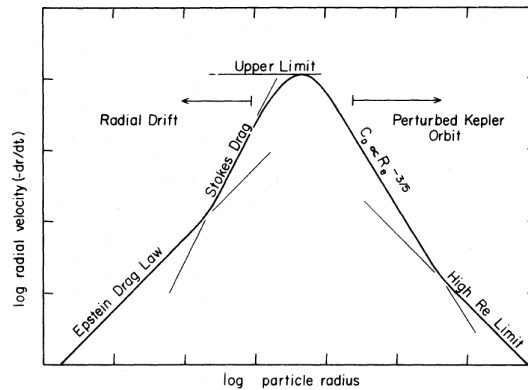


Figure 1.2: Schematic behavior of the relative radial velocity of fall depending on the size of the particle. We see that the smallest and the largest bodies fall very slow to the Sun with respect to intermediate sizes. The peak (Upper Limit) depends on the nebular structure. Taken from [123].

spiral into the Sun without being dragged. However, very small and very large objects also fall to the Sun, but with radial velocities much smaller. This explains the presence of large bodies like planets and the interplanetary dust in our solar system. Figure 1.2 shows very well this behavior.

**Tidal dissipation.** The effect of the tides exerted by the Moon on the Earth is a very well known phenomenon because it produces a periodic variation of the sea level. The physical mechanism involved is very common in celestial mechanics and it appears when we consider gravitational forces between extended bodies that are close enough to each other. The closest points experience a stronger attraction than those that are further away, so the tides are caused by this difference of forces. If the bodies are rigid or elastic, the tidal effects are conservative due to gravity. However, if the bodies are viscous, there are inelastic deformations that have a dissipative effect.

Consider an elastic body that has a spherical shape in absence of any external influence. If there is an external perturbing body, the tides deform the main body generating a new figure of equilibrium of oblate shape. The new shape is elongated in the direction to the perturber. The elastic response to the perturbation is immediate, but this is not the case for viscous bodies. A simple way to model the viscoelastic behavior in this context is to consider that there is a small delay between the perturbing force and the actual deformation of the body. This approach is synthesized in the following, with [42] as reference.

Let us take a system planet-satellite, where the satellite is an extended

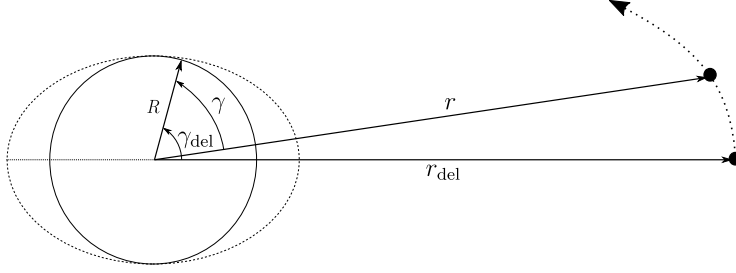


Figure 1.3: Schematic figure of the tides raised on the satellite by the delayed position of the planet.

body and the planet acts as a point mass. See Figure 1.3. Let  $\mathbf{R}$  be the position vector of a point at the surface of the satellite with respect to its center, and let  $\mathbf{r}$  be the position vector of the planet. Let  $R$  and  $r$  be the moduli respectively of  $\mathbf{R}$  and  $\mathbf{r}$ . Assume that  $\mathbf{R}$  and  $\mathbf{r}$  form an angle  $\gamma$ . The leading term of the potential created by the planet on the point of the surface has the usual expression  $-GM/r$ . Here  $M$  is the mass of the planet and  $G$  is the gravity constant. The next term in the expansion of the potential is the one responsible of the tides and is given by

$$\Phi_2(r, \gamma) = -G \frac{MR^2}{r^3} P_2(\cos \gamma),$$

where  $P_2(x) = (3x^2 - 1)/2$ . If the satellite is deformable, this potential gives rise to a displacement of the point  $\mathbf{R}$  to a point  $\tilde{\mathbf{R}}$ . If the satellite is viscous we can consider that the deformation is caused by the potential  $\Phi_2$  evaluated in a delayed position of the planet, that is given by  $r_{\text{del}}(t) = r(t - \Delta t)$ ,  $\gamma_{\text{del}} = \gamma + \alpha$ , where  $\Delta t$  is the time delay and  $\alpha$  is the lag angle. As a result, the point  $\tilde{\mathbf{R}}$  generates another potential onto a generic point  $\mathbf{r}_*$ . If the effect is small, we can assume a linear deformation that amends the potential with an additional term proportional to  $\Phi_2(r_{\text{del}}, \gamma_{\text{del}})$  and to the elastic Love number  $k_2$ . Since  $\Phi_2$  is proportional to  $P_2$ , from potential theory we know that the new potential must decrease with the distance as a power 3. Then, the new potential has the form

$$U = k_2 \left( \frac{R}{r_*} \right)^3 \Phi_2(r_{\text{del}}, \gamma_{\text{del}}) = -Gk_2 \frac{MR^5}{r_*^3 r_{\text{del}}^3} P_2(\cos \gamma_{\text{del}}), \quad (1.5)$$

where  $r_*$  is the modulus of  $\mathbf{r}_*$ . Here we assumed that the deformation is negligible with respect to the changes in  $r$  and  $\gamma$ , then,  $\tilde{\mathbf{R}} \approx \mathbf{R}$ . We can compute the force associated to this potential at the position of the planet. This force has a dissipative effect on the system as we can see in Section 1.3.2.

It is worth mentioning that the tidal force affects both to the orbital motion as well as to the spin motion of the bodies. However, in this thesis we will only focus on the tidal influence on the spin motion, i.e., the torque produced by the tidal force.

**Dissipative forces of electromagnetic origin.** For bodies that are small enough, electromagnetic forces become important with respect to the force of gravity. Probably, the main phenomenon considered in celestial mechanics that is of electromagnetic nature is the pressure exerted by the radiation emitted by stars. This pressure acts on the surface of the objects and produces a repulsive force. Thus, the larger is the surface of the object and smaller is its mass, the more important is such force. The emitted photons carry a momentum  $p$  and an energy  $E_p = pc$ , where  $c$  is the speed of light. Besides, the radiation flux of a star is given by  $\frac{L}{4\pi|\mathbf{x}|^2}$ , where  $L$  is the star luminosity (energy emitter per unit of time) and  $\mathbf{x}$  is the position vector with respect to the center of the star. Then, the force associated to the radiation pressure over a surface  $A$  oriented orthogonal to the direction of the light is

$$\mathbf{F}_r = \frac{AL}{4\pi c|\mathbf{x}|^3}\mathbf{x} = -\text{grad} \frac{\mu_r}{|\mathbf{x}|},$$

here grad is the gradient operator with respect to the coordinates of  $\mathbf{x}$  and  $\mu_r = \frac{AL}{4\pi c}$  is a constant. Note that the force  $\mathbf{F}_r$  has exactly the form of the gravity force (inverse square law) but points in the opposite direction. Then, the effect of the radiation pressure can be included into the Keplerian part of the gravity force by changing the standard gravitational parameter  $\mu$  of the star to  $\mu - \mu_r$ . This effect can be considered in other situations, for example, in a planet-satellite system we can assume that the star is so far away that the radiation pressure is constant. In any case, the effect of the radiation pressure alone is conservative.

However, an object can reflect, absorb or re-emit the radiation after it receives it. If there is total reflexion, the force we have to consider is twice the force  $\mathbf{F}_r$  we defined, because in the previous paragraph it was assumed a total absorption of the radiation. The case of the re-emission requires a more specific treatment, because it produces the dissipative effects, [17].

As already mentioned in Section 1.2.2, the Poynting-Robertson effect was studied in [108, 105, 110]. Consider the rest frame of a particle that is orbiting around a star. The re-emission of the radiation is isotropic assuming thermal equilibrium. However, as shown in Figure 1.4, in the rest frame of the Sun, the radiation become anisotropic due to the Doppler effect. In fact, the particle re-emits a factor  $2|\mathbf{v}|/c$  times more radiation in the forward

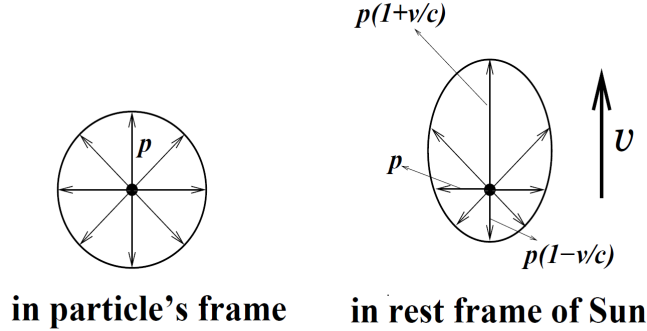


Figure 1.4: The Poynting-Robertson effect. Left: In the particle's frame, there is re-emission of photons with momentum  $p$  in all directions. Right: Due to the Doppler effect, the photons are emitted with momentum  $p(1 + \|\mathbf{v}\|/c)$  in the forward direction, whereas in the backwards direction they have momentum  $p(1 - \|\mathbf{v}\|/c)$ . Taken from [47].

direction than in the opposite direction. Here  $\mathbf{v} \in \mathbb{R}^3$  is the velocity of the particle. By conservation of momentum in the rest frame of the particle, there exists a force that acts opposite to the velocity given by

$$\mathbf{F} = -\frac{2\mu_r}{c\|\mathbf{x}\|^2}\mathbf{v}. \quad (1.6)$$

This force will be referred to as Poynting-Plummer-Danby (PPD) drag as in [14] and [39]. Since this dissipation occurs as an approximation of the Poynting-Robertson (PR) drag when the Doppler shift component is neglected, it is sometimes still called PR drag in the literature (see for example [47], pag. 115, [28], and [80]). To take into account the shape of the particle, its capacity to absorb, reflect or re-emit radiation there are some other constant factors that can be added to this force. A variant of this effect is produced by the solar wind, say, emission of massive particles instead of photons. The Yarkovsky effect is a similar phenomenon that arises if we consider that the particle rotates and it is not in thermal equilibrium.

According to [17], for particles of around  $0.1\mu\text{m}$  composed by iron, magnetite or graphite, the radiation force is larger than the force of gravity and those particles are blown out the solar system. Dust particles with sizes between  $1\mu\text{m} - 1\text{mm}$ , the Poynting-Robertson effect dominates and particles fall spiralling into the star. Larger particles usually collide between them before completing their orbits. Finally, the Yarkovsky effect dominates for particles of sizes of the order of meters, such as comets, meteoroids or asteroids.

## 1.3 The content of this thesis

### 1.3.1 The Kepler problem with singular drags

#### Model

The first problem we want to address is the dissipative Kepler problem. That is to say, we want to describe the motion of a particle moving in a Keplerian potential with an additional dissipative force. We take a family of dissipative forces opposed to the particle's motion and with a singularity at the origin. Let us take the family

$$\mathbf{F}_\beta(\mathbf{x}, \dot{\mathbf{x}}) = -\frac{k}{\|\mathbf{x}\|^\beta} \dot{\mathbf{x}}, \quad (1.7)$$

where  $k > 0$  and  $\beta > 0$  are parameters. We assume that  $k$  is a fixed positive number,  $\mathbf{x} \in \mathbb{R}^3 \setminus \{0\}$  is the position vector of the particle and  $\dot{\mathbf{x}} \in \mathbb{R}^3$  is its velocity. The parameter  $\beta$  distinguishes different models. For example, (1.7) has the form (1.6) if  $\beta = 2$ . This case, the PPD drag for dust particles, has attracted much attention from the theoretical point of view, see [108, 110, 105, 92, 39]. There are also numerical experiments, see [63]. If  $\beta = 0$ , (1.7) has the form (1.4) for bodies with small Reynolds numbers moving in homogeneous viscous fluids. This is the so-called linear drag or Stokes law. Note that in this case we do not have a singularity anymore. The linear drag has already been studied in several papers like [80, 81]. The linear drag and the PPD drag generate two very different global dynamics, whose main features we will recall below. Finally, (1.7) has the form (1.3) for a body moving into a gaseous solar nebula. Particularly, (1.7) represents different models depending on the density of the solar nebula as a function  $\rho = \rho(\|\mathbf{x}\|)$ , i.e., with radial symmetry. If, as in [123], we assume that the pressure and the temperature vary as  $P \propto r^{-a}$ ,  $T \propto r^{-b}$ , where  $r = \|\mathbf{x}\|$ , the density  $\rho$  will vary as a negative power of  $r$  as well. Then, to each model of the solar nebula, we would have a corresponding value of  $\beta$ . The equation of motion is then given by

$$\ddot{\mathbf{x}} + \frac{k}{\|\mathbf{x}\|^\beta} \dot{\mathbf{x}} = -\frac{\mathbf{x}}{\|\mathbf{x}\|^3}. \quad (1.8)$$

For simplicity, we study this normalized equation, in which all the quantities are dimensionless. Particularly, for a given  $\beta$ , the parameter  $k$  represents the strength of the dissipative force relative to the gravitational force, whose constant is normalized to 1. In our results we will see that the value of  $k$  is relevant for the asymptotic dynamics only in the case  $\beta = 3/2$ .

We note that (1.8) is a member of the larger class of dissipative Kepler problems considered by Poincaré in [106] when discussing the cosmogonique hypothesis of T.J.J. See (Section 1.2.2), namely,

$$\ddot{\mathbf{x}} + P_{\alpha,\beta}(\mathbf{x}, \dot{\mathbf{x}}) \frac{\dot{\mathbf{x}}}{\|\dot{\mathbf{x}}\|} = -\frac{\mathbf{x}}{\|\mathbf{x}\|^3}, \quad (1.9)$$

where  $P_{\alpha,\beta}(\mathbf{x}, \dot{\mathbf{x}}) = h\|\mathbf{x}\|^{-\beta}\|\dot{\mathbf{x}}\|^\alpha$ ,  $h$  is a positive fixed real number, and the parameters  $\alpha$  and  $\beta$  are positive. The family (1.9) can be included also in the general form of the drag forces (1.2) and (1.4) when the parameters depend on a power of the distance, as we mentioned for (1.7). Essentially, Poincaré found that orbits with negative energy spiral towards the singularity with increasing velocity<sup>4</sup>. Moreover, for  $\alpha$  and  $\beta$  sufficiently large, after each revolution the eccentricity decreases, leading to the circularization of orbits. Poincaré presented also a qualitative argument supporting that this effect occurs for a more general dissipative force opposed to the velocity, see Section 1.2.2. However, it turns out that such circularization of orbits does not take place for the particular cases that we mentioned: the linear drag ( $\alpha = 1, \beta = 0$ ) and the PPD drag ( $\alpha = 1, \beta = 2$ ).

In the first case, the fact that the linear drag does not circularize orbits was observed in [58]. Besides, the results presented in [82] and [83] show the following. Although some orbits circularize as they spiral down toward the singularity, for an open set of initial conditions, the value of the eccentricity of the corresponding orbit converges to a positive constant, being all values in  $]0, 1[$  attainable. Geometrically, these trajectories are spirals made of asymptotically self similar ellipses that shrink to the singularity. Moreover, it turns out that the angular velocity of these spirals increases exponentially with time. These results are obtained from the existence and continuity on the phase space of a first integral  $\mathbf{I}$ , defined as the limit, along the solutions, of the Runge-Lenz vector. We recall that this vector, also called eccentricity vector, is a first integral of the conservative Kepler problem, and defines the type of conic section corresponding to the orbit (its modulus is the eccentricity of the orbit) as well as its orientation (it is parallel to the axis containing the focus). Then, we can think of  $\mathbf{I}$  as an asymptotic eccentricity vector.

In [83] it is proved that the range of  $\mathbf{I}$  is the closed unit disk in the plane. This property expresses that all the non rectilinear orbits are of elliptic type, meaning that, eventually, their energy becomes negative. This last fact is stated in [81], where it is also established that the singularity is a global attractor, reached in infinite time by non rectilinear motions and in finite

---

<sup>4</sup>This fact had already been mentioned by Euler when discussing the motion of a planet in a resistive medium, see [44].

time by rectilinear ones. In each case, it is proved that the velocity tends to infinity.

In the case of the PPD drag (see [14], [17], [35], [39]), all the orbits which tend to the singularity, spiral only a finite number of times around it and achieve an asymptotic direction. This last property implies that their eccentricity tends to one. Moreover, all collisions occur in finite time and with finite velocity. Also, for this drag there exist solutions which escape to infinity. Essentially, these results are obtained in [39] by means of a qualitative study of (1.8). The fact that collision orbits are asymptotically rectilinear was previously observed in [14], where a more general class of drags is treated using a suitable transformation (called generalized Robertson transformation) to find explicit analytic solutions. The first step of such transformation is the Binet change of variables, exploited in [85], [92] to transform (1.8) with  $\beta = 2$  into a forced harmonic oscillator, that leads to a closed form for the orbit equation.

The PPD drag was studied also in other frameworks, such as the dissipative restricted Three-Body problem. In [28] and [80] the authors study the existence of periodic attractors. The actual Poynting-Robertson drag<sup>5</sup> was considered, for example in [9] to study its effect on the orbital evolution of grains of dust captured in mean motion resonances. Besides, in [71], the stability of motions near the Lagrangian points  $L_4$  and  $L_5$  was investigated.

## Objectives

In Chapter 2, we want to study the forward dynamics of the solutions of (1.8) with special emphasis on the following points.

1. We will try to characterize the asymptotic behavior of the solutions as much as we can for all  $\beta > 0$ ,  $k > 0$ . Recall that  $\beta$  distinguishes different models, and  $k$  gives the relative strength of the dissipation with respect to the gravitational force. We would like to find threshold values of the parameters such that the qualitative asymptotic behavior of the solution changes. Particularly, since the linear drag  $\beta = 0$  and the PPD drag  $\beta = 2$  generate two very different global dynamics, we want to explore if there are transitions of qualitative behavior for the different values of  $\beta$  in between.
2. We would like to know if, apart from the collisions with the singularity,

---

<sup>5</sup>For this dissipative force, the radial component of the velocity has a coefficient which is twice the one of the angular component.



there are escape orbits or even oscillatory solutions, say,

$$\limsup_{t \rightarrow \omega^-} \|\mathbf{x}(t)\| = +\infty, \quad \infty > \liminf_{t \rightarrow \omega^-} \|\mathbf{x}(t)\| \geq 0.$$

For example, we know that for  $\beta = 0$  all the solutions are collisions, but for  $\beta = 2$  there are also escapes. We would like to classify the resulting orbits.

3. We want to characterize the behavior of the collisions. Does a collision happen in infinite time? What is the energy and the velocity when the collision is reached? Is the number of turns around the singularity finite or infinite? Can we answer these questions for all the values of the parameters?
4. Also, we want to see if the first integral existing for  $\beta = 0$ , that is an asymptotic Runge-Lenz vector, is present for other values of  $\beta$ . Does it have the same properties as for  $\beta = 0$ ? The case  $\beta = 2$  seems a good candidate to start because the problem is integrable by quadratures.

## Results

The main results concerning the Kepler problem with a singular family of dissipations (1.8) are stated in Section 2.2 and Section 2.3. The problem has a planar structure (we restrict ourselves to  $\mathbf{x} \in \mathbb{C}$ ) and naturally divides into rectilinear solutions and non rectilinear ones. Regarding this division, there are some common and some particular results. Unless there is an explicit reference (for example, to the polar angle  $\theta$ ), the results would be valid for all the solutions. In the following,  $\omega$  denotes the supremum of the maximal interval of definition of a solution  $\mathbf{x}(t)$  of (1.8). Sometimes  $\omega$  appears as subscript of some quantity, for example, the limit of the polar angle  $\theta_\omega = \lim_{t \rightarrow \omega^-} \theta(t)$ . Analogous definitions hold for the energy  $E$ , the angular momentum  $M$ , the radial velocity  $u$ , etc.

In Section 2.1 we present a preliminary result, in Theorem 2.1. It states that, for non rectilinear collision orbits of (1.8), the energy and the angular momentum tend respectively to the values  $E_\omega = -\infty$  and  $M_\omega = 0$ .

In Section 2.2 we present an analysis of the dynamics as  $\beta$  increases. In particular, we detect some thresholds for different global behaviors.

In Theorems 2.2 and 2.5, we show that the global attractiveness of the singularity and the unboundedness of the angular velocity of solutions, which hold for  $\beta = 0$ , can be continued, respectively, for  $\beta \in (0, 1]$  and for  $\beta \in (0, 1)$ . Particularly, in Theorem 2.2 we claim that escapes are possible only

for  $\beta > 1$ . Recall that we already knew this for  $\beta = 2$ . Actually, it takes infinite time for a particle to escape, and it does with finite velocity and a non-negative finite energy. On the other hand, Theorem 2.5 determines that we can find a sequence  $\{t_n\}_{n=0}^{\infty}$  converging to  $\omega$ , such that the angular velocity of a non rectilinear collision becomes unbounded, say,  $\dot{\theta}(t_n) \rightarrow +\infty$ . These results suggest that, when  $\beta \in (0, 1)$ , all solutions collide with the singularity winding faster and faster infinite times around it, as they do in the case of the linear drag.

In Theorem 2.4 we show the variation of their polar angle  $\theta$  for different type of orbits. Escapes are only possible during the first turn around the origin, otherwise, if the solution makes more turns, it has to be a collision. Moreover, for escapes, the limit angle is bounded,  $\theta_\omega < \alpha_0 + \pi$ , where  $\alpha_0 \in (0, \pi)$  is the angle that forms the initial velocity  $\mathbf{v}(0)$  with the initial position vector  $\mathbf{x}(0)$ .

Theorem 2.3 allows us to classify the solutions because it rules out the possibility of oscillatory solutions. Here we show that escape and collision solutions are the only kind of solutions that can occur for (1.8). In consequence, the phase space associated to non rectilinear motions,  $\Omega^+$ , can be partitioned in the following three sets: the set of initial conditions of collisions orbits

$$\Omega_C^+ := \{(\mathbf{x}, \mathbf{v}) \in \Omega^+ : E_\omega = -\infty\},$$

the set of initial conditions of hyperbolic escapes, and the set of initial conditions of parabolic escapes, defined respectively by

$$\Omega_H^+ := \{(\mathbf{x}, \mathbf{v}) \in \Omega^+ : E_\omega > 0\} \quad \text{and} \quad \Omega_P^+ := \{(\mathbf{x}, \mathbf{v}) \in \Omega^+ : E_\omega = 0\}.$$

The last two sets are empty when  $\beta \in [0, 1]$ .

The case  $\beta \in [\frac{3}{2}, +\infty)$  for non rectilinear collisions is addressed in the next theorem, that we show explicitly.

**Theorem** (Theorem 2.6). *The following properties hold for non rectilinear collision orbits:*

- i) *If  $\beta > \frac{3}{2}$ , or if  $\beta = \frac{3}{2}$  and  $k > 2\sqrt{2}$ , there exists a limit polar angle at collision, achieved with zero angular velocity.*
- ii) *If  $\frac{3}{2} < \beta < 3$ , or if  $\beta = \frac{3}{2}$  and  $k > 2\sqrt{2}$ , collisions occur in finite time, whereas if  $\beta \geq 3$  they occur in infinite time.*
- iii) *If  $\frac{3}{2} < \beta < 2$ , or if  $\beta = \frac{3}{2}$  and  $k > 2\sqrt{2}$ , the limit velocity at collision is infinite, if  $\beta = 2$ , the limit velocity is finite and with modulus  $\frac{1}{k}$ , and if  $\beta > 2$  the limit velocity is zero.*

Here we give a fairly complete description of the qualitative dynamics of non rectilinear collision orbits. Namely, we show that when  $\beta > \frac{3}{2}$  such orbits are asymptotically rectilinear, a behavior that, as already mentioned above, was observed for  $\beta = 2$  in [14] and [39]. Moreover, we prove that the approach to zero occurs in finite time if  $\beta \in (\frac{3}{2}, 3)$ , and that  $\beta = 2$  is the threshold for the value of the terminal velocity. When  $\beta$  crosses this value, the terminal velocity passes from  $-\infty$  to 0. We extended these results to  $\beta = \frac{3}{2}$ , but only imposing that  $k > 2\sqrt{2}$ .

Unfortunately, we could not provide any result about the rotational properties, collision time or terminal velocity of non rectilinear solutions when  $\beta \in [1, \frac{3}{2})$ . However, in Section 1.3.1 we will present some conjectures about the dynamics at collision for  $\beta \in (0, \frac{3}{2})$ .

Theorem 2.7 gives a complete description of the rectilinear motions. We describe their collision time  $\omega$  (discussing whether it is finite or not), and the asymptotic behavior of their velocity,  $u_\omega$ , and energy,  $E_\omega$ . The results are summarized in the following table:

$\beta$	$]0, 1/2[$	$[1/2, 2[$	$2$	$]2, 3[$	$[3, \infty[$
$\omega$	finite				$+\infty$
$u_\omega$	$-\infty$		$-\frac{1}{k}$		0
$E_\omega$	finite		$-\infty$		

In Section 2.3, we show an interesting difference between the linear drag and the PPD drag. First note that equation (1.8) can be written as

$$\begin{cases} \dot{\mathbf{x}} = \mathbf{v} \\ \dot{\mathbf{v}} = -\frac{k}{|\mathbf{x}|^\beta} \mathbf{v} - \frac{\mathbf{x}}{|\mathbf{x}|^3} \end{cases} \quad (\mathbf{x}, \mathbf{v}) \in \Omega = (\mathbb{C} \setminus \{0\}) \times \mathbb{C}.$$

Let us define  $\mathbf{R}$ , the Runge-Lenz vector

$$\mathbf{R}(\mathbf{x}, \mathbf{v}) = \mathbf{v} \wedge (\mathbf{x} \wedge \mathbf{v}) - \frac{\mathbf{x}}{|\mathbf{x}|}.$$

The result of this section is contained in Theorem 2.8 and deals with the existence of a first integral  $\mathbf{I}$  for  $\beta = 2$ , like in [82] for  $\beta = 0$ . The vector field  $\mathbf{I}$  is an asymptotic Runge-Lenz vector, say, to each solution  $t \mapsto (\mathbf{x}(t), \mathbf{v}(t))$ , defined on the right maximal interval  $[0, \omega)$ , it corresponds the vector

$$\mathbf{I}(\mathbf{x}(t'), \mathbf{v}(t')) = \lim_{t \rightarrow \omega^-} \mathbf{R}(\mathbf{x}(t), \mathbf{v}(t))$$

for each  $t' \in [0, \omega)$ .

Theorem 2.8 is analogous to Theorem 2.1 in [82], where the properties of  $\mathbf{I}$  for  $\beta = 0$  are described. In such case,  $\mathbf{I}$  is continuous on  $\Omega$ . Moreover, Theorem 4.2 in [83] shows that the range of  $\mathbf{I}$  is the closed unit disk. When  $\beta = 2$ , Theorem 2.8 shows that  $\mathbf{I}$  has significantly different properties:  $\mathbf{I}$  is not continuous on  $\Omega$ , and its range is the exterior of the open unit disk. The discontinuity arises along any fixed parabolic orbit since such orbit is the limit of hyperbolic and collision orbits. We prove this fact only for  $\beta = 2$ , because in this case the problem is integrable. As to the range of  $\mathbf{I}$ , it expresses that, unlike the case  $\beta = 0$ , there are parabolic and hyperbolic orbits, and there are no elliptic motions winding infinite times around the singularity as they approach it.

## Methodology

Section 2.1 is devoted to introduce some preliminaries that are useful along Chapter 2. Here we show that our problem (1.8) has an intrinsic planar structure (the direction of the angular momentum is conserved) that can be split into rectilinear and non rectilinear motions. Also, the energy  $E$  and the angular momentum  $M$  are strictly decreasing functions of the time (except for rectilinear motions:  $M = 0$ ). This is used for the proof of the preliminary result, in Theorem 2.1, about the value of  $E_\omega$  and  $M_\omega$  for collisions.

In Section 2.2, we present several results on how the asymptotic behavior of the solution changes for different values of  $\beta$ . The first result, Theorem 2.2, deals with the existence of collision and escape orbits. Here we use some results that characterize the attractivity of the singularity. Using Lemma 6 in [33] we prove, with the family of functions (2.14), that all the solutions are bounded for  $0 < \beta \leq 1$ . Then, we apply Lemma 2.1, that says that any bounded solution is a collision. This is based on a generalization of La Salle's principle to singular systems, [83]. To prove the existence of escape orbits for  $\beta > 1$ , we use a family of unbounded positively invariant sets (2.17) that do not include the singularity. Then we prove the non existence of oscillatory solutions in Theorem 2.3 with similar arguments as in Lemma 2.1.

The following results deal only with non-rectilinear solutions. We rewrite (1.8) with the Binet transformation, that leads to a forced linear oscillator equation on  $\rho = 1/r$ , where  $r$  is the distance to the singularity. Using the variation of constants formula we obtain an expression for  $\rho$  (2.21), in terms of an integral that involves the angular momentum (2.23). Lemma 2.2 shows that the integral (2.23) increases after each turn. Its proof takes advantage of the monotonicity of the angular momentum. This is enough to prove Theorem 2.4, that characterizes the number of turns and the limit angle depending on the type of orbit (escape/collision). The second result is Theorem 2.5,

that states that for  $\beta \in (0, 1)$ , the angular velocity gets unbounded when reaching the singularity. This result is proved borrowing arguments from [81] on elementary inequalities using the equations of the system. Here we work on the regularized system (2.24) given by a time scaling  $dt = r^2 d\mu$ . To prove the next result we regularize with another time scaling  $dt = r^\beta d\tau$ . Theorem 2.6 gives a rather complete description for  $\beta > 3/2$  and  $\beta = 3/2$ ,  $k > 2\sqrt{2}$ . It shows the asymptotic value at the collision of the limit polar angle, the endpoint of the maximal time interval and the limit velocity. For the proof we apply repeatedly previous results on the behavior of the solutions. At the end of the proof of the item *ii*) of Theorem 2.6 we explain that in our problem we can eliminate the parameter  $k$  by a scaling of the solutions except when  $\beta = 3/2$ . In this case and with our tools we are able to characterize only solutions for  $k > 2\sqrt{2}$ . We do not know if this constraint on  $k$  is just a technical condition which arises due to our technique of proof, or if it reflects some deeper aspects of the dynamics.

The rectilinear problem is a planar problem that we study with analogous tools than those of [81, 83]. Theorem 2.7 gives a thorough description of the behavior of the rectilinear solutions for each range of the parameter  $\beta$ . In the proof, the phase space is divided by the isocline curves in different regions and we look for positively invariant regions that prove the results. For this purpose we define several families of curves and study how the vector field behaves on them. This theorem implies that the asymptotic expansions of solutions around the collision time given for  $\beta = 0$  in [81] still hold when  $\beta \in (0, \frac{1}{2})$ . However, we show that, unlike for the case  $\beta = 0$ , the presence of the singularity in the dissipation does not allow to regularize collisions by means of a generalized Levi-Civita transformation (2.49).

Section 2.3 is dedicated to prove Theorem 2.8 on the existence of the first integral **I**. We focus the proof on the discontinuity of such integral on the set of parabolic orbits (escapes whose energy tends to zero), because it is the main difference with respect to [81]. We base our proof on the fact that the limit polar angle  $\theta_\omega$  is a discontinuous function of the initial conditions. Particularly, the discontinuity arises when we continuously change from elliptic orbits (collisions) to hyperbolic ones (escapes whose energy tends to a positive value) passing through parabolic ones. We prove this by applying the expression of  $\rho = 1/r$  integrating the forced linear oscillator equation from the Binet transformation. For  $\beta = 2$ , the angular momentum has an explicit expression, so we have an explicit dependence on the polar angle  $\rho = \rho(\theta)$ . With this expression it is rather clear that  $\theta_\omega$  is different for elliptic orbits than for hyperbolic ones. In the proof we make a detailed description of the diffeomorphisms to undo the change of variables and get the desired result. Incidentally, we also show the range of **I**: for rectilinear solutions, collisions

and parabolic escapes,  $\mathbf{I}$  lies in the boundary of the unit disk, whereas for non rectilinear hyperbolic escapes,  $\mathbf{I}$  lies in the exterior of it.

### Discussion and perspectives

In this research we have considered a family of dissipative Kepler problems with drags of the form  $-\frac{k}{\|\mathbf{x}\|^\beta} \dot{\mathbf{x}}$ , and studied the changes in the forward dynamics as  $\beta$  increases. This family includes two physically meaningful dissipations: the Stokes drag ( $\beta = 0$ ) and the Poynting-Plummer-Danby drag ( $\beta = 2$ ).

We were able to detect a threshold value for the existence of escape orbits, namely  $\beta = 1$ , and we gave a fairly complete description of non rectilinear collision orbits for  $\beta \geq \frac{3}{2}$ , showing in particular that they are asymptotically rectilinear. Moreover, the integrability of the equation for  $\beta = 2$  allowed us to prove that the asymptotic Runge-Lenz vector, which is a non-trivial first integral, is not continuous on the phase space, unlike for the case  $\beta = 0$ . We think that the jump discontinuity in the parabolic orbits is a general property for those values of  $\beta$  for which there are hyperbolic escapes and asymptotically rectilinear collisions. The reason is that discontinuity follows essentially from the fact that  $\theta_\omega$  is defined by  $\rho(\theta_\omega^-) = 0$  for hyperbolic escapes, whereas for collisions  $\rho(\theta_\omega^-) = +\infty$ .

The dynamical behavior of non rectilinear collisions for the values of  $\beta$  in the complementary interval  $(0, \frac{3}{2})$  remains an open question. Our only contribution in this direction is the unboundedness of angular velocity of these solutions when  $\beta \in (0, 1)$ . However, the following informal argument, which we were not able to make rigorous, leads to a conjecture: substituting the third equation of (2.21) into the first, we obtain a fixed point equation of the form  $\rho = T(\rho)$ . From the results in [82], we see that, when  $\beta = 0$ , any fixed point defined for every  $\theta \geq 0$ , satisfies  $\rho(\theta) \approx \theta^{2/3}$  for large  $\theta$ . Then, if we look for fixed points defined for every  $\theta \geq 0$  when  $\beta > 0$ , we can try to find a space of functions satisfying  $\rho(\theta) \approx \theta^\alpha$ ,  $\alpha > 0$ , for large  $\theta$ , and which is invariant under  $T$ . We are led, heuristically, to  $\alpha = \frac{2}{3-2\beta}$ , which is correct for  $\beta = 0$ . Now, if  $\beta \in (0, \frac{3}{2})$ , it is not difficult to see that the previous asymptotic growth for  $\rho(\theta)$  implies that the collision time  $\omega$  is finite and that  $\dot{\theta}(t) \rightarrow +\infty$  as  $t \rightarrow \omega^-$ . This last property is consistent with Theorem 2.5. Due to the difficulty of numerical integration of singular systems, the simulations made to support our conjecture were inconclusive.

Finally, in our work we gave a complete description of the rectilinear collisions as  $\beta$  increases, including their asymptotic expansion for  $\beta \in (0, \frac{1}{2})$ . As a consequence, we were able to show that the presence of the singularity in the dissipation is an obstruction to the regularization of collisions.

We think that this research contributes to the understanding of the dissipative dynamics for more general dissipations. Particularly, as mentioned in the description of the model, we deal with a member of a larger family of dissipative Kepler problems

$$\ddot{\mathbf{x}} + k \frac{||\dot{\mathbf{x}}||^{\alpha-1}}{||\mathbf{x}||^{\beta}} \dot{\mathbf{x}} = -\frac{\mathbf{x}}{||\mathbf{x}||^3}, \quad \alpha, \beta > 0$$

that was considered by Poincaré and include very general drag forces (1.2). Here we considered the case  $\alpha = 1$  and it would be interesting to study other values, such as  $\alpha = 2$  because this is a common dependence for a body moving in a fluid, such as the atmosphere. In this way, another possibility is to study other dependence with respect to  $||\mathbf{x}||$ , such as the simple atmospheric model in [15] given by the factor  $\exp[-\alpha_0(||\mathbf{x}|| - R)]$ ,  $\alpha_0 > 0$ ,  $||\mathbf{x}|| > R$ , where  $R$  is the radius of the body.

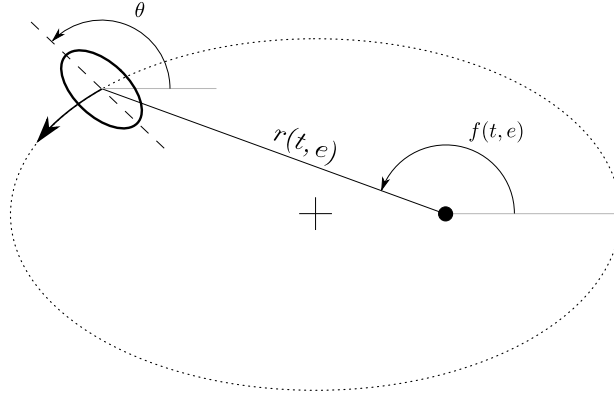


Figure 1.5: The spin-orbit problem

### 1.3.2 Stability of the 1:1 spin-orbit resonance

#### Model

The spin-orbit model is the most elementary model to study the rotational dynamics of a satellite about its center of mass when it orbits around a planet. Consider a satellite whose center of mass is moving around a planet in a Keplerian elliptical orbit of eccentricity  $e$ . We are interested in the spin of the satellite around its center of mass, so, we will identify the satellite with a tridimensional object and the planet with a point mass. Let the satellite be triaxial, with principal moments of inertia  $\mathcal{A} < \mathcal{B} < \mathcal{C}$ . The parameter  $\epsilon = \frac{3}{2} \frac{\mathcal{B} - \mathcal{A}}{\mathcal{C}}$  measures the equatorial oblateness of the satellite. For this ordering of moments of inertia,  $\epsilon \in (0, 3/2)$ . Assume that the spin axis of the satellite is perpendicular to the orbital plane and coincides with the smallest of its physical axes, which is associated to  $\mathcal{C}$ . This planar setting is a major simplification that reduces the problem to one degree of freedom (spin) plus time-dependence (orbit), allowing us to focus the study on the spin-orbit resonances.

Let us identify the orbital plane with the complex plane  $\mathbb{C}$ . Consider the planet fixed at the origin and let the position of the center of mass of the satellite be  $\mathbf{r} = r \exp[i f] \in \mathbb{C}$ , where  $r > 0$  and  $f$  are real and smooth functions of the time. Note that this point describes an ellipse with focus at the origin and eccentricity  $e \in [0, 1)$ , so, the polar coordinates  $r$  and  $f$  vary periodically with time and are known by the Kepler problem. Let us take convenient units of time so that the period is  $2\pi$ . In the usual terminology,  $f$  is called *true anomaly* and the time  $t$  is the *mean anomaly*. There is a third useful angle  $u$ , the *eccentric anomaly*, which is defined by the famous



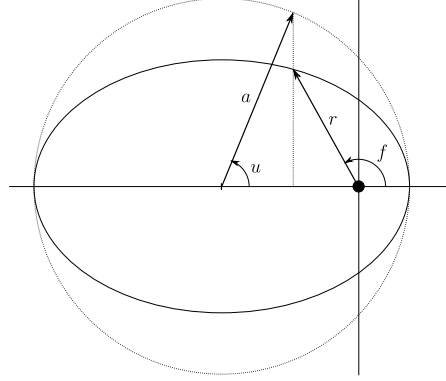


Figure 1.6: Some geometrical relations in a Keplerian ellipse.

Kepler's equation

$$t = u - e \sin u, \quad (1.10)$$

and let us determine the Keplerian ellipse simply by

$$r = a(1 - e \cos u), \quad (1.11)$$

where  $a$  is the semimajor axis of the ellipse.

Also, using the graphical definition of the eccentric anomaly, see Figure 1.6, we can write  $\mathbf{r}$  in terms of the eccentric anomaly as

$$r \exp[if] = a(\cos u - e + i\sqrt{1 - e^2} \sin u). \quad (1.12)$$

Note that for  $t = 0$  we assumed that  $f = u = 0$ , and consequently,  $f = u = \pi$  when  $t = \pi$ . We can take convenient units of length so that  $a = 1$ . The expressions eqs. (1.11) and (1.12) relate the true and eccentric anomalies. Moreover, Equations (1.10) to (1.12) define  $u = u(t, e)$ ,  $r = r(t, e)$  and  $f = f(t, e)$  as analytic functions in both entries.

Let  $\theta$  be the angle that determines the direction of the body's axis of the major elongation with respect to the major axis of the ellipse. See Figure 1.5. According to [51], the motion of the satellite is modelled by the following biparametric equation

$$\ddot{\theta} + \frac{\epsilon}{r(t, e)^3} \sin[2(\theta - f(t, e))] = \mathcal{T}_d(t, \dot{\theta}), \quad e \in [0, 1), \quad \epsilon \in (0, 3/2), \quad (1.13)$$

where  $\mathcal{T}_d$  is a dissipative torque, which has different forms depending on the model. The popular model introduced by MacDonald in [75] has been extensively used, taking as reference [51] or [99], for example. Although MacDonald studied only the case  $\mathcal{T}_d$  constant, later approaches, like [51] and

[115], suggest that it is more physically reasonable to take a MacDonald's torque with a linear dependence

$$\mathcal{T}_d(t, \dot{\theta}) = -\frac{C_M}{r(t, e)^6} \sin[2\Delta t(\dot{\theta} - \dot{f}(t, e))] \approx -\frac{\delta}{r(t, e)^6}(\dot{\theta} - \dot{f}(t, e)), \quad (1.14)$$

where  $1 \gg \delta = 2C_M\Delta t \geq 0$ , and  $C_M$  is a constant depending on the parameters of the bodies,

$$C_M = \frac{3GM^2R^2k_2}{2\mathcal{C}a^6},$$

where  $M$  is the mass of the planet,  $R$  and  $k_2$  are the mean radius and the Love number of the satellite. Here  $a$  is the semimajor axis of the orbit, that in our units equals 1. Hereafter (1.14) will be referred to as the *linear MacDonald torque*. According to [42], to obtain (1.14), the dissipation is modelled by assuming that there is a time delay between the deforming disturbance and the actual deformation of the body. This was explained in Section 1.2.3 and the delay was denoted by  $\Delta t$  (time lag). In our planar configuration, the torque  $\mathcal{T}_d$  can be derived from (1.5) by  $\mathcal{T}_d = -\frac{M}{\mathcal{C}}\partial_\gamma U$  evaluated at the position of the planet<sup>6</sup> ( $\gamma = 0$ ,  $r_* = r \approx r_{\text{del}}$ ). Let us show this. First,  $\partial_\gamma P_2(\cos \gamma_{\text{del}})$  at  $\gamma = 0$  equals  $\frac{3}{2}\sin(2\alpha)$ . Furthermore, if  $\hat{\mathbf{r}}_{\text{del}}$  and  $\hat{\mathbf{r}}$  are the unit vectors of the delayed and the current position of the planet,  $\hat{\mathbf{r}}_{\text{del}} \wedge \hat{\mathbf{r}} = (0, 0, \sin \alpha)$ , where  $\wedge$  is the vector product. Besides,  $\sin \alpha \approx \alpha$  if  $|\alpha|$  is small. We can approximate  $\hat{\mathbf{r}}_{\text{del}} \approx \hat{\mathbf{r}} - \frac{d\hat{\mathbf{r}}}{dt}\Delta t$ , then,

$$\hat{\mathbf{r}}_{\text{del}} \wedge \hat{\mathbf{r}} = \hat{\mathbf{r}} \wedge \frac{d\hat{\mathbf{r}}}{dt}\Delta t.$$

Note that we are in a non-inertial frame of reference that has an angular velocity  $\boldsymbol{\omega} = (0, 0, \dot{\theta})$ , then

$$\frac{d\hat{\mathbf{r}}}{dt} \equiv \left(\frac{d\hat{\mathbf{r}}}{dt}\right)_{\text{non-inertial}} = \left(\frac{d\hat{\mathbf{r}}}{dt}\right)_{\text{inertial}} - \boldsymbol{\omega} \wedge \hat{\mathbf{r}}.$$

Since  $\hat{\mathbf{r}} = (\cos f, \sin f, 0)$ , then

$$\hat{\mathbf{r}}_{\text{del}} \wedge \hat{\mathbf{r}} = (0, 0, \Delta t(\dot{f} - \dot{\theta})),$$

consequently, the lag angle (geometric lag) is  $\alpha \approx (\dot{f}(t, e) - \dot{\theta})\Delta t$ . This is enough to obtain (1.14).

The spin-orbit model has the structure of a periodically forced pendulum. It is nearly integrable for small eccentricities. It has attracted much attention

---

<sup>6</sup>Recall that, by the law of action-reaction, the torque exerted by the planet on the satellite is the opposite to the torque exerted by the satellite on the planet.

not only for its accurate physical implications but also for its mathematical richness. Some pioneer papers are [10] for the conservative case and [51] for the dissipative case. This model is useful to explain the synchronization of the rotational motion of the Moon and its orbital motion around the Earth. In other words, the Moon is in a 1:1 spin-orbit resonance, i.e., solutions of equation (1.13) that satisfy  $\theta(t + 2\pi) = \theta(t) + 2\pi$ . It is also known as synchronous resonance. This phenomenon is indeed very common in the Solar System for natural satellites that are close enough to their respective planets, [99]. Besides, Mercury, as an orbiting body around the Sun, is locked in a 3:2 spin-orbit resonance, for which  $\theta(t + 4\pi) = \theta(t) + 6\pi$ . This is also a very interesting resonance, see for example [34], [11] or [24]. According to [34], in its chaotic evolution, Mercury could have reached large orbital eccentricities that made possible the capture into this higher order resonance. It is accepted that the phenomenon of capture into resonances is driven by dissipative torques, caused by internal frictions within the satellite, [75]. The concept of stability of a resonance in the conservative regime is linked to the concept of capture in the dissipative case and both can be related. For example, [21] studies the KAM stability in the conservative case, whereas [25] proves the existence of quasiperiodic attractors for the dissipative problem, that bifurcate from the KAM tori of the conservative case. This last study belongs to a group of papers exploiting the weakly dissipative and nearly integrable Hamiltonian structure of the problem, [22, 24, 2]. We would like to remark the analytical treatment of the dissipative spin-orbit problem as a conformally symplectic system [20]. Also, it is worth mentioning that the system has a very strong connection with the standard map and its dissipative counterpart, see [19, 26]. The onset of chaos is another interesting feature of this problem. The oblateness of the satellite produces chaotic regions in the phase space that surround the libration regions of resonances. Chaotic zones can be very large due to overlapping of different resonances, [29]. A large eccentricity emphasizes this behavior, as in the case of Hyperion, [125], [124]. The spatial setting has a higher dimensional phase space and richer dynamics. For example, other types of resonances may appear. In [10], without the planar assumption, the synchronous resonance is found as a relative equilibrium, which is Lyapunov stable for circular orbits, only provided the ordering of the moments of inertia. By contrast, in [69], the authors study the onset of chaos due to deviations from perpendicularity of the spin axis and the orbital plane.

This thesis deals with the study of the stability of synchronous resonances of (1.13). Let us take the change of variable  $\Theta = 2(\theta - f)$  and a more general

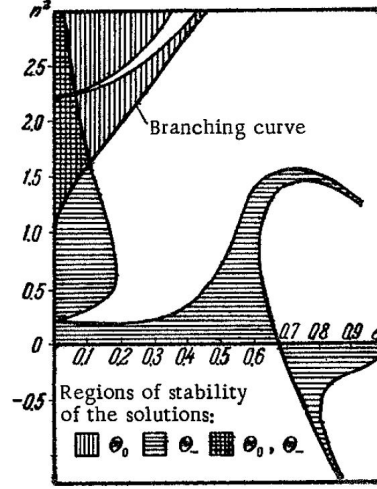


Figure 1.7: Figure 17 in [10]. This is a plot of linear stability of the odd  $2\pi$ -periodic solutions of (1.16) in the  $(\Lambda, e)$ -plane. Here  $\Lambda = n^2$ .

dissipation proportional to  $(\dot{\theta} - \dot{f})$ , such that (1.13) turns into

$$\ddot{\Theta} + \delta D(t, e) \dot{\Theta} + \frac{\Lambda}{r(t, e)^3} \sin \Theta = -2\ddot{f}(t, e), \quad e \in [0, 1), \Lambda = 2\epsilon \gg \delta \geq 0, \quad (1.15)$$

where  $D(t, e)$  is a positive analytic function, which is  $2\pi$ -periodic in  $t$ . Note that, for the linear MacDonald torque,  $D(t, e) = r(t, e)^{-6}$ . Equation (1.15) models a damped and forced pendulum of variable length and depends on three parameters  $e$ ,  $\Lambda$  and  $\delta$ . Since  $f(t + 2\pi, e) = f(t, e) + 2\pi$ , then, 1 : 1 resonances correspond to solutions of (1.15) satisfying  $\Theta(t + 2\pi) = \Theta(t)$ .

In [129] there is a numerical investigation of the non-dissipative problem<sup>7</sup>

$$\ddot{\Theta} + \frac{\Lambda}{r(t, e)^3} \sin \Theta = -2\ddot{f}(t, e), \quad e \in [0, 1), \Lambda \in (0, 3). \quad (1.16)$$

Particularly, [129] focuses on the periodic solutions of equation (1.16) with odd symmetry  $\Theta(-t) = -\Theta(t)$ . According to [129], in the indicated range of parameters, there are three odd periodic solutions, namely  $\Theta_-$ ,  $\Theta_+$  and  $\Theta_0$ . There is a branching curve, in which  $\Theta_+$  and  $\Theta_0$  coincide, that divides the region in two. The lower part is a region of uniqueness of  $\Theta_-$ . The regions of linear stability of the solutions and the branching curve are shown in Figure 1.7.

<sup>7</sup>The results of [129] (in Russian) have been summarized in [10]. The works [129, 10] consider the true anomaly  $f$  as independent variable, instead of the mean anomaly  $t$ .

## Objectives

Our main objective in Chapter 3 is to characterize the capture into the 1:1 resonance of the dissipative spin-orbit problem (1.13). We choose the 1:1 resonance because it is the simplest and most abundant one in the solar system. We want to achieve this goal using the full non-autonomous form (1.15) and without any previous assumption on the smallness of the eccentricity. With this approach we would like to address some particular questions.

1. We want to characterize the capture by finding an asymptotically stable solution of the dissipative problem. To do this, we would like to make a continuation of solutions of the conservative problem to the dissipative one. Here we expect to make an analytic continuation of solutions with odd symmetry.
2. First, we will explore the conservative problem. We can infer from Figure 1.7 that the solution  $\Theta_-$ , found in [129], is the continuation of the equilibrium of (1.16) for  $e = 0$ . We want to find regions of uniqueness and linear stability of  $\Theta_-$  with theoretical tools.
3. Once we have a region of linear stability, we want to make a continuation of  $\Theta_-$  to the dissipative problem (1.15) for  $\delta > 0$ . We want that the estimated region is large enough to make it useful for practical applications.
4. We expect such continuation to be asymptotically stable and would like to prove it. Furthermore, we want to make a quantitative continuation by finding an upper value of  $\delta$  for which the continuation is asymptotically stable.
5. To complete this process, we would like to obtain a diagram that provides the upper value of  $\delta$  for each point  $(e, \Lambda)$ . Also, we want to apply our results for real systems, such as the Earth-Moon system. Moreover, we would like to put our results on the dissipative parameter in contrast with real measurements of how the satellite dissipates energy.
6. Finally, we want to investigate the stability of  $\Theta_-$  for large eccentricities. It looks from Figure 1.7 that there is a bifurcation such that the solution  $\Theta_-$  is unstable for large eccentricities. We want to characterize theoretically this bifurcation.

## Results

The results of the second part of thesis are developed in Chapter 3.

We start discussing, in Section 3.1, the existence and uniqueness of a particular  $2\pi$ -periodic solution  $\Theta^*$  for the non-dissipative problem (1.16). This solution has an odd symmetry,  $\Theta^*(-t) = -\Theta^*(t)$ , and is two times the function  $\Theta_-$  defined in [129, 10], as it was described at the end of Section 1.3.2. Proposition 3.1 defines a region of uniqueness for such solution in the  $(e, \Lambda)$ -plane. The region is given by  $e \in (0, 1]$  and  $0 \leq \Lambda < \Lambda_1(e)$ , where the function  $\Lambda_1(e)$  is defined in (3.13). See Figure 1.8. In Lemma 3.2 we provide some properties of  $\Lambda_1(e)$ . Moreover, Proposition 3.1 claims that  $\Theta^*(t; e, \Lambda)$  is an analytic function in all its entries. Actually,  $\Theta^*$  is the analytic continuation of the trivial solution for  $e = 0$ .

In Proposition 3.2 we provide a region of linear stability of  $\Theta^*(t; e, \Lambda)$ . The region is given by

$$\left\{ (e, \Lambda) : e \in (0, 1), m(e) < \pi/4, 0 < \Lambda < \frac{1}{4}\Lambda_1(e), 0 < \Lambda < \Lambda_2(e) \right\}.$$

The functions  $m(e)$  and  $\Lambda_2(e)$  are defined respectively in (3.21) and (3.22). The functions  $\frac{1}{4}\Lambda_1(e)$  and  $\Lambda_2(e)$  define the upper limit of the stability region obtained theoretically. We can see these results illustrated in Figure 1.8. Note that we actually reach large eccentricities<sup>8</sup>, close to 0.4.

In Theorem 3.2, we make a continuation of the  $2\pi$ -periodic solution  $\Theta^*$  of (1.16) to the dissipative problem (1.15). In such case, the solution becomes asymptotically stable. More precisely, if  $(e, \Lambda)$  belongs to the region defined in Proposition 3.2, there exists a  $2\pi$ -periodic solution  $\Theta_\delta^*(t)$  of (1.15) that is continuous for  $\delta \in [0, \bar{\delta}]$  and  $\Theta_0^*(t) = \Theta^*(t; e, \Lambda)$  for each  $t \in \mathbb{R}$ . Here  $\bar{\delta}$  is a small quantifiable value. Particularly, if  $\delta > 0$ ,  $\Theta_\delta^*(t)$  is asymptotically stable. Let  $\Delta_0$  be the discriminant associated to the linearized equation at the solution  $\Theta^*(t; e, \Lambda)$ . We provide an explicit formula for  $\bar{\delta}$ , (3.36) with  $\bar{\delta} = \rho$ , that only involves the quantities  $e$ ,  $\Lambda$  and  $\Delta_0$ .

In Section 3.3.1 we discuss that our results are applicable to a family of torques generalizing the MacDonald torque. In Section 3.3.2 we make a diagram in the  $(e, \Lambda)$ -plane for different orders of magnitude of  $\bar{\delta}$  using the linear MacDonald torque. See Figure 1.9. Furthermore, we compute  $\bar{\delta}$  for a few systems, including the Earth-Moon system, shown in Table 1.1. Particularly, our estimates about asymptotic stability in the dissipative problem are consistent with the data from the Moon-Earth system.

---

<sup>8</sup>For example, recall that, according to [34], Mercury was captured in a higher spin-orbit resonance (3:2) because it had achieved large eccentricities in its evolution. Its current value is  $e = 0.2056$ .

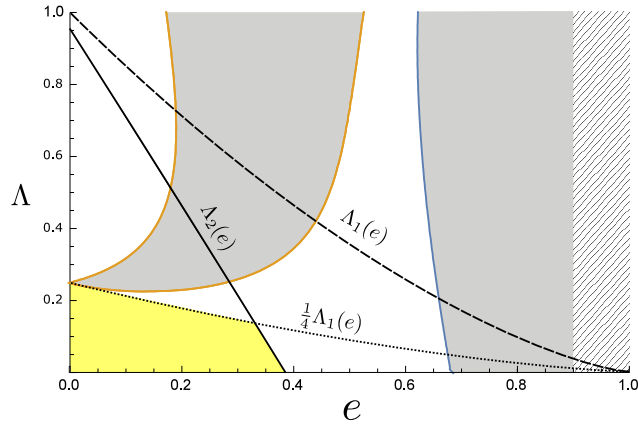


Figure 1.8: (Figure 3.2) Linear stability of  $\Theta^*(t; e, \Lambda)$ . The gray regions are linearly unstable and are computed numerically. Compare with Figure 1.7. The lines pattern indicates that for high eccentricity  $e \geq 0.9$  we did not compute the linear stability due to the proximity to the singularity. The yellow region is the region of linear stability with our theoretical results.

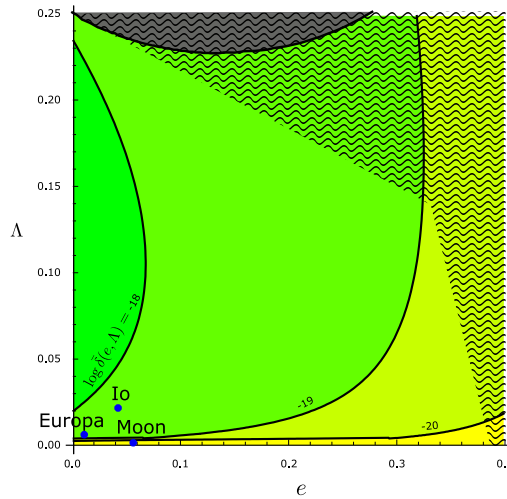


Figure 1.9: (Figure 3.5) Dissipative diagram for the linear MacDonald torque. The greener regions correspond to greater admissible  $\delta$ . We do not guarantee the existence of  $\Theta_\delta^*(t; e, \Lambda)$  for the region filled with the wavy pattern.

Satellite (Planet)	$e$	$\Lambda$	$\bar{\delta}$	$\Delta t(\bar{\delta})$
Moon (Earth)	0.0549	0.00069	$2.06 \cdot 10^{-20}$	11 min
Io (Jupiter)	0.0041	0.021	$9.69 \cdot 10^{-19}$	0.00057 min
Europa (Jupiter)	0.0094	0.0055	$2.85 \cdot 10^{-19}$	0.0064 min

Table 1.1: (Table 3.1) Estimates for some satellite-planet systems with strong spin-orbit interaction. The parameters  $e$  and  $\Lambda$  have been taken from [16] and other constants from [1]. The corresponding  $\bar{\delta}$  have been obtained numerically. The dependence of  $\Delta t$  with respect to  $\delta$  only depends on the parameters of the system.

Finally, Section 3.2 is devoted to prove that  $\Theta^*(t; e, \Lambda)$  is linearly unstable for high eccentricities, no matter how small  $\Lambda$  is considered. The variational equation at  $\Theta^*(t; e, \Lambda)$  is

$$\ddot{y} + \left( \frac{\Lambda}{r(t, e)^3} \cos[\Theta^*(t; e, \Lambda)] \right) y = 0. \quad (1.17)$$

In Theorem 3.1, we characterize the bifurcation of the instability region for large eccentricities shown in Figure 1.8. Here we define the curve  $e = E(\Lambda)$  of separation between stability and instability. It arises from the  $e$ -axis at some point  $e = e_* \approx 0.682$ . The result reads as follows.

**Theorem** (Theorem 3.1). *For some  $\varepsilon > 0$ , there exists a function  $E : [0, \varepsilon) \rightarrow (0, 1)$ ,  $\Lambda \mapsto E(\Lambda)$ , such that the equation (1.17) is unstable and has a non-trivial  $4\pi$ -periodic solution if  $e = E(\Lambda)$ . Moreover,  $E(0) = e_* \in (0, 1)$  and for each  $\bar{e} \in (e_*, 1)$  there exists a  $\bar{\Lambda} = \bar{\Lambda}(\bar{e}) \in (0, \varepsilon)$ , such that the equation (1.17) is unstable for the points  $(e, \Lambda)$  satisfying  $E(\Lambda) < e < \bar{e}$ ,  $0 < \Lambda < \bar{\Lambda}$ . In addition, the function  $E$  can be expressed as  $E(\Lambda) = \xi(\Lambda^{1/p})$ , where  $\xi(\zeta)$  is real analytic at  $\zeta = 0$  and  $p \geq 1$  is an integer.*

## Methodology

Recall from the objectives that we want to study the problem (1.15) in its full non-autonomous form and without any assumption of small eccentricities. This means that in our research we will not use the perturbative and averaging methods on Hamiltonian systems that are usual in the literature.

The results of Section 3.1 are proved as follows. The odd  $2\pi$ -periodic solution  $\Theta^*$  of the conservative problem (1.16) is also a solution of the Dirichlet problem (3.1) due to the symmetries of the original equation. Using the shooting method, we find out that, if the only solution of the linearization of



(3.1) is the trivial solution, then  $\Theta^*$  is the unique solution of (3.1). This is done using Lemma 3.1, that involves  $L^p$ -estimates on the linear coefficient. These estimates allow us to define the function  $\Lambda_1$  and the region of uniqueness given in Proposition 3.1. The estimates involve the optimal Sobolev inequalities (3.5). The analytic properties of the solution are proved by means of the implicit function theorem, in its real analytic version (Theorem 2.3.5 in [67]).

The linear stability of  $\Theta^*$  is given by a criterion for the stability of the first variation at  $\Theta^*$  (3.16). It is an example of Hill's equation. This criterion (3.17) is a generalization, using  $L^p$ -norms, of the Lyapunov criterion for stability of a Hill's equation. The inequalities of the criterion are considered separately. In one hand, we need  $L^p$ -estimates on the linear coefficient, as in the previous paragraph (Lemma 3.1). On the other hand, we can use a Green's function of a related problem to find upper and lower solutions for  $\Theta^*$ . This leads us to the definition of the function  $\Lambda_2$  appearing in Proposition 3.2.

Before making the continuation of  $\Theta^*$  to the dissipative regime, we prove in Section 3.2 that the solution is unstable for large eccentricities in Theorem 3.1. In this part we employ some techniques from complex analysis. Using some properties of (even) Hill's equations and the analyticity of the solution, we are able to characterize the bifurcation point  $e = e_*$  as a point where the integral  $I(e)$ , in (3.23), vanishes. This integral is analytic in  $e$  and we can prove that  $e = e_*$  exists by Bolzano's Theorem. To do this we compute  $I(e)$  in series expansion and prove that  $\lim_{e \rightarrow 1^-} I(e)$  is negative and finite (Lemma 3.3). We compute  $I(e)$  with the Residue Theorem and prove the uniform convergence of the limit. The additional properties that characterize the bifurcation curve  $e = E(\Lambda)$  are proved with Lemma 3.4. This lemma is a parametric version of Bolzano's Theorem that defines a curve in which a function of two variables vanishes and has a weaker transversality condition. To compensate, the lemma requires the function to be analytic in both variables, so we can prove it by means of the Weierstrass Preparation Theorem and the Decomposition Theorem (Theorems 6.3.1 and 4.2.7 in [67]).

In Section 3.3 we prove Theorem 3.2. Its proof is given by two lemmas. Lemma 3.5 allows the quantitative continuation of the solution and Lemma 3.7 guarantees that the continuation is asymptotically stable. We see the periodic solution as a fixed point of the Poincaré map, so, Lemma 3.5 is formulated as a quantitative version of the Implicit Function Theorem. The proof of Lemma 3.5 is given by the Contraction Mapping Theorem and a generalized version of the Mean-Value Theorem, [3]. Lemma 3.5 provides a formula for  $\bar{\delta}$  that is given in terms of bounds for the norms of derivatives of the Poincaré map. To assure such boundedness in our problem, it is nec-

essary a rather technical procedure based on an a priori bound in Lemma 3.6 and an auxiliary function given in (3.40). On the other hand, Lemma 3.7 is based on the concept of strong stability, in the sense of Krein, for a Hill's equation (if it is stable and also any small perturbation of it). Here we take advantage of the fact that a general perturbation of a Hill's equation can be converted into a Hill's equation by a change of variable. Strong stability guarantees that the perturbed equation is asymptotically stable by undoing the change of variable.

At the end of the section we apply our results concerning the dissipative problem. To compute  $\bar{\delta}$  we need to integrate numerically the conservative problem and its first variation. For simplicity, the numerical integrations are performed taking as independent variable the eccentric anomaly  $u$ . With this information we are able to produce the plot in Figure 1.9. We particularize our results to some real systems: Earth-Moon, Jupiter-Io and Jupiter-Europa. In the case of the Moon we have measurements of the velocity of propagation of seismic waves. This provides an estimate of the dissipative delay  $\Delta t$  of the model that is consistent with our results. We do not have the same information for Io and Europa, but our results are less realistic for those cases.

### Discussion and perspectives

In this research we have obtained some rigorous results concerning the existence and stability of the 1:1 resonant solution for the spin orbit problem, which is closely related to the capture into the resonance. The dissipative as well as the conservative version of the problem have attracted much attention. We have considered equation (1.13) as the reference model for the problem. Despite the rough simplification introduced by the linear MacDonald torque in the model, it seems reasonable to take the dissipative torque  $\mathcal{T}_d$  proportional to  $\dot{\theta} - \dot{f}$ . This inevitably leads us to the intricate pendulum-like equation (1.15). This starting point, though suggested in many articles, was never fully exploited, as far as we know. That is why we wanted to study this equation with an analytical point of view and without further modifications. This is in contrast with the literature, where either the numerical approach prevails, or the equation is modified. This modification can be produced by an average over a period or by an expansion in powers of the eccentricity  $e$ , in order to focus the study on small  $e$ . The pioneer works of Goldreich and Pale [51] and Beletskii [10] set the main research directions. The articles following [10] work in the conservative regime with  $f$  as independent variable, obtaining the so-called Beletskii equation.

In the literature we find different approaches to the stability of the solu-

tion. For instance, [51] poses the rough stability condition that the averaged dissipative torque does not exceed the maximum conservative torque. There are also more sophisticated approaches by A. Celletti and her collaborators, like the KAM stability in [21] for the conservative case, or the existence of quasiperiodic attractors in [25] for the dissipative problem, bifurcating from the KAM tori of the conservative case. See also other related articles like [24] and [50]. The articles that employ the Beletskii equation, such as [10], [89] and [88], do not average the equation. Indeed they study the  $2\pi$ -periodic solutions (there is not uniqueness) and consider the linear stability, particularly for the even solution  $\Theta^*(t)$ . They produce numerical stability diagrams similar to Figure 3.2, and notice, see for example [10], the complexity of the region of linear stability of  $\Theta^*(t)$  for high eccentricities.

The most similar approach to ours is that of [101], which studies the Beletskii equation with analytical tools. Its main result (Theorem 5) estimates a region of existence and Lyapunov stability of  $\Theta^*(t)$ . The authors use the method of upper and lower solutions to prove the existence of solution, but they do not guarantee the uniqueness as odd  $2\pi$ -periodic solution as we did in Proposition 3.1. Since we consider the dissipative model, we are interested in the asymptotic stability of the solution instead of the Lyapunov stability. For this purpose we need a region of strong linear stability, which is larger than the region obtained in Theorem 5, [101]. Using their computations, which correspond to  $L^\infty$ -norm estimates (recall that we used all the  $L^\alpha$ -norms to estimate our region), the resulting region of linear stability is given by

$$0 < \Lambda < \frac{(1-e)^3}{4}, \quad 0 < \Lambda < \frac{1}{\pi} \left( \frac{(1-e^2)^{3/2}}{2} - 8e \right).$$

We can check that this region is in fact included in our  $\Omega$ .

This research has several direct continuations. In one hand, the same study can be done to study the stability of higher spin-orbit resonances, such as the 3:2. In higher resonances the role of large eccentricities is even more important, as shown in [34] for the case of Mercury. Actually, if  $e = 0$ , the only possible asymptotically stable resonance is the 1:1, as we know for the equilibrium of the free damped pendulum, [86]. In this framework, we would have to look for asymptotically stable subharmonic solutions ( $2\pi n$ -periodic) of the pendulum equation (1.15). Another direction to explore is, as commented in Remark 3.3, the use of the results by Borg [77] (or similar) to look for other stability regions of higher order ( $\Lambda > 0.25$ ) for the synchronous resonance  $\Theta^*$ . Or, in addition, for the other odd solutions that appear for large  $\Lambda$ , as shown in Figure 1.7: do these solutions become asymptotically stable in the dissipative setting? On the other hand, we can try to apply

our techniques to a more general dissipative torque, so the model covers more realistic situations. See for example the models by S. Ferraz-Mello and collaborators using the Newtonian creep model, [46, 48]. Also, note that our results hold for the planar problem, we would like to know if the asymptotic stability of the solution holds for the three dimensional model. If this is the case, do we have to make important assumptions? Finally, as we will see, the next model and the applied techniques are based on the present work.

### 1.3.3 The spin-spin model and its double synchronous resonance

#### Model

We will call spin-spin model to a planar version of the Full Two-Body Problem. This is a natural extension of the well known spin-orbit problem for two extended bodies. As far as we know, it was first considered in [60] and we think it is of great value for future research.

The Full Two-Body Problem (F2BP) deals with the dynamics of two extended bodies interacting gravitationally. It has been extensively investigated, especially in the last two decades, due to an increasing interest on binary systems. Due to its complexity, most of the studies are numerical explorations of particular cases, [45]. There are some works with a more analytical approach dealing with relative equilibria and stability, [113] and [76]. The spin-spin model is motivated mainly by [12], [114], [36] and [7]. In one hand, [12] is focused on the evolution of the orbit and the spin axes of the bodies in the secular F2BP (averaging over fast angles). This paper points out that the mutual influence in the spin dynamics is contained in the terms of order  $1/r^5$  of the expansion of the potential energy of the system, where  $r$  is the distance between the bodies. On the other hand, [114] studies the relative equilibria and stability in the planar case, i.e., the spin axes of the bodies are perpendicular to the orbital plane, that is also a common equatorial plane. [36] studies the observability of non-planar stable oscillations around the double synchronous equilibrium in binary asteroids. In [114] and [36], only terms up to  $1/r^3$  of the potential energy are considered, so the resulting system is equivalent to two uncoupled spin-orbit problems. The planar spin-spin coupling was first studied in [7], making an analogous study as the classical paper [51] on the spin-orbit coupling. Particularly, [7] studies the spin of the body 1, identified with two point masses slightly separated from each other (dumbbell model), that moves in a circular orbit around the body 2, an ellipsoid with uniform rotation. They focus on the case when the orbital motion is slow and the angular velocity of the body 1 becomes commensurable with the angular velocity of the body 2 (spin-spin resonance).

The spin-spin model deals with the complete coupled dynamics of the F2BP in the planar and ellipsoidal case. As usual in the spin-orbit problem, we also assume that the orbital motion is Keplerian. This reduces the high dimensional phase space of the F2BP to a problem of two degrees of freedom (spins) plus time-dependence (orbit). For a small non-zero orbital eccentricity, it has the structure of a nearly integrable system of coupled pendula that

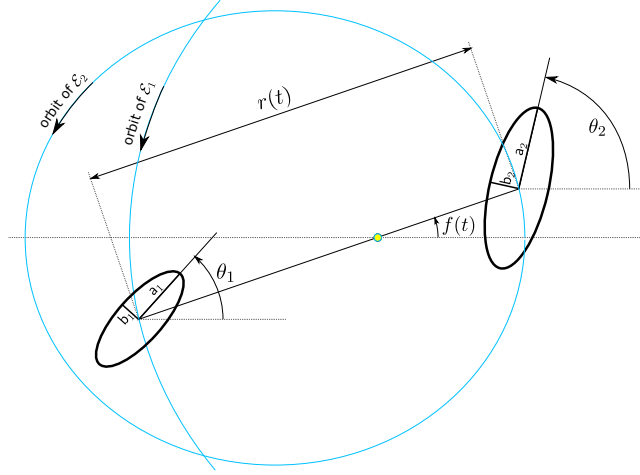


Figure 1.10: The planar spin-spin problem.

is periodically forced. This setting is suited to study the phenomena related to spin-orbit and spin-spin resonances. Furthermore, the intrinsic dissipative nature of the capture into resonances supports the relevance of this model. The reason is that the most used family of dissipative torques, the MacDonald torques in (1.14), is of order  $1/r^6$ , whereas the spin-spin coupling appears at order  $1/r^5$ . In addition to the questions related to the spin-orbit problem, this model of coupled oscillators opens new questions that were not possible to consider before. In [60] there is a first study of this kind. It deals with the stability of relative equilibria and the chaotic behavior associated to the spin-spin-orbit resonances (simultaneous spin-orbit and spin-spin resonances) of the problem due to the Chirikov diffusion.

Consider two homogeneous ellipsoids  $\mathcal{E}_1$  and  $\mathcal{E}_2$  with respective masses  $M_j$ ,  $j = 1, 2$ , principal moments of inertia  $\mathcal{A}_j < \mathcal{B}_j < \mathcal{C}_j$  and corresponding principal semi-axes  $a_j > b_j > c_j$ . Assume that the orbital motion of the ellipsoids is the same as for two point masses, say, the centers of the ellipsoids describe coplanar Keplerian orbits of eccentricity  $e \in [0, 1)$  with a common focus at the center of mass of the system. Moreover, assume that the spin axis of each body is the principal axis associated to  $c_j$  and is perpendicular to the orbital plane.

Now proceed as for the spin-orbit problem. We identify the orbital plane with the complex plane  $\mathbb{C}$ . Consider the center of mass of the system fixed at the origin and let the center of each ellipsoid be  $\mathbf{r}_j$ , then,  $M_1\mathbf{r}_1 + M_2\mathbf{r}_2 = 0$ . If we define the relative position vector  $\mathbf{r} = \mathbf{r}_2 - \mathbf{r}_1$  and choose the units of mass such that  $M_1 + M_2 = 1$ , then,  $\mathbf{r}_1 = -M_2\mathbf{r}$  and  $\mathbf{r}_2 = M_1\mathbf{r}$ . The orbital motion is defined by  $\mathbf{r}$ , which can be written as  $\mathbf{r} = r \exp(if) \in \mathbb{C}$ ,

where  $r > 0$  and  $f$  vary periodically with time. Here the vector  $\mathbf{r}$  describes an ellipse of eccentricity  $e \in [0, 1)$  and semi-major axis  $a$  with focus at the origin. Then, the functions  $f(t)$  and  $r(t)$  are known by the Kepler problem given by eqs. (1.10) to (1.12).

Let us take convenient units of time so that the period is  $2\pi$ . Here we do not take  $a = 1$  as for the spin-orbit problem because we will see that the size of the orbit is now an important factor. Recall Kepler's third law for the Two-Body Problem

$$G(M_1 + M_2) \left( \frac{T}{2\pi} \right)^2 = a^3, \quad (1.18)$$

where  $G$  is the Gravitational constant and  $T$  is the orbital period. In consequence,  $G = a^3$  in our units. For our model to be completely non-dimensional and adequate to the scale of the system, we take convenient units of length such that  $\mathcal{C}_1 + \mathcal{C}_2 = 1$ . In these units the semimajor axes  $\mathbf{a}_j$  of the ellipsoids are of order 1, whereas  $a$  should be much larger.

If  $t$ ,  $M$  and  $l$  stand for time, mass and length respectively, the relation between our system of units and any other one is the following

$$t_{\text{ours}} = \frac{2\pi}{T}t, \quad M_{\text{ours}} = \frac{M}{M_1 + M_2}, \quad l_{\text{ours}} = l \sqrt{\frac{M_1 + M_2}{\mathcal{C}_1 + \mathcal{C}_2}}.$$

It is worth mentioning that, if  $I$  is any magnitude with units of moment of inertia, then the conversion is given simply by

$$I_{\text{ours}} = \frac{I}{\mathcal{C}_1 + \mathcal{C}_2}.$$

The value of the gravitational constant  $G$  in any system of units must respect Kepler's third law (1.18).

Let  $\theta_j$  be the polar angle of the principal direction associated to  $\mathbf{a}_j$  with respect to the orbit's major axis. See Figure 1.10. The spin dynamics of the ellipsoids is modelled by the following coupled system of ordinary differential equations

$$\mathcal{C}_j \ddot{\theta}_j = \mathcal{T}_j^{\text{C}}(t, \theta_1, \theta_2) + \mathcal{T}_j^{\text{D}}(t, \dot{\theta}_j), \quad j = 1, 2, \quad (1.19)$$

where  $\mathcal{T}_j^{\text{C}}$  and  $\mathcal{T}_j^{\text{D}}$  are respectively the *conservative* and *dissipative* torques acting on  $\mathcal{E}_j$ .

The *conservative* torque is derived from a potential energy, see Section 4.1,

and it takes the form

$$\begin{aligned} \mathcal{T}_j^C(t, \theta_1, \theta_2) = & - \left( \frac{a}{r(t)} \right)^3 \frac{\Lambda_j}{2} \sin(2\theta_j - 2f(t)) \\ & - \left( \frac{a}{r(t)} \right)^5 \sum_{(m_1, m_2) \in \Xi} \frac{m_j \Lambda_{m_2}^{m_1}}{2} \sin(2m_1(\theta_1 - f(t)) + 2m_2(\theta_2 - f(t))), \end{aligned} \quad (1.20)$$

where

$$\Xi = \{(m_1, m_2) \in \mathbb{Z}^2 : |m_1| + |m_2| \leq 2\}.$$

The parameters  $\Lambda_j$  and  $\Lambda_{m_2}^{m_1}$  are positive small quantities depending on the physical parameters of the bodies and on  $a$ . These parameters satisfy  $\Lambda_{m_2}^{m_1} = \Lambda_{-m_2}^{-m_1} < \Lambda_j < 3\mathcal{C}_j$ . Note that if all the constants  $\Lambda_{m_2}^{m_1}$  in (1.20) vanish, the system (1.19) is formed by two uncoupled spin-orbit problems in  $\theta_1$  and  $\theta_2$ . The coupling of the system is contained in the terms  $(m_1, m_2)$  of type  $(\pm 1, \pm 1)$  and  $(\pm 1, \mp 1)$ , whereas the rest of them are high order spin-orbit terms.

On the other hand, for the *dissipative* torques we take the form (1.14), that in our case is given by

$$\mathcal{T}_j^D(t, \dot{\theta}_j) = -C_{M,j} \left( \frac{a}{r(t)} \right)^6 \sin(2\Delta t_j(\dot{\theta}_j - \dot{f}(t))) \approx -\delta_j \mathcal{C}_j \left( \frac{a}{r(t)} \right)^6 (\dot{\theta}_j - \dot{f}(t)),$$

where  $1 \gg \delta_j \mathcal{C}_j = 2C_{M,j} \Delta t_j \geq 0$ , and  $C_{M,j}$  are constants depending on the parameters of the bodies. Note that between the definitions of  $\mathcal{T}_j^D$  and  $\mathcal{T}_d$  there is a factor  $\mathcal{C}$  different. It is worth mentioning that there is no physical reason for both lags  $\Delta t_j$  (or both  $\delta_j$ ) to match.

Note that if  $\mathcal{T}_j^D = 0$ , the system (1.19) has a Hamiltonian structure. The corresponding Hamiltonian has two degrees of freedom and time dependence and it is given by

$$H(\theta_1, \theta_2, p_{\theta_1}, p_{\theta_2}, t) = \frac{p_{\theta_1}^2}{2\mathcal{C}_1} + \frac{p_{\theta_2}^2}{2\mathcal{C}_2} + \mathcal{V}(t, \theta_1, \theta_2), \quad (1.21)$$

where

$$\begin{aligned} \mathcal{V}(t, \theta_1, \theta_2) = & -\frac{1}{4} \left( \frac{a}{r(t)} \right)^3 \sum_{j=1}^2 \Lambda_j \cos(2\theta_j - 2f(t)) \\ & - \frac{1}{4} \left( \frac{a}{r(t)} \right)^5 \sum_{(m_1, m_2) \in \Xi} \Lambda_{m_2}^{m_1} \cos(2m_1(\theta_1 - f(t)) + 2m_2(\theta_2 - f(t))). \end{aligned}$$



Due to the explicit time dependence of the Hamiltonian, the energy of the system is not constant even though  $\mathcal{T}_j^D \equiv 0$ . However, if  $\mathcal{T}_j^D \equiv 0$ , the system (1.19) will be called *conservative*, because no dissipative forces are involved in the physical derivation of the model. On the other hand, if  $\mathcal{T}_j^D$  is not identically zero for all time, then we will call it *dissipative*. In the following, particularly in Chapter 4, we will use the terms *conservative* and *dissipative* in italic font to remark this point. In Section 4.1 we will see also a purely conservative version of the model involving  $(r, f, \theta_1, \theta_2)$  as unknown functions of time, eqs. (4.14) and (4.15).

There are solutions of (1.19) that are especially relevant. Since the spin-orbit problem is a particular case of (1.19), a solution satisfying  $\theta_1(t + 2\pi n_o) = \theta_1(t) + 2\pi n_s$ , with  $n_s, n_o \in \mathbb{Z}$ , is called  $n_s : n_o$  spin-orbit resonance of the ellipsoid  $\mathcal{E}_1$ . The same holds for  $\mathcal{E}_2$ . Spin-spin resonances arise when the spin rates of the two ellipsoids become commensurable. In [7] these resonances were studied independently from the orbital rate. There are some solutions in which the ellipsoids are simultaneously in a spin-orbit and a spin-spin resonance (studied in [60]). The simplest of these resonances is the double synchronous resonance of equation (1.19), that is, solutions satisfying  $\theta_j(t + 2\pi) = \theta_j(t) + 2\pi$ , for both  $j = 1, 2$ . In other words, the spin of both ellipsoids synchronize with the orbital motion at the same time.

In this thesis we will deal with the capture into the double synchronous resonance of equation (1.19). In the same way as for the spin-orbit problem in the previous section, let us take the change of variable  $\Theta_j = 2(\theta_j - f)$ , such that the system (1.19) turns into

$$\begin{aligned} \mathcal{C}_j \ddot{\Theta}_j + \delta_j \mathcal{C}_j \left( \frac{a}{r(t)} \right)^6 \dot{\Theta}_j + \left( \frac{a}{r(t)} \right)^3 \Lambda_j \sin \Theta_j \\ + \left( \frac{a}{r(t)} \right)^5 \sum_{(m_1, m_2) \in \Xi} m_j \Lambda_{m_2}^{m_1} \sin(m_1 \Theta_1 + m_2 \Theta_2) = -2\mathcal{C}_j \ddot{f}(t). \end{aligned} \quad (1.22)$$

The system (1.22) models a couple of damped and forced pendula of variable length. Since  $f(t + 2\pi) = f(t) + 2\pi$ , then, double synchronous resonances correspond to solutions of (1.22) satisfying  $\Theta_j(t + 2\pi) = \Theta_j(t)$  for both  $j = 1, 2$ .

Similarly to the spin-orbit problem, we will consider also the *conservative* version of (1.22), say,

$$\begin{aligned} \mathcal{C}_j \ddot{\Theta}_j + \left( \frac{a}{r(t)} \right)^3 \Lambda_j \sin \Theta_j \\ + \left( \frac{a}{r(t)} \right)^5 \sum_{(m_1, m_2) \in \Xi} m_j \Lambda_{m_2}^{m_1} \sin(m_1 \Theta_1 + m_2 \Theta_2) = -2\mathcal{C}_j \ddot{f}(t). \end{aligned} \quad (1.23)$$

In Section 4.1 we will make the derivation of the conservative model from the Lagrangian of the physical system and obtain the expression of  $\Lambda_j$  and  $\Lambda_{m_2}^{m_1}$  in terms of physical parameters.

### Objectives

We have two objectives in Chapter 4. On one hand, we want to make a thorough derivation of the model presented in Section 1.3.3. On the other hand, we want to characterize the capture into the double synchronous resonance of (1.19) in a similar way as we do for the spin-orbit problem in the second part of the thesis (Chapter 3). That is, by using the full non-autonomous equation (1.22) and avoiding a requirement of small eccentricity. Again, the double synchronous resonance is the most important full resonance of the problem and we know several examples in the solar system. We summarize our specific goals as follows.

1. First, we want to derive the Euler-Lagrange equations of motion of the conservative system. This will involve the computation of the potential energy of the F2BP up to order  $1/r^5$ . Although this was done in other works [12, 76, 13], we want to do it independently in order to find the expansion of the potential of the planar problem at any order.
2. We would like to find a parametric description of the problem such that we can study different systems and make an effective comparison between them. Accordingly, we want to find the number of independent parameters of the problem. Can we associate a physical meaning to them? Are realistic all the values of the parameters? These questions will be related to the assumption that the orbits to be Keplerian. We want to clarify this point.
3. We will study the *conservative* problem. We want to explore the solutions with odd symmetry, because, at least for the uncoupled problem, it is equivalent to two spin-orbit problems. Can we find a region of uniqueness and linear stability for that solution? What techniques are

necessary now that we have one more degree of freedom? Are the estimated regions (much) smaller compared to those of the spin-orbit problem? About the corresponding regions found with numerical methods: How do they change when we increase the coupling?

4. After the region of linear stability is found, we want to make a continuation of the odd solution to the *dissipative* setting. We would like to be able to prove that this continuation is asymptotically stable. In this process, do we have to include additional requirements with respect to the spin-orbit problem? Can we do a quantitative continuation?
5. Then, we want to apply our results. In one hand, we can use real binaries in the solar system and see if our results are compatible. On the other hand, we can study some families of representative systems. For example, the case of identical bodies or the case in which one body is twice larger than the other one. Here the following question arises: can we reduce the number of parameters of the problem to facilitate the comparison between systems?

## Results

The results of the third part of the thesis are given in Chapter 4.

In Section 4.1, we derive the equations of motion of the full planar system

$$\begin{aligned} \mathcal{C}_1 \ddot{\theta}_1 &= -\partial_{\theta_1} V, & \mathcal{C}_2 \ddot{\theta}_2 &= -\partial_{\theta_2} V, \\ \mu \ddot{r} &= \mu r \dot{f}^2 - \partial_r V, & \ddot{f} &= -\frac{1}{\mu r^2} \partial_f V - 2 \frac{\dot{r} \dot{f}}{r}. \end{aligned}$$

They depend on the potential energy. Its full expansion is found to be

$$\begin{aligned} V = & -\frac{GM_1 M_2}{r} \sum_{\substack{(l_1, m_1) \in \Upsilon \\ (l_2, m_2) \in \Upsilon}} \Gamma_{l_2, m_2}^{l_1, m_1} \left(\frac{R_1}{r}\right)^{2l_1} \left(\frac{R_2}{r}\right)^{2l_2} \times \\ & \times \mathcal{Z}_{2l_1, 2m_1}^1 \mathcal{Z}_{2l_2, 2m_2}^2 \cos(2m_1(\theta_1 - f) + 2m_2(\theta_2 - f)), \end{aligned}$$

where  $\Upsilon = \{(l, m) \in \mathbb{Z}^2 : 0 \leq |m| \leq l\}$ , the constants  $\Gamma_{l_2, m_2}^{l_1, m_1}$  are defined in (4.13),  $R_j$  is the mean radius of  $\mathcal{E}_j$ , and  $\mathcal{Z}_{2l_j, 2m_j}^j$  are the Stokes coefficients of  $\mathcal{E}_j$  computed with respect to its fixed body frame, they are defined in (4.9). The first terms of the expansion are

$$\begin{aligned}
V_0 &= -\frac{GM_1M_2}{r}. \\
V_2 &= -\frac{GM_2}{4r^3} (q_1 + 3d_1 \cos(2(\theta_1 - f))) - \frac{GM_1}{4r^3} (q_2 + 3d_2 \cos(2(\theta_2 - f))), \\
V_4 &= -\frac{3G}{4^3r^5} \{12q_1q_2 + \frac{15}{7}[\frac{M_2}{M_1}d_1^2 + 2\frac{M_2}{M_1}q_1^2 + \frac{M_1}{M_2}d_2^2 + 2\frac{M_1}{M_2}q_2^2] \\
&\quad + d_1M_2 \left\{ [20\frac{q_2}{M_2} + \frac{100}{7}\frac{q_1}{M_1}] \cos(2(\theta_1 - f)) + 25\frac{d_1}{M_1} \cos(4(\theta_1 - f)) \right\} \\
&\quad + d_2M_1 \left\{ [20\frac{q_1}{M_1} + \frac{100}{7}\frac{q_2}{M_2}] \cos(2(\theta_2 - f)) + 25\frac{d_2}{M_2} \cos(4(\theta_2 - f)) \right\} \\
&\quad + 6d_1d_2 \cos(2(\theta_1 - \theta_2)) + 70d_1d_2 \cos(2(\theta_1 + \theta_2) - 4f)\},
\end{aligned}$$

where  $d_j = \mathcal{B}_j - \mathcal{A}_j$ ,  $q_j = 2\mathcal{C}_j - \mathcal{B}_j - \mathcal{A}_j$ .  $V_0$  contains the dynamics of two point masses,  $V_2$  the uncoupled spin-orbit dynamics and  $V_4$  the spin-spin coupled dynamics between  $\theta_1$  and  $\theta_2$ . The coupling terms appear in the last line of  $V_4$ . The assumption of Keplerian orbital motion leads us to the equations of motion for  $j = 1, 2$ ,

$$\begin{aligned}
0 &= \ddot{\theta}_j + \frac{\lambda_j}{2} \left\{ \left( \frac{a}{r(t)} \right)^3 \sin(2\theta_j - 2f(t)) + \right. \\
&\quad + \left( \frac{a}{r(t)} \right)^5 \left[ \frac{5}{4} \left( \hat{q}_{3-j} + \frac{5}{7}\hat{q}_j \right) \sin(2\theta_j - 2f(t)) + \frac{25\hat{d}_j}{8} \sin(4\theta_j - 4f(t)) + \right. \\
&\quad \left. \left. + \frac{3\hat{d}_{3-j}}{8} \sin(2\theta_j - 2\theta_{3-j}) + \frac{35\hat{d}_{3-j}}{8} \sin(2\theta_{3-j} + 2\theta_j - 4f(t)) \right] \right\},
\end{aligned}$$

where the parameters of the problem are defined as

$$\lambda_j = 3\frac{d_j}{\mathcal{C}_j} \frac{\mu}{M_j}, \quad \hat{d}_j = \frac{d_j}{M_j a^2}, \quad \hat{q}_j = \frac{q_j}{M_j a^2}.$$

The parameters have the following physical meaning:  $\lambda_j$  measures equatorial oblateness of  $\mathcal{E}_j$ ,  $\hat{d}_j$  measures the equatorial oblateness of  $\mathcal{E}_j$  with respect to the size of the orbit and  $\hat{q}_j$  measures the flattening of  $\mathcal{E}_j$  with respect to the size of the orbit. Not all the parameters are free, there are only six independent ones ( $e; \mathcal{C}_1, \lambda_1, \lambda_2, \hat{d}_1, \hat{q}_1$ ). Moreover, we see that spin of the ellipsoid  $\mathcal{E}_2$  is affected by the spin-spin coupling with a strength essentially given by  $\hat{d}_1$ , and vice versa. The equations can be written in terms of the *conservative* torque in the compact form (1.20). The parameters of both forms are related by the expressions in eqs. (4.23) to (4.26).

In Section 4.2 we prove our theoretical results on the double synchronous resonance of the *conservative* problem (1.23). The next theorems define (in the space of parameters) regions of uniqueness and linear stability of the

odd  $2\pi$ -periodic solution that is the continuation of the equilibrium of the equation for  $e = 0$ .

**Theorem** (Theorem 4.1). *Assume that  $e \in [0, 1)$  and the parameters of the problem satisfy*

$$1 > \frac{1}{(1-e)^3} \max \left\{ \frac{\Lambda_1}{\mathcal{C}_1}(1 + \alpha_1), \frac{\Lambda_2}{\mathcal{C}_2}(1 + \alpha_2) \right\},$$

where

$$\alpha_j \frac{\Lambda_j}{\mathcal{C}_j} = \frac{1}{(1-e)^2} \sum_{(m_1, m_2) \in \Xi} \left( \frac{m_j^2}{\mathcal{C}_j} + \frac{|m_1 m_2|}{\sqrt{\mathcal{C}_1 \mathcal{C}_2}} \right) \Lambda_{m_2}^{m_1}.$$

Then, there exists a unique odd  $2\pi$ -periodic solution for (1.23), denoted by  $(\Theta_1^*(t), \Theta_2^*(t))$ .

**Theorem** (Theorem 4.2). *Assume that the parameters of the model satisfy the following conditions.*

$$\frac{1}{\pi^2} > \frac{1}{(1-e)^3} \left( \frac{\Lambda_1}{\mathcal{C}_1} + \frac{\Lambda_2}{\mathcal{C}_2} \right) + \frac{1}{(1-e)^5} \sum_{(m_1, m_2) \in \Xi} \left( \frac{m_1^2}{\mathcal{C}_1} + \frac{m_2^2}{\mathcal{C}_2} \right) \Lambda_{m_2}^{m_1},$$

$$\begin{aligned} \frac{1}{4\pi} > M := & \frac{1}{(1-e)^3} \max \left\{ \frac{\Lambda_1}{\mathcal{C}_1}, \frac{\Lambda_2}{\mathcal{C}_2} \right\} + \\ & + \frac{1}{(1-e)^5} \sum_{(m_1, m_2) \in \Xi} \max \left\{ \frac{|m_1|}{\mathcal{C}_1}, \frac{|m_2|}{\mathcal{C}_2} \right\} \Lambda_{m_2}^{m_1} + \frac{4e\sqrt{1-e^2}}{(1-e)^4}, \end{aligned}$$

$$\cos(2\pi^2 M) \min \left\{ \frac{\Lambda_1}{\mathcal{C}_1}, \frac{\Lambda_2}{\mathcal{C}_2} \right\} > \max \left\{ \alpha_1 \frac{\Lambda_1}{\mathcal{C}_1}, \alpha_2 \frac{\Lambda_2}{\mathcal{C}_2} \right\},$$

Then the solution  $(\Theta_1^*(t), \Theta_2^*(t))$  is strongly linearly stable.

The definition of strong linear stability in the sense of Krein is given in Definition 4.2. Strong linear stability can be used in Section 3.3 to make a continuation of the solution to the dissipative setting, as we did for the spin-orbit problem in Chapter 3. This is done in Theorem 4.3. Here we assume that the parameters of the problem satisfy the conditions of Theorem 4.2 and that  $|\delta_j|$  are small enough. In such case, there exists a solution  $\Psi^*(t, \delta_1, \delta_2)$  of (1.22) for  $\delta_j \geq 0$ , that is analytic in all the entries and such that  $\Psi^*(t, 0) = (\Theta_1^*(t), \Theta_2^*(t))$  for each  $t \in \mathbb{R}$ . Moreover, if  $|\Lambda_{m_2}^{m_1}|$  are small enough,  $\Psi^*(t, \delta_1, \delta_2)$  is asymptotically stable. Note that here we require that  $|\Lambda_{m_2}^{m_1}|$  and  $|\delta_j|$  are small enough, in contrast with the quantitative result in

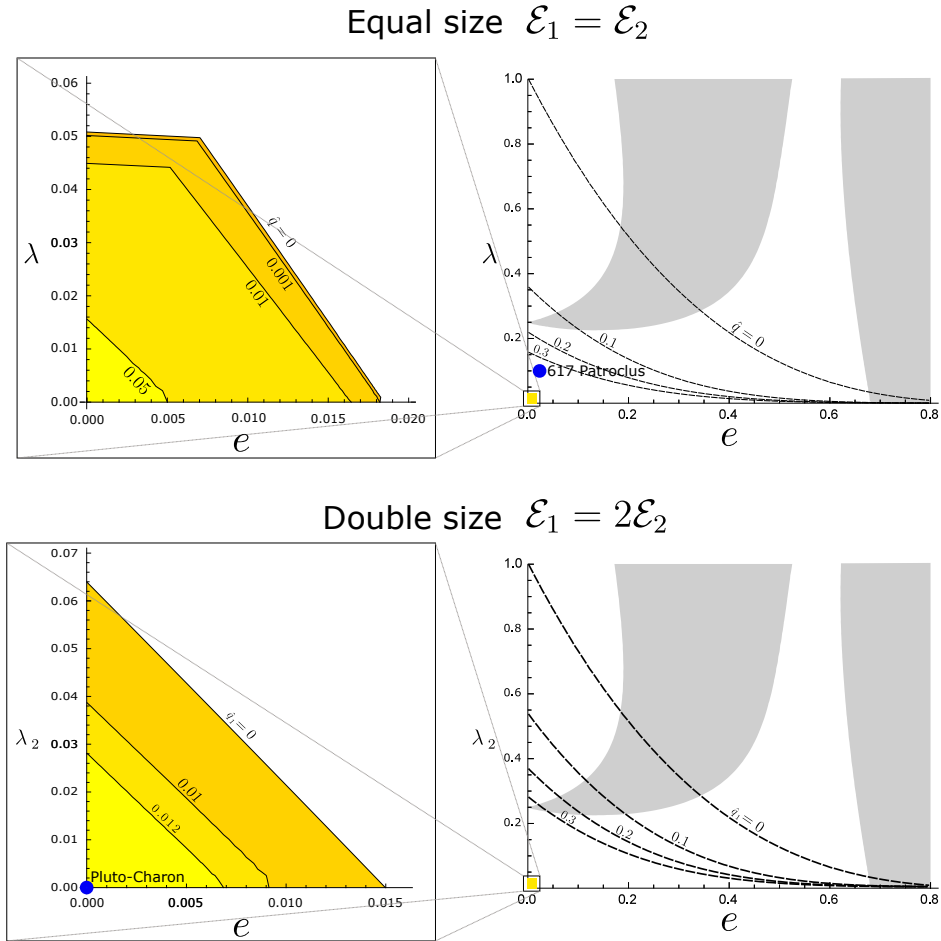


Figure 1.11: (Figure 4.2) Stability diagrams in the  $(e, \lambda)$ -plane of the synchronous resonance of the spin-spin model. Top: both bodies are equal. Bottom: one body is double the size of the other. The double synchronous resonance is unique under the dashed lines (right) and linearly stable under the black lines (left) for the indicated value of  $\hat{q}$ . In the left we see zoomed views of the stable regions. The more yellow is the region indicates that stability is guaranteed for larger values of  $\hat{q}$ . The gray regions in the right are unstable for the uncoupled system (spin-orbit), i.e., with  $\hat{q} = 0$ .

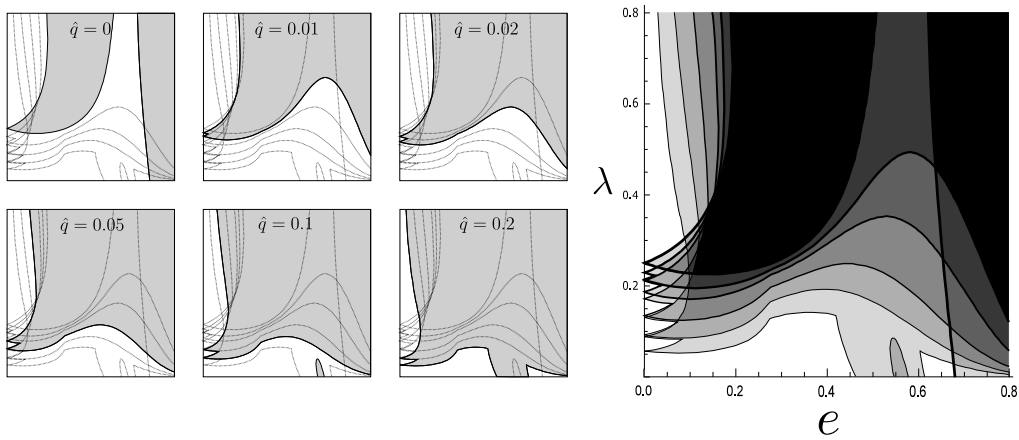


Figure 1.12: (Figure 4.4) Stability diagrams in the  $(e, \lambda)$ -plane in the case of equal bodies. The six plots in the left show the unstable region in gray for different values of  $\hat{q}$ . The image in the right shows the six diagrams superimposed. Darker tones of gray indicate more overlapping between unstable regions.

Theorem 3.2 for the spin-orbit problem. We discuss at the end of Section 3.3 the technical limitations that did not allow to make a quantitative result.

In Section 4.4 we explain how to apply our results to real cases and use the Pluto-Charon system and the binary asteroid 617 Patroclus as two representative examples. In the case of Pluto and Charon, all of our results are consistent, but the case of 617 Patroclus is only covered by our result on the uniqueness of the solution (Theorem 4.1). This study leads to a discussion of the extension of the theoretical regions obtained. In correspondence with our results (we provide only sufficient conditions for uniqueness and linear stability), we reduce the coupling of the system to a single parameter ( $\hat{q}_1$ ). This allows us to produce the diagrams in Figure 1.11 to two cases: In one hand, the case of identical bodies, that we compare with the asteroid 617 Patroclus. On the other hand, the case when  $\mathcal{E}_1$  is twice the size of  $\mathcal{E}_2$ , that we compare with the Pluto-Charon system. We discuss the technical reasons that make the shown regions much smaller than those of the spin-orbit model (Figure 1.8).

Finally, we describe in detail the change of the regions of linear stability (computed numerically) when we increase the coupling. The plots are shown in Figure 1.12. This is done for the case of identical bodies. We conclude giving an upper estimate for  $\hat{q} \approx 10^{-2}$ , under which the orbits are close to be Keplerian, and we can use the model as stated.

## Methodology

We derive the equations of motion of the model in Section 4.1. We start by computing the expansion of the potential energy of the Full Two Body Problem in terms of the Stokes coefficients of the two bodies, (4.6). To achieve this we use the translation formula of the (solid) spherical harmonics in (4.3). The Stokes coefficients with respect to the inertial frame are related to the ones computed in each fixed body frame by (4.7). Here, the Wigner  $D$ -matrices, that in our planar case are diagonal, perform the rotation of the components. We use properties of symmetry of the ellipsoids to obtain the full expansion of the potential energy of the system in (4.12), whose first terms are given in (4.16). With this potential we can write the Euler-Lagrange equations of the system eqs. (4.14) and (4.15). Then we disregard the non-Keplerian terms only in the orbital part and obtain the equations of the spin-spin model (4.27). Here we define the adimensional parameters of the system with physical meaning.

In Section 4.2 we obtain results to the *conservative* spin-spin model, analogous to those of Section 3.1 for the spin-orbit problem: we find regions of uniqueness and linear stability of a  $2\pi$ -periodic solution with odd symmetry in the space of parameters. We call this solution  $\Theta^*$  as in Section 3.1, although here it has two components. In this case we do not intend to maximize the size of the uniqueness and stability regions because the increase of one degree of freedom adds many technical difficulties. Again  $\Theta^*$  is the solution of a Dirichlet problem (4.31). We prove that such solution exists using Brouwer's fixed-point theorem. For the uniqueness we prove that the only solution of the linear Dirichlet problem (4.33) is the trivial one (Lemma 4.1). To do this we employ the partial ordering of symmetric matrices (Definition 4.1) and other basic properties of the spectral radius and matrix norms. Then, we deal with the variational equation at  $\Theta^*$ , that is a linear Hamiltonian system with periodic coefficients. We define strong stability (in the sense of Krein) for such systems in Definition 4.2 and use a test of strong stability to prove Theorem 4.2. To fulfil the inequalities in the test (4.40), we apply again basic properties of the spectral radius, matrix norms and also an a priori bound in Lemma 4.2.

In Section 4.3, to make the continuation of the solution to the dissipative setting (Theorem 4.3) we use Proposition 4.3 and Theorem 3.2. Proposition 4.3 reproduces some classical results on the continuation of periodic solutions, [31]. The first item of Proposition 4.3 guarantees that the continuation exists and is unique. To apply this item we use Proposition 4.2, a basic result on strong stability. Then, we need to prove that the new solution is asymptotically stable. This is proved by applying Theorem 3.2 to each of



the equations of the system in the uncoupled case  $\Lambda_{m_2}^{m_1} = 0$ . To complete the proof, we can see the complete system as a perturbation of the uncoupled one and apply the second item of Proposition 4.3. We dedicate the end of the section to explain why we require a small coupling  $|\Lambda_{m_2}^{m_1}|$  in the last part of the proof. Basically, the full coupled system requires a deeper theoretical study because we did not find a straightforward generalization to higher dimensions of the method used in Lemma 3.7 for the spin-orbit problem.

In Section 4.4, we apply the results. We make a direct application to the Pluto-Charon binary and to the binary asteroid 617 Patroclus. This leads us to a discussion about why the estimated regions for the spin-spin model are much smaller than those for the spin-orbit problem in Chapter 3. We conclude that the techniques of the latter are much finer: In Chapter 3 we develop generalized Lyapunov criteria using  $L^p$ -norms, with  $p \in [1, \infty]$ , see [128], and upper and lower solutions to bound the amplitude of the solution. Instead, for the spin-spin model we use the stability test given by (4.40), that is of type  $L^\infty$ , and a rougher bound for the amplitude of the solution in Lemma 4.2. Finally, we make a qualitative description of Figure 1.12, that shows the numerical plots of linear stability regions of  $\Theta^*$  for the case of identical bodies when we change the coupling parameter  $\hat{q}$ . For a stable linear Hamiltonian system with periodic coefficients with two degrees of freedom,  $\sum_{n=1}^4 |\lambda_n| = 4$ , where  $\lambda_n$  are the Floquet multipliers of the variational equation at  $\Theta^*$  (Section 4.2.3). On the other hand, if  $\sum_{n=1}^4 |\lambda_n| > 4$ , the system is unstable. Then, we find the separatrix of stability/instability by taking the limit of the curves given implicitly by  $\sum_{n=1}^4 |\lambda_n| = 4 + \epsilon$  as  $\epsilon \rightarrow 0^+$ .

## Discussion and perspectives

In this research we deal with a simplified mathematical model for the rotational dynamics in the Full Two-Body Problem. As far as we know, it was first studied in [60], although here we put more emphasis on the mathematical formulation of the problem for future studies. This model is a straightforward continuation of the spin-orbit problem. In consequence, we hope it will be of interest for physical applications as well as for theoretical studies. We have approached the problem from a theoretical point of view, but always keeping what we think is the essence of the physical problem: the dissipative effects are fundamental to explain the universe we observe today. In this sense, the spin-spin model not only broaden the scope of the spin-orbit problem in a higher dimensional phase space, but also contributes to fill the gap between the conservative and the dissipative effects considered in the spin-orbit problem. More precisely, if the *dissipative* torque (of order  $1/r^6$ ) is important in the evolution of a satellite, then, we should consider also the spin-spin

interaction (of order  $1/r^5$ ). Of course these two effects are more important when the bodies are closer to each other. In fact, in the spin-spin model the strength of the terms of order  $1/r^5$  is given by parameters that compare the shape of the bodies with the size of the orbit, say,  $\hat{d}_j$  and  $\hat{q}_j$ . In contrast, the spin-orbit problem only regards the equatorial oblateness of the satellite  $d_j/\mathcal{C}_j$ . It is reasonable to think that the different types of interactions, say, point-point, spin-orbit and spin-spin, must have their own specific relevance in different ranges of parameters. This shows that the non-Keplerian behavior of the full Lagrangian model (4.14), (4.15), should be investigated more deeply. Here the full expansion of the potential energy, given in (4.12), may also play a role. Moreover, as [36] shows, non-planar oscillations around solutions of the planar problem can be studied and are of practical interest.

In the present research, we have made a brief theoretical study that allowed us to point out the importance of the double synchronous resonance and compare it with the synchronous resonance of the spin-orbit problem. Particularly, in a similar way than in Chapter 3, we determine sufficient conditions for the existence of an asymptotically stable periodic solution (capture into resonance). Besides, note that our estimates do not intend to be optimal at all. Instead, we illustrate a way to extend to the spin-spin model the tools used for the spin-orbit model, as well as to compare them. Furthermore, in this sense we have included some numerical diagrams of linear stability in Figure 4.4 that show us how the spin-spin interaction alters the schemes of the spin-orbit model.

We have applied our study to two real systems in double synchronous resonance. In one hand, Pluto and Charon are representative of a large binary with one body much larger than the other one, see [41]. On the other hand, the binary asteroid 617 Patroclus is an archetype of a small system of similar components, see [36], [79]. Here we propose a way how to make an effective comparison between different systems. Note that the convenient choice of units and parameters helps to clarify the comparison. As we expected, the best candidates to apply the spin-spin model are binary asteroids. They are very abundant in the solar system, e.g., about 15% of the near-Earth asteroids are thought to be binaries. For a detailed discussion on the applications of the general spin-spin model and its full Lagrangian version, we refer to [7] and the bibliography therein. With our study on the double synchronous resonance we hope to contribute to the study of the spin-spin resonances made in [7]. Whereas they focus on the synchronization of both spins for slow circular orbital motion ( $\dot{f} \ll \dot{\theta}_j$ ), we consider the full synchronization including the orbit with arbitrary eccentricity. According to [36], most of the equal mass binaries are expected to be in the double synchronous state. In [99], Section 4.14, they provide a formula for a critical mass ratio of the

components for this state to be possible. We want to remark also that, apart from the application to binary asteroids and large natural satellites, the spin-spin interaction can be relevant for artificial satellites whose rotation state along an orbit is important. For instance, communication satellites in equatorial orbits or even spacecraft exploring small bodies.

Finally, we think that the theoretical interest of the model is large, even beyond the phenomena already observed in the spin-orbit problem. For example, in the spin-orbit problem we can apply the notion of KAM stability because KAM tori confine regions in the phase space. However this does not happen in the spin-spin model due to the increase in the phase space dimension (two degrees of freedom and time dependence). In fact, it is expected that Arnold diffusion takes place in this case. In general, the weak coupling and the Hamiltonian character of the system makes it suitable to apply perturbative techniques. Particular questions may be investigated, such as chaos by overlapping of resonances (see [60]), stochastic phenomena, normally hyperbolic manifolds, scattering maps, among other phenomena, see [29].



# Chapter 2

## The Kepler problem with singular drags

### 2.1 Some preliminaries

In this section we present some preliminary considerations and establish some notation for the dissipative Kepler problem (1.8). We rewrite equation (1.8) in an equivalent form as the first order system

$$\begin{cases} \dot{\mathbf{x}} = \mathbf{v} \\ \dot{\mathbf{v}} = -\frac{k}{\|\mathbf{x}\|^\beta} \mathbf{v} - \frac{\mathbf{x}}{\|\mathbf{x}\|^3}, \end{cases} \quad (2.1)$$

defined in the phase space  $\Omega = (\mathbb{R}^3 \setminus \{0\}) \times \mathbb{R}^3$ . Given an initial condition  $(\mathbf{x}_0, \mathbf{v}_0) \in \Omega$ , the unique maximal solution of (2.1) such that  $\mathbf{x}(0) = \mathbf{x}_0$  and  $\mathbf{v}(0) = \mathbf{v}_0$  will be denoted by  $(\mathbf{x}(t), \mathbf{v}(t))$  or by  $\phi^t(\mathbf{x}_0, \mathbf{v}_0)$ , where  $\phi^t$  is the flow of the system (2.1). The corresponding interval of definition will be indicated by  $(\alpha, \omega)$ .

The energy  $E$  and the angular momentum  $\mathcal{M}$ , defined respectively by

$$E(\mathbf{x}, \mathbf{v}) = \frac{1}{2} \|\mathbf{v}\|^2 - \frac{1}{\|\mathbf{x}\|}, \quad \mathcal{M}(\mathbf{x}, \mathbf{v}) = \mathbf{x} \wedge \mathbf{v},$$

are no longer conserved quantities for (2.1), since their derivatives along any solution of (2.1) satisfy

$$\dot{E}(t) = -k \frac{\|\mathbf{v}(t)\|^2}{\|\mathbf{x}(t)\|^\beta}, \quad \dot{\mathcal{M}}(t) = -\frac{k}{\|\mathbf{x}(t)\|^\beta} \mathcal{M}(t). \quad (2.2)$$

It follows that the energy is strictly decreasing along the solutions of (2.1), and that the angular momentum of any solution satisfies

$$\mathcal{M}(t) = \mathcal{M}_0 e^{-\int_0^t \frac{k}{\|\mathbf{x}(s)\|^\beta} ds}, \quad \mathcal{M}_0 := \mathbf{x}_0 \wedge \mathbf{v}_0. \quad (2.3)$$

Then, either  $\mathcal{M}(t) \equiv 0$  on  $(\alpha, \omega)$ , and the corresponding orbit is rectilinear, or  $\mathcal{M}(t) \neq 0$  on  $(\alpha, \omega)$ , and the corresponding orbit is planar since  $\frac{\mathcal{M}(t)}{\|\mathcal{M}(t)\|}$  is a conserved vector. In this second case,  $\|\mathcal{M}(t)\|$  is strictly decreasing.<sup>1</sup>

Due to the invariance of our problem with respect to the group of isometries of  $\mathbb{R}^3$ , we can study the dynamics of (2.1) in the phase space  $\Omega = \{(\mathbf{x}, \mathbf{v}) \in (\mathbb{C} \setminus \{0\}) \times \mathbb{C}\}$ , where we have set  $\mathbf{x} = x_1 + ix_2$ ,  $\mathbf{v} = v_1 + iv_2$ . Moreover, denoting by  $M = x_1 v_2 - x_2 v_1$  the scalar angular momentum of a solution, in order to study the rotational properties of non rectilinear motions, it will be sufficient to restrict ourselves to the set  $\Omega^+ = \{(\mathbf{x}, \mathbf{v}) \in \Omega : M > 0\}$ . The manifold  $\Omega^0 = \{(\mathbf{x}, \mathbf{v}) \in \Omega : M = 0\}$  corresponds to rectilinear motions.

We rewrite now system (2.1) using polar coordinates in  $\mathbb{C} \setminus \{0\}$ . Considering the change of variables  $\mathbf{x} = r \exp(i\theta)$  we see that the new coordinates satisfy the system

$$\begin{cases} \dot{r} = u \\ \dot{u} = r\varphi^2 - k\frac{u}{r^\beta} - \frac{1}{r^2} \\ \dot{\varphi} = -\frac{k + 2ur^{\beta-1}}{r^\beta}\varphi, \end{cases} \quad (2.4)$$

where  $\varphi = \dot{\theta} \geq 0$  and  $u \in \mathbb{R}$ . Of course, motions in  $\Omega^+$  will correspond to  $\varphi > 0$ , whereas the equality  $\varphi = 0$  singles out the rectilinear motions in  $\Omega^0$ . When dealing with rectilinear motions in Subsection 3.4, we will identify  $\Omega^0$  with the set  $\{(r, u) : r > 0, u \in \mathbb{R}\}$ .

In what follows, we will consider just the forward dynamics of (1.8). Accordingly, all the solutions will be considered on their right maximal interval  $[0, \omega)$ .

Throughout the paper, the subscript  $\omega$  attached to a time dependent function will denote the limit of that function as  $t \rightarrow \omega^-$ . For simplicity, we will generally omit the dependence of such limit on initial conditions  $(\mathbf{x}_0, \mathbf{v}_0)$ . For example, since the energy and the scalar angular momentum are decreasing along the solutions of (1.8) we will write

$$E_\omega = \lim_{t \rightarrow \omega^-} E(\phi^t(\mathbf{x}_0, \mathbf{v}_0)) \in [-\infty, E(0)]$$

---

<sup>1</sup>Jacobi, in his book on mechanics [59], had already considered the dissipative Kepler problem corresponding to (1.9) with drag  $P_{1,\beta}$ , finding that the motions are planar and have decreasing energy and decreasing scalar angular momentum. We note that these properties actually hold for any dissipation opposite to the velocity.

and

$$M_\omega = \lim_{t \rightarrow \omega^-} M(\phi^t(\mathbf{x}_0, \mathbf{v}_0)) \in [0, M(0)].$$

Throughout the paper we will make use of the following definition.

**Definition 2.1.** *A solution of (1.8) defined on the right maximal interval  $[0, \omega[$  is called a collision solution if*

$$\lim_{t \rightarrow \omega} \mathbf{x}(t) = 0. \quad (2.5)$$

We will say that the collision occurs in finite time if  $\omega$  is finite, and that it occurs in infinite time if  $\omega = +\infty$ .

In the first result we determine the values of  $E_\omega$  and  $M_\omega$  for collision solutions.

**Theorem 2.1.** *Collisions always occur with zero angular momentum and energy equals to minus infinity.*

**Proof.** From the expression of the energy

$$E(t) = \frac{u^2(t)}{2} + \frac{r^2(t)\dot{\theta}^2(t)}{2} - \frac{1}{r(t)} = \frac{u^2(t)}{2} + \frac{M^2(t)}{2r^2(t)} - \frac{1}{r(t)},$$

we see that in the case of a collision, since  $r(t) \rightarrow 0^+$  as  $t \rightarrow \omega^-$ , it must be  $M_\omega = 0$ . Otherwise, we would get  $E_\omega = +\infty$ , which is not possible since  $E(t)$  is a decreasing function.

To prove the second part of the statement, we start by observing that, by (2.3),

$$M(t) = M(0)e^{-k\tau(t)},$$

where

$$\tau(t) = \int_0^t \frac{ds}{r^\beta(s)}. \quad (2.6)$$

Since  $M_\omega = 0$ , we get that, for collision solutions,

$$\tau_\omega = \int_0^\omega \frac{ds}{r^\beta(s)} = +\infty. \quad (2.7)$$

Now we can conclude our proof arguing by contradiction. Assume that  $E_\omega \in \mathbb{R}$ . Since for a collision solution there exists a  $t_0 \in [0, \omega)$  such that

$$E(t) > E_\omega \geq \frac{1}{2} - \frac{1}{r(t)}$$

for all  $t \in [t_0, \omega)$ , then, on this interval,

$$|\mathbf{v}(t)|^2 = 2E(t) + \frac{2}{r(t)} > 1.$$

As a consequence, we get

$$\dot{E}(t) = -k \frac{|\mathbf{v}(t)|^2}{r^\beta(t)} < -\frac{k}{r^\beta(t)}.$$

Integrating this inequality from  $t_0$  to  $t$ , we get  $E(t) < E(t_0) - k\tau(t)$ . But now, from (2.7) we get  $E_\omega = -\infty$ , contradicting the assumption. Then,  $E_\omega = -\infty$  and our proof is complete. ■



## 2.2 Forward dynamics

### 2.2.1 A threshold for the existence of escape orbits and non existence of oscillatory ones

In this subsection we first address the problem of the existence of escape orbits for (1.8). From [81] we know that escapes do not exist for  $\beta = 0$ , since in this case the singularity is a global attractor. However, the influence of the singularity at infinity becomes weaker and weaker as  $\beta$  increases, and escapes are expected to exist when  $\beta$  crosses some threshold value. The results in [39] show that escape rectilinear orbits exist for  $\beta = 2$ , implying that such threshold is less than or equal to 2. In Theorem 2.2 below we show that the threshold is  $\beta = 1$ . We also show, in Theorem 2, that no oscillatory solutions exist for (1.8). We first give the following auxiliary lemma. We point out that this result holds for  $\omega$  finite or infinite.

**Lemma 2.1.** *For any  $\beta > 0$ , let  $\mathbf{x}(t)$  be a solution of (1.8) defined on the right maximal interval  $[0, \omega)$ .*

*i) If  $\liminf_{t \rightarrow \omega^-} |\mathbf{x}(t)| < +\infty$ , then*

$$\liminf_{t \rightarrow \omega^-} |\mathbf{x}(t)| = 0. \quad (2.8)$$

*ii) If  $\mathbf{x}(t)$  is bounded on  $[0, \omega)$ , then it is a collision solution.*

**Proof.** To prove *i)*, we argue by contradiction. Assume that there exists a positive real number  $\delta_*$  such that

$$\liminf_{t \rightarrow \omega^-} |\mathbf{x}(t)| = 2\delta_*. \quad (2.9)$$

Then, there exists a sequence  $\{t_n\} \subset [0, \omega[$  that satisfies  $t_n \rightarrow \omega$ ,  $|\mathbf{x}(t_n)| \rightarrow 2\delta_*$ , and

$$|\mathbf{x}(t_n)| \geq \delta_*, \quad \text{for any } n. \quad (2.10)$$

Since the energy is decreasing along solutions, from (2.10) we have

$$\frac{|\mathbf{v}(t_n)|^2}{2} \leq E(0) + \frac{1}{|\mathbf{x}(t_n)|} \leq E(0) + \frac{1}{\delta_*}, \quad (2.11)$$

for any  $n$ . It follows that there exists  $(\mathbf{x}_*, \mathbf{v}_*) \in \Omega$  which is a limit point of  $(\mathbf{x}(t_n), \mathbf{v}(t_n))$ . By the general theory of ODEs and the maximality of  $(\mathbf{x}(t), \mathbf{v}(t))$ , we conclude that  $\omega = +\infty$ . Then, we can apply the extension

of La Salle's principle to singular systems given in [83], Proposition 2.2, with  $V = E$ , and conclude that

$$L_\omega(\mathbf{x}, \mathbf{v}) \cap \Omega = \emptyset, \quad (2.12)$$

where  $L_\omega(\mathbf{x}, \mathbf{v})$  is the  $\omega$ -limit set of the solution  $t \mapsto (\mathbf{x}(t), \mathbf{v}(t))$ . Since  $(\mathbf{x}_*, \mathbf{v}_*) \in L_\omega(\mathbf{x}, \mathbf{v}) \cap \Omega$  we get a contradiction, and our proof of *i*) is concluded.

To get *ii*) we start by noticing that, if  $\omega = +\infty$ , the conclusion follows immediately as in [83]. If  $\omega < +\infty$ , we show that

$$\limsup_{t \rightarrow \omega^-} |\mathbf{x}(t)| = 0, \quad (2.13)$$

arguing by contradiction. Assume that (2.13) does not hold, and let  $2\delta^* > 0$  be the value of the upper limit. Then, there exists a sequence  $\{t_n\} \subset [0, \omega)$  converging to  $\omega$  as  $n \rightarrow \infty$ , such that  $|\mathbf{x}(t_n)| \rightarrow 2\delta^*$  and  $|\mathbf{x}(t_n)| \geq \delta^*$ . Now, the same argument already used in *i*) leads to the contradiction that  $\omega = +\infty$ . Our proof is concluded. ■

**Theorem 2.2.** *If  $0 < \beta \leq 1$  all the orbits of (1.8) tend to the singularity, whereas if  $\beta > 1$  there are also escape orbits. Escapes occur in infinite time with a finite velocity, which can have an arbitrarily large modulus, and with non-negative finite energy.*

**Proof.** We start the proof of the first claim by showing that for  $0 < \beta \leq 1$  all the solutions are bounded in the future.

Let  $w = |\dot{\mathbf{x}}|$  and consider the following family of functions

$$\Lambda_\beta(r, w) := \begin{cases} \frac{k}{1-\beta} r^{1-\beta} + w & \text{if } 0 < \beta < 1, \\ k \ln r + w & \text{if } \beta = 1. \end{cases} \quad (2.14)$$

Let  $t \mapsto \mathbf{x}(t)$  be a solution of (1.8) defined on the right maximal interval  $[0, \omega)$ . Define  $r_0 := r(0)$  and  $w_0 := w(0)$ . We will show that

$$\Lambda_\beta(r(t), 0) \leq \Lambda_\beta(r_0, w_0), \quad t \in [0, \omega),$$

which implies immediately that  $r(t)$  is bounded for all  $t \in [0, \omega)$ . We argue by contradiction. Assume that there exists  $t_1 \in [0, \omega)$  such that  $r_1 := r(t_1)$  satisfies

$$\Lambda_\beta(r_1, 0) > \Lambda_\beta(r_0, w_0) \geq \Lambda_\beta(r_0, 0).$$

Then,  $r_1 > r_0$ , and, if we let  $w_1 := w(t_1)$  we have

$$\Lambda_\beta(r_1, w_1) > \Lambda_\beta(r_0, w_0). \quad (2.15)$$

Let  $\Lambda_\beta(t) := \Lambda_\beta(r(t), w(t))$ . If  $t \in [0, t_1]$  is such that  $\dot{r}(t) > 0$ , then

$$\dot{\Lambda}_\beta(t) = k \frac{\dot{r}}{r^\beta} - k \frac{w}{r^\beta} - \frac{\dot{r}}{r^2 w} < 0, \quad 0 < \beta \leq 1.$$

The inequality holds since  $w \geq \dot{r}$ . Moreover, let  $t'$  and  $t''$  be two values such that  $0 < t' < t'' \leq t_1$  and  $r(t') = r(t'')$ , then, from  $E(t'') < E(t')$ , it follows that  $w(t'') < w(t')$ , and consequently,  $\Lambda_\beta(t'') \leq \Lambda_\beta(t')$ . By Lemma 6 in [33], applied with  $a = 0$ ,  $b = t_1$ ,  $y(t) = r(t)$  and  $z(t) = -\Lambda_\beta(t)$ , we get that

$$-\Lambda_\beta(t_1) = -\Lambda_\beta(r_1, w_1) \geq -\Lambda_\beta(0) = -\Lambda_\beta(r_0, w_0),$$

contradicting (2.15). We conclude that all solutions of (1.8) are bounded on  $[0, \omega[$ . The first part of the statement follows now from *ii*) of Lemma 2.1.

In order to prove the second claim, we rewrite system (2.4) introducing the scalar angular momentum  $M = r^2 \dot{\theta}$  as a variable, getting the following system:

$$\begin{cases} \dot{r} = u \\ \dot{u} = \frac{M^2}{r^3} - k \frac{u}{r^\beta} - \frac{1}{r^2} \\ \dot{M} = -k \frac{M}{r^\beta}. \end{cases} \quad (2.16)$$

Consider the set

$$B := \{(r, u, M) : r > 1, u \in \mathbb{R}, M \geq 0\},$$

and the following family of functions  $f_c : B \rightarrow \mathbb{R}$  depending on the positive parameter  $c$ :

$$f_c(r, u, M) := c + \frac{1}{\ln r} - u.$$

We claim that, for fixed  $c > 0$ , there exists  $r_* > 1$  such that the set

$$B_c := \{(r, u, M) \in B : r \geq r_*, f_c(r, u, M) \leq 0\} \quad (2.17)$$

is positively invariant with respect to the flow of system (2.16). Denote by  $\mathcal{V}(r, u, M)$  the vector field associated to (2.16) and by  $\phi^t(r, u, M)$  the corresponding flow. A computation shows that on the surface  $f_c(r, u, M) = 0$  we have

$$(\mathcal{V} \cdot \nabla f_c)|_{f_c=0} = -\frac{c}{r \ln^2 r} - \frac{1}{r \ln^3 r} - \frac{M^2}{r^3} + \frac{kc}{r^\beta} + \frac{k}{r^\beta \ln r} + \frac{1}{r^2},$$

where the dot denotes the Euclidean inner product. As  $\beta > 1$ , it follows that there exists a sufficiently large  $r_* > 1$  such that, for any initial condition  $(r, u, M) \in B_c$  satisfying  $f_c(r, u, M) = 0$ , the following inequality holds

$$\frac{d}{dt} f_c(\phi^t(r, u, M))|_{t=0} = (\mathcal{V} \cdot \nabla f_c)(r, u, M) < 0.$$

Since for  $(r_*, u, M) \in B_c$  we have that  $u = \dot{r} > 0$ , and since the set  $\{M = 0\} \cap B$  is positively invariant, we conclude that  $B_c$  is positively invariant for  $\phi^t$ . Taking into account that  $M(t)$  is decreasing, we have

$$\dot{u} = \frac{M^2}{r^3} - k \frac{u}{r^\beta} - \frac{1}{r^2} \leq \frac{M^2(0)}{r^3} - \frac{kc}{r^\beta} - \frac{k}{r^\beta \ln r} - \frac{1}{r^2},$$

and, by choosing if necessary a larger  $r_*$ , we may assume that  $\dot{u} < 0$  in  $B_c$ . Consider now a solution of (2.16) with initial condition in  $B_c$ . Then,  $u(t)$  is decreasing on  $[0, \omega)$  and

$$c \leq \lim_{t \rightarrow \omega} u(t) = u_\omega \leq u(0).$$

If  $\omega$  were finite, from  $\dot{r} = u$  we would get that  $r_* \leq r(t) \leq r(0) + u(0)\omega$  on  $[0, \omega[$ . Since on this interval it holds also  $0 \leq M(t) \leq M(0)$ , we would have a maximal solution of (2.16) contained in a compact set of the phase space. We conclude that  $\omega = +\infty$ , and then

$$r_* + ct \leq r(t) \rightarrow +\infty$$

as  $t \rightarrow +\infty$ . The existence of escape solutions is proved.

By the identity

$$|\mathbf{v}(t)|^2 = u^2(t) + r^2(t)\dot{\theta}^2(t) = u^2(t) + \frac{M^2(t)}{r^2(t)},$$

and the boundedness of  $M(t)$ , we see that the value of the asymptotic velocity for escapes is exactly  $u_\omega$ . For initial conditions in  $B_c$ , we get that  $u_\omega \geq c$ , where  $c$  may be fixed arbitrarily large. Furthermore, the limit energy verifies  $E_\omega = u_\omega^2/2$ . Our proof is concluded. ■

The arguments used in Lemma 2.1 to prove the attractiveness of the singularity can be adapted to show that collisions and escapes are the only possible types of solutions for (1.8). This is done in the next result.

We recall that a solution  $t \mapsto \mathbf{x}(t)$  of (1.8), defined on the right maximal interval  $[0, \omega[$ , is called oscillatory if it satisfies

$$\limsup_{t \rightarrow \omega^-} |\mathbf{x}(t)| = +\infty, \quad \liminf_{t \rightarrow \omega^-} |\mathbf{x}(t)| = 0. \quad (2.18)$$

Actually, in the definition of an oscillatory solution, it is usually required only that the lower limit of  $|\mathbf{x}(t)|$  is finite, but Lemma 2.1 rules out any value different from zero.

**Theorem 2.3.** *Equation (1.8) does not admit oscillatory solutions.*

**Proof.** If  $\beta \in ]0, 1]$  the statement is trivially true, since all solutions are collision solutions. The case  $\beta > 1$  can be proved arguing by contradiction. If  $\mathbf{x}(t)$  is an oscillatory solution, there exist a  $d > 0$  and a sequence  $\{t_n\} \subset [0, \omega)$  converging to  $\omega$  such that  $|\mathbf{x}(t_n)| = d$  for any  $n$ . Then, we get a contradiction in the same way as in the proof of the item *ii*) in Lemma 2.1. We omit the details. ■

**Remark 2.1.** *According to Lemma 2.1, a bounded solution is attracted to the singularity. Actually, a closer look at the proof shows that this behavior, as well as the statement of Theorem 2.3, hold for any (sufficiently regular) drag such that the energy along the motions is strictly decreasing. In our framework, a general example is provided by a force of the form  $-D(\mathbf{x}, \dot{\mathbf{x}})\dot{\mathbf{x}}$ , where the function  $D$  is strictly positive and sufficiently smooth on  $\Omega$ . In fact, in this case  $\dot{E}(t) = -D(\mathbf{x}(t), \dot{\mathbf{x}}(t))|\dot{\mathbf{x}}(t)|^2 < 0$ ,  $t \in [0, \omega)$ . We conclude that, for such class of dissipations, the only attractor is the singularity.*

It may be interesting to observe that a dissipative Kepler problem with a different kind of attractor is obtained in [30], where a simplified model of tidal dissipation is discussed. The general class of dissipations considered there is radial, as illustrated by the example of dissipative force  $-\epsilon(\mathbf{x} \cdot \dot{\mathbf{x}})\mathbf{x}$ . For this dissipative Kepler problem, each orbit is attracted to a circular orbit depending on the initial conditions.

**Remark 2.2.** *Note that Theorem 2.3 and Theorem 2.1 imply that  $\Omega^+$  can be partitioned in the following three sets: the set of initial conditions of collisions orbits*

$$\Omega_C^+ := \{(\mathbf{x}, \mathbf{v}) \in \Omega^+ : E_\omega = -\infty\},$$

*the set of initial conditions of hyperbolic escapes, and the set of initial conditions of parabolic escapes, defined respectively by*

$$\Omega_H^+ := \{(\mathbf{x}, \mathbf{v}) \in \Omega^+ : E_\omega > 0\} \quad \text{and} \quad \Omega_P^+ := \{(\mathbf{x}, \mathbf{v}) \in \Omega^+ : E_\omega = 0\}.$$

*The last two sets are empty when  $\beta \in [0, 1]$ .*

Of course, an analogous partition holds for  $\Omega$ , but we will not need this fact in what follows.

### 2.2.2 Non-rectilinear motions

In this subsection we focus on some qualitative properties of the non rectilinear motions of (1.8). We show that, for any  $\beta > 1$ , an escape solution cannot make a full turn around the singularity, i.e., the variation of the polar angle is less than  $2\pi$ . As to collision solutions, we prove several facts. Firstly, for any  $\beta > 0$ , their angular momentum tends to zero and their energy goes to  $-\infty$ . Secondly, if  $\beta \in (0, 1)$ , their angular velocity is unbounded. Thirdly, collision solutions are asymptotically rectilinear for  $\beta > \frac{3}{2}$ . In this case we discuss the time to collision and the terminal velocity as  $\beta$  increases. We are able to extend our results to the case  $\beta = \frac{3}{2}$ , but just for  $k$  sufficiently large. This is due to the fact that  $\frac{3}{2}$  is the only value of the parameter  $\beta$  for which  $k$  cannot be eliminated from equation (1.8) by a rescaling of the solutions.

#### Variation of the polar angle of escape orbits

In order to prove our result about escapes, we rewrite (1.8) using the well known Binet transformation, which we recall here. Since for any solution in  $\Omega^+$  we have  $M(t) = r^2(t)\dot{\theta}(t) > 0$ , for any  $t \in [0, \omega)$ , the function  $t \mapsto \theta(t)$  is an increasing diffeomorphism between  $J_t = [0, \omega)$  and the interval  $J_\theta = [\theta_0 := \theta(0), \theta_\omega = \theta(\omega^-))$ . The inverse function  $\theta \mapsto t(\theta)$  is then used to re-parameterize the solutions of system (2.4), in which  $r$  is replaced by the new variable  $\rho = \frac{1}{r}$ . Then, the maximal solutions  $t \mapsto (\mathbf{x}(t), \mathbf{v}(t))$ ,  $t \in J_t$ , of (2.1) in the set  $\Omega^+$  are transformed into the maximal solutions  $\theta \mapsto y(\theta) = (\rho(\theta), \zeta(\theta), \theta, M(\theta))$ ,  $\theta \in J_\theta$ , of the differential system

$$y' = g(y) := \left( \zeta, \frac{1}{M^2} - \rho, 1, -\frac{k}{\rho^{2-\beta}} \right), \quad (2.19)$$

where the prime denotes derivation with respect to  $\theta$  and

$$y = (\rho, \zeta, \theta, M) \in (0, +\infty) \times \mathbb{R} \times \mathbb{R} \times (0, +\infty).$$

The previous transformation may be defined by the time rescaling  $t = t(\theta)$  and by the change of variables

$$(\mathbf{x}, \mathbf{v}) = U(y) := \left( \frac{1}{\rho} e_r(\theta), -M\zeta e_r(\theta) + \rho M e_\theta(\theta) \right), \quad (2.20)$$

where we identify  $\theta$  modulo  $2\pi$  and  $e_r(\theta) = e^{i\theta}$ ,  $e_\theta(\theta) = ie_r(\theta)$ .

The first two equations of system (2.19) are equivalent to the second order scalar equation of a forced linear oscillator, namely  $\rho'' + \rho = \frac{1}{M^2}$ . Given an initial condition  $(\mathbf{x}_0, \mathbf{v}_0) \in \Omega^+$ , we set  $y_0 := (\rho_0, \zeta_0, \theta_0, M_0) = U^{-1}(\mathbf{x}_0, \mathbf{v}_0)$ , in which  $\theta_0 = \arg \mathbf{x}_0$  is defined modulo  $2\pi$ . In what follows we will consider  $\theta_0 \in$

$[0, 2\pi)$ . By the variation of constants formula we see that the corresponding solution satisfies the coupled system

$$\begin{aligned}\rho(\theta) &= \rho_0 \cos(\theta - \theta_0) + \zeta_0 \sin(\theta - \theta_0) + \int_{\theta_0}^{\theta} \frac{\sin(\theta - \eta)}{M^2(\eta)} d\eta \\ \zeta(\theta) &= \rho'(\theta) \\ M(\theta) &= M_0 - \int_{\theta_0}^{\theta} \frac{k}{\rho^{2-\beta}(\eta)} d\eta\end{aligned}\tag{2.21}$$

on  $[\theta_0, \theta_\omega)$ . We can rewrite the first equation as

$$\rho(\theta) = -\kappa \sin(\theta - \alpha_0 - \theta_0) + \Phi(\theta),\tag{2.22}$$

where  $\alpha_0 = \arccos\left(-\frac{\zeta_0}{\kappa}\right) \in (0, \pi)$  is the angle between  $\mathbf{x}_0$  and  $\mathbf{v}_0$ , and where we have defined

$$\Phi(\theta) := \int_{\theta_0}^{\theta} \frac{\sin(\theta - \eta)}{M^2(\eta)} d\eta, \quad \kappa = \sqrt{\rho_0^2 + \zeta_0^2}.\tag{2.23}$$

Note that a solution of  $y' = g(y)$  defined on  $[0, \theta_\omega)$  corresponds to an escape solution of (1.8) if and only if

$$\rho(\theta) > 0 \text{ on } [0, \theta_\omega) \quad \text{and} \quad \lim_{\theta \rightarrow \theta_\omega^-} \rho(\theta) = 0.$$

We are now in a position to prove our result about escapes. To simplify our notations, we assume that  $\theta_0 = 0$ .

**Theorem 2.4.** *Escapes can only occur during the first turn around the origin. Moreover, the limit angle  $\theta_\omega$  satisfies*

$$\theta_\omega < \alpha_0 + \pi.$$

*If a solution does more than one turn, then it corresponds to a collision orbit.*

The theorem will be an immediate consequence of the following lemma, whose proof is based on the fact that  $M(\theta)$  is a strictly decreasing function.

**Lemma 2.2.** *The function  $\Phi$  defined in (2.23) satisfies the following properties:*

- i)  $\Phi(\theta) > 0$  for all  $\theta \in (0, \theta_\omega)$ .
- ii) If  $\theta_\omega > 2\pi$ , then  $\Phi(\theta) > \Phi(\theta - 2\pi)$  for all  $\theta \in [2\pi, \theta_\omega)$ .

**Proof.** From the sign of  $\sin(\theta - \eta)$  we see that

$$I_1 := \int_{\theta-2\pi}^{\theta} \frac{\sin(\theta - \eta)}{M^2(\eta)} d\eta > 0, \quad I_2 := \int_{\theta-2\pi}^{\theta-\pi} \frac{\sin(\theta - \eta)}{M^2(\eta)} d\eta < 0.$$

By the second inequality, it follows that

$$|I_2| = \int_{\theta-2\pi}^{\theta-\pi} \frac{|\sin(\theta - \eta)|}{M^2(\eta)} d\eta = \int_{\theta-\pi}^{\theta} \frac{|\sin(\theta - \bar{\eta} + \pi)|}{M^2(\bar{\eta} - \pi)} d\bar{\eta} = \int_{\theta-\pi}^{\theta} \frac{\sin(\theta - \bar{\eta})}{M^2(\bar{\eta} - \pi)} d\bar{\eta}.$$

Since  $\frac{1}{M(\eta)}$  is strictly increasing, we have  $I_1 > |I_2|$ , and then

$$\int_{\theta-2\pi}^{\theta} \frac{\sin(\theta - \eta)}{M^2(\eta)} d\eta = I_2 + I_1 > 0, \quad \text{for any } \theta \in [0, \theta_\omega).$$

This inequality implies both assertions of the lemma. ■

**Proof.** (of Theorem 2.4)

If a solution of (1.8) makes one complete turn around the origin, it follows that

$$\rho(\theta) > 0, \quad \text{for any } \theta \in [0, 2\pi] \subset [0, \theta_\omega).$$

Property *ii)* of Lemma 2.2 implies

$$\liminf_{\theta \rightarrow \theta_\omega} \rho(\theta) \geq \rho(\theta_\omega - 2\pi) > 0,$$

and  $|\mathbf{x}(\theta)| = \frac{1}{\rho(\theta)}$  is bounded on  $[0, \theta_\omega)$ . From Remark 2.1, such solution is a collision solution. To end our proof, we observe that *i)* of Lemma 2.2 and (2.22) imply that, for an escape solution,  $\theta_\omega \in (\alpha_0, \alpha_0 + \pi)$ . ■

### A rotational property of collision orbits for $\beta \in (0, 1)$

Next result shows that the rotational property of solutions obtained for the linear drag in Proposition 2.5 in [81] continue to hold when  $\beta \in (0, 1)$ .

**Theorem 2.5.** *Let  $\beta \in (0, 1)$ . Given a non rectilinear solution  $t \mapsto \mathbf{x}(t) = r(t) \exp(i\theta(t))$ , there exists a sequence  $t_n \rightarrow \omega^-$  such that*

$$\dot{\theta}(t_n) \rightarrow +\infty.$$



**Proof.** We start by regularizing system (2.1) using the time rescaling  $d\mu = \frac{dt}{r^2}$ . We obtain the  $C^1$  system

$$\begin{cases} \frac{dr}{d\mu} = r^2 u \\ \frac{du}{d\mu} = -kur^{2-\beta} + r^3 \varphi^2 - 1 \\ \frac{d\varphi}{d\mu} = -(kr^{2-\beta} + 2ur)\varphi \end{cases} \quad (2.24)$$

on the set  $r \geq 0, u \in \mathbb{R}, \varphi > 0$ .

Then, multiplying the first equation by  $kr^{-\beta}$ , adding it to the second equation and integrating the result, we obtain that any solution

$$\mu \mapsto (r(\mu), u(\mu), \varphi(\mu))$$

satisfies the following equality:

$$u(\mu) + k \frac{r^{1-\beta}(\mu)}{1-\beta} = \int_0^\mu r^3(\sigma) \varphi^2(\sigma) d\sigma + C_0 - \mu, \quad (2.25)$$

where  $C_0 := u(0) + k \frac{r^{1-\beta}(0)}{1-\beta}$ , on its right maximal interval  $I_\mu = [0, \mu_\omega)$ .

Now we argue by contradiction. Assume that  $\varphi(\mu)$  is bounded on  $I_\mu$ . Then, it must be  $\mu_\omega = +\infty$ . Otherwise, if we assume that  $\mu_\omega < +\infty$ , we are led to a contradiction as follows. From (2.25) we infer that  $u(\mu)$  is bounded on  $I_\mu$ . As a consequence, from the third equation of the system we see that  $\varphi(\mu)$  is bounded away from zero on  $I_\mu$ . But then the solution  $\mu \mapsto (r(\mu), u(\mu), \varphi(\mu))$  is contained in a compact set of the phase space for all  $\mu \in I_\mu$ , contradicting its maximality. We conclude that  $\mu_\omega = +\infty$ . Now the argument proceeds as in [81]. Since  $r(\mu) \rightarrow 0$  as  $\mu \rightarrow +\infty$ , there exists a sequence  $\mu_n \rightarrow +\infty$  such that  $u(\mu_n) \rightarrow 0$ . By the boundedness of  $\varphi$  on  $I_\mu$ , there exists  $\bar{\mu}$  such that  $r^3(\sigma) \varphi^2(\sigma) < \frac{1}{2}$  for any  $\sigma \geq \bar{\mu}$ . Then, from (2.25) we get that for any  $\mu_n > \bar{\mu}$  it holds the inequality

$$u(\mu_n) + k \frac{r^{1-\beta}(\mu_n)}{1-\beta} \leq \int_0^{\bar{\mu}} r^3(\sigma) \varphi^2(\sigma) d\sigma + \frac{\mu_n - \bar{\mu}}{2} + C_0 - \mu_n.$$

Taking the limit for  $n \rightarrow +\infty$ , we get the contradiction  $0 \leq -\infty$ . We conclude that  $\varphi(\mu)$  is unbounded on  $[0, +\infty)$ , and the same property holds for  $\dot{\theta}(t)$  on  $[0, \omega)$ . ■

**Asymptotic dynamics of collision solutions for  $\beta \geq \frac{3}{2}$** 

To get our next results we start with a suitable rescaling of time in system (2.4), given by  $d\tau = \frac{dt}{|\mathbf{x}|^\beta}$ . We obtain the following equivalent system in the new time  $\tau$

$$\begin{cases} \frac{dr}{d\tau} = r^\beta u, \\ \frac{du}{d\tau} = -ku + r^{\beta+1}\varphi^2 - r^{\beta-2}, \\ \frac{d\varphi}{d\tau} = -(k + 2ur^{\beta-1})\varphi. \end{cases} \quad (2.26)$$

The associated vector field is non singular for  $\beta \geq 2$ . In this case, it can be extended continuously to the collision manifold  $r = 0$ , on which it possesses a unique equilibrium  $r = 0, u = 0, \varphi = 0$ . For  $\beta \geq 3$  the vector field is  $C^1$  on the set  $r \geq 0, u \in \mathbb{R}, \varphi \geq 0$ .

By (2.7), collision solutions in  $\Omega^+$  are defined on the right maximal interval  $[0, \tau_\omega = +\infty)$ , and on such interval,  $\varphi(\tau) = \dot{\theta}(t(\tau)) > 0$ . Since  $\tau \mapsto t(\tau)$  is an increasing diffeomorphism, the polar angle  $\theta(t(\tau))$  is an increasing function of  $\tau$  and, moreover, by (2.6) we get

$$\frac{d\theta}{d\tau} = \dot{\theta} \frac{dt}{d\tau} = \dot{\theta}(t(\tau))r^\beta(t(\tau)) > 0. \quad (2.27)$$

**Theorem 2.6.** *The following properties hold for collision orbits:*

- i) *If  $\beta > \frac{3}{2}$ , or if  $\beta = \frac{3}{2}$  and  $k > 2\sqrt{2}$ , there exists a limit polar angle at collision, achieved with zero angular velocity.*
- ii) *If  $\frac{3}{2} < \beta < 3$ , or if  $\beta = \frac{3}{2}$  and  $k > 2\sqrt{2}$ , collisions occur in finite time, whereas if  $\beta \geq 3$  they occur in infinite time.*
- iii) *If  $\frac{3}{2} < \beta < 2$ , or if  $\beta = \frac{3}{2}$  and  $k > 2\sqrt{2}$ , the limit velocity at collision is infinite, if  $\beta = 2$ , the limit velocity is finite and with modulus  $\frac{1}{k}$ , and if  $\beta > 2$  the limit velocity is zero.*

**Proof.**

- i) Since  $E_\omega = -\infty$  and  $r$  is bounded for collision orbits, we can take initial conditions such that  $E(0) < 0$  and  $0 < r(t) < 1$  on  $[0, \omega)$ . Then,

$$\frac{u^2(t)}{2} - \frac{1}{r(t)} < E(t) = \frac{|\mathbf{v}(t)|^2}{2} - \frac{1}{r(t)} < 0,$$

or equivalently,  $u^2 r < 2$ . It follows that, for any  $\beta \geq \frac{3}{2}$ , we have

$$u^2 r^{2\beta-2} < 2r^{2\beta-3} \leq 2,$$

which implies

$$ur^{\beta-1} > -\sqrt{2}r^{\frac{2\beta-3}{2}} \geq -\sqrt{2}, \quad \text{for any } \beta \geq \frac{3}{2}. \quad (2.28)$$

Consider now the evolution of the angular velocity given by the last equation of (2.26). By (2.28) we get the inequality

$$\frac{d\varphi}{d\tau} = -(k + 2ur^{\beta-1})\varphi < -(k - 2\sqrt{2})\varphi, \quad (2.29)$$

and hence

$$0 < \varphi(t(\tau)) < \varphi(0)e^{-(k-2\sqrt{2})\tau}. \quad (2.30)$$

Taking into account that  $\varphi = \dot{\theta}$  and (2.27), we can integrate (2.30) obtaining

$$\theta(t(\tau)) < \theta(0) + \varphi(0) \int_0^\tau r^\beta(t(\bar{\tau}))e^{-(k-2\sqrt{2})\bar{\tau}} d\bar{\tau}.$$

For  $k > 2\sqrt{2}$  the integrand function in the right hand side of the inequality is integrable on  $[0, +\infty)$ , since  $r$  is bounded on this interval. Then,  $\tau \mapsto \theta(t(\tau))$  is an increasing function, bounded from above on  $[0, +\infty)$ . We conclude that, if  $\beta \geq \frac{3}{2}$  and  $k > 2\sqrt{2}$ , there exists  $\lim_{\tau \rightarrow +\infty} \theta(t(\tau)) = \lim_{t \rightarrow \omega^-} \theta(t) = \theta_\omega$ , and is finite. Moreover, (2.30) implies that  $\lim_{\tau \rightarrow +\infty} \dot{\theta}(t(\tau)) = \lim_{t \rightarrow \omega^-} \dot{\theta}(t) = 0^+$ .

To finish the proof of *i*), we show that, if  $\beta > \frac{3}{2}$ , the restriction on the values of  $k$  may be removed. In fact, one can check that, when  $\beta \neq \frac{3}{2}$ , fixed arbitrarily two different values of  $k$ , the solutions of the two corresponding equations (1.8) can be transformed ones into the others by a suitable scaling of the form  $\tilde{\mathbf{x}}(t) = p\mathbf{x}(qt)$ ,  $p, q > 0$ . In particular, for  $\beta > \frac{3}{2}$ , let us consider  $k = k_1 \leq 2\sqrt{2}$ . Then, the scaling  $\tilde{\mathbf{x}}(t) = p\mathbf{x}(p^{-\frac{3}{2}}t)$ , with  $p > 0$  and  $p^{\beta-\frac{3}{2}} > 2\sqrt{2}/k_1$ , transforms any solution of (1.8) with  $k = k_1$  into a solution of the same equation with  $k = k_2 = p^{\beta-\frac{3}{2}}k_1 > 2\sqrt{2}$ . Since the scaling preserves the asymptotic behavior of the solutions as well as the orientation of time, the proof of *i*) is concluded.

- ii) To study if  $\omega$  is finite or not, it will be convenient to deal directly with system (2.4). As above, without loss of generality, we may assume that  $E(t) < 0$ ,  $0 < r(t) < 1$  on  $[0, \omega)$ . Moreover, since we are considering  $\beta > \frac{3}{2}$  or  $\beta = \frac{3}{2}$  and  $k > 2\sqrt{2}$ , by (2.30) we may assume also  $0 < \varphi(t) = \varphi(\tau(t)) < 1$  on  $[0, \omega)$ .

From the second equation in (2.4) we see that, whenever  $u \geq 0$ , it holds

$$\dot{u} = -k \frac{u}{r^\beta} + r \left( \varphi^2 - \frac{1}{r^3} \right) < -k \frac{u}{r^\beta} + r \left( 1 - \frac{1}{r^3} \right) < 0.$$

Then, there exists  $t_1 \in ]0, \omega)$  such that  $u(t) < 0$  on  $[t_1, \omega)$ . As a consequence,  $r(t)$  is a decreasing function on  $[t_1, \omega)$ , and we can take  $r$  as independent variable by considering the time rescaling  $t = t(r)$ ,  $r \in (0, r_1 := r(t_1)]$ . It follows that  $\omega$  satisfies the equality

$$\omega - t_1 = \int_{r_1}^0 \frac{dr}{u(t(r))}.$$

Since  $r^3 \varphi^2 \rightarrow 0$  as  $t \rightarrow \omega^-$ , we can assume that  $r^3(t) \varphi^2(t) < 1/2$  on  $[t_1, \omega)$ . Then, from (2.4) we get the inequality

$$r^2 \frac{du}{dr} = \frac{r^3 \varphi^2}{u} - \frac{k}{r^{\beta-2}} - \frac{1}{u} > -\frac{k}{r^{\beta-2}} - \frac{1}{2u}. \quad (2.31)$$

Integrating (2.31) on any interval of the form  $[r_*, r_1]$ , with  $0 < r_* < r_1$ , we obtain

$$r_1^2 u(t_1) - r_*^2 u(t(r_*)) - 2 \int_{r_*}^{r_1} r u(t(r)) dr > -k \int_{r_*}^{r_1} \frac{dr}{r^{\beta-2}} - \frac{1}{2} \int_{r_*}^{r_1} \frac{dr}{u(t(r))}. \quad (2.32)$$

By the inequality  $u^2 r < 2$ , it follows that, for all  $\gamma > 1/2$ ,  $ur^\gamma \rightarrow 0$  as  $r \rightarrow 0^+$ . Then, the left hand side of (2.32) has a finite limit, say  $l^*$ , when  $r_* \rightarrow 0^+$ . Passing to the limit in (2.32), we arrive to the following inequality:

$$l^* > -k \int_0^{r_1} \frac{dr}{r^{\beta-2}} + \frac{1}{2}(\omega - t_1).$$

Now, if  $\beta < 3$ , the integral is convergent, and then it must be  $\omega < +\infty$ .

In the case  $\beta \geq 3$ , we can proceed analogously, by integrating on the interval  $[r_*, r_1]$  the inequality

$$r^2 \frac{du}{dr} = \frac{r^3 \varphi^2}{u} - \frac{k}{r^{\beta-2}} - \frac{1}{u} < -\frac{k}{r^{\beta-2}} - \frac{1}{u},$$

and then taking the limit as  $r_* \rightarrow 0^+$ . We obtain the inequality

$$l_* < -k \int_0^{r_1} \frac{dr}{r^{\beta-2}} + (\omega - t_1),$$

where  $l_*$  denotes the finite limit of the left hand side of the integrated inequality. Since when  $\beta \geq 3$  the integral is divergent, it must be  $\omega = +\infty$ .

The proof of *ii)* is concluded.

- iii)* We know that, if  $\beta > \frac{3}{2}$ , or if  $\beta = \frac{3}{2}$  and  $k > 2\sqrt{2}$ , the limit velocity at collisions depends only on the radial component  $u$ , because the angular component  $r\varphi$  goes to zero. Additionally, in the previous item it was proved that  $u$  gets eventually negative.

To prove our claims we will use the second equation of system (2.26). Note that  $r^{\beta+1}\varphi^2 \rightarrow 0$  as  $r \rightarrow 0^+$  for any  $\beta > 0$ , but the behavior of the term  $r^{\beta-2}$  will depend on the sign of  $\beta - 2$ .

If  $\beta < 2$ , we have that  $r^{\beta-2} \rightarrow +\infty$  as  $r \rightarrow 0^+$ . Then, for any  $a > 0$ , we can take initial conditions such that, for all  $\tau > 0$ ,

$$\frac{du}{d\tau} = -ku + r^{\beta+1}\varphi^2 - r^{\beta-2} < -ku - a,$$

or, equivalently,

$$\frac{d}{d\tau} (ue^{k\tau}) < -ae^{k\tau}.$$

Integrating this inequality we get

$$u(t(\tau)) < -\frac{a}{k} + \left(u(0) + \frac{a}{k}\right) e^{-k\tau},$$

which implies

$$\limsup_{\tau \rightarrow +\infty} u(t(\tau)) \leq -\frac{a}{k}.$$

Since  $a$  can be chosen arbitrary large, we conclude that  $u \rightarrow u_\omega = -\infty$ .

On the other hand, if  $\beta > 2$ , we have that  $r^{\beta-2} \rightarrow 0$  as  $r \rightarrow 0^+$ . Then, for any  $a > 0$  we can take initial conditions such that, for all  $\tau > 0$ ,

$$\frac{du}{d\tau} = -ku + r^{\beta+1}\varphi^2 - r^{\beta-2} > -ku - a.$$

Analogously to the previous case, we conclude that

$$-\frac{a}{k} \leq \liminf_{\tau \rightarrow +\infty} u(t(\tau)) \leq 0,$$

for any arbitrarily small  $a$ . Then,  $u \rightarrow u_\omega = 0$ .

Finally, for the threshold value  $\beta = 2$ , since  $r^3\varphi^2 \rightarrow 0$ , fixed any arbitrarily small positive  $\epsilon$ , we can use the inequality  $0 < r^3\varphi^2 < \epsilon$  in the second equation of (2.26). We obtain, in a similar manner than above, that

$$-\frac{1}{k} \leq \liminf_{\tau \rightarrow +\infty} u(t(\tau)) \leq \limsup_{\tau \rightarrow +\infty} u(t(\tau)) \leq -\frac{1-\epsilon}{k},$$

which leads to the conclusion that  $u \rightarrow u_\omega = -1/k$ .

■

### 2.2.3 Rectilinear motions

In order to give a more complete description of the forward dynamics of (1.8), in this subsection we address the rectilinear collisions of (1.8).

We recall that the rectilinear motions of (1.8) verify the second order equation

$$\ddot{r} + k \frac{\dot{r}}{r^\beta} + \frac{1}{r^2} = 0, \quad (2.33)$$

equivalent to the following first order system (which, of course, corresponds to the first two equations of system (2.4) with  $\varphi = 0$ ),

$$\begin{cases} \dot{r} = u \\ \dot{u} = -k \frac{u}{r^\beta} - \frac{1}{r^2}, \end{cases} \quad (2.34)$$

on the phase space  $\Omega^0 = \{(r, u) : r > 0, u \in \mathbb{R}\}$ .

We have the following result.

**Theorem 2.7.** *The terminal time  $\omega$ , the terminal velocity  $u_\omega$  and the terminal energy  $E_\omega$  of collision solutions depend on  $\beta$  according to the following table:*

$\beta$	$]0, 1/2[$	$[1/2, 2[$	$2$	$]2, 3[$	$[3, \infty[$
$\omega$	finite				$+\infty$
$u_\omega$	$-\infty$		$-\frac{1}{k}$	0	
$E_\omega$	finite	$-\infty$			

**Proof.** This proof borrows some ideas from the ones of Proposition 2.4 in [83] and of Proposition 3.1 in [81], mainly in Case I. The corresponding steps are presented below with less detail.

We recall that our phase space is the half-plane  $\Omega^0 = \{(r, u) : r > 0, u \in \mathbb{R}\}$ . The isocline of system (2.34) associated to  $\dot{r} = 0$  is the half line defined by  $u = 0$ , whereas for  $\dot{u} = 0$  the isocline is defined by

$$u = -\frac{r^{\beta-2}}{k}.$$

These curves determine the following disjoint open regions in the phase space:

$$\begin{aligned} A_0 &= \{(r, u) \in \Omega^0 : u > 0\}, & A_1 &= \{(r, u) \in \Omega^0 : 0 > k u > -r^{\beta-2}\}, \\ A_2 &= \{(r, u) \in \Omega^0 : k u < -r^{\beta-2}\}. \end{aligned} \quad (2.35)$$

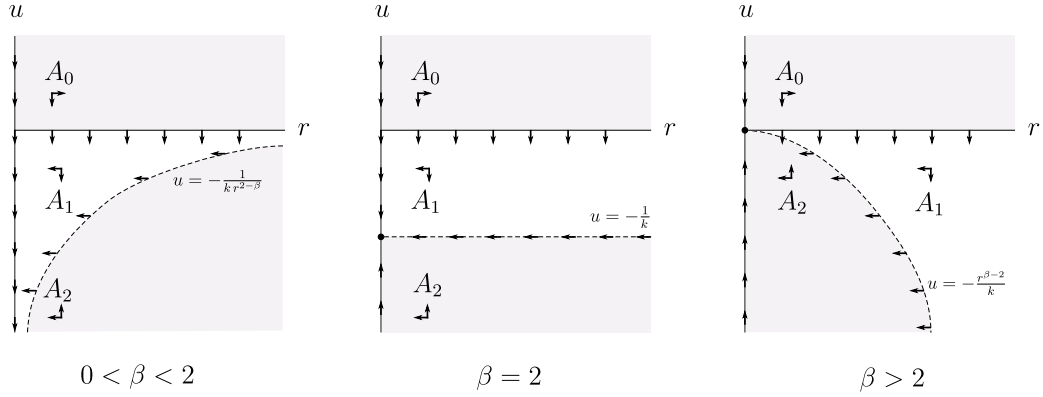


Figure 2.1: Dependence on  $\beta$  of the regions defined by the isoclines in the regularized systems.

The set  $A_0$  is negatively invariant with respect to the flow of (2.34) for all  $\beta > 0$ , whereas for  $\beta \in (0, 2)$ ,  $A_1$  is positively invariant and  $A_2$  is negatively invariant. For  $\beta > 2$ , the set  $A_2$  is positively invariant. We distinguish three cases.

**Case 1:**  $\beta \in (0, 2)$ .

We prove first that  $\omega$  is finite. If it were infinite, there should exist a sequence  $t_n \rightarrow +\infty$  such that  $u(t_n) \rightarrow 0$ . However, this is not possible, because one can easily check that all collision solutions enter eventually into the positively invariant set  $A_1$ , where  $u = \dot{r}$  is negative and decreasing.

In what follows, we consider the regularization of system (2.34) given by the time rescaling  $d\mu = \frac{dt}{r^2}$ , already considered in the proof of Theorem 2.5. Of course, we obtain a system made by the first two equations of (2.24) with  $\varphi \equiv 0$ , namely,

$$\begin{cases} \frac{dr}{d\mu} = r^2 u, \\ \frac{du}{d\mu} = -k r^{2-\beta} u - 1. \end{cases} \quad (2.36)$$

System (2.36) is defined in the extended phase space  $\bar{\Omega}^0 = \Omega^0 \cup \{(r, u) : r = 0, u \in \mathbb{R}\}$  and the line  $r = 0$  is an isocline orbit associated to  $\frac{dr}{d\mu} = 0$  (see the left panel of Figure 2.1).

Let us prove now that, when  $\beta \in (0, 2)$ , the velocity at collision satisfies  $u_\omega = -\infty$ . We argue by contradiction. Assume that  $\mu \mapsto (r(\mu), u(\mu))$  is a collision solution such that  $u_\omega \in (-\infty, 0)$ . We can take initial conditions  $(r(0), u(0)) \in A_1$  so that  $u(\mu)$  is negative for all  $\mu > 0$ . Then, from the first equation of (2.36), we see that



$$\frac{1}{r(\mu)} = \frac{1}{r(0)} + \int_0^\mu |u(\sigma)| d\sigma. \quad (2.37)$$

Letting  $\mu \rightarrow \mu_\omega$ , we have that the left hand side tends to  $+\infty$ , and since  $u(\tau)$  is bounded on  $[0, \mu_\omega)$ , from (2.37) we get  $\mu_\omega = +\infty$ . But then, from the second equation of (2.36), it follows that

$$\lim_{\mu \rightarrow +\infty} \frac{du}{d\mu} = -1,$$

and this would imply that  $u_\omega = -\infty$ , contradicting the hypothesis that  $u_\omega$  is finite. We conclude that  $u_\omega = -\infty$ .

Now let us see how the energy behaves when an orbit approaches the collision.

Consider first the case  $\beta \in (0, 1)$ . System (2.36) has the first integral

$$H(r, u, \mu) = u + \frac{k}{1-\beta} r^{1-\beta} + \mu, \quad (2.38)$$

obtained by setting  $\varphi \equiv 0$  in (2.25).

Let  $(r_0, u_0)$  be an initial condition in  $A_1$ , and let  $H_0 := H(r_0, u_0, 0)$ , so that by (2.38) we have

$$u(\mu) + \frac{k}{1-\beta} r^{1-\beta}(\mu) + \mu = H_0. \quad (2.39)$$

Since  $u(\mu) \rightarrow -\infty$  and  $r(\mu) \rightarrow 0$  as  $\mu \rightarrow \mu_\omega$ , from (2.39) we infer that  $\mu_\omega = +\infty$ . Then, from the same equality it follows that  $\frac{u(\mu)}{\mu} \rightarrow -1$  as  $\mu \rightarrow +\infty$ , and from (2.37) we get that  $\mu^2 r(\mu) \rightarrow 2$  as  $\mu \rightarrow +\infty$ .

By (2.2), we see that  $\frac{dE}{d\mu} = r^2 \frac{dE}{dt} = -k r^{2-\beta} u^2$ . Then, using the two limits established above for  $u$  and  $r$ , we get that

$$\mu^{2(1-\beta)} \frac{dE}{d\mu}(\mu) \rightarrow -2^{2-\beta} k,$$

as  $\mu \rightarrow \infty$ . As a consequence,

$$E_\omega = E(0) + \int_0^\infty \frac{dE}{d\mu}(\sigma) d\sigma$$

is finite if  $\beta \in (0, 1/2)$ , whereas  $E_\omega = -\infty$  if  $\beta \in [1/2, 1)$ .

Let us consider now  $\beta \in [1, 2)$ .

In this case the approach through the first integral (given by  $H = u + k \log r + \mu$ , when  $\beta = 1$ , and by (2.38), when  $\beta > 1$ ) does not allow to find out the asymptotic expansion of the solutions as they approach collision.

However, we argue as follows. It is easy to see that in  $A_1$  the trajectories of system (2.36) may be written in the form  $u = \chi(r)$ ,  $r \in (0, r_0]$ . If we evaluate the slope of such orbits at the points of the form  $u = -r^{\beta-1}$ , we get

$$\left. \frac{du}{dr} \right|_{u=-r^{\beta-1}} = \frac{1}{r^\beta} \left( \frac{1}{r} - k \right),$$

which is positive for  $0 < r < 1/k$ . This implies that the region

$$D := \left\{ (r, u) : 0 < r < \frac{1}{k}, -\frac{1}{kr^{2-\beta}} < u < -r^{\beta-1} \right\} \subset A_1$$

is positively invariant. On the other hand, note that

$$\frac{dE}{dr} = \frac{1}{u} \frac{dE}{dt} = -k \frac{u}{r^\beta} > 0.$$

Then, for every orbit  $u = \chi(r)$  such that  $(r_0, \chi(r_0)) \in D$ , as a consequence of the invariance of  $D$ , we have

$$\frac{k}{r} < \left. \frac{dE}{dr} \right|_{u=\chi(r)} < \frac{1}{r^2},$$

and we conclude that

$$E_\omega = E(0) + \int_{r_0}^0 \left. \frac{dE}{dr} \right|_{u=\chi(r)} dr = -\infty.$$

**Case 2:**  $\beta = 2$ .

This case is solved in [39]. The explicit solution is given by

$$u(\mu) = \left( u_0 + \frac{1}{k} \right) e^{-k\mu} - \frac{1}{k}, \quad \frac{1}{r(\mu)} = \frac{1}{r(0)} - \int_0^\mu u(\sigma) d\sigma, \quad \mu \in [0, \infty).$$

From these expressions it is easy to see that  $\omega < +\infty$ ,  $u_\omega = -1/k$  and  $E_\omega = -\infty$ .

**Case 3:**  $\beta > 2$ .

In order to study the collisions for  $\beta > 2$ , it is convenient to consider the time rescaling  $d\tau = \frac{dt}{r^\beta}$ , introduced previously to get system (2.26). We obtain the following regular system, which corresponds to the first two equations of (2.26) with  $\varphi \equiv 0$ ,

$$\begin{cases} \frac{dr}{d\tau} = r^\beta u \\ \frac{du}{d\tau} = -k u - r^{\beta-2}, \end{cases} \quad (2.40)$$

on the extended phase space  $\bar{\Omega}^0$ .

We note that the origin is an equilibrium of system (2.40) which attracts the points of the invariant line  $r = 0$  (see the right panel of Figure 2.1).

One can see easily that all collision orbits will enter eventually in the positively invariant region  $A_2$ . Then, without loss of generality, we will consider only initial conditions in  $A_2$ . Actually, since in this region we have  $\frac{du}{d\tau} > 0$  and  $\frac{dr}{d\tau} < 0$ , all solutions are bounded on  $[0, \tau_\omega)$ . This fact implies that all solutions starting in  $A_2$  are collision ones, since otherwise an equilibrium of the system should exist in  $A_2$ . Moreover, any segment of orbit contained in  $A_2$  may be expressed in the form  $u = \chi(r)$ , with  $r$  in a suitable interval of the form  $(0, \tilde{r})$ , with  $0 < r_0 < \tilde{r}$ . Notice that, on this interval,  $\chi(r)$  satisfies the scalar differential equation

$$\frac{du}{dr} := f(r, u) = -\frac{k}{r^\beta} - \frac{1}{r^2 u}. \quad (2.41)$$

When  $\beta \geq 3$  the vector field associated to (2.40) is continuously differentiable on  $\bar{\Omega}^0$  and, by the general theory of ODEs, we conclude that all solutions starting in  $A_2$  tend to the equilibrium  $(0, 0)$  in infinite  $\tau$  time. We conclude that  $u_\omega = 0$ .

This cannot be guaranteed without further considerations for  $\beta \in (2, 3)$ . In fact, in this range of values the regularized vector field is not Lipschitz continuous in the points of the form  $(0, u) \in \bar{\Omega}^0$ . As a consequence, in such points uniqueness of solutions may fail, and all we can conclude by the general theory is that, for collision solutions, we have  $-\infty < u_\omega \leq 0$ . Let us prove that, actually,  $u_\omega = 0$ . Define the function  $h_\lambda(r) := -\lambda r^{\beta-2}$ , where  $\lambda > 1/k$ . Note that  $A_2 = \cup_{\{\lambda > 1/k\}} \{(r, h_\lambda(r)) : r > 0\}$ . Evaluating the slope field  $du/dr$  at  $u = h_\lambda(r)$ , we get

$$\left( \frac{du}{dr} \Big|_{h_\lambda} \right) / \frac{dh_\lambda}{dr} = \frac{k\lambda - 1}{\lambda^2(\beta - 2)r^{2\beta-3}}. \quad (2.42)$$

Hence, for any fixed  $\lambda > 1/k$  there exists only one point  $r = r_\lambda$  such that the graph of the function  $h_\lambda(r)$  is tangent to an orbit, and is given by

$$r_\lambda := \left( \frac{k\lambda - 1}{\lambda^2(\beta - 2)} \right)^{\frac{1}{2\beta-3}}. \quad (2.43)$$

Moreover, by (2.42) it follows that

$$\frac{dh_\lambda}{dr} \leq f(r, h_\lambda(r)), \quad \text{if } r \geq r_\lambda. \quad (2.44)$$

As a consequence, by the comparison theorem for ODEs, the orbit  $u = \chi(r)$  of (2.41) that is tangent to the curve  $u = h_\lambda(r)$  in  $r = r_\lambda$  satisfies

$$\chi(r) \geq h_\lambda(r),$$

for any  $r \in (0, r_\lambda)$ .

Note that (2.43) is a second degree equation in  $\lambda$ . Solving it, we obtain two local inverses of the function  $\lambda \mapsto r_\lambda$ , namely the functions

$$\lambda_\pm(r) := \frac{1}{r^{2\beta-3}} \frac{k \pm \sqrt{k^2 - 4(\beta-2)r^{2\beta-3}}}{2(\beta-2)},$$

defined for  $0 < r \leq R$ , where

$$R := \left( \frac{k^2}{4(\beta-2)} \right)^{\frac{1}{2\beta-3}}.$$

Now we use  $\lambda_\pm(r)$  to construct the two following auxiliary functions:

$$h_\pm(r) = h_{\lambda_\pm(r)}(r) := -\frac{1}{r^{\beta-1}} \frac{k \pm \sqrt{k^2 - 4(\beta-2)r^{2\beta-3}}}{2(\beta-2)},$$

also defined for  $0 < r \leq R$ .

The functions  $h_+$  and  $h_-$  satisfy the following properties. They are, respectively, strictly decreasing and strictly increasing on  $(0, R]$ , and such that  $h_-(r) > h_+(r)$  on  $(0, R)$ , with  $h_-(R) = h_+(R) := u_R$ . Moreover, they have the following behavior as  $r \rightarrow 0^+$ :

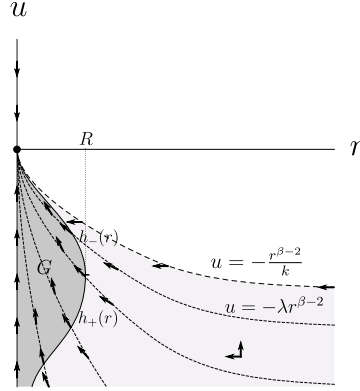
$$h_-(r) = -\frac{r^{\beta-2}}{k} + o(r^{\beta-2}) \rightarrow 0 \text{ and } h_+ \rightarrow -\infty. \quad (2.45)$$

Finally, the range of  $h_+$  is  $(-\infty, u_R]$ , and the one of  $h_-$  is  $[u_R, 0)$ . We are now ready to prove that on collision orbits  $u_\omega = 0$ .

We start by defining the positively invariant set

$$G := \{(r, u) : 0 < r \leq R, h_+(r) \leq u \leq h_-(r)\} \subset A_2.$$

Given an initial condition  $(r_0, u_0) \in G$ , let us consider the corresponding orbit  $u = \chi(r)$ ,  $r \in (0, \tilde{r})$ . Since there exists a value  $\lambda > 1/k$  such that  $h_-(r) > \chi(r) > -\lambda r^{\beta-2}$  for all  $0 < r < R$ , we conclude that the orbit will go towards the equilibrium as  $r \rightarrow 0^+$ . If  $(r_0, u_0) \in A_2 \setminus G$  the corresponding orbit will eventually enter in  $G$ . In fact, if there exists an orbit  $u = \bar{\chi}(r)$  for which this is not the case, we can find  $\bar{\lambda} = \lambda_-(\tilde{r})$  such that  $u = h_{\bar{\lambda}}(r)$  intersects  $u = \bar{\chi}(r)$  in a point  $\hat{r} > \tilde{r}$  for which it holds the inequality  $\frac{dh_{\bar{\lambda}}}{dr}(\hat{r}) > f(\hat{r}, h_{\bar{\lambda}}(\hat{r}))$ . By

Figure 2.2: Illustration of the proof for  $\beta \in (2, 3)$ .

(2.44), there exists a second point,  $r_* > \hat{r} > \bar{r}$ , such that the curve  $u = h_{\bar{\chi}}(r)$  is tangent to an orbit (the first being  $\bar{r}$ ), which is absurd.

Then,  $u_\omega = 0$  for all collision orbits also for  $\beta \in (2, 3)$ . Taking into account what was proved previously, we conclude that  $u_\omega = 0$  for any  $\beta > 2$ . It follows immediately that the energy  $E = u^2/2 - 1/r$  tends to  $E_\omega = -\infty$ .

Also, since

$$\omega = \int_{r_0}^0 \frac{dr}{\chi(r)}, \quad (2.46)$$

by (2.45) and by the inequality  $-\lambda r^{\beta-2} < \chi(r) < h_-(r)$  for any  $r \in (0, R)$ , we see that  $1/|\chi(r)|$  is integrable on the interval  $(0, r_0]$  if  $\beta \in (2, 3)$ , in which case  $\omega$  is finite, whereas it is not integrable if  $\beta \geq 3$ , and then  $\omega = +\infty$ . Our proof is concluded. ■

From Theorem 2.7, we see that, when  $\beta \in (0, \frac{1}{2})$ , the collision time, as well as the corresponding energy, are finite. It is not difficult to prove that also the ejection time and ejection energy<sup>2</sup> are finite. These properties are sufficient to infer that the asymptotic expansions of solutions around collision and ejection times obtained in [81] for  $\beta = 0$  are still valid for  $\beta \in (0, \frac{1}{2})$ . Namely, at collision we have

$$r(t) = \left(\frac{9}{2}\right)^{1/3} (\omega - t)^{2/3} + O((\omega - t)^{4/3}), \quad t \rightarrow \omega^-, \quad (2.47)$$

$$\dot{r}(t) = -\frac{2}{3} \left(\frac{9}{2}\right)^{1/3} (\omega - t)^{-1/3} + O((\omega - t)^{1/3}), \quad t \rightarrow \omega^-. \quad (2.48)$$

<sup>2</sup>An ejection solution is a solution such that  $\lim_{t \rightarrow \alpha^+} \mathbf{x}(t) = 0$ , and  $\alpha$  is the ejection time.

The analogous expansion at ejection is obtained just by replacing  $\omega - t$  with  $t - \alpha$  and by reversing the sign of  $\dot{r}$  in (2.48). We point out that these expansions hold also for the rectilinear motions of a periodically forced Kepler problem ([102]), as well as for a perturbed two body problem, with a perturbation of the form  $P(t, \mathbf{x}, \dot{\mathbf{x}})$ , which, unlike in our case, is bounded ([116]).

However, unlike in the case of the linear drag, when  $\beta \in (0, \frac{1}{2})$  the ejection-collision solutions cannot be embedded in a regular flow. Let us explain this point. The Levi-Civita transformation, developed in the conservative setting, was used effectively in [81] to regularize the dynamics of (1.8) for  $\beta = 0$ . But, for  $\beta > 0$ , the natural generalization of this transformation leads to a system that, although non singular, does not define a flow. To show this, consider the Levi-Civita-like transformation  $\mathbf{x} = x_1 + ix_2 = w^2$ ,  $d\nu = \frac{dt}{|\mathbf{x}|^{\beta+1}}$  (the classical Levi-Civita transformation corresponds to  $\beta = 0$ ). This transformation maps solutions of (1.8) into solutions of the non singular system

$$\frac{dw}{d\nu} = |w|^{2\beta}v, \quad \frac{dv}{d\nu} = \frac{E}{2}|w|^{2\beta}w - |w|^2v, \quad \frac{dE}{d\nu} = -(2E|w|^2 + 1) \quad (2.49)$$

contained in the invariant manifold  $\mathcal{M} \subset \mathbb{C}^2 \times \mathbb{R}$  of equation  $E|w|^2 + 1 - 2|v|^2 = 0$ .

We notice that an ejection-collision solution,  $t \mapsto r(t)$ , defined on the maximal finite interval  $(\alpha, \omega)$  is transformed into a solution  $\nu \mapsto \Xi(\nu) = (w(\nu), v(\nu), E(\nu))$  of (2.49), defined on the finite, but not maximal, interval

$$I_S = \left( \nu_\alpha := - \int_\alpha^0 \frac{1}{r^{\beta+1}(\sigma)} d\sigma, \nu_\omega := \int_0^\omega \frac{1}{r^{\beta+1}(\sigma)} d\sigma \right).$$

A maximal solution of (2.49) which extends  $\Xi$  outside  $I_S$  is obtained by considering the function  $\Xi_\alpha(\nu) := \left(0, \frac{1}{\sqrt{2}}, E_\alpha - \nu + \nu_\alpha\right)$  on  $(-\infty, \nu_\alpha)$ , where  $E_\alpha$  is the energy at ejection, and the function  $\Xi_\omega(\nu) := \left(0, -\frac{1}{\sqrt{2}}, E_\omega - \nu + \nu_\beta\right)$  on  $[\nu_\omega, +\infty)$ . Since  $\Xi_\alpha(\nu)$ ,  $\nu \in \mathbb{R}$ , is also a maximal solution of (2.49), it follows that uniqueness of solutions fails at the point  $(0, \frac{1}{\sqrt{2}}, E_\alpha)$ .

This behavior agrees with the fact that, when  $\beta \in (0, \frac{1}{2})$ , the regularized vector field is not locally Lipschitz continuous at points of the form  $(0, v, E)$  with  $v \neq 0$ .

In a conservative setting, the study of the existence of a regularized flow by means of a change of variables analogous to the Levi-Civita transformation has been considered in [87].

## 2.3 The asymptotic Runge-Lenz vector for $\beta = 2$

In this section we consider the case of the Poynting-Plummer-Danby drag. We show that a careful analysis of equation (2.22) allows a complete description of the orbit structure for such a case, improving the results in [39]. Such description will be contained in the main result of this section, where we discuss the properties of the limit  $\mathbf{I}$  of the Runge-Lenz vector

$$\mathbf{R}(\mathbf{x}, \mathbf{v}) = \mathbf{v} \wedge (\mathbf{x} \wedge \mathbf{v}) - \frac{\mathbf{x}}{|\mathbf{x}|}$$

along the solutions of (1.8) with  $\beta = 2$ . We recall that  $\mathbf{R}$  is a first integral of the classical Kepler problem, with the following geometrical meaning: for non rectilinear orbits, which are conic sections,  $\mathbf{R}$  is parallel to the symmetry axis which contains the focus, and its modulus is the eccentricity of the orbit. For this reason it is also referred to as eccentricity vector.

The vector  $\mathbf{I}$ , which can be thought of as an asymptotic eccentricity vector, was considered in [82] to study the dynamics of (1.8) when  $\beta = 0$  (see Remark 2.3 below). In our case, its properties will be obtained by taking the limit of  $\mathbf{R}$  along the solutions of (2.19) and then going back to the  $(\mathbf{x}, \mathbf{v})$  variables. This is equivalent to take the limit of  $\mathbf{R}$  along the flow of (2.1). In fact, if  $\gamma^\theta$  denotes the flow of (2.19), we have

$$\phi^t = U \circ \gamma^\theta \circ U^{-1}, \quad (2.50)$$

where  $U$  was defined in (2.20) and  $t$  and  $\theta$  are explicitly related by  $t = t(\theta, y) = \int_{\theta_0}^\theta \lambda(\gamma^\sigma(y)) d\sigma$ , with  $\lambda(y) = \frac{1}{\rho^2 M}$ . The pair  $(U, \lambda)$  establishes the so called equivalence in the extended sense of the vector fields (2.1) and (2.19), see [95].

**Theorem 2.8.** *There exists a vector field*

$$\mathbf{I} : \Omega \rightarrow \mathbb{R}^2, \quad \mathbf{I} = \mathbf{I}(\mathbf{x}, \mathbf{v}),$$

*satisfying*

*i)  $\mathbf{I}(\sigma\mathbf{x}, \sigma\mathbf{v}) = \sigma\mathbf{I}(\mathbf{x}, \mathbf{v})$ , for each  $(\mathbf{x}, \mathbf{v}) \in \Omega$  and each rotation*

$$\sigma = \begin{pmatrix} \cos \theta & -\sin \theta \\ \sin \theta & \cos \theta \end{pmatrix}.$$

- ii)  $\mathbf{I}$  is smooth on the sets  $\Omega_H^+$  and  $\Omega_C^+$ , corresponding, respectively, to hyperbolic and collision orbits, and is discontinuous on the set  $\Omega_P^+$ , corresponding to parabolic orbits.

Moreover,

$$\mathbf{I}(\Omega) = \mathbb{R}^2 \setminus \text{int}(\mathbb{D}),$$

where  $\mathbb{D}$  is the closed unit disk in  $\mathbb{R}^2$ .

- iii) Each solution  $t \mapsto (\mathbf{x}(t), \mathbf{v}(t))$  of (2.1) with  $\beta = 2$ , defined on the right maximal interval  $[0, \omega)$ , satisfies

$$\mathbf{I}(\mathbf{x}(t'), \mathbf{v}(t')) = \lim_{t \rightarrow \omega^-} \mathbf{R}(\mathbf{x}(t), \mathbf{v}(t))$$

for each  $t' \in [0, \omega)$ .

**Remark 2.3.** This theorem is analogous to Theorem 2.1 in [82], where the properties of  $\mathbf{I}$  for  $\beta = 0$  are considered. In particular, in [82] it is found that  $\mathbf{I}$  is continuous on  $\Omega$ . Moreover, taking also into account an improvement of Theorem 4.2 presented in [83], it is established that the range of  $\mathbf{I}$  is the closed unit disk. When  $\beta = 2$ , item ii) shows that  $\mathbf{I}$  has significantly different properties:  $\mathbf{I}$  is not continuous on  $\Omega$ , and its range is the exterior of the open unit disk. We will see that the discontinuity arises along any fixed parabolic orbit since such orbit is the limit of hyperbolic orbits and of collision ones. We prove this fact only for  $\beta = 2$ , because in this case the problem is integrable, and we could make use of explicit closed formulas in our computations. As to the range of  $\mathbf{I}$ , it somewhat expresses that, unlike the case  $\beta = 0$ , there are parabolic and hyperbolic orbits, and there are no elliptic motions winding infinite times around the singularity as they approach it.

**Proof.**

We start by proving that  $\mathbf{I}$ , as defined in iii), exists on  $\Omega^+$  and that the properties stated in ii) hold. To carry out our analysis we will use the Binet variables. Consider the initial condition

$$(\mathbf{x}_0, \mathbf{v}_0) = U(\rho_0, \zeta_0, \theta_0, M_0) = \left( \frac{1}{\rho_0} e_r(\theta_0), -\zeta_0 M_0 e_r(\theta_0) + \rho_0 M_0 e_\theta(\theta_0) \right) \in \Omega^+,$$

and consider the corresponding solution of system (2.19), given by (2.21), (2.22) and (2.23), with  $\beta = 2$ . In this case

$$M(\theta) = M_0 - k(\theta - \theta_0) = k(\theta_M - \theta + \theta_0),$$

where  $\theta_M = M_0/k$ , and we have the following explicit formula:



$$\rho(\theta) = -\kappa \sin(\theta - \alpha_0 - \theta_0) + \int_{\theta_0}^{\theta} \frac{\sin(\theta - \eta)}{k^2(\theta_M - \eta + \theta_0)^2} d\eta. \quad (2.51)$$

Collision solutions correspond to  $\theta_\omega = \theta_M$ , and are such that

$$\rho(\theta) > 0, \quad \theta \in [\theta_0, \theta_\omega), \quad \rho(\theta_\omega^-) = +\infty.$$

Escape solutions correspond to  $\theta_\omega < \theta_M$ , and satisfy

$$\rho(\theta) > 0, \quad \theta \in [\theta_0, \theta_\omega), \quad \rho(\theta_\omega^-) = 0.$$

By Theorem 2.4, we also know that for escapes  $\theta_\omega \in (\theta_0 + \alpha_0, \theta_0 + \alpha_0 + \pi)$ . If we define the set

$$A = \{(\theta, \theta_M) : \theta_0 < \theta < \theta_0 + \theta_M, \theta_0 + \alpha_0 \leq \theta \leq \theta_0 + \alpha_0 + \pi\}$$

and the smooth family of functions  $F_{\rho_0, \zeta_0, \theta_0} : A \rightarrow \mathbb{R}$ ,

$$F_{\rho_0, \zeta_0, \theta_0}(\theta, \theta_M) := \rho(\theta) = -\kappa \sin(\theta - \alpha_0 - \theta_0) + \int_{\theta_0}^{\theta} \frac{\sin(\theta - \eta)}{k^2(\theta_M - \eta + \theta_0)^2} d\eta, \quad (2.52)$$

then the limit angle  $\theta_\omega$  of an escape orbit will satisfy the implicit equation

$$F_{\rho_0, \zeta_0, \theta_0}(\theta_\omega, \theta_M) = 0.$$

We will show below that this equation defines implicitly  $\theta_\omega$  as a function of  $y_0 = U^{-1}(\mathbf{x}_0, \mathbf{v}_0)$  which is continuous in  $\Omega_H^+ \cup \Omega_P^+$  and smooth on  $\Omega_H^+$ .

For simplicity, in what follows we omit the dependence on the parameters of  $F$  and of the functions implicitly defined. We also set  $\theta_0 = 0$  for our computations, but will remove this restriction in our conclusions.

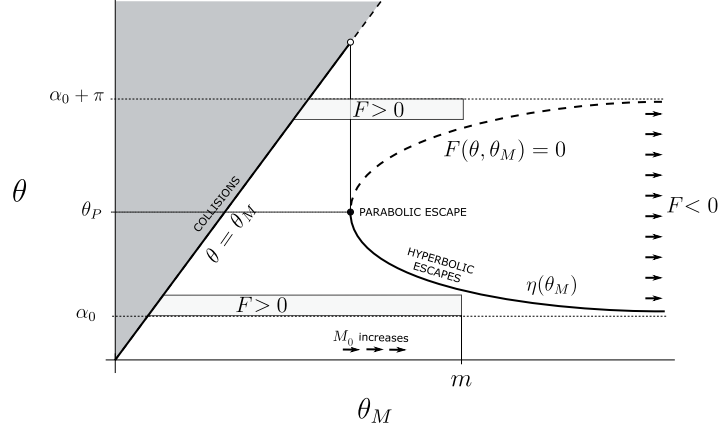
In the same way we proved that  $\Phi(\theta) > 0$  in  $i)$  of Lemma 2.2, we obtain the inequality

$$\partial_{\theta_M} F(\theta, \theta_M) = -2 \int_0^{\theta} \frac{\sin(\theta - \eta)}{k^2(\theta_M - \eta)^3} d\eta < 0,$$

so that for each fixed  $\theta \in (0, \theta_M) \cap [\alpha_0, \alpha_0 + \pi]$ , the map  $\theta_M \mapsto F(\theta, \theta_M)$  is strictly decreasing on  $(\theta, +\infty)$ . For each  $\theta \in (\alpha_0, \alpha_0 + \pi)$  we have

$$\lim_{\theta_M \rightarrow \infty} F(\theta, \theta_M) = -\kappa \sin(\theta - \alpha_0) < 0, \quad (2.53)$$

and since


 Figure 2.3: Discontinuity of  $\theta_\omega$  : graphical illustration of the proof.

$$\frac{\sin(\theta_M - \eta)}{(\theta_M - \eta)^2} = \frac{1}{\theta_M - \eta} + O((\theta_M - \eta)^2),$$

we get

$$\lim_{\theta \rightarrow \theta_M^-} F(\theta, \theta_M) = +\infty,$$

for any fixed  $\theta_M > \alpha_0$ . By Bolzano's theorem and the implicit function theorem, there exists a smooth function  $\theta_M = \psi(\theta)$  defined on  $(\alpha_0, \alpha_0 + \pi)$  such that  $F(\theta, \psi(\theta)) = 0$ .

From (2.52) and *i*) of Lemma 2.2, it follows that  $F(\alpha_0, \theta_M) > 0$  and  $F(\alpha_0 + \pi, \theta_M) > 0$ . Then, fixed any  $m > 0$ , there exists  $\delta > 0$  such that  $F > 0$  on  $([\alpha_0, \alpha_0 + \delta] \times [0, m]) \cap A$  and on  $([\pi + \alpha_0 - \delta, \pi] \times [0, m]) \cap A$ , see Figure 2.3. From (2.53) we conclude that

$$\lim_{\theta \searrow \alpha_0} \psi(\theta) = \lim_{\theta \nearrow \alpha_0 + \pi} \psi(\theta) = +\infty,$$

and as a consequence  $\psi(\theta)$  has at least a minimum. Actually, for all  $\theta$  such that  $\psi'(\theta) = 0$ , we have

$$\psi''(\theta) = -\frac{\partial_\theta^2 F(\theta, \psi(\theta))}{\partial_{\theta_M} F(\theta, \psi(\theta))} > 0,$$

since  $\partial_{\theta_M} F(\theta, \psi(\theta)) < 0$  and  $\partial_\theta^2 F(\theta, \psi(\theta)) = \frac{1}{k^2(\psi(\theta) - \theta)^2} > 0$ . Then, the minimum point, say  $\theta = \theta_P$ , is unique and it is the only critical point of  $\psi$ . The subscript indicates that the minimum point is associated to a parabolic escape, as we will see.

It follows that  $\psi$  admits a decreasing left inverse  $\eta : [\psi(\theta_P), +\infty) \rightarrow (\alpha_0, \theta_P]$ , which is continuous on  $[\psi(\theta_P), +\infty)$  and smooth on  $(\psi(\theta_P), +\infty)$ .

Fixed  $\theta_M \in [\psi(\theta_P), +\infty)$ , the angle  $\theta_\omega = \eta(\theta_M) \in (\alpha_0, \theta_P]$  is the limit angle of the escape solution  $\theta \mapsto \rho(\theta) = F_{\rho_0, \zeta_0, 0}(\theta, \theta_M)$ ,  $\theta \in [0, \theta_\omega)$ , corresponding to initial conditions  $(\rho_0, \zeta_0, 0, M)$ . We notice that if  $\theta_M \in [\psi(\theta_P), +\infty)$ , it is

$$\zeta(\theta_\omega) = \rho'(\theta_\omega) = \partial_\theta F(\theta_\omega, \psi(\theta_M)) \leq 0,$$

where the equality holds if and only if  $\theta_\omega = \theta_P$ . By definition of  $U$ , we have

$$v = -\zeta M e_r(\theta) + \rho M e_\theta(\theta).$$

We infer that, if  $\theta_M > \psi(\theta_P)$ , the corresponding orbit is hyperbolic, since the terminal velocity  $v_\omega$  satisfies

$$v_\omega = -\zeta(\theta_\omega) M(\theta_\omega) e_r(\theta_\omega) \neq 0, \quad M(\theta_\omega) > 0,$$

whereas, if  $\theta_M = \psi(\theta_P)$ , the corresponding orbit is parabolic, since  $v_\omega = 0$ .

To complete our analysis, we note that, if  $\alpha_0 < \theta_M < \psi(\theta_P)$ , then the solution  $\theta \mapsto \rho(\theta) = F_{\rho_0, \zeta_0, 0}(\theta, \theta_M)$ ,  $\theta \in [0, \theta_\omega)$  corresponds to a collision solution with limit angle  $\theta_\omega = \theta_M$ . Summarizing, the limit angle  $\theta_\omega$ , as shown by Figure 2.3, is defined by the function

$$\theta_\omega = \begin{cases} \theta_M & \text{if } \theta_M < \psi(\theta_P), \\ \eta(\theta_M) & \text{if } \theta_M \geq \psi(\theta_P). \end{cases}$$

We conclude that this map is a smooth function of  $y_0 = (\rho_0, \zeta_0, \theta_0, M_0)$  if  $\theta_\omega \neq \theta_P$  (that is, on hyperbolic and on collision orbits) and is discontinuous at  $\theta_M = \psi(\theta_P)$  (that is, on parabolic orbits), since

$$\lim_{\theta_M \rightarrow \psi(\theta_P)^-} \theta_\omega = \psi(\theta_P) > \theta_P = \lim_{\theta_M \rightarrow \psi(\theta_P)^+} \theta_\omega. \quad (2.54)$$

Then, taking into account (2.50), if  $(\mathbf{x}_0, \mathbf{v}_0) \in \Omega^+$  there exists

$$\mathbf{I}(\mathbf{x}_0, \mathbf{v}_0) = \lim_{t \rightarrow \omega} \mathbf{R}(\mathbf{x}(t), \mathbf{v}(t)) = \lim_{\theta \rightarrow \theta_\omega} \mathbf{R} \circ U \circ \gamma^\theta \circ U^{-1}(\mathbf{x}_0, \mathbf{v}_0)$$

and is given by

$$\mathbf{I}(\mathbf{x}_0, \mathbf{v}_0) = \begin{cases} -e_r(\theta_M) & \text{if } \theta_M < \psi(\theta_P), \\ -\zeta(\theta_\omega) M^2(\theta_\omega) e_\theta(\theta_\omega) - e_r(\theta_\omega) & \text{if } \theta_M \geq \psi(\theta_P), \end{cases}$$

where for simplicity of notations we have not indicated explicitly the composition with  $U^{-1}$  of the functions  $\theta_M$ ,  $\theta_\omega$  and  $\theta_P$ . It follows that  $\mathbf{I}$  is smooth on  $\Omega_H^+ \cup \Omega_C^+$ , since this property holds for  $\theta_\omega$ .

To prove that  $\mathbf{I}$  is discontinuous on parabolic orbits, fix any  $(\mathbf{x}_0, \mathbf{v}_0) = U(\rho_0, \zeta_0, \theta_0, M_0) \in \Omega_P^+$ . Then, we can consider solutions of (2.19) with initial conditions of the form

$$(\mathbf{x}_0, \mathbf{v}_0) = (\rho_0, \zeta_0, \theta_0, M_*) \in \Omega_H^+ \cup \Omega_C^+$$

with  $M_*$  in a neighborhood of  $M_0$ . By (2.54)

$$\lim_{\theta_{M_*} \rightarrow \psi(\theta_P)^+} \mathbf{I} \circ U = -e_r(\theta_P) \neq \lim_{\theta_{M_*} \rightarrow \psi(\theta_L)^-} \mathbf{I} \circ U = -e_r(\psi(\theta_P)),$$

so that  $\mathbf{I}$  is discontinuous on  $\Omega_P^+$ .

Note that  $\mathbf{I}$ , as defined by property *iii*) of the statement, exists on all  $\Omega$ . In fact, on the rectilinear motions, it is  $\mathbf{I}(\mathbf{x}_0, \mathbf{v}_0) = -\frac{\mathbf{x}_0}{|\mathbf{x}_0|}$ . On solutions with negative scalar angular momentum, one can easily adapt the argument used in  $\Omega^+$ , getting also the corresponding regularity results.

To complete the proof of the theorem, we observe that *i*) holds since the  $SO(2)$  invariance of  $\mathbf{R}$  is inherited by  $\mathbf{I}$ . Then, by *i*), the continuity of  $\mathbf{I}$  on  $\Omega_H^+$  and the property

$$\lim_{\theta_\omega \rightarrow (\alpha_0)^+} |\mathbf{I} \circ U| = +\infty,$$

it follows that

$$\mathbf{I}(\Omega) = \mathbb{R}^2 \setminus \text{int}(\mathbb{D}),$$

where  $\mathbb{D}$  is the closed unit disk in  $\mathbb{R}^2$ . ■

# Chapter 3

## Stability of the synchronous spin-orbit resonance

### 3.1 Linear stability of the synchronous resonance

The main result of this section is at the end of it, in Proposition 3.2. It determines a region of linear stability written in terms of the functions  $\Lambda_1(e)$ , defined in the first subsection, and  $\Lambda_2(e)$ , defined in the second one.

#### 3.1.1 Uniqueness of the odd $2\pi$ -periodic solution

Note that equation (1.16) is invariant under the change  $(t, \Theta) \rightarrow (-t, -\Theta)$ , since  $f(-t, e) = -f(t, e)$  and  $r(-t, e) = r(t, e)$ . Then, if  $\Theta(t)$  is a solution of (1.16), so it is  $-\Theta(-t)$ . On the other hand, for  $e = 0$ , the equation (1.16) becomes the free pendulum equation  $\ddot{\Theta} + \Lambda \sin \Theta = 0$ . In this case we know that for  $\Lambda \leq 1$ , the only  $2\pi$ -periodic solutions are the equilibria  $\Theta \equiv 0$  and  $\Theta \equiv \pi$ . Since the trivial solution is the stable one, it is natural to look for the  $2\pi$ -periodic continuation of such solution for  $e \neq 0$  in the family of the odd solutions of (1.16), which is equivalent to solve the Dirichlet problem

$$\begin{cases} \ddot{\Theta} + \frac{\Lambda}{r(t,e)^3} \sin \Theta = -2\ddot{f}(t, e), \\ \Theta(0) = \Theta(\pi) = 0. \end{cases} \quad (3.1)$$

It is well known from nonlinear analysis that this problem has at least one solution because equation (1.16) can be written as

$$\ddot{\Theta} = F(t, \Theta), \quad (3.2)$$

with  $F(t, \Theta)$  bounded. Making explicit<sup>1</sup> the dependence with respect to the parameters we can write

$$F(t, \Theta; e, \Lambda) = -\frac{\Lambda}{r(t, e)^3} \sin \Theta - 2\ddot{f}(t, e). \quad (3.3)$$

We are going to present a simple proof of the existence of solution, based on the shooting method (see [100]). This will be a convenient way to introduce some notation.

Let  $\Theta(t) = \vartheta(t, v)$  be the solution of (3.2) satisfying initial conditions  $\Theta(0) = 0$ ,  $\dot{\Theta}(0) = v \in \mathbb{R}$ . Solutions of the problem (3.1) are in correspondence with the solutions of the equation  $\vartheta(\pi, v) = 0$ . From equation (3.2) we know that  $\vartheta$  satisfies the following integral equation

$$\vartheta(t, v) = vt + \int_0^t (t-s)F(s, \vartheta(s, v))ds.$$

Moreover, since there exists a positive number  $M \geq |F(t, \Theta)|$ , then

$$|\vartheta(t, v) - vt| \leq M\frac{t^2}{2},$$

for each  $t \in \mathbb{R}$ . Using this estimate for  $t = \pi$ , we conclude that

$$\lim_{v \rightarrow \pm\infty} \vartheta(\pi, v) = \pm\infty.$$

In consequence, the equation  $\vartheta(\pi, v) = 0$  must have at least one solution.

We know now that the Dirichlet problem (3.1) has a solution, however, it is not necessarily unique. For instance, in the circular case ( $e = 0$ ), if  $\Lambda \leq 1$  the only solution of the problem (3.1) is  $\Theta(t) \equiv 0$ , while if  $\Lambda > 1$  there are additional solutions, see [86]. We would like to determine a region of parameters  $(e, \Lambda)$  where there is uniqueness for the problem (3.1).

The shooting method is also useful to prove uniqueness by proving that  $\vartheta(\pi, v)$  is monotone, which is equivalent to say that the partial derivative  $\partial_v \vartheta(\pi, v)$  never vanishes. From the theorem of differentiability with respect to initial conditions, we know that  $y(t) = \partial_v \vartheta(t, v)$  is the solution of the variational equation

$$\ddot{y} + \left( \frac{\Lambda}{r(t, e)^3} \cos[\vartheta(t, v; e, \Lambda)] \right) y = 0, \quad (3.4)$$

---

<sup>1</sup>Sometimes we will make explicit the dependence on the parameters of the problem in this way, for example, a solution  $\Theta(t)$  of (3.2) would be referred as  $\Theta(t; e, \Lambda)$

with initial conditions  $y(0) = 0, \dot{y}(0) = 1$ . Note that in (3.4) we have made explicit the dependence upon the parameters of  $\vartheta$ . We conclude that the problem (3.1) has a unique solution as soon as the equation (3.4) has the trivial solution  $y(t) \equiv 0$  as the unique solution satisfying the Dirichlet conditions  $y(0) = y(\pi) = 0$ . This condition will be checked for every  $v \in \mathbb{R}$ .

To do this we will employ the Sobolev inequality

$$K_l(p) \|\xi\|_p^2 \leq \|\dot{\xi}\|_2^2, \quad (3.5)$$

where  $\xi$  is any function in the space  $H_0^1[0, l]$ ,  $\|\cdot\|_p$  is the  $L^p$ -norm, which is defined by

$$\|\xi\|_p = \begin{cases} \left( \int_0^l |\xi(t)|^p dt \right)^{1/p}, & \text{if } 1 \leq p < \infty, \\ \text{ess sup}_{t \in [0, l]} |\xi(t)|, & \text{if } p = \infty, \end{cases}$$

and the constant  $K_l(p)$  is optimal for (3.5) by definition,

$$K_l(p) = \inf_{\xi \in H_0^1[0, l] \setminus \{0\}} \frac{\|\dot{\xi}\|_2^2}{\|\xi\|_p^2},$$

see [118], [18]. This constant has an explicit expression in terms of special functions since, according to [128],

$$K_l(p) = \begin{cases} \frac{2\pi}{p l^{1+2/p}} \left( \frac{2}{2+p} \right)^{1-2/p} \left( \frac{\Gamma(1/p)}{\Gamma(1/2+1/p)} \right)^2, & \text{if } 1 \leq p < \infty, \\ \frac{4}{l}, & \text{if } p = \infty, \end{cases} \quad (3.6)$$

where  $\Gamma$  is the usual Gamma function. The last expression can be employed to check that  $K_l(p)$  is continuous for all  $p \in [1, \infty]$ .

In order to prove the following lemma let us also recall Hölder's inequality for  $\xi \in L^p[0, l]$  and  $\chi \in L^q[0, l]$ , with  $1/p + 1/q = 1$ ,

$$\|\xi \cdot \chi\|_1 \leq \|\xi\|_p \|\chi\|_q. \quad (3.7)$$

**Lemma 3.1.** *Let  $a \in C[0, l]$  be a function such that its positive part*

$$a^+(t) = \max\{0, a(t)\},$$

*satisfies*

$$\|a^+\|_\alpha < K_l \left( \frac{2\alpha}{\alpha - 1} \right), \quad (3.8)$$

with  $\alpha \in [1, \infty]$ . Then, the unique solution of the Dirichlet problem

$$\begin{cases} \ddot{y} + a(t)y = 0, \\ y(0) = y(l) = 0, \end{cases} \quad (3.9)$$

is the trivial solution.

This Lemma is a particular case of Corollary 2.2 in [18], in its Dirichlet version (Section 2.3). As we see in Remark 2.1 and in Section 2.3 of [18], we do not need to impose the condition  $\int_0^l a(t)dt > 0$ , since, in the terminology of [18], our problem is *nonresonant*.

**Proof.** We proceed by contradiction. Multiply the equation in (3.9) by  $y(t) \not\equiv 0$  and integrate by parts,

$$\int_0^l \dot{y}(t)^2 dt = \int_0^l a(t)y(t)^2 dt \leq \int_0^l a^+(t)y(t)^2 dt, \quad (3.10)$$

i.e.

$$\|\dot{y}\|_2^2 \leq \|a^+ y^2\|_1,$$

from (3.7) we get

$$\|\dot{y}\|_2^2 \leq \|a^+\|_p \|y^2\|_q,$$

for any numbers such that  $1 \leq p, q \leq \infty$  satisfying  $1/p + 1/q = 1$ . Additionally, from (3.5) we get

$$K_l(\beta) \|y\|_\beta^2 \leq \|a^+\|_p \|y^2\|_q,$$

for any number such that  $1 \leq \beta \leq \infty$ . Let us take  $q = \beta/2$  in the last inequality and assume that  $y(t) \not\equiv 0$ , consequently

$$K_l(\beta) \leq \|a^+\|_{\frac{\beta}{\beta-2}},$$

where we have used that  $\|y\|_\beta^2 = \|y^2\|_{\beta/2}$ . The last inequality contradicts the hypothesis (3.8). In consequence,  $y(t) \equiv 0$ . ■

The previous Lemma can be applied to equation (3.4) in the interval  $[0, \pi]$  for each  $\alpha \in [1, \infty]$ . To do this we define the following function

$$\Lambda_0(e, \alpha) = \frac{K_\pi\left(\frac{2\alpha}{\alpha-1}\right)}{\|r(\cdot, e)^{-3}\|_\alpha}, \quad (3.11)$$

which has an explicit expression in terms of the hypergeometric function and the  $\Gamma$  function, and it is continuous in both of its variables. Let us show this



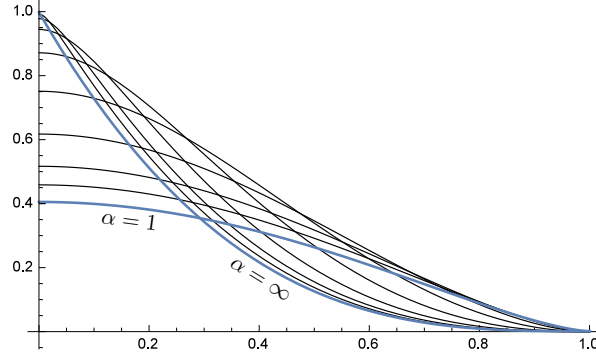


Figure 3.1: The functions  $e \mapsto \Lambda_0(e, \alpha)$  for different values of  $\alpha$ .

point. We can compute that

$$\|r(\cdot, e)^{-3}\|_\alpha = \begin{cases} \frac{\pi}{(1-e^2)^{3/2}}, & \text{if } \alpha = 1, \\ \left( \frac{\pi {}_2F_1(1/2, 3\alpha - 1; 1; 2e/(1+e))}{(1+e)^{3\alpha-1}} \right)^{1/\alpha}, & \text{if } 1 < \alpha < \infty, \\ (1-e)^{-3}, & \text{if } \alpha = \infty, \end{cases} \quad (3.12)$$

where  $\|\cdot\|_\alpha$  denotes the  $L^\alpha[0, \pi]$ -norm and  ${}_2F_1$  is the hypergeometric function. The continuous dependence of the function  $\|r(\cdot, e)^{-3}\|_\alpha$  with respect to  $e$  and  $\alpha < \infty$  is guaranteed by the classical theorem in integration theory. Moreover, it is also guaranteed for  $\alpha = \infty$ , because it is well known that the  $L^\alpha$ -norm of a function converges to its  $L^\infty$ -norm as  $\alpha \rightarrow \infty$ . The function  $K_l(p)$  is continuous for each  $p \in [1, \infty)$  since  $\Gamma(x)$  is continuous for all  $x > 0$ . It is also continuous for  $p = \infty$  because  $\Gamma(1/2) = \sqrt{\pi}$  and  $\Gamma(1/p) = p + \mathcal{O}(1)$  as  $p \rightarrow \infty$ . Consequently,  $\Lambda_0(e, \alpha)$  is continuous in both entries.

The graphs of  $\Lambda_0(\cdot, \alpha)$ , for some values of  $\alpha$ , are plotted in Figure 3.1.

Now we are able to define the function

$$\Lambda_1(e) = \max_{\alpha \in [1, \infty]} \Lambda_0(e, \alpha), \quad (3.13)$$

which allow us to state Proposition 3.1, that is the main result of this section. But before, let us state some properties of  $\Lambda_1$ .

**Lemma 3.2.** *The function  $\Lambda_1$  defined in (3.13) is continuous, strictly decreasing and*

$$\Lambda_1(0) = 1, \quad \lim_{e \rightarrow 1^-} \Lambda_1(e) = 0.$$

**Proof.** The continuity of  $\Lambda_0(e, \alpha)$  implies that the function  $\Lambda_1(e)$  is bounded in  $[0, \bar{e}]$ , for all  $\bar{e} \in (0, 1)$ , since,

$$|\Lambda_1(e)| \leq \max_{[0, \bar{e}] \times [1, \infty]} |\Lambda_0(e, \alpha)|.$$

Then, the continuity of  $\Lambda_1(e)$  is equivalent to say that the set  $\{(e, \Lambda_1(e)) : e \in [0, \bar{e}]\}$  is closed in  $\mathbb{R}^2$ .

Since  $\Lambda_1$  is bounded, we can take a sequence  $e_n \in [0, \bar{e}]$  converging to  $e$  such that  $\Lambda_1(e_n)$  converges to a some  $\zeta$ . Then we have to prove that  $\Lambda_1(e) = \zeta$ .

By definition of  $\Lambda_1$ , for each  $n$  there exists  $\alpha_n \in [1, \infty]$  such that  $\Lambda_1(e_n) = \Lambda_0(e_n, \alpha_n)$ . We can take a subsequence  $\alpha_{\sigma(n)}$  converging to a some  $\hat{\alpha}$ . Due to the continuity of  $\Lambda_0$  and because  $\Lambda_1(e_{\sigma(n)}) = \Lambda_0(e_{\sigma(n)}, \alpha_{\sigma(n)})$ , we get that  $\Lambda_1(e) \geq \Lambda_0(e, \hat{\alpha}) = \zeta$ . On the other hand, we can take a  $\alpha_* \in [1, \infty]$  such that  $\Lambda_1(e) = \Lambda_0(e, \alpha_*)$ . Again, since  $\Lambda_1(e_n) \geq \Lambda_0(e_n, \alpha_*)$ , then,  $\zeta \geq \Lambda_0(e, \alpha_*) = \Lambda_1(e)$ . Consequently,  $\Lambda_1(e) = \zeta$ .

To prove that  $\Lambda_1$  is monotone, recall the definitions made in (1.11). We can evaluate the integral  $\|r(\cdot, e)^{-3}\|_\alpha$ ,  $\alpha \in [1, \infty)$  using the change of variable of the eccentric anomaly  $t = u - e \sin u$  and get

$$\|r(\cdot, e)^{-3}\|_\alpha^\alpha = \int_0^\pi \frac{du}{(1 - e \cos u)^{3\alpha-1}}, \quad (3.14)$$

differentiating with respect to  $e$  and applying properties of the cosine we obtain

$$\begin{aligned} \frac{d}{de} \|r(\cdot, e)^{-3}\|_\alpha^\alpha &= (3\alpha - 1) \int_0^\pi \frac{\cos u}{(1 - e \cos u)^{3\alpha}} du \\ &= (3\alpha - 1) \int_0^{\pi/2} \left( \frac{1}{(1 - e \cos u)^{3\alpha}} - \frac{1}{(1 + e \cos u)^{3\alpha}} \right) \cos u \, du. \end{aligned}$$

The last integral is clearly positive and, since

$$\frac{d}{de} \|r(\cdot, e)^{-3}\|_\alpha^\alpha = \alpha \|r(\cdot, e)^{-3}\|_\alpha^{\alpha-1} \frac{d}{de} \|r(\cdot, e)^{-3}\|_\alpha,$$

the function  $\|r(\cdot, e)^{-3}\|_\alpha$  is increasing in  $e$ . In consequence, according to the definition (3.11), each  $\Lambda_0(\cdot, \alpha)$  is strictly decreasing for  $\alpha \in [1, \infty)$ . The same can be said about  $\Lambda_0(\cdot, \infty)$  since, according to (3.12),  $\|r(\cdot, e)^{-3}\|_\infty = (1 - e)^{-3}$ . This implies also that  $\Lambda_1$  is monotone.

Now let us prove that  $\Lambda_1(0) = 1$ . First note that it is easy to check that  $\Lambda_0(0, \infty) = K_\pi(2) = 1$ , then  $\Lambda_1(0) \geq 1$ . On the other hand, we can

apply Theorem 5 in [128] to our equation (3.16), which for  $e = 0$  is simply  $\ddot{y} + \Lambda y = 0$ . In this case, the first anti-periodic eigenvalue is  $1/4$ . Then, using the identities (3.18) again and the definition of  $\Lambda_0(0, \alpha)$ , we get the following inequalities

$$1 > \Lambda_0(0, 1), \quad 1 \geq \Lambda_0(0, \alpha), \quad \alpha \in (1, \infty],$$

which lead to  $\Lambda_1(0) \leq 1$ . This proves the claim.

Now consider the asymptotic behavior. Note that the integrand in (3.14) is positive and has a singularity at  $u = 0$  for  $e = 1$ . Actually, it behaves as  $u^{-2(3\alpha-1)}$  as  $u \rightarrow 0^+$ , making the integral divergent. This is the reason why  $\|r(\cdot, e)^{-3}\|_\alpha \rightarrow \infty$  as  $e \rightarrow 1^-$  for each  $\alpha \in [1, \infty)$ , and, as a result,  $\Lambda_0(e, \alpha) \rightarrow 0$ . The same happens for the case  $\alpha = \infty$  as we did before. To be able to take the maximum, the limit  $\Lambda_0(e, \alpha) \rightarrow 0$  as  $e \rightarrow 1^-$  should be uniform, but so far we have shown only the pointwise convergence. To obtain this property we can apply Dini's Theorem (see Theorem 7.13 in [112]) thanks to the fact that  $\Lambda_0(e, \alpha)$  is continuous in the compact set of values  $\alpha \in [1, \infty]$  for each  $e$ , and it is monotone in  $e$  for each  $\alpha$ . We can take any set of values  $\{e_n\} \subset [0, 1)$ , such that  $e_n < e_{n+1}$ , and  $e_n \rightarrow 1^-$  as  $n \rightarrow \infty$ , and apply the mentioned theorem to the functions  $f_n(\alpha) = \Lambda_0(e_n, \alpha)$ . As a result,  $\Lambda_0(e, \alpha) \rightarrow 0$  uniformly in  $\alpha$  as  $e \rightarrow 1^-$ , which guarantees that  $\Lambda_1(e) \rightarrow 0$ . ■

The main result of this section is the following.

**Proposition 3.1.** *Assume that  $e \in (0, 1]$  and  $0 \leq \Lambda < \Lambda_1(e)$ . Then, there exists a unique solution of the Dirichlet problem (3.1), denoted by  $\Theta^*(t; e, \Lambda)$ . The function*

$$(t, e, \Lambda) \in [0, \pi] \times [0, 1) \times [0, \Lambda_1(e)) \quad \mapsto \quad \Theta^*(t; e, \Lambda),$$

*is analytic in the real sense.*

**Proof.** The previous discussions lead directly to the existence and uniqueness of the solution. To prove the analytic character, we observe that, in terms of the previous notation, the solution corresponds to  $\Theta^*(t; e, \Lambda) = \vartheta(t, v(e, \Lambda); e, \Lambda)$ , where  $v = v(e, \Lambda)$  is the unique solution of

$$\vartheta(\pi, v; e, \Lambda) = 0.$$

Now we can apply the implicit function theorem, in its real analytic version (Theorem 2.3.5 in [67]), because the solution  $\vartheta$  is analytic in all the entries due to the analytic character of the equation (1.16). Also, the derivative  $\partial_v \vartheta(\pi, v; e, \Lambda)$  does not vanish as long as  $v \in \mathbb{R}$ ,  $e \in [0, 1)$  and  $0 \leq \Lambda < \Lambda_1(e)$ , due to Lemma 3.1. These considerations lead easily to the proof of the claim. ■

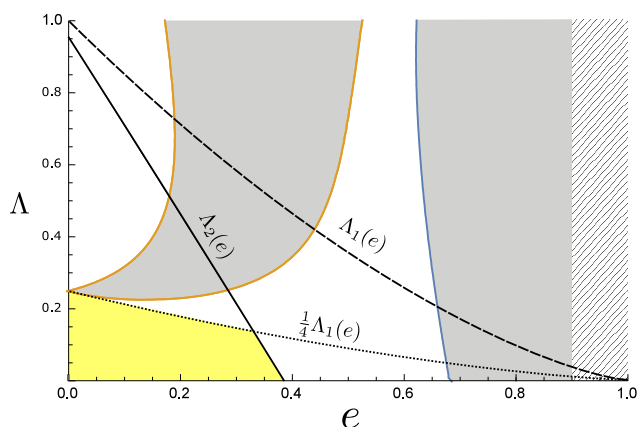


Figure 3.2: Stability diagram of  $\Theta^*(t; e, \Lambda)$  computed numerically: the gray regions are linearly unstable. The lines pattern indicates that for high eccentricity  $e \geq 0.9$  we did not compute the linear stability due to the proximity to the singularity. The yellow region is the stable region by a Lyapunov-type criterion.

**Remark 3.1.** *Being more precise, in terms of complex analysis, the function  $\Theta^*(t; e, \Lambda)$  has a holomorphic extension to some open subset of  $\mathbb{C}^3$  containing  $[0, \pi] \times [0, 1) \times [0, \Lambda_1(e))$ .*

**Remark 3.2.** *Note that there are two special cases for which  $\Theta^*$  can be computed*

$$\Theta^*(t; e, 0) = 2(t - f(t, e)), \quad \Theta^*(t; 0, \Lambda) = 0. \quad (3.15)$$

Now we are interested in the stability properties of the solution  $\Theta^*(t; e, \Lambda)$ , which should be seen as  $2\pi$ -periodic and odd from now on. In the following we will find a region of parameters where the linearized equation of (1.16) at  $\Theta^*$ , say,

$$\ddot{y} + \left( \frac{\Lambda}{r(t, e)^3} \cos[\Theta^*(t; e, \Lambda)] \right) y = 0, \quad (3.16)$$

is stable (linear stability). See Figure 3.2.

For this purpose we are going to apply Theorem 1 from [128], which is a generalization of the classical Lyapunov criterion for the stability of a Hill's equation using  $L^\alpha$  norms. According to it, given a Hill's equation

$$\ddot{y} + a(t)y = 0, \quad a(t+T) = a(t),$$

with  $a \in L^\alpha[0, T]$ , the equation is stable if

$$\int_0^T a(t)dt > 0 \quad \text{and} \quad \|a^+\|_\alpha < K_T \left( \frac{2\alpha}{\alpha - 1} \right). \quad (3.17)$$

See also a similar result by Borg in [77], Section 5.2.

In the present setting we want to consider  $T = 2\pi$ , so we have to do the computations in the interval  $[0, 2\pi]$ , instead of  $[0, \pi]$ , as we did before. We know that the following relations hold

$$K_{2l}\left(\frac{2\alpha}{\alpha-1}\right) = \frac{2^{\frac{1}{\alpha}}}{4} K_l\left(\frac{2\alpha}{\alpha-1}\right), \quad \int_0^{2\pi} \frac{dt}{r(t, e)^{3\alpha}} = 2 \int_0^{\pi} \frac{dt}{r(t, e)^{3\alpha}}. \quad (3.18)$$

The first identity comes from the definition of  $K_l(p)$  in (3.6). In consequence, the second inequality in (3.17) is satisfied for equation (3.16) if  $0 < \Lambda < \frac{1}{4}\Lambda_1(e)$ . We rule out the case  $\Lambda = 0$  because it does not satisfy the second inequality.

### 3.1.2 Upper and lower solutions

We see from Figure 3.2 that the condition  $0 < \Lambda < \frac{1}{4}\Lambda_1(e)$  is not sufficient to obtain stability. We are going to define another function  $\Lambda_2(e)$ , which let us guarantee that the first inequality in (3.17) is satisfied for equation (3.16). Let us impose that  $\cos[\Theta^*(t; e, \Lambda)] > 0$ , or, equivalently,

$$|\Theta^*(t; e, \Lambda)| < \frac{\pi}{2}, \quad t \in [0, 2\pi]. \quad (3.19)$$

Due to the symmetry of this solution, it is sufficient to find the estimate on the half-interval  $[0, \pi]$ . This can be done with the method of upper and lower solutions. See for example [37].

Let  $\psi(t)$  be a solution of the Dirichlet problem

$$\ddot{\psi} = -\frac{\Lambda}{r(t, e)^3}, \quad \psi(0) = \psi(\pi) = 0.$$

By the maximum principle, the function  $\psi$  is positive on  $(0, \pi)$  and can be expressed as

$$\psi(t) = -\Lambda \int_0^\pi \frac{G(t, s)}{r(s, e)^3} ds,$$

where  $G(t, s)$  is the Green's function associated to the operator  $L[\psi] = \ddot{\psi}$  with Dirichlet conditions  $\psi(0) = \psi(\pi) = 0$ , and whose expression is

$$G(t, s) = \begin{cases} -s(\pi - t)/\pi & \text{if } s \in [0, t], \\ -t(\pi - s)/\pi & \text{if } s \in [t, \pi]. \end{cases}$$

Note that  $G(t, s) \leq 0$ , and that  $|G(t, s)| \leq |G(s, s)|$ , then,

$$\psi(t) \leq \frac{\Lambda}{\pi} \int_0^\pi \frac{s(\pi - s)}{r(s, e)^3} ds. \quad (3.20)$$

We can use  $\psi$  to produce the following functions

$$\psi_\pm(t) = 2(t - f(t, e)) \pm \psi(t).$$

These functions are upper and lower solutions of our problem, since they satisfy

$$\psi_+(t) > \psi_-(t), \quad \ddot{\psi}_-(t) \geq F(t, \psi_-(t)), \quad \ddot{\psi}_+(t) \leq F(t, \psi_+(t)),$$

where  $F(t, \Theta)$  was defined by the expressions eqs. (3.2) and (3.3), and contains the nonlinear terms of our equation. Consequently,

$$\psi_+(t) \geq \Theta^*(t; e, \Lambda) \geq \psi_-(t), \quad t \in [0, \pi].$$

Let us look for bounds that do not depend on  $t$ . Consider the function  $\chi(t) = f(t, e) - t$ . Since  $\chi(0) = \chi(\pi) = 0$  and computing that

$$\ddot{f}(t, e) = -\frac{2e\sqrt{1-e^2}\sin[u(t, e)]}{(1-e\cos[u(t, e)])^4} < 0, \quad t \in (0, \pi),$$

we can say that  $\chi(t), t \in [0, \pi]$ , is positive and has a unique maximum  $m(e)$  in the interval  $(0, \pi)$ , say,

$$m(e) = 2 \arctan \sqrt{\frac{(1+e)(e-1+(1-e^2)^{\frac{1}{4}})}{(1-e)(e+1-(1-e^2)^{\frac{1}{4}})}} - \arccos\left(\frac{1-\sqrt[4]{1-e^2}}{e}\right) + \sqrt{e^2 - (1-\sqrt[4]{1-e^2})^2}. \quad (3.21)$$

According to this discussion, define the function

$$\Lambda_2(e) = \frac{\frac{\pi^2}{2} - 2\pi m(e)}{\int_0^\pi \frac{t(\pi-t)}{r(t, e)^3} dt}, \quad (3.22)$$

then, the condition (3.19) is satisfied if  $0 < \Lambda < \Lambda_2(e)$ . The stability result is summarized in the following Proposition.

**Proposition 3.2.** *For each value  $e \in (0, 1)$  such that  $m(e) < \pi/4$ , if  $0 < \Lambda < \frac{1}{4}\Lambda_1(e)$  and  $0 < \Lambda < \Lambda_2(e)$ , the solution  $\Theta^*(t; e, \Lambda)$  is linearly stable.*

**Remark 3.3.** *We can see in Figure 3.2 that the yellow region determined by Proposition 3.2 is just the first linear stability region of the solution. We have focused in this zone because, physically, the most relevant application is to the case of the major natural satellites in the solar system, which are generally close to be spherical. See [16] for a detailed study of periodic solutions in a large range of  $\Lambda$ . Besides, an extension of our results to higher stability regions can be done using the mentioned results by Borg in [77].*

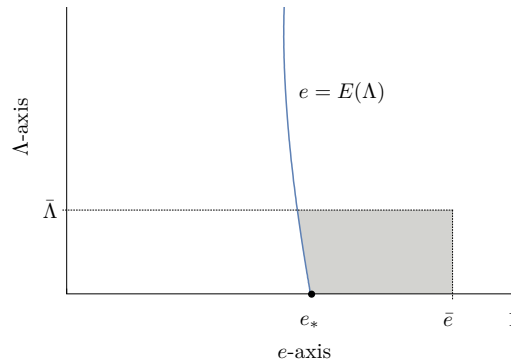


Figure 3.3: Bifurcation of stability at  $e = e_*$ . The shaded region is unstable.

## 3.2 Instability for high eccentricity

The numerical calculation of the instability regions in Figure 3.2 shows that there exists instability for high eccentricities, whose boundary bifurcates from  $\Lambda = 0$  at some value of the eccentricity that we will call  $e = e_*$ . As it is described in [10], Chapter 2, Section 7.3, Zlatoustov and collaborators already showed this behavior with computer simulations in [129]. In this section we will prove the existence of such bifurcation branch for small  $\Lambda$ . Assume that  $e$  and  $\Lambda$  are in the conditions of Proposition 3.1 and let  $\Theta^*(t; e, \Lambda)$  be the odd  $2\pi$ -periodic solution obtained for the Dirichlet problem (3.1). The next result also concerns the stability of the variational equation (3.16).

**Theorem 3.1.** *For some  $\varepsilon > 0$ , there exists a function  $E : [0, \varepsilon) \rightarrow (0, 1)$ ,  $\Lambda \mapsto E(\Lambda)$ , such that the equation (3.16) is unstable and has a non-trivial  $4\pi$ -periodic solution if  $e = E(\Lambda)$ . Moreover,  $E(0) = e_* \in (0, 1)$  and for each  $\bar{e} \in (e_*, 1)$  there exists a  $\bar{\Lambda} = \bar{\Lambda}(\bar{e}) \in (0, \varepsilon)$ , such that the equation (3.16) is unstable for the points  $(e, \Lambda)$  satisfying  $E(\Lambda) < e < \bar{e}$ ,  $0 < \Lambda < \bar{\Lambda}$ . In addition, the function  $E$  can be expressed as  $E(\Lambda) = \xi(\Lambda^{1/p})$ , where  $\xi(\zeta)$  is real analytic at  $\zeta = 0$  and  $p \geq 1$  is an integer.*

The proof of this result will provide some additional information. The number  $e_*$  solves the equation  $I(e) = 0$ , where,

$$I(e) := \int_{-\pi}^{\pi} \frac{\cos[2(t - f(t, e))]}{r(t, e)^3} dt. \quad (3.23)$$

Numerical computations suggest that  $e_*$  is the only root of  $I(e)$  and  $e_* \approx 0.682\dots$



The general theory of Hill's equation deals with the study of

$$\ddot{y} + a(t)y = 0, \quad (3.24)$$

where  $a$  is a continuous and  $2\pi$ -periodic function, see [77]. As it is well known, the discriminant  $\Delta = \Delta[a]$  is a real number such that (3.24) is stable if  $|\Delta| < 2$  (elliptic case) and unstable if  $|\Delta| > 2$  (hyperbolic case). When  $|\Delta| = 2$  (parabolic case) the equation might be stable or unstable. In this last case, there is at least one  $4\pi$ -periodic solution and, only if all the solutions of (3.24) are  $4\pi$ -periodic (coexistence), the equation is stable.

According to Theorem 3.1, the specific equation (3.16) is parabolic-unstable on the curve  $e = E(\Lambda)$  and hyperbolic-unstable on the shaded region of the Figure 3.3. In particular, this hyperbolicity implies that  $\Theta^*(t; e, \Lambda)$  is unstable, in the Lyapunov sense, as solution of the nonlinear equation (1.16).

Incidentally, we notice that Zhang's conditions (3.17) really imply that (3.24) is elliptic-stable. In our particular case, it means that equation (3.16) is elliptic on the conditions of Proposition 3.2.

To describe the strategy for the proof of Theorem 3.1 we first recall some facts on the linear equation (3.24) when the coefficient  $a(t)$  is even. Note that this is the case for (3.16). Let  $y_1$  and  $y_2$  be the normalized solutions, i.e., solutions obtained with initial conditions  $y_1(0) = 1, \dot{y}_1(0) = 0, y_2(0) = 0, \dot{y}_2(0) = 1$ . The discriminant is expressed in terms of these solutions by the formula

$$\Delta^2 - 4 = 4\dot{y}_1(2\pi)y_2(2\pi), \quad (3.25)$$

which let us decide the stability in a convenient way.

For the equation (3.16), we have that  $y_1(t) = y_1(t; e, \Lambda)$  and  $y_2(t) = y_2(t; e, \Lambda)$ . Particularly, for  $\Lambda = 0$  we observe that for all  $t \in \mathbb{R}, e \in [0, 1)$ ,

$$y_1(t; e, 0) \equiv 1, \quad y_2(t; e, 0) \equiv t. \quad (3.26)$$

Assuming that  $\Lambda < \frac{1}{4}\Lambda_1(e)$ , let us prove that  $y_2(2\pi; e, \Lambda) > 0$ . Since  $y_2$  is a non-trivial solution, we can apply Lemma 3.1 for  $l = 2\pi$ , and conclude that  $y_2(2\pi; e, \Lambda) \neq 0 = y_2(0; e, \Lambda)$ . From (3.26),  $y_2(2\pi; e, 0) > 0$  for each  $e \in [0, 1)$ , then, by continuity,  $y_2(2\pi; e, \Lambda) > 0$ .

In consequence, by (3.25), if  $\dot{y}_1(2\pi; e, \Lambda)$  is negative/positive, the equation will be stable/unstable. Additionally, the fact that  $y_2(2\pi; e, \Lambda) \neq 0$  implies, by Theorems 1.1 and 1.2 in [77], that  $y_2$  is not  $4\pi$ -periodic. Therefore, if  $\dot{y}_1(2\pi; e, \Lambda) = 0$ , then, the equation (3.24) will be parabolic-unstable. Since  $\dot{y}_1(2\pi; e, 0) = 0$  for each  $e$ , the division formula can be applied to write

$$\dot{y}_1(2\pi; e, \Lambda) = \Lambda\Psi(e, \Lambda), \quad (3.27)$$

with

$$\Psi(e, \Lambda) = \int_0^1 \partial_\Lambda \dot{y}_1(2\pi; e, s\Lambda) ds,$$

which is a real analytic function in both variables. This comes from the fact that any solution  $y = y(t; e, \Lambda)$  of (3.16) is analytic in all its entries due to the real analytic version of the theorem of differentiability of solutions with respect to the parameters. Fix a value  $e \in [0, 1)$  and note that, according to the expansion of  $\dot{y}_1(2\pi, e, \Lambda)$  around  $\Lambda = 0$ , we have

$$\Psi(e, 0) = \partial_\Lambda \dot{y}_1(2\pi; e, 0).$$

Differentiating the equation (3.16) with respect to  $\Lambda$  and evaluating at  $\Lambda = 0$ , we obtain

$$\partial_\Lambda \ddot{y}(t; e, 0) + \frac{\cos[\Theta^*(t; e, 0)]}{r(t, e)^3} y(t; e, 0) = 0,$$

which can be integrated with initial condition  $\partial_\Lambda \dot{y}_1(0; e, 0) = 0$  and give as a result that

$$\partial_\Lambda \dot{y}_1(2\pi; e, 0) = - \int_0^{2\pi} \frac{\cos[2(t - f(t, e))]}{r(t, e)^3} dt.$$

Due to the periodicity of the integrand and considering the definition (3.23), we can change the interval of integration from  $[0, 2\pi]$  to  $[-\pi, \pi]$  and identify  $\Psi(e, 0) = -I(e)$ .

The standard theory of integrals depending on parameters implies that  $I(e)$  is a real analytic function defined on  $e \in [0, 1)$ . Moreover, since  $f(t, 0) = t$  and  $r(t, 0) = 1$ , we see that  $I(0) = 2\pi > 0$ . The following result implies that  $I(e)$  has a change of sign. Hence,  $I(e_*) = 0$  for some  $e_* \in (0, 1)$ .

**Lemma 3.3.** *The function  $I(e)$  has a negative finite limit as  $e \rightarrow 1^-$ .*

The proof of this result is delicate because it is not possible to interchange the limit with the integral sign. Let us explain this point. Since the integrand is even, we just consider the integral (3.23) on the interval  $(0, \pi)$ . At first glance we see that the limit of the integrand is

$$\lim_{e \rightarrow 1^-} \frac{\cos[2(t - f(t, e))]}{r(t, e)^3} = \frac{\cos[2t]}{r(t, 1)^3}$$

because, as  $e \rightarrow 1^-$ ,  $f(t, e) \rightarrow \pi$  for all  $t \in (0, \pi)$ . From the definition of  $r(t, 1)$ , we get the expansion  $r(t, 1)^3 = 9t^2/2 + O(t^4)$ , i.e., the integrand has a pole of order 2 at  $t = 0$ . Therefore,

$$\int_0^\pi \frac{\cos[2t]}{r(t, 1)^3} dt = +\infty.$$

However, the delicate point comes from the fact that, for  $e$  close to 1, the value of  $f(t, e)$  increases from 0 to  $\pi$  very fast. This results in a fast-changing argument of the cosine and, ultimately, a change of sign of the integrand in (3.23) for smaller and smaller  $t > 0$ . In this situation we cannot apply any classical technique, such as the dominated convergence theorem or Fatou's lemma.

In order to prove Lemma 3.3, we will first apply the Residue Theorem to compute  $I(e)$  for  $e \in (0, 1)$ , and then we let  $e$  go to 1. All this hard work is postponed to the end of the section.

Once we have found  $e_*$  such that  $\Psi(e_*, 0) = 0$ , it seems natural to find the function  $e = E(\Lambda)$  as a solution of the implicit function problem

$$\Psi(E(\Lambda), \Lambda) = 0, \quad E(0) = e_*.$$

A direct application of the implicit function theorem does not seem easy. The number  $e_*$  is not known explicitly and the transversality condition  $\partial_\Lambda \Psi(e_*, 0) \neq 0$  leads to a complicated integral with no clear sign.

Taking advantage of the analytic character of the function  $\Psi$ , we will apply the following parametric version of Bolzano's Theorem. The proof of Theorem 3.1 will follow as a direct consequence.

**Lemma 3.4.** *Let  $\Upsilon : [0, l_1) \times [0, l_2) \rightarrow \mathbb{R}$ ,  $l_1, l_2 > 0$ , be a real analytic function of two variables  $\Upsilon = \Upsilon(x, y)$  such that,*

$$\Upsilon(0, 0) < 0 < \liminf_{x \rightarrow l_1^-} \Upsilon(x, 0). \quad (3.28)$$

*Then, there exists a value  $x_* \in (0, l_1)$  and a function  $\varphi : [0, \varepsilon) \rightarrow (0, l_1)$ , such that*

$$\varphi(0) = x_*, \quad \Upsilon(\varphi(y), y) = 0, \quad \text{for each } y \in [0, \varepsilon), \quad (3.29)$$

*and, for each  $\bar{x} \in (x_*, l_1)$ , there exists a  $\bar{y} > 0$  such that*

$$\Upsilon(x, y) > 0, \quad \text{if } \varphi(y) < x, \quad x < \bar{x}, \quad 0 < y < \bar{y}. \quad (3.30)$$

*Moreover, there exists some positive integer  $p \geq 1$  such that  $\varphi(y) = \tilde{\varphi}(y^{1/p})$ , where  $\tilde{\varphi}(\zeta)$  is analytic at  $\zeta = 0$ .*

**Proof.** The function  $\Upsilon(\cdot, 0)$  is analytic in  $[0, l_1)$  and changes sign, then it has a finite number of zeros. We will say that a zero  $x_0 \in (0, l_1)$  of this function is *transversal* if

$$\Upsilon(x_0 + \sigma, 0)\Upsilon(x_0 - \sigma, 0) < 0,$$

for every small enough  $\sigma > 0$ . The function  $\Upsilon(\cdot, 0)$  has at least one transversal zero due to the condition (3.28).

Define the set of zeros

$$Z = \{(x, y) \in [0, l_1] \times [0, l_2] : \Upsilon(x, y) = 0\}.$$

We say that a zero  $x_0 \in (0, l_1)$  of  $\Upsilon(\cdot, 0)$  has a *continuation* if the point  $(x_0, 0)$  is non-isolated in  $Z$ . Transversal zeros have always a continuation. This is a consequence of Bolzano's Theorem. Given a transversal zero  $x_0$ , for small  $\varepsilon > 0$ ,

$$\Upsilon(x_0 + \sigma, y)\Upsilon(x_0 - \sigma, y) < 0 \quad \text{if } 0 < y < \varepsilon.$$

Therefore,  $Z$  has a point lying in the segment  $[x_0 - \sigma, x_0 + \sigma] \times \{y\}$ . The converse is not true, sometimes non-transversal zeros have a continuation. We illustrate the previous definitions with the example

$$\Upsilon(x, y) = (y - x + 1)^2(y + x - 2)(x - 3)^2.$$

This function satisfies the conditions of the Lemma if  $l_1 > 3, l_2 > 0$ . Additionally,  $\Upsilon(\cdot, 0)$  has three zeros, say,  $x_0 = 2$  (transversal),  $x_1 = 1$  (non-transversal with continuation) and  $x_2 = 3$  (non-transversal without continuation).

Let  $x_* \in (0, l_1)$  be the largest zero of  $\Upsilon(\cdot, 0)$  having a continuation. Now, we are going to use several theorems on real analytic functions of two variables in order to characterize the continuation set of the point  $(x_*, 0)$ .

First, we apply the Weierstrass Preparation Theorem (Theorem 6.3.1 in [67]) to the function  $\Upsilon$  at the point  $(x_*, 0)$ . To do this, note that some coefficient of the power series expansion of  $\Upsilon(x, 0)$  at  $x = x_*$  does not vanish (otherwise  $\Upsilon(x, 0) \equiv 0$ ). Then, the function  $\Upsilon(x, y)$  can be decomposed as

$$\Upsilon(x, y) = W(x - x_*, y)Y(x, y), \quad (x, y) \in U,$$

where  $U$  is a small neighborhood of  $(x_*, 0)$ ,  $Y(x, y)$  is a non-vanishing real analytic function defined on  $U$  and  $W(x, y)$  is a Weierstrass polynomial. This means that there exists an integer  $N \geq 1$  such that

$$W(x, y) = x^N + A_{N-1}(y)x^{N-1} + \cdots + A_1(y)x + A_0(y),$$

where the functions  $A_n(y)$ ,  $n = 0, \dots, N - 1$ , are real analytic at  $y = 0$  and  $A_n(0) = 0$ . As a result, the equation  $\Upsilon = 0$  is equivalent to  $W = 0$  in  $U$ .

Second, we can apply the Decomposition Theorem (Theorem 4.2.7 in [67]) to  $W$ . We deduce that there exists a finite number  $q$  of functions

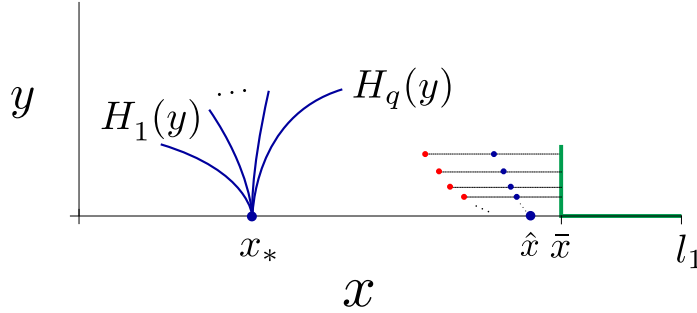


Figure 3.4: Illustration of the contradiction argument. Green, red and blue correspond to values of  $\Upsilon$  that are positive, negative and zero, respectively.

$H_1, H_2, \dots, H_q$ , defined on  $[0, \varepsilon)$  where  $H_j(0) = x_*$ ,  $j = 1, \dots, q$ ;  $H_1(y) < H_2(y) < \dots < H_q(y)$  if  $y \in (0, \varepsilon)$ , and such that, for some neighborhood  $V \subset U$  of  $(x_*, 0)$ , we can characterize the continuation set as

$$Z \cap V = \{(H_j(y), y) : y \in [0, \varepsilon), j = 1, \dots, q\}.$$

Moreover, there exists an integer  $p \geq 1$  such that  $H_j(y) = \tilde{H}_j(y^{1/p})$ , where each  $\tilde{H}_j(\zeta)$  is analytic at  $\zeta = 0$ . We define  $\varphi = H_q$  and  $\tilde{\varphi} = \tilde{H}_q$ . Then, the identities (3.29) are automatically satisfied.

It remains to check that the inequality (3.30) holds. We start with a preliminary observation: given a point  $(x, y) \in V$  with  $x > \varphi(y)$ , then,  $\Upsilon(x, y) > 0$ . This is a consequence of the way we have chosen  $\varphi = H_q$ . Consider  $\chi \in (x_*, x_* + \sigma)$ , with  $\sigma > 0$  small enough such that the point  $(\chi, 0) \in V$ . The point  $(\chi, 0)$  is connected to every point within the region  $\{(x, y) \in V : x > \varphi(y)\}$ . Since  $\Upsilon(\chi, 0) > 0$ , the same is true for all the points in the region.

Let us now prove (3.30) by a contradiction argument concerning the definition of  $x_*$ . Assume the existence of a number  $\bar{x} \in (x_*, l_1)$  and a sequence of points  $\{(x_n, y_n)\}$  satisfying

$$\Upsilon(x_n, y_n) \leq 0, \quad \varphi(y_n) < x_n, \quad x_n < \bar{x}, \quad y_n > 0, \quad y_n \xrightarrow[n \rightarrow \infty]{} 0.$$

Figure 3.4 illustrates the argument for strict inequalities  $\Upsilon(x_n, y_n) < 0$ . It is not restrictive to assume that  $\bar{x}$  is sufficiently close to  $l_1$  in order to guarantee that  $\bar{x} \notin V$  and  $\Upsilon(\bar{x}, 0) > 0$ . Let us fix  $\varepsilon_1 > 0$  such that  $\Upsilon(\bar{x}, y) > 0$  if  $y \in [0, \varepsilon_1]$ . Letting  $n \rightarrow \infty$  in the inequality  $x_n > \varphi(y_n)$ , we deduce that  $\liminf_{n \rightarrow \infty} x_n \geq x_*$ .

From the previous discussions we know that  $(x_n, y_n) \notin V$ . Then, there exists some positive number  $\nu > 0$  such that  $x_n > x_* + \nu$  for large  $n$ . Also,

we can assume  $y_n \leq \varepsilon_1$ . For each  $n$ , the function  $\Upsilon(\cdot, y_n)$  must have a zero in the interval  $[x_n, \bar{x})$ , say  $\hat{x}_n \in [x_n, \bar{x})$ . After extracting a subsequence we can assume that  $\hat{x}_n$  converges to some  $\hat{x} \in [x_* + \nu, \bar{x}]$ . Then,  $(\hat{x}, 0)$  is a non-isolated point in  $Z$ . Which contradicts the definition of  $x_*$  as the largest of such points. ■

**Proof of Lemma 3.3.** We will employ some techniques from complex analysis. They are motivated by the following observation: after the change of variable  $t = u - e \sin u$ , we can express the integral in the form

$$I(e) = \int_{-\pi}^{\pi} \frac{\cos[2(u - e \sin u - f(u, e))]}{(1 - e \cos u)^2} du,$$

where the true anomaly  $f$  is written in terms of the eccentric anomaly  $u$ , as defined by eqs. (1.11) and (1.12). Then, it is indeed the composition of  $f(t, e)$  with  $t = u - e \sin u$ .

Using some trigonometric identities  $I(e)$  can be written as an integral in the family

$$\int_{-\pi}^{\pi} (R_1(\cos u, \sin u) \sin(2e \sin u) + R_2(\cos u, \sin u) \cos(2e \sin u)) du,$$

where  $R_1(x, y)$  and  $R_2(x, y)$  are rational functions. The simpler family of trigonometric integrals

$$\int_{-\pi}^{\pi} R(\cos u, \sin u) du,$$

is often analyzed using the change of variables  $z = \exp[iu]$  and the Residue Theorem. We will show that this trick also works in our situation.

First it is convenient to observe that

$$\int_{-\pi}^{\pi} \frac{\sin[2(u - e \sin u - f(u, e))]}{(1 - e \cos u)^2} du = 0,$$

because the integrand is odd. Therefore, our integral can be expressed as

$$I(e) = \int_{-\pi}^{\pi} \frac{\exp[2i(u - e \sin u - f(u, e))]}{(1 - e \cos u)^2} du. \quad (3.31)$$

After the change of variable  $z = \exp[iu]$ , we can interpret  $I(e)$  as an integral over the curve  $\gamma$ , where  $\gamma$  is the unit circle with counter-clockwise orientation. To find the integrand we employ the formulas

$$\cos u = \frac{1}{2} \left( z + \frac{1}{z} \right), \quad \sin u = \frac{1}{2i} \left( z - \frac{1}{z} \right),$$

leading to

$$1 - e \cos u = -\frac{e}{2z}(z - \zeta_-)(z - \zeta_+),$$

where  $\zeta_{\pm} = \frac{1 \pm \sqrt{1-e^2}}{e}$ . Note that  $\zeta_-$  and  $\zeta_+$  are positive real numbers with  $\zeta_- \zeta_+ = 1$  and  $\zeta_- < 1$ .

From (1.12) we can compute that

$$\exp[if(u, e)] = -\zeta_+ \frac{z - \zeta_-}{z - \zeta_+}.$$

Straightforward computations show that

$$I(e) = \frac{4}{ie^2 \zeta_+^2} \int_{\gamma} h(z, e) dz,$$

where

$$h(z, e) = \frac{z^3 \exp[-e(z - \frac{1}{z})]}{(z - \zeta_-)^4}.$$

For each  $e \in (0, 1)$ , the meromorphic function  $h(\cdot, e)$  has two singularities at  $z = \zeta_-$  and  $z = 0$ , both inside the unit circle. Therefore, making explicit the dependence on  $e$  and using the Residue Theorem,

$$I(e) = \frac{8\pi}{e^2 \zeta_+(e)^2} [\text{Res}(h(\cdot, e), \zeta_-(e)) + \text{Res}(h(\cdot, e), 0)].$$

The singularity at  $z = \zeta_-(e)$  is a pole of order 4. Then,

$$\text{Res}(h(\cdot, e), \zeta_-(e)) = \frac{1}{6} \frac{d^3 g}{dz^3}(\zeta_-(e), e),$$

with  $g(z, e) = z^3 \exp[-e(z - \frac{1}{z})]$ . The function  $g(\cdot, 1)$  is holomorphic in  $|z| > 0$ . Moreover,

$$g(z, e) \rightarrow g(z, 1) \quad \text{as } e \rightarrow 1^-, \quad z \neq 0,$$

and the convergence is uniform for  $z$  lying in any compact subset of  $\mathbb{C} \setminus \{0\}$ . In particular,

$$\frac{d^3 g}{dz^3}(z, e) \rightarrow \frac{d^3 g}{dz^3}(z, 1) \quad \text{as } e \rightarrow 1^-.$$

This shows that the residue  $\text{Res}(h(\cdot, e), \zeta_-(e))$  has a limit when  $e \rightarrow 1^-$ . We are going to prove that this is also the case for the residue at the origin.

The function  $h(\cdot, 1)$  is holomorphic in  $0 < |z| < 1$  and

$$h(z, e) \rightarrow h(z, 1) \quad \text{as } e \rightarrow 1^-, \quad 0 < |z| < 1.$$

The convergence is uniform on compact subsets. In particular on the circle  $\tilde{\gamma} = \{z \in \mathbb{C} : |z| = 1/2\}$ . Then, as  $e \rightarrow 1^-$ ,

$$\operatorname{Res}(h(\cdot, e), 0) = \frac{1}{2\pi i} \int_{\tilde{\gamma}} h(z, e) dz \rightarrow \frac{1}{2\pi i} \int_{\tilde{\gamma}} h(z, 1) dz = \operatorname{Res}(h(\cdot, 1), 0).$$

We conclude that  $I(e)$  has a limit, namely,

$$\lim_{e \rightarrow 1^-} I(e) = 8\pi \left[ \frac{1}{6} \frac{d^3 g}{dz^3}(1, 1) + \operatorname{Res}(h(\cdot, 1), 0) \right]. \quad (3.32)$$

To complete the proof we must show that this number is negative. This will involve some computations, first,

$$\frac{1}{6} \frac{d^3 g}{dz^3}(1, 1) = -\frac{1}{3}. \quad (3.33)$$

The function  $h(\cdot, 1)$  has an essential singularity at  $z = 0$ . To compute the residue we factorize  $h(\cdot, 1)$  in the form

$$h(z, 1) = \mu(z)\nu(z),$$

with

$$\mu(z) = \frac{z^3}{(z-1)^4} \exp[-z], \quad \nu(z) = \exp \frac{1}{z}.$$

Then,  $\mu$  is holomorphic in the disk  $|z| < 1$  and has an expansion

$$\mu(z) = \sum_{n=0}^{\infty} \mu_n z^n, \quad |z| < 1.$$

The function  $\nu$  has an essential singularity at  $z = 0$  with Laurent expansion

$$\nu(z) = \sum_{n=0}^{\infty} \frac{1}{n!} z^{-n}, \quad |z| > 0.$$

The residue of  $h(\cdot, 1)$  can be computed from the Laurent expansion. More precisely,

$$\operatorname{Res}(h(\cdot, 1), 0) = \sum_{n=0}^{\infty} \frac{\mu_n}{(n+1)!}. \quad (3.34)$$

From the binomial series  $(1-z)^{-d} = \sum_{n=0}^{\infty} \binom{n+d-1}{n} z^n$ , we know that

$$\frac{1}{(z-1)^4} = \sum_{n=0}^{\infty} \binom{n+3}{n} z^n, \quad |z| < 1,$$



and

$$z^3 \exp[-z] = \sum_{n=3}^{\infty} \frac{(-1)^{n+1}}{(n-3)!} z^n, \quad z \in \mathbb{C},$$

we deduce that

$$\mu_0 = \mu_1 = \mu_3 = 0, \quad \mu_n = \sum_{k=0}^{n-3} \binom{k+3}{k} \frac{(-1)^{n-k+1}}{(n-k-3)!}, \quad n \geq 3.$$

Combining this formula with (3.34),

$$\operatorname{Res}(h(\cdot, 1), 0) = \sum_{n=0}^{\infty} \sum_{k=0}^{n-3} \binom{k+3}{k} \frac{(-1)^{n-k+1}}{(n+1)!(n-k-3)!}$$

Letting  $n - k - 3 = j$ ,

$$\begin{aligned} \operatorname{Res}(h(\cdot, 1), 0) &= \sum_{k=0}^{\infty} \sum_{j=0}^{\infty} \binom{k+3}{k} \frac{(-1)^j}{j!(j+k+4)!} \\ &< \sum_{k=0}^{\infty} \sum_{j=0}^{\infty} \binom{k+3}{k} \frac{1}{j!(j+k+4)!} \\ &< \sum_{j=0}^{\infty} \frac{1}{j!} \sum_{k=0}^{\infty} \binom{k+3}{k} \frac{1}{(k+4)!} = \exp[1] \sum_{k=0}^{\infty} \binom{k+3}{k} \frac{1}{(k+4)!} \end{aligned}$$

Finally, we observe that

$$\sum_{k=0}^{\infty} \binom{k+3}{k} \frac{1}{(k+4)!} = \frac{1}{3!} \sum_{k=0}^{\infty} \frac{1}{(k+4)k!} < \frac{1}{4!} \sum_{k=0}^{\infty} \frac{1}{k!} = \frac{\exp[1]}{24}.$$

Thus,

$$\operatorname{Res}(h(\cdot, 1), 0) < \frac{\exp[2]}{24} < \frac{1}{3},$$

and the proof follows from (3.32), (3.33) and this inequality. ■

### 3.3 The synchronous resonance in the dissipative regime

Recall that the dissipative spin-orbit problem is modelled by the equation

$$\ddot{\Theta} + \delta D(t, e) \dot{\Theta} + \frac{\Lambda}{r(t, e)^3} \sin \Theta = -2\ddot{f}(t, e), \quad e \in [0, 1), \Lambda \gg \delta \geq 0, \quad (3.35)$$

with  $D(t, e)$  positive, analytic and  $2\pi$ -periodic in  $t$ . We know from Proposition 3.2 that, for  $\delta = 0$ , there exists an odd  $2\pi$ -periodic solution  $\Theta^*(t; e, \Lambda)$ , which is linearly stable in the set

$$\Omega = \{(e, \Lambda) : 0 < e < 1, 0 < \Lambda < \frac{1}{4}\Lambda_1(e), 0 < \Lambda < \Lambda_2(e)\}.$$

Furthermore, this solution is elliptic in the following sense, the discriminant associated to the linearized equation at  $\Theta^*(t; e, \Lambda)$ , say  $\Delta_0 = \Delta_0(e, \Lambda)$ , satisfies  $|\Delta_0| < 2$ .

We will prove that this periodic solution can be continued in the presence of friction, although the odd symmetry is lost.

**Theorem 3.2.** *Assume that  $(e, \Lambda) \in \Omega$ . Then, there exists a number  $\bar{\delta} > 0$  and a real analytic function*

$$(t, \delta) \in \mathbb{R} \times [0, \bar{\delta}] \quad \mapsto \quad \Theta_\delta^*(t) \in \mathbb{R},$$

*satisfying*

- i)  $\Theta_\delta^*(t)$  is an asymptotically stable  $2\pi$ -periodic solution of (3.35),*
- ii)  $\Theta_0^*(t) = \Theta^*(t; e, \Lambda)$  for each  $t \in \mathbb{R}$ .*

In principle, this theorem is consequence of well known classical results (see for instance Theorem 1.1 and 1.2 in Chapter 14, [31]). However, we will prove it independently because our proof will provide an explicit formula for  $\bar{\delta}$ . This formula will involve the quantities  $e$ ,  $\Lambda$  and  $\Delta_0$  only.

Let  $\Theta_\delta(t)$  be a solution of (3.35) satisfying  $\Theta_\delta(0) = \Theta_0 \in \mathbb{R}$ ,  $\dot{\Theta}_\delta(0) = \omega_0 \in \mathbb{R}$ . To make explicit the dependence on initial conditions, consider  $x = (\Theta_0, \omega_0)^\top \in \mathbb{R}^2$  and

$$\phi_t(\delta, x) = \begin{pmatrix} \Theta_\delta(t) \\ \omega_\delta(t) \end{pmatrix}, \quad \text{with} \quad \omega_\delta(t) = \dot{\Theta}_\delta(t).$$

Define the function

$$\mathcal{F}(\delta, x) = \phi_{2\pi}(\delta, x) - x.$$

The zeros of this function are in correspondence with the  $2\pi$ -periodic solutions of (3.35). Since we know that  $\Theta^*(t; e, \Lambda)$  is the odd  $2\pi$ -periodic solution for  $\delta = 0$ , we are going to study the implicit function problem

$$\mathcal{F}(\delta, \chi(\delta)) = 0, \quad \chi(0) = \begin{pmatrix} 0 \\ \dot{\Theta}^*(0; e, \Lambda) \end{pmatrix}.$$

The solution  $x = \chi(\delta)$  of this problem will produce a branch of periodic solutions in the conditions of Theorem 3.2.

The proof of Theorem 3.2 will consist of two steps. First, we will apply a quantitative version of the Implicit Function Theorem in order to find  $\chi(\delta)$ , defined on  $\delta \in [0, \bar{\delta}]$ . Once the branch is constructed, we will prove the asymptotic stability of the solution.

In the next lemma we will employ the following notation.

Given a function  $(\delta, x) \in [0, 1] \times \mathbb{R}^n \mapsto \mathcal{G}(\delta, x) \in \mathbb{R}^n$ . The partial derivative  $\partial_\delta \mathcal{G}(\delta, x)$  will be interpreted as a vector in  $\mathbb{R}^n$ , whereas  $\partial_x \mathcal{G}(\delta, x)$  and  $\partial_{\delta x} \mathcal{G}(\delta, x) = \partial_\delta(\partial_x \mathcal{G}(\delta, x))$  are linear maps represented by matrices in  $\mathbb{R}^{n \times n}$ . Let  $x_i$  be the  $i$ -th component of  $x \in \mathbb{R}^n$ , then,  $\partial_{xx} \mathcal{G}(\delta, x)$  is a bilinear map given by

$$\partial_{xx} \mathcal{G}(\delta, x)[u, v] = \sum_{i=1}^n \sum_{j=1}^n \frac{\partial^2 \mathcal{G}(\delta, x)}{\partial x_i \partial x_j} u_i v_j, \quad u, v \in \mathbb{R}^n.$$

The norm in  $\mathbb{R}^n$  is denoted by  $\|\cdot\|$ . The same notation will be employed for the induced norm in spaces of multilinear forms. See [40], Chapter 5, Section 7. Given a point  $\zeta \in \mathbb{R}^n$  and a positive number  $r > 0$ , the closed ball centered at  $\zeta$  of radius  $r$  is denoted by  $\bar{B}_r(\zeta)$ .

**Lemma 3.5.** *Let  $\mathcal{G} : [0, \delta_*] \times \mathbb{R}^n \rightarrow \mathbb{R}^n$ , with  $\delta_* > 0$ , and  $\mathcal{G} = \mathcal{G}(\delta, x)$ , be a function of class  $C^2$  such that there exists  $(\partial_x \mathcal{G}(\delta_0, x_0))^{-1}$  and  $\mathcal{G}(\delta_0, x_0) = 0$  for a certain point  $(\delta_0, x_0) \in [0, \delta_*] \times \mathbb{R}^n$ .*

*Assume that there exist uniform bounds  $C_1 \geq \|\partial_\delta \mathcal{G}\|$ ,  $C_{12} \geq \|\partial_{\delta x} \mathcal{G}\|$ ,  $C_{22} \geq \|\partial_{xx} \mathcal{G}\|$  for all  $(\delta, x) \in [0, \delta_*] \times \mathbb{R}^n$  and  $C_0 > \|(\partial_x \mathcal{G}(\delta_0, x_0))^{-1}\|$ .*

*Define the positive constants*

$$\rho = \begin{cases} \frac{C_{12} - C_0 C_1 C_{22}}{C_0 C_{12}^2} & \text{if } 2C_0 C_1 C_{22} < C_{12}, \\ \frac{1}{4C_0^2 C_1 C_{22}} & \text{if } 2C_0 C_1 C_{22} \geq C_{12}, \end{cases} \quad (3.36)$$

and

$$R = R(\rho) = \frac{1 - \sqrt{1 - 4C_0^2 C_1 C_{22} \rho}}{2C_0 C_{22}}, \quad (3.37)$$

then, there exists a  $C^2$  function  $\chi : \bar{B}_\rho(\delta_0) \cap [0, \delta_*] \rightarrow \bar{B}_R(x_0)$  satisfying  $x_0 = \chi(\delta_0)$  and

$$\mathcal{G}(\delta, \chi(\delta)) = 0, \quad \delta \in \bar{B}_\rho(\delta_0) \cap [0, \delta_*].$$

**Proof.** The proof follows along the standard methods using the Contraction mapping theorem. See for instance Section 3.4 in [68]. We give some hints to reproduce the values of  $\rho$  and  $R$  in eqs. (3.36) and (3.37). Define

$$L(\delta, x) = x - M^{-1}\mathcal{G}(\delta, x), \quad M = \partial_x \mathcal{G}(\delta_0, x_0),$$

so that our problem is equivalent to the fixed point equation  $x = L(\delta, x)$ . We see that

$$\partial_x \mathcal{G}(\delta, x) - M = \int_0^1 \partial_{\delta_x} \mathcal{G}(\delta_\lambda, x_\lambda)(\delta - \delta_0) d\lambda + \int_0^1 \partial_{xx} \mathcal{G}(\delta_\lambda, x_\lambda)(x - x_0) d\lambda,$$

$$\partial_x \mathcal{G}(\delta_0, x) - M = \int_0^1 \partial_{xx} \mathcal{G}(\delta_0, x_\lambda)(x - x_0) d\lambda,$$

where  $\delta_\lambda = \lambda\delta + (1 - \lambda)\delta_0$ ,  $x_\lambda = \lambda x + (1 - \lambda)x_0$ ,  $\lambda \in [0, 1]$ . Consequently, since  $\partial_x L(\delta, x) = \mathbf{1} - M^{-1}\partial_x \mathcal{G}(\delta, x)$ , we can use the bounds of the derivatives of  $\mathcal{G}$  to get that

$$\|\partial_x L(\delta, x)\| \leq C_0(C_{12}\rho + C_{22}R), \quad \|\partial_x L(\delta_0, x)\| \leq C_0 C_{22}R, \quad (3.38)$$

for each  $x \in \bar{B}_R(x_0)$  and  $\delta \in \bar{B}_\rho(\delta_0)$ . From the second expression in (3.38) and the generalized version of the mean-value theorem for vector-valued functions, see [3], we get

$$\|L(\delta_0, x) - L(\delta_0, x_0)\| \leq C_0 C_{22}R^2 \quad x \in \bar{B}_R(x_0).$$

Proceeding analogously with  $\partial_\delta L$ , we obtain

$$\|L(\delta, x) - L(\delta_0, x)\| \leq C_0 C_1 \rho \quad x \in \bar{B}_R(x_0), \quad \delta \in \bar{B}_\rho(\delta_0).$$

Note that  $L(\delta_0, x_0) = x_0$  by definition, then,

$$\begin{aligned} \|L(\delta, x) - x_0\| &\leq \|L(\delta, x) - L(\delta_0, x)\| + \|L(\delta_0, x) - L(\delta_0, x_0)\| \\ &\leq C_0(C_1\rho + C_{22}R^2). \end{aligned}$$

Let  $X$  be the complete metric space composed by continuous functions

$$\chi : \bar{B}_\rho(\delta_0) \cap [0, \delta_*] \rightarrow \bar{B}_R(x_0), \quad \chi(\delta_0) = x_0.$$

The distance in  $X$  is induced by the uniform norm. Consider the operator  $L(\delta, \cdot) : X \rightarrow X$ . From the previous computations, this operator is well defined, i.e.,  $L(\delta, X) \subseteq X$ , as long as

$$C_0(C_1\rho + C_{22}R^2) \leq R.$$

Moreover, from the first inequality in (3.38),  $L(\delta, \cdot)$  is a contraction if

$$C_0(C_{12}\rho + C_{22}R) < 1.$$

The parameters  $\rho$  and  $R$  in (3.36) and (3.37) are the values such that the last two inequalities are satisfied and the value of  $\rho$  is the largest possible. The Banach principle leads to a continuous solution of the functional equation. The implicit function theorem can be applied at each  $(\delta, \chi(\delta))$  to deduce that this solution is indeed  $C^2$ . ■

**Remark 3.4.** Note that  $\chi$  is a real analytic function if  $\mathcal{G}$  is real analytic.

**Remark 3.5.** By direct substitution of (3.36), we get that  $0 \leq 1 - 4C_0^2C_1C_{22}\rho < 1$ , and

$$\rho \in \left(0, \frac{1}{4C_0^2C_1C_{22}}\right], \quad R \in \left(0, \frac{1}{2C_0C_{22}}\right].$$

We will work with  $n = 2$  and the maximum norm

$$\|x\| = \max\{|x_1|, |x_2|\}, \quad x = \begin{pmatrix} x_1 \\ x_2 \end{pmatrix}.$$

The corresponding norms in the spaces of multilinear maps (see [40]) are given by

$$\begin{aligned} \|\partial_\delta \mathcal{G}(\delta, x)\| &= \max_{i \in \{1,2\}} |\partial_\delta \mathcal{G}_i(\delta, x)|, \\ \|\partial_{\delta x} \mathcal{G}(\delta, x)\| &= \max_{i \in \{1,2\}} \left\{ \sum_{j \in \{1,2\}} \left| \frac{\partial^2 \mathcal{G}_i(\delta, x)}{\partial \delta \partial x_j} \right| \right\}, \\ \|\partial_{xx} \mathcal{G}(\delta, x)\| &= \max_{i \in \{1,2\}} \left\{ \sum_{j,k \in \{1,2\}} \left| \frac{\partial^2 \mathcal{G}_i(\delta, x)}{\partial x_k \partial x_j} \right| \right\}. \end{aligned}$$

It will be clear from the computations of the bounds of the previous norms that Lemma 3.5 cannot be directly applied to the function  $\mathcal{F}$ . Actually, the norm of  $\partial_\delta \mathcal{F}(\delta, x)$  has not a uniform bound in  $(\delta, x) \in \mathbb{R}^2$ . To overcome this difficulty, we will observe that there is a partial a priori bound for the periodic solutions of (3.35).

**Lemma 3.6.** *Let  $\Theta(t)$  be a  $2\pi$ -periodic solution of (3.35). Then,*

$$|\dot{\Theta}(t)| \leq C \quad \text{for each } t \in \mathbb{R},$$

with  $C := \Lambda \int_0^{2\pi} \frac{dt}{r(t,e)^3} + 2 \int_0^{2\pi} |\ddot{f}(t,e)| dt$ .

**Proof.** Note that if  $\Theta(t)$  satisfies (3.35), then  $\omega(t) = \dot{\Theta}(t)$  satisfies the equation

$$\dot{\omega} + \delta D(t,e)\omega = b_0(t), \quad b_0(t) = -2\ddot{f}(t,e) - \frac{\Lambda}{r(t,e)^3} \sin[\Theta(t)],$$

by variation of constants we see that if  $\omega_0 = \omega(t_0)$ ,

$$\omega(t) = \omega_0 \exp\left(-\delta \int_{t_0}^t D(s,e) ds\right) + \int_{t_0}^t b_0(s) \exp\left(-\delta \int_s^t D(\tau,e) d\tau\right) ds,$$

and, since  $D$  is positive,

$$|\omega(t)| \leq |\omega_0| + \int_{t_0}^{t_0+2\pi} |b_0(s)| ds \leq |\omega_0| + C, \quad (3.39)$$

where we defined

$$C = 2\|\ddot{f}(\cdot, e)\|_1 + \Lambda\|r(\cdot, e)^{-3}\|_1,$$

where  $\|\cdot\|_1$  is the  $L^1[0, 2\pi]$ -norm.

Since the solution  $\Theta(t)$  is  $2\pi$ -periodic, then, we could choose  $t_0$  such that  $\dot{\Theta}(t_0) = \omega_0 = 0$ . Then,  $C$  is a bound for  $|\dot{\Theta}(t)|$ . ■

Note that an analogous bound cannot be obtained for  $\Theta(t)$ . Due to the periodicity of the equation,  $\Theta(t) + 2n\pi$  is also a solution for each  $n \in \mathbb{Z}$ .

Let us define the function  $\mathcal{M} : \mathbb{R} \rightarrow \mathbb{R}$ , and the map  $\mathcal{R} : \mathbb{R}^2 \rightarrow \mathbb{R}^2$  such that

$$\mathcal{M}(\zeta) = \begin{cases} \arctan(\zeta + C) - C & \text{if } \zeta < -C, \\ \zeta & \text{if } |\zeta| \leq C, \\ \arctan(\zeta - C) + C & \text{if } \zeta > C, \end{cases} \quad \mathcal{R}(x) = \begin{pmatrix} x_1 \\ \mathcal{M}(x_2) \end{pmatrix}. \quad (3.40)$$

We observe that  $\mathcal{R}$  is  $C^2$  and satisfies

- $\mathcal{R}$  is the identity on the strip  $S_C = \{(x_1, x_2)^\top : |x_2| \leq C\}$ .
- $\mathcal{R}(\mathbb{R}^2 \setminus S_C) \cap S_C = \emptyset$ .

From these properties and Lemma 3.6 it is easy to deduce that, if  $x \in S_C$ , the equation  $\mathcal{F}(\delta, x) = 0$  is equivalent to  $\mathcal{G}(\delta, x) = 0$ , where,

$$\mathcal{G}(\delta, x) = \mathcal{F}(\delta, \mathcal{R}(x)).$$

Here by equivalence we mean that both equations have the same solutions.

We can now find bounds for the norms of the derivatives of  $\mathcal{G}$ . Consider a vector  $x = (\Theta_0, \omega_0)^\top \in \mathbb{R}^2$  and let  $\Theta = \Theta(t; \delta, x)$  be the solution of (3.35) with initial conditions  $\Theta(0) = \Theta_0$ ,  $\dot{\Theta}(0) = \omega_0$  for fixed  $(e, \Lambda)$ . Let us call  $\omega(t; \delta, x) = \dot{\Theta}(t; \delta, x)$  and

$$\phi_t(\delta, x) = \begin{pmatrix} \Theta(t; \delta, x) \\ \omega(t; \delta, x) \end{pmatrix}.$$

Note that  $\Phi(t) = \partial_x \phi_t(\delta, x) \in \mathbb{R}^{2 \times 2}$  is the matrix solution of

$$\dot{y} = A(t)y, \quad y(0) = \mathbf{1},$$

where

$$A(t) = \begin{pmatrix} 0 & 1 \\ -\frac{\Lambda}{r(t,e)^3} \cos[\Theta(t; \delta, x)] & -\delta D(t, e) \end{pmatrix},$$

then, for  $0 \leq s \leq t \leq T = 2\pi$ ,

$$\Phi(t)\Phi(s)^{-1} = \mathbf{1} + \int_s^t A(\tau)\Phi(\tau)\Phi(s)^{-1}d\tau,$$

taking matrix norms and using Gronwall's inequalities, we have that

$$\|\Phi(t)\Phi(s)^{-1}\| \leq \exp\left(\int_s^t \|A(\tau)\|d\tau\right) \leq \exp\left(\int_0^T \|A(\tau)\|d\tau\right).$$

Using the maximum norm we get

$$\|A(\tau)\| \leq \begin{cases} \max\{1, \Lambda|r(\tau, e)^{-3}\} & \text{if } \delta = 0, \\ \max\{1, \Lambda|r(\tau, e)^{-3} + \delta|D(\tau, e)|\} & \text{if } \delta > 0, \end{cases}$$

in consequence, using the subscript 0 for the case  $\delta = 0$ , we have that

$$\|\Phi_0(t)\Phi_0(s)^{-1}\| \leq \kappa_0 = \exp\left(\max\{T, \Lambda\|r(\cdot, e)^{-3}\|_1\}\right),$$

where  $\|\cdot\|_1$  is the  $L^1[0, T]$ -norm. Note that, for  $\delta = 0$ , it is also true that  $\|A(\tau)^\top\| \leq \max\{T, \Lambda|r(\tau, e)^{-3}\}$ , then,  $\|\Phi_0(t)^\top\| \leq \kappa_0$ . Fixing a value  $\delta_* > 0$ , for  $\delta \in (0, \delta_*]$  we have

$$\|\Phi(t)\Phi(s)^{-1}\| \leq \kappa = \exp\left(\max\{T, \Lambda\|r(\cdot, e)^{-3}\|_1 + \delta_*\|D(\cdot, e)\|_1\}\right).$$

The previous bounds are valid for all the initial conditions  $x \in \mathbb{R}^2$ .

For

$$\mathcal{G}(\delta, x) = \mathcal{F}(\delta, \mathcal{R}(x)) = \phi_T(\delta, \mathcal{R}(x)) - \mathcal{R}(x),$$

where  $\mathcal{R}$  is defined in (3.40), we want to find some positive constants such that

$$C_1 \geq \|\partial_\delta \mathcal{G}(\delta, x)\|, \quad C_{12} \geq \|\partial_{\delta x} \mathcal{G}(\delta, x)\|, \quad C_{22} \geq \|\partial_{xx} \mathcal{G}(\delta, x)\|.$$

Computing the derivatives,

$$\partial_\delta \mathcal{G}(\delta, x) = \partial_\delta \phi_T(\delta, \mathcal{R}(x)),$$

$$\partial_{\delta x} \mathcal{G}(\delta, x) = \partial_{\delta x} \phi_T(\delta, \mathcal{R}(x)) \partial_x \mathcal{R}(x),$$

$$\frac{\partial^2 \mathcal{G}}{\partial x_i \partial x_j}(\delta, x) = \partial_{xx} \phi_T(\delta, \mathcal{R}(x)) \left[ \frac{\partial \mathcal{R}}{\partial x_i}, \frac{\partial \mathcal{R}}{\partial x_j} \right] + (\partial_x \phi_T(\delta, \mathcal{R}(x)) - \mathbb{1}) \left[ \frac{\partial^2 \mathcal{R}}{\partial x_i \partial x_j} \right],$$

where, in the last expression,  $\partial_{xx} \phi_T$  is considered as a bilinear map and  $(\partial_x \phi_T - \mathbb{1})$  as a linear map. We can see that the non-vanishing derivatives of  $\mathcal{R}$  appearing above are

$$\frac{\partial \mathcal{R}}{\partial x_1} = \begin{pmatrix} 1 \\ 0 \end{pmatrix}, \quad \frac{\partial \mathcal{R}}{\partial x_2} = \begin{pmatrix} 0 \\ \mathcal{M}'(x_2) \end{pmatrix}, \quad \frac{\partial^2 \mathcal{R}}{\partial x_2^2} = \begin{pmatrix} 0 \\ \mathcal{M}''(x_2) \end{pmatrix},$$

then, particularly,

$$\frac{\partial^2 \mathcal{G}}{\partial x_1^2}(\delta, x) = \frac{\partial^2 \phi_T}{\partial x_1^2}(\delta, \mathcal{R}(x)), \quad \frac{\partial^2 \mathcal{G}}{\partial x_1 \partial x_2} = \frac{\partial^2 \phi_T}{\partial x_1 \partial x_2}(\delta, \mathcal{R}(x)) \mathcal{M}'(x_2),$$

$$\frac{\partial^2 \mathcal{G}}{\partial x_2^2}(\delta, x) = (\mathcal{M}'(x_2))^2 \frac{\partial^2 \phi_T}{\partial x_2^2}(\delta, \mathcal{R}(x)) + (\partial_x \phi_T(\delta, \mathcal{R}(x)) - \mathbb{1}) \begin{pmatrix} 0 \\ \mathcal{M}''(x_2) \end{pmatrix}.$$

Taking into account that  $|\mathcal{M}'(x_2)| \leq 1$  and  $|\mathcal{M}''(x_2)| \leq 3\sqrt{3}/8$ , the constants  $C_1$ ,  $C_{12}$  and  $C_{22}$  are going to be defined in terms of bounds for the derivatives of  $\phi_T(\delta, \mathcal{R}(x))$ .

The function  $\partial_\delta \phi_t(\delta, x)$  is a solution of

$$\dot{y} = A(t)y + b_1(t), \quad y(0) = 0,$$

where

$$b_1(t) = \begin{pmatrix} 0 \\ -D(t, e)\omega(t; \delta, x) \end{pmatrix}.$$

By variation of constants

$$\partial_\delta \phi_t(\delta, x) = \int_0^t \Phi(t)\Phi(s)^{-1} b_1(s) ds,$$



then, in order to find a bound for  $\|\partial_\delta \phi_T(\delta, \mathcal{R}(x))\|$ , first we need to find a bound for  $|\omega(t; \delta, \mathcal{R}(x))|$ . Note that the expression (3.39) is valid for all the initial conditions  $\omega_0 = \omega(0; \delta, x)$ , but in our case  $|\mathcal{M}(\omega_0)| \leq C + \pi/2$ , then,

$$|\omega(t; \delta, \mathcal{R}(x))| \leq 2C + \pi/2.$$

Consequently,

$$\|\partial_\delta \phi_T(\delta, \mathcal{R}(x))\| \leq \int_0^T \|\Phi(T)\Phi(s)^{-1}\| \|b_1(s)\| ds \leq C_1 = \kappa \|D(\cdot, e)\|_1 (2C + \pi/2).$$

We see that  $\partial_{\delta x} \phi_t(\delta, x)$  is a matrix solution of

$$\dot{y} = A(t)y + b_{12}(t), \quad y(0) = 0,$$

where

$$b_{12}(t) = \begin{pmatrix} 0 & 0 \\ \frac{\Lambda}{r(t,e)^3} \partial_\delta \Theta(t; \delta, x) \sin[\Theta(t; \delta, x)] & -D(t, e) \end{pmatrix} \Phi(t),$$

then,

$$\|\partial_{\delta x} \phi_T(\delta, \mathcal{R}(x))\| \leq \int_0^T \|\Phi(T)\Phi(s)^{-1}\| \|b_{12}(s)\| ds \leq C_{12},$$

with  $C_{12} = \kappa^2 (C_1 \Lambda \|r(\cdot, e)^{-3}\|_1 + \|D(\cdot, e)\|_1)$ .

Finally, we observe that  $\frac{\partial^2 \phi_t}{\partial x_i \partial x_j}$  is solution of

$$\dot{y} = A(t)y + b_{22}^{ij}(t), \quad y(0) = 0,$$

where

$$b_{22}^{ij}(t) = \begin{pmatrix} 0 \\ \frac{\Lambda}{r(t,e)^3} \frac{\partial \Theta}{\partial x_i} \frac{\partial \Theta}{\partial x_j} \sin \Theta \end{pmatrix}.$$

Then

$$\left\| \frac{\partial^2 \phi_T}{\partial x_i \partial x_j}(\delta, \mathcal{R}(x)) \right\| \leq \int_0^T \|\Phi(T)\Phi(s)^{-1}\| \|b_{22}^{ij}(s)\| ds \leq \kappa^3 \Lambda \|r(\cdot, e)^{-3}\|_1.$$

In consequence,

$$\|\partial_{xx} \mathcal{G}(\delta, x)\| \leq \sum_{i,j \in \{1,2\}} \left\| \frac{\partial^2 \mathcal{G}}{\partial x_i \partial x_j} \right\| \leq C_{22} = 4\kappa^3 \Lambda \|r(\cdot, e)^{-3}\|_1 + \frac{3\sqrt{3}(1+\kappa)}{8}.$$

Finally, in our case,  $\delta_0 = 0$  and  $x_0 = (0, \dot{\Theta}^*(0))^\top$ . We know that  $|\dot{\Theta}^*(0)| \leq C$ , since  $\Theta^*(t)$  is a  $T$ -periodic solution, then,  $\mathcal{R}(x_0) = x_0$  and  $\partial_x \mathcal{R}(x_0) = \mathbf{1}$ , so, we have to find a bound for the norm of

$$(\partial_x \mathcal{G}(0, x_0))^{-1} = (\partial_x \phi_T(0, x_0) - \mathbf{1})^{-1}.$$

For any matrix  $M \in \mathbb{R}^{2 \times 2}$ ,

$$M^{-1} = -\frac{JM^\top J}{\det M}, \quad J = \begin{pmatrix} 0 & 1 \\ -1 & 0 \end{pmatrix},$$

since  $\|J\| = 1$ , then,

$$\|M^{-1}\| \leq \frac{\|M^\top\|}{|\det M|},$$

on the other hand, define  $\Delta_0 = \text{Tr}(\partial_x \phi_T(0, x_0))$ , since  $\partial_x \phi_T(0, x_0)$  is a symplectic matrix, we have that  $\det(\partial_x \phi_T(0, x_0)^\top - \mathbf{1}) = 2 - \Delta_0$ . In consequence,

$$\|(\partial_x \mathcal{G}(0, x_0))^{-1}\| \leq C_0 = \frac{1 + \kappa_0}{|2 - \Delta_0|}.$$

Summarizing, we have obtained

$$C_0 = \frac{1 + \kappa_0}{|2 - \Delta_0|}, \quad C_1 = \kappa \|D(\cdot, e)\|_1 (2C + \pi/2),$$

$$C_{12} = \kappa^2 (C_1 \Lambda \|r(\cdot, e)^{-3}\|_1 + \|D(\cdot, e)\|_1),$$

$$C_{22} = 4\kappa^3 \Lambda \|r(\cdot, e)^{-3}\|_1 + \frac{3\sqrt{3}(1 + \kappa)}{8},$$

where  $\|\cdot\|_1$  is the  $L^1[0, 2\pi]$ -norm and the constants  $\kappa_0$  and  $\kappa$  are defined by

$$\kappa_0 = \exp(\max\{2\pi, \Lambda \|r(\cdot, e)^{-3}\|_1\}),$$

$$\kappa = \exp(\max\{2\pi, \Lambda \|r(\cdot, e)^{-3}\|_1 + \delta_* \|D(\cdot, e)\|_1\}),$$

where the constant  $\delta_* \in (0, 1/4)$  can be chosen arbitrarily as long as the computed value  $\bar{\delta}$  remains smaller than the chosen  $\delta_*$ . We will take  $\delta_* = 0.01$  for the linear MacDonald torque in Section 3.3.2.

The parameters  $\rho$  and  $R$  are now determined by (3.36) and (3.37). We find the function  $\chi(\delta)$  defined on  $[0, \rho]$ , such that

$$\|\chi(\delta) - \chi(0)\| \leq R. \tag{3.41}$$

Once we have constructed the branch of periodic solutions  $\Theta = \Theta_\delta^*(t)$ , we analyze the stability properties. The next Lemma on linear equations is tailored for our purposes.

**Lemma 3.7.** *Let  $a, b, c : \mathbb{R} \rightarrow \mathbb{R}$  be continuous and  $T$ -periodic functions, also,  $c \in C^1$  and  $\int_0^T c(t)dt > 0$ . Let  $K > 0$  be a constant such that*

$$\left| b(t) - \frac{1}{4}c(t)^2 - \frac{1}{2}\dot{c}(t) \right| < K, \quad t \in [0, T].$$

*Let  $\Delta_0$  be the discriminant of  $\ddot{y} + a(t)y = 0$  and assume that  $|\Delta_0| < 2$ . Assume that*

$$\|\Phi_0(t)\Phi_0(s)^{-1}\| \leq \kappa_0, \quad 0 \leq s < t \leq T,$$

*where  $\Phi_0(t)$  is the matrix solution of  $\ddot{y} + a(t)y = 0$ , such that  $\Phi_0(0) = \mathbb{1}$ , and  $\|\cdot\|$  denotes the matrix norm induced by the maximum norm in  $\mathbb{R}^2$ . Then, the equation*

$$\ddot{y} + c(t)\dot{y} + (a(t) + b(t))y = 0 \quad (3.42)$$

*is asymptotically stable if*

$$K < \frac{1}{\kappa_0 T} \ln \left( 1 + \frac{2 - |\Delta_0|}{2\kappa_0} \right). \quad (3.43)$$

**Proof.** The change of variables  $\eta(t) = \exp\left(\frac{1}{2}\int_0^t c(s)ds\right)y(t)$ , transforms (3.42) into

$$\ddot{\eta} + \left(a(t) + \tilde{b}(t)\right)\eta = 0,$$

where

$$\tilde{b}(t) = b(t) - \frac{1}{4}c(t)^2 - \frac{1}{2}\dot{c}(t).$$

We observe that (3.42) is asymptotically stable if the equation for  $\eta$  is stable. If we call  $Y = \begin{pmatrix} \eta \\ \dot{\eta} \end{pmatrix}$ , we obtain the equation

$$\dot{Y} = \left(A_0(t) + \tilde{b}(t)N\right)Y,$$

where

$$A_0(t) = \begin{pmatrix} 0 & 1 \\ -a(t) & 0 \end{pmatrix}, \quad N = \begin{pmatrix} 0 & 0 \\ -1 & 0 \end{pmatrix}.$$

Let  $\Phi(t)$  be the matrix solution with  $\Phi(0) = \mathbb{1}$ . Then, by variation of constants, the equation is equivalent to

$$\Phi(t) = \Phi_0(t) + \int_0^t \Phi_0(t)\Phi_0(s)^{-1}\tilde{b}(t)N\Phi(s)ds.$$

Since the maximum norm of  $N$  is 1, then,

$$\|\Phi(t)\| \leq \kappa_0 + \kappa_0 \mu \int_0^t \|\Phi(s)\| ds.$$

Using Gronwall's Lemma,

$$\|\Phi(t)\| \leq \kappa_0 \exp(\kappa_0 \mu t),$$

in consequence,

$$\|\Phi(t) - \Phi_0(t)\| \leq \kappa_0^2 \mu \int_0^t \exp(\kappa_0 \mu s) ds = \kappa_0 (\exp(\kappa_0 \mu t) - 1).$$

For any real square matrix  $M$ ,  $|\operatorname{Tr} M| \leq 2r_s(M) \leq 2\|M\|$ , where  $r_s$  is the spectral radius. If  $\Delta = \operatorname{Tr} \Phi(T)$  and, using hypothesis (3.43),

$$|\Delta - \Delta_0| \leq 2\kappa_0 (\exp(\kappa_0 \mu T) - 1) < 2 - |\Delta_0|.$$

We conclude that  $|\Delta| < 2$ . ■

The variational equation of (3.35) at  $\Theta_\delta^*(t)$  is

$$\ddot{y} + \delta D(t, e) \dot{y} + \frac{\Lambda}{r(t, e)^3} \cos[\Theta_\delta^*(t)] y = 0.$$

We can interpret this equation as a perturbation of the equation for  $\delta = 0$ . In the framework of (3.42),

$$a(t) = \frac{\Lambda}{r(t, e)^3} \cos[\Theta_0^*(t)],$$

$$b(t) = \frac{\Lambda}{r(t, e)^3} (\cos[\Theta_\delta^*(t)] - \cos[\Theta_0^*(t)]), \quad c(t) = \delta D(t, e).$$

To estimate  $|b(t)|$  we observe that  $\eta(t) = \Theta_\delta^*(t) - \Theta_0^*(t)$  satisfies the linear equation

$$\ddot{\eta} + P(t)\eta = Q(t), \tag{3.44}$$

where

$$P(t) = \frac{\Lambda}{r(t, e)^3} \frac{\sin[\Theta_\delta^*(t)] - \sin[\Theta_0^*(t)]}{\Theta_\delta^*(t) - \Theta_0^*(t)}, \quad Q(t) = -\delta D(t, e) \dot{\Theta}_\delta^*(t)$$

In view of Lemma 3.6 we deduce that  $|Q(t)| \leq \rho C D(t, e)$ . Also,  $|P(t)| \leq \frac{\Lambda}{r(t, e)^3}$ . These estimates, together with (3.41) and (3.37) lead to

$$|\Theta_\delta^*(t) - \Theta_0^*(t)| \leq \kappa_0 R(\rho) + \kappa_0 \rho C \|D(\cdot, e)\|_1, \tag{3.45}$$

where  $\|\cdot\|_1$  is the  $L^1[0, 2\pi]$ -norm. Let us prove this. By variation of constants in (3.44) we get that

$$\begin{pmatrix} \eta(t) \\ \dot{\eta}(t) \end{pmatrix} = \hat{\Phi}(t) \begin{pmatrix} \eta(0) \\ \dot{\eta}(0) \end{pmatrix} + \int_0^t \hat{\Phi}(t)\hat{\Phi}^{-1}(s) \begin{pmatrix} 0 \\ Q(s) \end{pmatrix} ds,$$

where  $\hat{\Phi}(t)$  is the matrix solution of the homogeneous equation  $\ddot{\eta} + P(t)\eta = 0$ . Note that, since  $|P(t)| \leq \frac{\Lambda}{r(t,e)^3}$ , we have that

$$\|\hat{\Phi}(t)\| \leq \kappa_0 = \exp\left(\max\{2\pi, \Lambda\|r(\cdot, e)^{-3}\|_1\}\right),$$

exactly as in the computation of  $\kappa_0$ . Moreover, note that

$$\left\| \begin{pmatrix} \eta(0) \\ \dot{\eta}(0) \end{pmatrix} \right\| = \|\chi(\delta) - \chi(0)\| \leq R,$$

since  $|Q(t)| \leq \rho CD(t, e)$ , we get that

$$|\Theta_\delta^*(t) - \Theta_0^*(t)| \leq \kappa_0 R + \kappa_0 \rho C \|D(\cdot, e)\|_1.$$

Consequently,

$$|b(t)| \leq \frac{\kappa_0 \Lambda}{r(t, e)^3} (R(\rho) + \rho C \|D(\cdot, e)\|_1),$$

and we can take a suitable  $K = K(\rho)$ , say,

$$K(\rho) = \kappa_0 \Lambda \|r(\cdot, e)^{-3}\|_\infty (R(\rho) + \rho C \|D(\cdot, e)\|_1) + \frac{\rho^2}{4} \|D(\cdot, e)\|_\infty^2 + \frac{\rho}{2} \|\dot{D}(\cdot, e)\|_\infty.$$

Note that, by (3.37),  $K(\rho)$  is an increasing continuous function for  $\rho \in (0, \frac{1}{4C_0^2 C_1 C_{22}}]$  and such that  $K(\rho) \rightarrow 0^+$  as  $\rho \rightarrow 0^+$ . In consequence, the function  $\Theta_\delta^*(t)$  obtained by Lemma 3.5 is asymptotically stable as long as

$$\rho < K^{-1} \left( \frac{1}{\kappa_0 T} \ln \left( 1 + \frac{2 - |\Delta_0|}{2\kappa_0} \right) \right).$$

In principle, we do not know if the value of  $\rho$  defined by (3.36) satisfies this inequality. However, since the solution  $\Theta_\delta^*(t)$  is defined for all  $\delta \in [0, \rho]$ , we can always take a smaller value of  $\rho$ , say  $\delta$ , satisfying the previous inequality so that  $\Theta_\delta^*(t)$  is asymptotically stable for all  $\delta \in [0, \delta]$ . With this, we have proved Theorem 3.2.

### 3.3.1 The dissipative function $D(t, e)$

In addition of being a planar model, equation (3.35) models the dissipative spin-orbit with the strong assumption that the dissipative torque is proportional to  $\dot{\Theta}$ . This is obvious for the so-called linear MacDonald torque in (1.14), for which  $D(t, e) = r(t, e)^{-6}$ , in this case we will be able to find analytically the constants of our estimates, except for  $\Delta_0$ , which can be found numerically.

Let us sketch a procedure to make applicable our results to other dissipative torques. We take [42] as reference. In general, to compute the dissipative torque  $\mathcal{T}_d$  we start from a potential  $U$  depending on the position of the perturbing body, so that  $\mathcal{T}_d = rF_z$ , where  $F_z$  is the  $z$ -component of the force  $F = -\text{grad} U$ . It is common to expand  $U$  in power series of  $1/r$ , via Legendre polynomials, and assume that the dissipation is introduced by including a constant small time delay  $\Delta t$  in the position of the perturber. This gives rise to the torque of equation (28) in [42]. If we take only the leading term of the expansion we get the linear MacDonald torque, equation (30), [42]. Note that, in the expanded torque (28), [42], we work with  $i = 0$ ,  $M_1 = M_1^*$ ,  $r = r^*$ , and  $\lambda = \lambda^*$ . Consequently, we can see that each term of the expansion is proportional to  $\sin(-m\Delta t\dot{\Theta}/2) \approx -m\Delta t\dot{\Theta}/2$  and we can write the torque in the form  $-\delta D(t, e)\dot{\Theta}$ . Actually, different orders of approximation would give rise to different functions  $D(t, e)$ . However, we must mention that this procedure does not guarantee that  $D(t, e)$  is positive, which is important to find an upper bound  $C \geq |\dot{\Theta}_\delta^*(t)|$ , see Lemma 3.6, involved in the computation of other constants of our estimates.

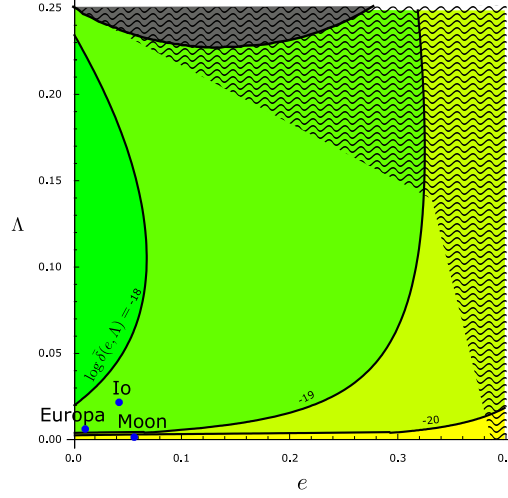


Figure 3.5: Dissipative diagram for the linear MacDonald torque. The greener regions correspond to greater admissible  $\delta$ . We do not guarantee the existence of  $\Theta_\delta^*(t; e, \Lambda)$  for the region filled with the wavy pattern.

### 3.3.2 Quantitative estimates for the linear MacDonald torque

In general we see that

$$\|r(\cdot, e)^{-3}\|_\infty = \frac{1}{(1-e)^3}, \quad \|r(\cdot, e)^{-3}\|_1 = \frac{2\pi}{(1-e^2)^{3/2}},$$

$$\|\ddot{f}(\cdot, e)\|_1 = \frac{8e}{\sqrt{1-e^2}},$$

while for the linear MacDonald torque

$$\|D(\cdot, e)\|_\infty = \frac{1}{(1-e)^6}, \quad \|D(\cdot, e)\|_1 = \frac{8 + 24e^2 + 3e^4}{4(1-e^2)^{9/2}}\pi,$$

$$\|\dot{D}(\cdot, e)\|_\infty \leq \frac{6e}{(1-e)^8}.$$

Taking  $\delta_* = 0.01$ , we can compute the maximum admissible  $\bar{\delta} = \bar{\delta}(e, \Lambda)$  and divide the  $(e, \Lambda)$ -diagram in regions corresponding to different orders of magnitude of  $\bar{\delta}$ . See Figure 3.5.

In the case of the Moon-Earth system, for which  $e = 0.0549$ ,  $\Lambda = 0.00069$ , we obtain that the 1 : 1 resonance is asymptotically stable for all  $\delta$  smaller than  $\bar{\delta} = 2.06 \cdot 10^{-20}$ . This is actually a very small value, however, if we

Satellite (Planet)	$e$	$\Lambda$	$\bar{\delta}$	$\Delta t(\bar{\delta})$
Moon (Earth)	0.0549	0.00069	$2.06 \cdot 10^{-20}$	11 min
Io (Jupiter)	0.0041	0.021	$9.69 \cdot 10^{-19}$	0.00057 min
Europa (Jupiter)	0.0094	0.0055	$2.85 \cdot 10^{-19}$	0.0064 min

Table 3.1: Estimates for some satellite-planet systems with strong spin-orbit interaction. The parameters  $e$  and  $\Lambda$  have been taken from [16] and other constants from [1]. The corresponding  $\bar{\delta}$  has been obtained numerically. The dependence of  $\Delta t$  with respect to  $\delta$  only depends on the parameters of the system.

evaluate the corresponding maximum admissible delay we get  $\Delta t(\bar{\delta}) = 11$  min. Which means that, if the Moon's response is delayed 11 minutes or less, its asymptotic stability is guaranteed by our computations. Consider a seismic event occurring at the center of the Moon and reaching the surface in 11 minutes. If the Moon were homogeneous, the necessary velocity of propagation would be of 2.74 km/s. This is reasonably consistent with the available data from the interior of the Moon, for which the speed of p-waves ranges from 1.0 km/s to 8.5 km/s, according to Table 24.2 in [122]. On the contrary, as we see in Table 3.1, we are less optimistic with respect to the direct applicability of these estimates for Io and Europa, since we get too small values of  $\Delta t$ . We do not know the ultimate reason for this shortcoming. The roughness of our estimates could be the underlying reason. The limitations of the model could also explain it. One of the referees has informed us about more accurate models involving a multi-layer structure for the satellite, like in [120]. In the framework of our study, the disparity comes from one parameter. The delay is given by

$$\Delta t = \frac{\delta}{2C_M} \frac{T_{orb}}{2\pi} = \delta \frac{Ca^6}{3GM_p^2 R_s^5 k_{2,s}} \frac{T_{orb}}{2\pi}, \quad (3.46)$$

where  $T_{orb}$  is the orbital period,  $a$  is the semimajor axis of the orbit,  $G$  is the gravitational constant,  $M_p$  is the mass of the planet,  $R_s$  is the mean radius of the satellite and  $k_{2,s}$  is its Love number (elasticity). The small values of  $\Delta t$  for Io and Europa are mainly due to the large mass of Jupiter, which is around 300 times the mass of the Earth. The rest of the parameters in (3.46) are comparable for the three systems.



# Chapter 4

## The spin-spin model and its double synchronous resonance

### 4.1 Derivation of the conservative spin-spin model

In this section we will compute the equations of motion of the ellipsoids with respect to the inertial frame with origin at the barycenter of the system. We will compute the expansion of the potential energy of the system in Section 4.1.1 and particularize it to the planar problem in Section 4.1.2. Section 4.1.3 is devoted to find the equations of motion of the full system of four variables  $(r, f, \theta_1, \theta_2)$ , in terms of the gravitational potential energy  $V = V(r, f, \theta_1, \theta_2)$ . In Section 4.1.4 we fix the Keplerian orbit and obtain the final model in terms of physical parameters of the system.

#### 4.1.1 Potential of the Full Two-Body Problem

The expansion of the potential energy in the Full Two-Body Problem has been obtained in several papers, see [119] for example. In this subsection, and in order to introduce some notation, we present a short derivation of the spherical harmonics expansion, following the approach of [76] and [13]. See also a similar approach in [84] and [32]. We start from the formula

$$V = -G \int \int \frac{dM_1(\mathbf{x}_1) dM_2(\mathbf{x}_2)}{|\mathbf{x}_1 - \mathbf{x}_2|},$$

where each  $\mathbf{x}_j \in \mathbb{R}^3$  is the position vector (with respect to the barycenter of the system) of the mass element  $dM_j(\mathbf{x}_j)$  corresponding to the ellipsoid  $\mathcal{E}_j$ .

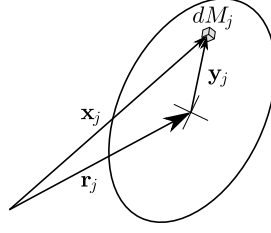


Figure 4.1: Position vectors of the element of mass of an ellipsoid.

Making the change of variables  $\mathbf{y}_j = \mathbf{x}_j - \mathbf{r}_j$ , illustrated in Figure 4.1, and defining  $\mathbf{y} = \mathbf{y}_1 - \mathbf{y}_2$ , we obtain

$$V = -G \int \int \frac{dM_1(\mathbf{y}_1) dM_2(\mathbf{y}_2)}{|\mathbf{r} - \mathbf{y}|}.$$

Recall that  $\mathbf{r} = \mathbf{r}_2 - \mathbf{r}_1$ . The usual expansion in spherical harmonics gives us

$$V = -G \sum_{(l,m) \in \Upsilon} Q_{l,m} \frac{Y_{l,m}(\hat{\mathbf{r}})}{|\mathbf{r}|^{l+1}}, \quad (4.1)$$

where

$$\Upsilon = \{(l, m) \in \mathbb{Z}^2 : 0 \leq |m| \leq l\}$$

and the multipolar moments of the system  $Q_{l,m}$  are defined by

$$Q_{l,m} = \int \int |\mathbf{y}|^l \bar{Y}_{l,m}(\hat{\mathbf{y}}) dM_1(\mathbf{y}_1) dM_2(\mathbf{y}_2), \quad (4.2)$$

where the upper bar indicates complex conjugation. We use the Schmidt semi-normalization<sup>1</sup> of the spherical harmonics in the same way as in [13]. Assume that, in the inertial frame,  $\mathbf{r}$  has spherical coordinates  $(r, \vartheta, \phi)$ , then, the spherical harmonics are defined by

$$Y_{l,m}(\vartheta, \phi) = (-1)^m \sqrt{\frac{(l-m)!}{(l+m)!}} P_{l,m}(\cos \vartheta) \exp(im\phi),$$

where the associated Legendre polynomials are given by

$$P_{l,m}(x) = \frac{1}{2^l l!} (1-x^2)^{m/2} \frac{d^{l+m}}{dx^{l+m}} (x^2-1)^l, \quad x \in [-1, 1].$$

<sup>1</sup>With this choice, the Legendre polynomials can be written in terms of the spherical harmonics as

$$P_l(\hat{\mathbf{r}} \cdot \hat{\mathbf{y}}) = \sum_{m=-l}^l Y_{l,m}(\hat{\mathbf{r}}) \bar{Y}_{l,m}(\hat{\mathbf{y}}).$$

Note that, since  $\mathbf{y} = \mathbf{y}_1 - \mathbf{y}_2$ , we cannot factorize the integral in (4.2) into factors that involve quantities associated to each body separately. However we can express this integral as a sum of factorized terms. For this we can define the auxiliary normalized solid harmonics

$$\mathcal{Y}_{l,m}(\mathbf{x}) = \frac{|\mathbf{x}|^l Y_{l,m}(\hat{\mathbf{x}})}{\sqrt{(l-m)!(l+m)!}}, \quad \mathbf{x} \in \mathbb{R}^3,$$

and apply the translation formula, given in equation (313) in [117],

$$\mathcal{Y}_{l,m}(\mathbf{y}_1 - \mathbf{y}_2) = \sum_{\lambda_1, \mu_1} \sum_{\lambda_2, \mu_2} \mathcal{Y}_{\lambda_1, \mu_1}(\mathbf{y}_1) \mathcal{Y}_{\lambda_2, \mu_2}(-\mathbf{y}_2), \quad (4.3)$$

where  $\lambda_j$  and  $\mu_j$  are integers running all the values such that

$$0 \leq \lambda_j \leq l, \quad \lambda_1 + \lambda_2 = l; \quad -\lambda_j \leq \mu_j \leq \lambda_j, \quad \mu_1 + \mu_2 = m.$$

Then, using the parity relation  $Y_{l,m}(-\hat{\mathbf{x}}) = (-1)^l Y_{l,m}(\hat{\mathbf{x}})$ , the expression (4.2) becomes

$$\begin{aligned} \frac{Q_{l,m}}{\sqrt{(l-m)!(l+m)!}} = \\ \sum_{\lambda_1, \mu_1} \sum_{\lambda_2, \mu_2} (-1)^{\lambda_2} \frac{M_1 R_1^{\lambda_1} Z_{\lambda_1, \mu_1}^1}{\sqrt{(\lambda_1 - \mu_1)!(\lambda_1 + \mu_1)!}} \frac{M_2 R_2^{\lambda_2} Z_{\lambda_2, \mu_2}^2}{\sqrt{(\lambda_2 - \mu_2)!(\lambda_2 + \mu_2)!}}, \end{aligned} \quad (4.4)$$

where, the complex Stokes coefficients<sup>2</sup> of each ellipsoid are given by

$$Z_{\lambda, \mu}^j = \frac{1}{M_j R_j^\lambda} \int |\mathbf{y}_j|^\lambda \bar{Y}_{\lambda, \mu}(\hat{\mathbf{y}}_j) dM_j(\mathbf{y}_j), \quad (4.5)$$

and  $R_j$  is the mean radius of  $\mathcal{E}_j$ .

Finally, since in the potential energy the summation range is  $0 \leq l \leq \infty$ ,  $-l \leq m \leq l$ , which are all the possible terms, then, from (4.1) and (4.4) we

---

<sup>2</sup>The quantities  $Z_{l,m}^j$  provide the expansion of the potential created for the body  $\mathcal{E}_j$ . They are related to the usual parameters  $C_{l,m}^j$  and  $S_{l,m}^j$  by

$$C_{l,m}^j + iS_{l,m}^j = (-1)^m \frac{2}{1 + \delta_{m,0}} \sqrt{\frac{(l-m)!}{(l+m)!}} \bar{Z}_{l,m}^j, \quad m \geq 0,$$

where  $\delta_{m,n}$  is the Kronecker delta.

can write

$$V = -\frac{GM_1M_2}{|\mathbf{r}|} \sum_{\substack{(\lambda_1, \mu_1) \in \Upsilon \\ (\lambda_2, \mu_2) \in \Upsilon}} (-1)^{\lambda_2} \gamma_{\lambda_2, \mu_2}^{\lambda_1, \mu_1} \left(\frac{R_1}{|\mathbf{r}|}\right)^{\lambda_1} \left(\frac{R_2}{|\mathbf{r}|}\right)^{\lambda_2} \times \\ \times Z_{\lambda_1, \mu_1}^{(1)} Z_{\lambda_2, \mu_2}^{(2)} Y_{\lambda_1 + \lambda_2, \mu_1 + \mu_2}(\hat{\mathbf{r}}), \quad (4.6)$$

where we defined the constants

$$\gamma_{\lambda_2, \mu_2}^{\lambda_1, \mu_1} = \sqrt{\frac{(\lambda_1 + \lambda_2 - \mu_1 - \mu_2)! (\lambda_1 + \lambda_2 + \mu_1 + \mu_2)!}{(\lambda_1 - \mu_1)! (\lambda_1 + \mu_1)! (\lambda_2 - \mu_2)! (\lambda_2 + \mu_2)!}}.$$

### 4.1.2 Potential of the ellipsoidal spin-spin model

Note that the terms in the expansion (4.6), and in particular  $Z_{\lambda,\mu}^j$ , have to be computed with respect to the inertial frame. Let us call  $\mathcal{E}_j$ -frame to the fixed body frame of each ellipsoid, formed by its center and its principal directions associated respectively to  $\mathbf{a}_j$ ,  $\mathbf{b}_j$  and  $\mathbf{c}_j$ . Let  $\mathcal{Z}_{\lambda,\mu}^j$  be the Stokes coefficients computed with respect to the  $\mathcal{E}_j$ -frame. The  $\mathcal{E}_j$ -frame is rotated, with respect to the inertial frame, with the rotation labelled by the Euler  $z$ - $y$ - $z$  angles  $(\alpha, \beta, \gamma) = (\theta_j, 0, 0)$ .

Let  $\mathbf{x} \in \mathbb{R}^3$  be a vector with spherical coordinates  $(|\mathbf{x}|, \vartheta_j, \phi_j)$  with respect to the  $\mathcal{E}_j$ -frame and  $(|\mathbf{x}|, \vartheta, \phi)$  with respect to the reference frame formed by the center of the body  $\mathcal{E}_j$  and the directions parallel to those of the inertial frame. The relation between spherical harmonics  $Y_{l,m}(\hat{\mathbf{x}})$  computed with respect to both systems of reference is the following

$$Y_{l,m}(\vartheta_j, \phi_j) = \sum_{m'=-l}^l Y_{l,m'}(\vartheta, \phi) \bar{D}_{m,m'}^l(\alpha, \beta, \gamma)$$

where  $D_{m,m'}^l(\alpha, \beta, \gamma)$  is the  $(m, m')$ -element of the Wigner  $D$ -matrix associated to the rotation given by the Euler  $z$ - $y$ - $z$  angles  $(\alpha, \beta, \gamma)$ , see [117]. Then, from (4.5),

$$Z_{\lambda,\mu}^j = \sum_{\mu'=-\lambda}^{\lambda} D_{\mu,\mu'}^{\lambda}(\alpha, \beta, \gamma) \mathcal{Z}_{\lambda,\mu'}^j. \quad (4.7)$$

From the definition of the Wigner  $D$ -matrices, see for instance equation (186) in [117], in our planar case they are diagonal  $D_{\mu,\mu'}^{\lambda}(\theta_j, 0, 0) = \delta_{\mu,\mu'} \exp(-i\mu'\theta_j)$ , where  $\delta_{\mu,\mu'}$  is the Kronecker delta. Then,

$$Z_{\lambda,\mu}^j = \mathcal{Z}_{\lambda,\mu}^j \exp(-i\mu\theta_j).$$

Now we can express (4.6) in terms of  $\mathcal{Z}_{\lambda,\mu}^j$ . In [5] an expansion of the potential created by a homogeneous ellipsoid was computed. Incidentally, a complicated general expression for  $\mathcal{Z}_{\lambda,\mu}^j$  was computed there as well. In the next Proposition we summarize some remarkable properties of those quantities.

**Proposition 4.1.** *Let  $\mathcal{Z}_{l,m}$  be Stokes coefficients of an homogeneous ellipsoid computed in its own fixed body frame. They have the following properties*

1.  $\mathcal{Z}_{l,m} \in \mathbb{R}$ .
2.  $\mathcal{Z}_{l,m} \equiv 0$  if either  $l$  or  $m$  are odd numbers.

3.  $\mathcal{Z}_{l,-2n} = \mathcal{Z}_{\lambda,2n}$ , with  $n$  integer.

**Proof.**

- Let us choose convenient units such that both the mass and the mean radius of the ellipsoid equal 1. Take spherical coordinates  $(r, \vartheta, \phi)$  in the fixed body frame, then, the distance  $r_{\mathcal{E}}(\vartheta, \phi)$  from the center of the ellipsoid  $\mathcal{E}$  to its surface is given by

$$\frac{1}{r_{\mathcal{E}}(\vartheta, \phi)^2} = \sin^2 \vartheta \left( \frac{\cos^2 \phi}{a^2} + \frac{\sin^2 \phi}{b^2} \right) + \frac{\cos^2 \vartheta}{c^2}$$

then, if we take the density  $\rho$ , from (4.5),

$$\begin{aligned} \mathcal{Z}_{l,m} &= (-1)^m \rho \sqrt{\frac{(l-m)!}{(l+m)!}} \times \\ &\quad \times \int_{\phi=0}^{2\pi} \int_{\vartheta=0}^{\pi} \int_{r=0}^{r_{\mathcal{E}}(\vartheta, \phi)} r^{l+2} dr P_{l,m}(\cos \vartheta) \exp(-im\phi) d\cos \vartheta d\phi \\ &= \frac{(-1)^m \rho}{l+3} \sqrt{\frac{(l-m)!}{(l+m)!}} \times \\ &\quad \times \int_{\phi=0}^{2\pi} \int_{\vartheta=0}^{\pi} r_{\mathcal{E}}(\vartheta, \phi)^{l+3} P_{l,m}(\cos \vartheta) \exp(-im\phi) d\cos \vartheta d\phi \quad (4.8) \end{aligned}$$

Since  $r_{\mathcal{E}}(\vartheta, -\phi) = r_{\mathcal{E}}(\vartheta, \phi)$ , if we take the change of variable  $\phi = -\phi'$ , we obtain that  $\mathcal{Z}_{l,m}$  equals its complex conjugate, then, it must be real.

- We can change variables  $\mathbf{y}_i = -\mathbf{y}'$  in (4.5),

$$\begin{aligned} \mathcal{Z}_{l,m} &= \int \int \int_{-\mathbf{y}' \text{ inside } \mathcal{E}} |-\mathbf{y}'|^l \bar{Y}_{l,m}(-\hat{\mathbf{y}}') dM(-\mathbf{y}') \\ &= (-1)^3 \int \int \int_{\mathbf{y}' \text{ inside } \mathcal{E}} |\mathbf{y}'|^l \bar{Y}_{l,m}(-\hat{\mathbf{y}}') (-1)^3 dM(\mathbf{y}') \\ &= (-1)^l \mathcal{Z}_{l,m}, \end{aligned}$$

where we used  $Y_{l,m}(-\hat{\mathbf{x}}) = (-1)^l Y_{l,m}(\hat{\mathbf{x}})$ . Then,  $\mathcal{Z}_{l,m} \equiv 0$  if  $l$  is odd. Note that this particular result is independent of the reference frame.

From (4.8) we see that  $\mathcal{Z}_{l,m}$  is computed integrating the function

$$I(\vartheta) = \int_{\phi=0}^{2\pi} r_{\mathcal{E}}(\vartheta, \phi)^{l+3} \exp(-im\phi) d\phi$$

Since  $r_{\mathcal{E}}(\vartheta, \phi)$  depends on  $\phi$  through  $\sin^2 \phi$  and  $\cos^2 \phi$ , we know that  $r_{\mathcal{E}}(\vartheta, \pi - \phi) = r_{\mathcal{E}}(\vartheta, \phi)$ . Now, if we take the change of variables  $\phi = \pi - \phi'$ , we obtain that  $I(\vartheta) = (-1)^m \bar{I}(\vartheta)$ . Since  $I(\vartheta)$  must be real, then,  $I(\vartheta) \equiv 0$  for odd  $m$ .

3. If we apply the symmetry relation  $Y_{l,m}(\mathbf{x}) = (-1)^m \bar{Y}_{l,-m}(\mathbf{x})$  we can easily see that  $\mathcal{Z}_{l,-m} = (-1)^m \bar{\mathcal{Z}}_{l,m}$ . Since  $m$  is even and  $\mathcal{Z}_{l,m}$  is real, we have finished the proof.

■

**Remark 4.1.** *Regarding these properties, a convenient expression to compute numerically  $\mathcal{Z}_{2k,2n}$ , with  $k \geq 0$  and  $n$  integers, is*

$$\begin{aligned} \mathcal{Z}_{2k,2n} &= \frac{3}{4\pi R^{2k}} \sqrt{\frac{(2k-2n)!}{(2k+2n)!}} \int_{\mathbf{B}} \operatorname{Re}((\mathbf{a}Z - i\mathbf{b}Y)^{2n}) \times \\ &\times \frac{[(\mathbf{a}X)^2 + (\mathbf{b}Y)^2 + (\mathbf{c}Z)^2]^k}{[(\mathbf{a}X)^2 + (\mathbf{b}Y)^2]^n} P_{2k,2n} \left( \frac{\mathbf{c}Z}{\sqrt{(\mathbf{a}X)^2 + (\mathbf{b}Y)^2 + (\mathbf{c}Z)^2}} \right) dX dY dZ, \end{aligned} \quad (4.9)$$

where  $R$  is the mean radius of the ellipsoid,  $\mathbf{a}$ ,  $\mathbf{b}$  and  $\mathbf{c}$  are its principal semi-axes,  $\operatorname{Re}$  indicates the real part and  $\mathbf{B}$  is the unit ball, defined by  $X^2 + Y^2 + Z^2 \leq 1$ . Moreover,  $\mathcal{Z}_{2k,2n}$  can be written only in terms of  $M$  and the principal moments of inertia because

$$\mathbf{a} = \sqrt{\frac{5(-\mathcal{A} + \mathcal{B} + \mathcal{C})}{2M}}, \quad \mathbf{b} = \sqrt{\frac{5(\mathcal{A} - \mathcal{B} + \mathcal{C})}{2M}}, \quad \mathbf{c} = \sqrt{\frac{5(\mathcal{A} + \mathcal{B} - \mathcal{C})}{2M}}.$$

Recalling the definitions of  $q$  and  $d$  in (4.17), the first non-vanishing Stokes coefficients are given by

$$\mathcal{Z}_{0,0} = 1, \quad \mathcal{Z}_{2,0} = -\frac{1}{2} \frac{q}{MR^2}, \quad \mathcal{Z}_{2,2} = \sqrt{\frac{3}{8}} \frac{d}{MR^2}, \quad (4.10)$$

$$\mathcal{Z}_{4,0} = \frac{15}{56} \frac{d^2 + 2q^2}{M^2 R^4}, \quad \mathcal{Z}_{4,2} = -\frac{15}{28} \sqrt{\frac{5}{3}} \frac{dq}{M^2 R^4}, \quad \mathcal{Z}_{4,4} = \frac{15}{8} \sqrt{\frac{5}{14}} \frac{d^2}{M^2 R^4}, \quad (4.11)$$

and it seems that, in general,  $\mathcal{Z}_{2k,2n}$  has the form of a homogeneous polynomial of degree  $k$  with respect to  $q/(MR^2)$  and  $d/(MR^2)$ .

In order to simplify expression (4.6), recall that  $\mathbf{r}$  is the vector pointing from the center of  $\mathcal{E}_1$  to the center of  $\mathcal{E}_2$ . Then, the spherical coordinates of  $\mathbf{r}$  with respect to the inertial frame are  $(r, \vartheta = \pi/2, \phi = f)$ . The non-vanishing terms of (4.6) are such that  $\lambda_j = 2l_j$  and  $\mu_j = 2m_j$ . Let us call from now on  $l = l_1 + l_2$  and  $m = m_1 + m_2$ . We can apply the formula

$$Y_{2l,2m}(\pi/2, f) = \sqrt{\frac{(2l-2m)!}{(2l+2m)!}} P_{2l,2m}(0) e^{2imf},$$

and the following property of the associated Legendre polynomials

$$P_{2l,2m}(0) = \frac{(-1)^{l-m}}{4^l} \frac{(2l+2m)!}{(l-m)!(l+m)!},$$

see for instance equation (68) in [117]. Then, we can write the potential keeping only the real part of  $V$ , so that the final expression potential is

$$\begin{aligned} V = & -\frac{GM_1M_2}{r} \sum_{\substack{(l_1, m_1) \in \Upsilon \\ (l_2, m_2) \in \Upsilon}} \Gamma_{l_2, m_2}^{l_1, m_1} \left(\frac{R_1}{r}\right)^{2l_1} \left(\frac{R_2}{r}\right)^{2l_2} \times \\ & \times \mathcal{Z}_{2l_1, 2m_1}^1 \mathcal{Z}_{2l_2, 2m_2}^2 \cos(2m_1(\theta_1 - f) + 2m_2(\theta_2 - f)), \end{aligned} \quad (4.12)$$

where

$$\begin{aligned} \Gamma_{l_2, m_2}^{l_1, m_1} = & \frac{(-1)^{l-m}}{4^l \sqrt{(2l_1 - 2m_1)!(2l_1 + 2m_1)!(2l_2 - 2m_2)!(2l_2 + 2m_2)!}} \times \\ & \times \frac{(2l-2m)!(2l+2m)!}{(l-m)!(l+m)!}. \end{aligned} \quad (4.13)$$

The first terms of the expansion (4.12) can be computed using (4.10) and (4.11). The terms corresponding to  $l = l_1 + l_2$ , for  $l = 0, 1$  and  $2$ , are shown in (4.16).



### 4.1.3 The planar Lagrangian model

Let the Lagrangian of the system be  $L = T - V$ , where  $T$  is the kinetic energy and  $V$  the potential energy of the system. Recall that the positions of the bodies are  $\mathbf{r}_1 = -M_2\mathbf{r}$  and  $\mathbf{r}_2 = M_1\mathbf{r}$ , where the relative position vector is defined by  $\mathbf{r} = \mathbf{r}_2 - \mathbf{r}_1 = r \exp(if)$ . Besides, for each body, the angle  $\theta_j$  defines the orientation of the axis associated to  $\mathbf{a}_j$ . We are going to use  $r$ ,  $f$ ,  $\theta_1$  and  $\theta_2$ , depicted in Figure 1.10, as the Lagrangian variables of our system. The total orbital kinetic energy is given by

$$T_{orb} = \frac{1}{2}(M_1\dot{\mathbf{r}}_1^2 + M_2\dot{\mathbf{r}}_2^2) = \frac{\mu}{2}\dot{\mathbf{r}}^2 = \frac{\mu}{2}(\dot{r}^2 + r^2\dot{f}^2),$$

where  $\mu = M_1M_2$  is the reduced mass of the system (recall  $M_1 + M_2 = 1$ ). While the rotational kinetic energy is  $T_{rot} = \frac{1}{2}\mathcal{C}_1\dot{\theta}_1^2 + \frac{1}{2}\mathcal{C}_2\dot{\theta}_2^2$ . In the previous subsection we derived the full expression of the potential energy of the system  $V = V(r, f, \theta_1, \theta_2)$ , equation (4.12). The Euler-Lagrange equations corresponding to the Lagrangian  $L = T_{orb}(r, \dot{r}, \dot{f}) + T_{rot}(\dot{\theta}_1, \dot{\theta}_2) - V(r, f, \theta_1, \theta_2)$  are

$$\mathcal{C}_1\ddot{\theta}_1 = -\partial_{\theta_1}V, \quad \mathcal{C}_2\ddot{\theta}_2 = -\partial_{\theta_2}V, \quad (4.14)$$

$$\mu\ddot{r} = \mu r\dot{f}^2 - \partial_rV, \quad \ddot{f} = -\frac{1}{\mu r^2}\partial_fV - 2\frac{\dot{r}\dot{f}}{r}. \quad (4.15)$$

Note that, in the case of ellipsoids, the expansion of the potential energy (4.12) has the form  $V = \sum_{n=0}^{\infty} V_{2n}$ , where  $V_{2n}$  is proportional to  $1/r^{2n+1}$ . The first terms of the expansion are

$$V_0 = -\frac{GM_1M_2}{r}.$$

$$V_2 = -\frac{GM_2}{4r^3}(q_1 + 3d_1 \cos(2(\theta_1 - f))) - \frac{GM_1}{4r^3}(q_2 + 3d_2 \cos(2(\theta_2 - f))),$$

$$\begin{aligned} V_4 = & -\frac{3G}{4^3r^5} \{12q_1q_2 + \frac{15}{7}[\frac{M_2}{M_1}d_1^2 + 2\frac{M_2}{M_1}q_1^2 + \frac{M_1}{M_2}d_2^2 + 2\frac{M_1}{M_2}q_2^2] \\ & + d_1M_2 \left\{ [20\frac{q_2}{M_2} + \frac{100}{7}\frac{q_1}{M_1}] \cos(2(\theta_1 - f)) + 25\frac{d_1}{M_1} \cos(4(\theta_1 - f)) \right\} \\ & + d_2M_1 \left\{ [20\frac{q_1}{M_1} + \frac{100}{7}\frac{q_2}{M_2}] \cos(2(\theta_2 - f)) + 25\frac{d_2}{M_2} \cos(4(\theta_2 - f)) \right\} \\ & + 6d_1d_2 \cos(2(\theta_1 - \theta_2)) + 70d_1d_2 \cos(2(\theta_1 + \theta_2) - 4f)\}, \end{aligned} \quad (4.16)$$

where we defined the parameters

$$d_j = \mathcal{B}_j - \mathcal{A}_j, \quad q_j = 2\mathcal{C}_j - \mathcal{B}_j - \mathcal{A}_j. \quad (4.17)$$

Note that  $d_j$  is proportional to  $C_{22}^{(j)}$ , whereas  $q_j$  is proportional to  $C_{20}^{(j)}$ , where  $C_{nm}^{(j)}$  are the usual coefficients in the expansion of the gravitational potential of the ellipsoid  $\mathcal{E}_j$ . The quantity  $d_j/\mathcal{C}_j$  measures the oblateness of the section of the ellipsoid in the plane of motion, whereas,  $q_j/\mathcal{C}_j$  measures the flattening with respect to the plane. If  $\mathcal{A}_j \leq \mathcal{B}_j \leq \mathcal{C}_j$ , then,  $q_j \geq d_j \geq 0$ . Note that the term  $V_0$  contains the dynamics of two point masses,  $V_2$  the uncoupled spin-orbit dynamics and  $V_4$  the spin-spin coupled dynamics between  $\theta_1$  and  $\theta_2$ . The coupling terms appear in the last line of (4.16).

#### 4.1.4 The Keplerian assumption

The complete dynamics of the system is given by Equations (4.14) and (4.15), with  $V$  in (4.12). In this paper we impose that the orbital motion is Keplerian, i.e., we keep only  $V_0$  in the orbital part (4.15). Besides, in the spin part (4.14), we truncate  $V$  ignoring terms of order  $1/r^7$  and higher, then  $V \approx V_0 + V_2 + V_4$ . The resulting system is

$$\mathcal{C}_1 \ddot{\theta}_1 = -\partial_{\theta_1}(V_0 + V_2 + V_4), \quad \mathcal{C}_2 \ddot{\theta}_2 = -\partial_{\theta_2}(V_0 + V_2 + V_4), \quad (4.18)$$

$$\mu \ddot{r} = \mu r \dot{f}^2 - \partial_r V_0, \quad \ddot{f} = -\frac{1}{\mu r^2} \partial_f V_0 - 2 \frac{\dot{r} \dot{f}}{r}. \quad (4.19)$$

Note that, since  $\partial_{\theta_j} V_0 = 0$ , the system (4.19) is now decoupled from (4.18). Its solution is  $r = r(t)$ ,  $f = f(t)$  given by Equations (1.10) to (1.12) and depends on the eccentricity of the orbit  $e$  and its semimajor axis  $a$ .

Let us now write  $V_2$  and  $V_4$  in a more convenient way. The quantity  $M_j a^2$  is a sort of orbital moment of inertia of the body  $\mathcal{E}_j$ . Then, we can define

$$\hat{d}_j = \frac{d_j}{M_j a^2}, \quad \hat{q}_j = \frac{q_j}{M_j a^2}, \quad (4.20)$$

so that  $\hat{d}_j$  measures the equatorial oblateness of  $\mathcal{E}_j$  with respect to the size of the orbit and  $\hat{q}_j$  measures the flattening of  $\mathcal{E}_j$  with respect to the size of the orbit.

Taking into account that in our units  $G = a^3$ , the terms  $V_2$  and  $V_4$  can be written in a compact way as

$$V_2 = -\frac{1}{4} \left( \frac{a}{r(t)} \right)^3 (\Lambda_0 + \Lambda_1 \cos(2\theta_1 - 2f(t)) + \Lambda_2 \cos(2\theta_2 - 2f(t))) \quad (4.21)$$

and

$$V_4 = -\frac{1}{4} \left( \frac{a}{r(t)} \right)^5 \sum_{(m_1, m_2) \in \Xi} \Lambda_{m_2}^{m_1} \cos(2m_1(\theta_1 - f(t)) + 2m_2(\theta_2 - f(t))) \quad (4.22)$$

where

$$\Xi = \{(m_1, m_2) \in \mathbb{Z}^2 : |m_1| + |m_2| \leq 2\},$$

and the following  $\Lambda$  parameters are defined by

$$\Lambda_1 = 3d_1 M_2, \quad \Lambda_2 = 3d_2 M_1, \quad (4.23)$$

$$\Lambda_0^1 = \Lambda_0^{-1} = \frac{5}{56} (7\hat{q}_2 + 5\hat{q}_1) \Lambda_1, \quad \Lambda_1^0 = \Lambda_{-1}^0 = \frac{5}{56} (7\hat{q}_1 + 5\hat{q}_2) \Lambda_2, \quad (4.24)$$

$$\Lambda_0^2 = \Lambda_0^{-2} = \frac{25}{32} \hat{d}_1 \Lambda_1, \quad \Lambda_2^0 = \Lambda_{-2}^0 = \frac{25}{32} \hat{d}_2 \Lambda_2, \quad (4.25)$$

$$\Lambda_1^1 = \Lambda_{-1}^{-1} = \frac{35}{16} \hat{d}_1 \Lambda_2 = \frac{35}{16} \hat{d}_2 \Lambda_1, \quad \Lambda_1^{-1} = \Lambda_{-1}^1 = \frac{3}{16} \hat{d}_1 \Lambda_2 = \frac{3}{16} \hat{d}_2 \Lambda_1 \quad (4.26)$$

$$\Lambda_0 = q_1 M_2 + q_2 M_1, \quad \Lambda_0^0 = \frac{9}{4} \hat{q}_1 q_2 M_1 + \frac{15}{112} (\Lambda_1 \hat{d}_1 + 6 \hat{q}_1 q_1 M_2 + \Lambda_2 \hat{d}_2 + 6 \hat{q}_2 q_2 M_1).$$

With the last definitions we can write equations (4.18) as  $\mathcal{C}_j \ddot{\theta} = \mathcal{T}_j^C$ , where  $\mathcal{T}_j^C = -\partial_{\theta_j} (V_2 + V_4)$  are the *conservative* torques of the spin-spin model shown in (1.20). This can be checked with the expressions (4.21) and (4.22). Note that  $m_j \Lambda_{m_2}^{m_1}$  is in all cases proportional to the corresponding  $\Lambda_j$ . Then, the equations of the *conservative* spin-spin model (4.18) can be written in terms of the physical parameters in the following symmetric way for  $j = 1, 2$ ,

$$\begin{aligned} 0 = \ddot{\theta}_j + \frac{\lambda_j}{2} \left\{ \left( \frac{a}{r(t)} \right)^3 \sin(2\theta_j - 2f(t)) + \right. \\ \left. + \left( \frac{a}{r(t)} \right)^5 \left[ \frac{5}{4} \left( \hat{q}_{3-j} + \frac{5}{7} \hat{q}_j \right) \sin(2\theta_j - 2f(t)) + \frac{25 \hat{d}_j}{8} \sin(4\theta_j - 4f(t)) \right. \right. \\ \left. \left. + \frac{3 \hat{d}_{3-j}}{8} \sin(2\theta_j - 2\theta_{3-j}) + \frac{35 \hat{d}_{3-j}}{8} \sin(2\theta_{3-j} + 2\theta_j - 4f(t)) \right] \right\}, \quad (4.27) \end{aligned}$$

where

$$\lambda_j = \frac{\Lambda_j}{\mathcal{C}_j} = 3 \frac{d_j}{\mathcal{C}_j} \frac{\mu}{M_j}.$$

It is worth mentioning that the terms with  $\hat{q}_j$  and  $\hat{d}_j$  in (4.27) were missing in the model used in [7] due to the dumbbell simplification for one of the bodies in the derivation of the equations. Not all the parameters appearing in (4.27) are free because the following identities hold

$$\mathcal{C}_1 + \mathcal{C}_2 = 1, \quad \Lambda_1 \hat{d}_2 = \Lambda_2 \hat{d}_1, \quad \Lambda_1 \hat{q}_2 = \Lambda_2 \hat{q}_1. \quad (4.28)$$

In consequence, our model depends on six independent parameters with physical meaning ( $e; \mathcal{C}_1, \lambda_1, \lambda_2, \hat{d}_1, \hat{q}_1$ ). Moreover, in (4.27) we see that spin of the ellipsoid  $\mathcal{E}_2$  is affected by the spin-spin coupling with a strength essentially given by  $\hat{d}_1$ , and vice versa.

## 4.2 Linear stability of the double synchronous resonance in the conservative model

In this section we deal with the *conservative* system with the notation in (1.23), that is more convenient for our purpose. The main result is Theorem 4.2. It determines a region of linear stability of the double synchronous resonance in the space of parameters of the system.

### 4.2.1 Existence of the odd $2\pi$ -periodic solution

The system (1.23) can be written as

$$\mathcal{C}\ddot{\Theta} + F(t, \Theta) = 0, \quad (4.29)$$

where

$$\Theta = \begin{pmatrix} \Theta_1 \\ \Theta_2 \end{pmatrix}, \quad \mathcal{C} = \begin{pmatrix} \mathcal{C}_1 & 0 \\ 0 & \mathcal{C}_2 \end{pmatrix}, \quad \mathcal{C}_j > 0,$$

and  $F(t, \Theta)$  is the bounded function given by

$$\begin{aligned} F(t, \Theta) &= \left(\frac{a}{r(t)}\right)^3 \begin{pmatrix} \Lambda_1 \sin \Theta_1 \\ \Lambda_2 \sin \Theta_2 \end{pmatrix} + \\ &+ \left(\frac{a}{r(t)}\right)^5 \sum_{(m_1, m_2) \in \Xi} \begin{pmatrix} m_1 \\ m_2 \end{pmatrix} \Lambda_{m_2}^{m_1} \sin(m_1 \Theta_1 + m_2 \Theta_2) + 2\ddot{f}(t) \begin{pmatrix} \mathcal{C}_1 \\ \mathcal{C}_2 \end{pmatrix}. \end{aligned} \quad (4.30)$$

Note that equation (4.29) is invariant under the change  $(t, \Theta) \rightarrow (-t, -\Theta)$ , since  $f(-t) = -f(t)$  and  $r(-t) = r(t)$ . Then, if  $\Theta(t)$  is a solution of (4.29), so it is  $-\Theta(-t)$ . On the other hand, for  $e = 0$ , we have  $f(t) = t$  and  $r(t) = a$ , meaning that the system (4.29) is that of two coupled free pendula. For this case, the trivial solution  $\Theta(t) \equiv 0$  is a stable equilibrium. Then, for  $e \neq 0$ , it is natural to look for the  $2\pi$ -periodic continuation of  $\Theta(t) \equiv 0$  in the family of the odd solutions of (4.29), say, solutions satisfying  $\Theta(-t) = -\Theta(t)$ . This is equivalent to solve the Dirichlet problem

$$\begin{cases} \mathcal{C}\ddot{\Theta} + F(t, \Theta) = 0, \\ \Theta(0) = \Theta(\pi) = 0. \end{cases} \quad (4.31)$$

It is well known from nonlinear analysis that the system (4.31) has at least one solution because  $F(t, \Theta)$  is bounded. We can give a simple proof for this. Let  $\Theta(t) = \vartheta(t, v)$  be the solution of (4.29) satisfying initial conditions  $\Theta(0) = 0$ ,  $\dot{\Theta}(0) = v \in \mathbb{R}^2$ . Solutions of the problem (4.31) are in correspondence

with the solutions of the equation  $\vartheta(\pi, v) = 0$ . From (4.29), we know that  $\vartheta$  satisfies the following integral equation

$$\vartheta(t, v) = vt - \int_0^t (t-s) \mathcal{C}^{-1} F(s, \vartheta(s, v)) ds. \quad (4.32)$$

Let  $\|\cdot\|$  be a norm in  $\mathbb{R}^2$ , for instance, the maximum norm or the Euclidean one. We will employ the same notation for the corresponding induced matrix norm in  $\mathbb{R}^{2 \times 2}$ . Since there exists a positive number  $M \geq \|\mathcal{C}^{-1} F(t, \Theta)\|$ , then

$$\|\vartheta(t, v) - vt\| \leq M \frac{t^2}{2},$$

for each  $t \in \mathbb{R}$ . If we take  $t = \pi$ , then,  $\|\Phi(v)\| \leq M\pi/2$ , with  $\Phi(v) = v - \vartheta(\pi, v)/\pi$  and  $v \in \mathbb{R}^2$ . Hence, we can apply Brouwer's fixed-point theorem to guarantee that  $\Phi(v)$  has a fixed point for some  $v_0$  satisfying  $\|v_0\| \leq M\pi/2$ . For such point we have that  $\vartheta(\pi, v_0) = 0$ , and the corresponding  $\vartheta(t, v_0)$  satisfies (4.31).

### 4.2.2 Uniqueness of the solution

We know now that the Dirichlet problem (4.31) has a solution, however, it is not necessarily unique. For instance, if  $\Lambda > 1$ , there is not a unique solution for the free pendulum equation  $\ddot{x} + \Lambda \sin x = 0$ ,  $x \in \mathbb{R}$ , with Dirichlet conditions  $x(0) = x(\pi) = 0$ . See [86]. We would like to determine sufficient conditions on the space of parameters of the system such that there is uniqueness for the problem (4.31).

We can prove uniqueness by a contradiction argument. Define the following matrix

$$\mathcal{C}^{1/2} = \begin{pmatrix} \sqrt{\mathcal{C}_1} & 0 \\ 0 & \sqrt{\mathcal{C}_2} \end{pmatrix}$$

and its inverse  $\mathcal{C}^{-1/2} = (\mathcal{C}^{1/2})^{-1}$ . Let  $\Theta^{(0)}(t)$  and  $\Theta^{(1)}(t)$  be two non-identical solutions of (4.31). Then, we can check that  $y(t) = \mathcal{C}^{1/2}(\Theta^{(1)}(t) - \Theta^{(0)}(t))$  is a solution of the Dirichlet problem

$$\begin{cases} \ddot{y} + A(t)y = 0, \\ y(0) = y(\pi) = 0, \end{cases} \quad (4.33)$$

with  $A(t)$  a symmetric<sup>3</sup> matrix given by

$$\mathcal{C}^{1/2}A(t)\mathcal{C}^{1/2} = \int_0^1 \partial_{\Theta}F(t, \Theta^{(\lambda)}(t)) \, d\lambda, \quad (4.34)$$

where  $\Theta^{(\lambda)}(t) = \lambda\Theta^{(1)}(t) + (1 - \lambda)\Theta^{(0)}(t)$  and

$$F(t, \Theta) = \begin{pmatrix} F_1(t, \Theta) \\ F_2(t, \Theta) \end{pmatrix}, \quad \partial_{\Theta}F(t, \Theta) = \begin{pmatrix} \frac{\partial F_1}{\partial \Theta_1} & \frac{\partial F_1}{\partial \Theta_2} \\ \frac{\partial F_2}{\partial \Theta_1} & \frac{\partial F_2}{\partial \Theta_2} \end{pmatrix}.$$

The statement of uniqueness is given in Theorem 4.1. We can prove it by guaranteeing that (3.9) has only the trivial solution. In the proof we are going to apply the following lemma to (4.33) for a generic matrix  $A(t) \in \mathbb{R}^{d \times d}$ . But first we need some definitions. Let  $\langle \cdot, \cdot \rangle$  be the Euclidean inner product in  $\mathbb{R}^d$  and  $\|\cdot\|$  its corresponding norm. Let  $\mathbb{1}$  be the unit matrix in  $\mathbb{R}^{d \times d}$ .

**Definition 4.1.** *Let  $A_1, A_2 \in \mathbb{R}^{d \times d}$  be two symmetric matrices. We say that  $A_1 \leq A_2$  if, for the corresponding quadratic forms,  $\langle A_1 y, y \rangle \leq \langle A_2 y, y \rangle$  for all  $y \in \mathbb{R}^d$ .*

**Lemma 4.1.** *Assume that, for some  $\gamma < 1$ , the matrix  $A(t) \in \mathbb{R}^{d \times d}$  is such that  $A(t) \leq \gamma \mathbb{1}$  for each  $t \in [0, \pi]$ . Then, the only solution of  $\ddot{y} + A(t)y = 0$ ,  $y \in \mathbb{R}^d$ , with Dirichlet conditions  $y(0) = y(\pi) = 0$  is the trivial one.*

<sup>3</sup>In this paper we use properties of linear systems with symmetric coefficient matrices.  $\mathcal{C}^{-1}\partial_{\Theta}F(t, \Theta)$  is not symmetric, but we obtain the desired structure using  $\mathcal{C}^{1/2}$ . See [126].

**Proof.** Proceed by contradiction. Let  $y(t)$  be a non-trivial solution of  $\ddot{y} + A(t)y = 0$ ,  $y(0) = y(\pi) = 0$ , then,

$$\int_0^\pi \langle \ddot{y}(t), y(t) \rangle + \int_0^\pi \langle A(t)y(t), y(t) \rangle = 0,$$

integrating by parts it follows that

$$\int_0^\pi \|\dot{y}(t)\|^2 = \int_0^\pi \langle A(t)y(t), y(t) \rangle.$$

Let  $y_n(t)$  be the components of the vector  $y(t)$ . From the Sobolev inequality  $\int_0^\pi |y_n(t)|^2 \leq \int_0^\pi |\dot{y}_n(t)|^2$ , see [128] or [91], we get that

$$\int_0^\pi \|y(t)\|^2 \leq \int_0^\pi \langle A(t)y(t), y(t) \rangle.$$

This contradicts the hypothesis  $A(t) \leq \gamma \mathbf{1}$  for some  $\gamma < 1$ . Then,  $y(t)$  must be the trivial solution. ■

Let us define the matrix  $\tilde{A}(t, \Theta) = \mathcal{C}^{-1/2} \partial_\Theta F(t, \Theta) \mathcal{C}^{-1/2}$ ,

$$\begin{aligned} \tilde{A}(t, \Theta) &= \left( \frac{a}{r(t)} \right)^3 \begin{pmatrix} \frac{\Lambda_1}{\mathcal{C}_1} \cos \Theta_1 & 0 \\ 0 & \frac{\Lambda_2}{\mathcal{C}_2} \cos \Theta_2 \end{pmatrix} \\ &+ \left( \frac{a}{r(t)} \right)^5 \sum_{(m_1, m_2) \in \Xi} \begin{pmatrix} \frac{m_1^2}{\mathcal{C}_1} & \frac{m_1 m_2}{\sqrt{\mathcal{C}_1 \mathcal{C}_2}} \\ \frac{m_1 m_2}{\sqrt{\mathcal{C}_1 \mathcal{C}_2}} & \frac{m_2^2}{\mathcal{C}_2} \end{pmatrix} \Lambda_{m_2}^{m_1} \cos(m_1 \Theta_1 + m_2 \Theta_2). \end{aligned} \quad (4.35)$$

We will use the maximum norm

$$\|y\| = \max\{|y_1|, |y_2|\}, \quad y = \begin{pmatrix} y_1 \\ y_2 \end{pmatrix},$$

and its induced norm in matrices

$$\|A\| = \max\{|A_{11}| + |A_{12}|, |A_{21}| + |A_{22}|\}, \quad A = \begin{pmatrix} A_{11} & A_{12} \\ A_{21} & A_{22} \end{pmatrix}.$$

**Theorem 4.1.** Assume that  $e \in [0, 1)$  and the parameters of the problem satisfy

$$1 > \frac{1}{(1-e)^3} \max\left\{ \frac{\Lambda_1}{\mathcal{C}_1} (1 + \alpha_1), \frac{\Lambda_2}{\mathcal{C}_2} (1 + \alpha_2) \right\}, \quad (4.36)$$

where

$$\alpha_j \frac{\Lambda_j}{\mathcal{C}_j} = \frac{1}{(1-e)^2} \sum_{(m_1, m_2) \in \Xi} \left( \frac{m_j^2}{\mathcal{C}_j} + \frac{|m_1 m_2|}{\sqrt{\mathcal{C}_1 \mathcal{C}_2}} \right) \Lambda_{m_2}^{m_1}. \quad (4.37)$$

Then, there exists a unique solution of the Dirichlet problem (4.31), denoted by  $\Theta^*(t)$ .



**Proof.** Using the fact that  $a/r \leq 1/(1-e)$  by (1.11), equations (4.36) and (4.37) imply that  $1 > \|\tilde{A}(t, \Theta)\|$  for all  $(t, \Theta) \in \mathbb{R}^3$ , where we use the maximum norm. Furthermore, if  $\rho(A)$  is the spectral radius of  $A$ , the well known inequality  $\|\tilde{A}(t, \Theta)\| \geq \rho(\tilde{A}(t, \Theta))$  guarantees that  $\gamma \mathbf{1} \geq \tilde{A}(t, \Theta)$  for some  $\gamma < 1$ . Then,  $\gamma \mathbf{1} \geq A(t)$  for  $A(t)$  defined in (4.34). Now a direct application of Lemma 4.1 finishes the proof. ■

**Remark 4.2.** Note that, as in the spin-orbit problem, there are two special cases for which  $\Theta^*$  can be computed explicitly for some combination of parameters satisfying (4.36). If  $\Lambda_j = 0$  and  $\Lambda_{m_2}^{m_1} = 0$  for  $m_1 m_2 \neq 0$ , for each  $e \in (0, 1)$  the solution is the synchronous resonance of the uncoupled system

$$\Theta^*(t) = 2(t - f(t, e)) \begin{pmatrix} 1 \\ 1 \end{pmatrix}. \quad (4.38)$$

On the other hand, if  $e = 0$  the solution is  $\Theta^*(t) = 0$ .

### 4.2.3 Linear stability of the solution

Now we are interested in the stability properties of the solution  $\Theta^*(t)$ , which should be seen as  $2\pi$ -periodic and odd from now on. In the following we will find a region of parameters guaranteeing stability of the (scaled) linearized system of (1.23) at the periodic solution  $\Theta^*$ , say,

$$\ddot{y} + A(t)y = 0, \quad (4.39)$$

where we take the symmetric matrix  $A(t)$  now defined by

$$A(t) = \tilde{A}(t, \Theta^*(t)) = \mathcal{C}^{-1/2} \partial_{\Theta} F(t, \Theta^*(t)) \mathcal{C}^{-1/2},$$

and  $\tilde{A}(t, \Theta)$  was defined in (4.35).

Recall from Section 1.3.3 that the *conservative* spin-spin model has a time-dependent Hamiltonian structure given by (1.21). The variational equations associated to periodic solutions, like (4.39), are linear Hamiltonian systems with periodic coefficients. We will abbreviate them by LPH systems<sup>4</sup>. These systems have some special properties that we will use in the following. For the general theory see [126] or [43]. For example, assume that  $\varphi$  is a Floquet multiplier of an LPH system. Then, its inverse  $\varphi^{-1}$ , its complex conjugate  $\bar{\varphi}$  and  $\bar{\varphi}^{-1}$  are also multipliers and have the same multiplicity as  $\varphi$ . This is stated in Corollary 6 of Chapter 1.1 of [43]. Let us point out two interesting consequences. First, a necessary condition for stability of an LPH system is that all its Floquet multipliers must have modulus 1. Second, an LPH system can never be asymptotically stable. In order to do continuation of periodic solutions to the *dissipative* regime we will need the concept of strong stability for LPH systems.

**Definition 4.2.** *Let  $A_0(t) \in \mathbb{R}^{d \times d}$  be a fixed symmetric and  $T$ -periodic matrix. Assume that there exists a number  $\varepsilon > 0$  such that the equation  $\ddot{y} + A_*(t)y = 0$  is stable for all  $A_*(t) \in \mathbb{R}^{d \times d}$  symmetric and  $T$ -periodic satisfying  $\int_0^T \|A_*(t) - A_0(t)\| < \varepsilon$ . Then,  $\ddot{y} + A_0(t)y = 0$  is strongly stable.*

In other words, if an LPH system is strongly stable, then, any sufficiently small perturbation of it is stable. The perturbation should keep the Hamiltonian structure. Let us illustrate this with an example of the so-called Mathieu equation. Consider the  $2\pi$ -periodic equation

$$\ddot{x} + \frac{1}{4}(1 + \epsilon \cos t)x = 0, \quad x \in \mathbb{R}.$$

---

<sup>4</sup>The linear system  $\mathcal{C}\ddot{y} + \partial_{\Theta} F(t, \Theta^*(t))y = 0$  is an LPH system in the general sense. However, for simplicity, we particularize the general theory to (4.39).

For  $\epsilon = 0$  it is stable, but not strongly stable, because we can always find a small number  $\epsilon \neq 0$  such that the corresponding equation is not stable. This is called parametric resonance, see [4].

Strong stability can be characterized with the Floquet multipliers of the system. For example, take an LPH system whose multipliers belong to the unit circle. If the multiplicity of all the multipliers is one, then the system is strongly stable. However, the converse is not true. M. Krein developed a theory to determine if a system is strong stable with further algebraic properties of the multipliers. For our purpose of making continuation of periodic solutions the following property is relevant.

**Proposition 4.2.** *Assume that  $\ddot{y} + A(t)y = 0$ , with  $A(t) \in \mathbb{R}^{d \times d}$  symmetric and  $T$ -periodic, is strongly stable. Then, neither 1 nor  $-1$  are Floquet multipliers of the system.*

We will not prove this property because it is a particular result of the general theory. Nonetheless, it can be inferred by the paragraph previous to Theorem 10 in Chapter 1.2 of [43], that is the main result of Krein's theory.

Some sufficient conditions for strong stability of (4.39) are given by the following Lyapunov-like stability criterion, from Test 4, in [126], Chapter III, Section 7.

**Stability test 4.1.** *The equation  $\ddot{y} + A(t)y = 0$ , with  $A(t) \in \mathbb{R}^{d \times d}$  symmetric and  $2\pi$ -periodic, is strongly stable provided that, for all  $x \in \mathbb{R}^d \setminus \{0\}$ ,*

$$\int_0^{2\pi} \langle A(t)x, x \rangle dt > 0 \quad \text{and} \quad \int_0^{2\pi} \text{Tr}(A(t)) dt < \frac{2}{\pi}. \quad (4.40)$$

This stability test is the main tool for the proof of the next theorem.

**Theorem 4.2.** *Assume that the parameters of the model satisfy the following conditions.*

$$\frac{1}{\pi^2} > \frac{1}{(1-e)^3} \left( \frac{\Lambda_1}{\mathcal{C}_1} + \frac{\Lambda_2}{\mathcal{C}_2} \right) + \frac{1}{(1-e)^5} \sum_{(m_1, m_2) \in \Xi} \left( \frac{m_1^2}{\mathcal{C}_1} + \frac{m_2^2}{\mathcal{C}_2} \right) \Lambda_{m_2}, \quad (4.41)$$

$$\begin{aligned} \frac{1}{4\pi} > M := & \frac{1}{(1-e)^3} \max \left\{ \frac{\Lambda_1}{\mathcal{C}_1}, \frac{\Lambda_2}{\mathcal{C}_2} \right\} + \\ & + \frac{1}{(1-e)^5} \sum_{(m_1, m_2) \in \Xi} \max \left\{ \frac{|m_1|}{\mathcal{C}_1}, \frac{|m_2|}{\mathcal{C}_2} \right\} \Lambda_{m_2} + \frac{4e\sqrt{1-e^2}}{(1-e)^4}, \end{aligned} \quad (4.42)$$

$$\cos(2\pi^2 M) \min \left\{ \frac{\Lambda_1}{\mathcal{C}_1}, \frac{\Lambda_2}{\mathcal{C}_2} \right\} > \max \left\{ \alpha_1 \frac{\Lambda_1}{\mathcal{C}_1}, \alpha_2 \frac{\Lambda_2}{\mathcal{C}_2} \right\}, \quad (4.43)$$

with  $\alpha_j$  defined in (4.37). Then the solution  $\Theta^*(t)$  is strongly linearly stable.

Note that the second condition of (4.40) is guaranteed by (4.41). The first condition of (4.40) is a bit more complicated, but its proof is immediate by the following two lemmas.

**Lemma 4.2.** *The components of the solution  $\Theta^*(t)$  satisfy the following bounds  $|\Theta_j^*(t)| \leq 2\pi^2 M$ ,  $|\dot{\Theta}_j^*(t)| \leq 2\pi M$  provided that  $M \geq \|\mathcal{C}^{-1}F(t, \Theta^*(t))\|$ .*

**Proof.** Integrating the identity  $\ddot{\Theta}^*(t) + \mathcal{C}^{-1}F(t, \Theta^*(t)) = 0$  and taking the first component,

$$\dot{\Theta}_1^*(t) = \dot{\Theta}_1^*(t_0) - \int_{t_0}^t u_1 \mathcal{C}^{-1}F(s, \Theta^*(s)) ds,$$

where  $u_1$  is the row vector  $(1, 0)$ . Then, for  $t \in [t_0, t_0 + 2\pi]$ ,

$$|\dot{\Theta}_1^*(t)| \leq |\dot{\Theta}_1^*(t_0)| + \int_{t_0}^{t_0+2\pi} \|\mathcal{C}^{-1}F(s, \Theta^*(s))\| ds \leq |\dot{\Theta}_1^*(t_0)| + 2\pi M,$$

where  $\|\cdot\|$  indicates a matrix norm induced by a norm in  $\mathbb{R}^2$ . Since  $\Theta_1^*(t)$  is  $2\pi$ -periodic, we can choose  $t_0$  such that  $\dot{\Theta}_1^*(t_0) = 0$ . The same is applicable to  $\Theta_2$  for a possibly different  $t_0$ , consequently,  $|\dot{\Theta}_j^*(t)| \leq 2\pi M$  for all  $t$ . Furthermore, since  $\Theta_1^*(0) = 0$ ,

$$\Theta_1^*(t) = \int_0^t \dot{\Theta}_1^*(s) ds,$$

and, due to the odd symmetry of  $\Theta_1^*(t)$ , it is enough to consider  $t \in [0, \pi]$ . Then,  $|\Theta_1^*(t)| \leq 2\pi^2 M$ . The same is true for  $\Theta_2^*(t)$ . ■

**Lemma 4.3.** *The conditions (4.42) and (4.43) are sufficient so that  $A(t) = \tilde{A}(t, \Theta^*(t)) \geq \gamma \mathbf{1}$  for some  $\gamma > 0$ .*

**Proof.** The proof this lemma is based on the following fact. Considering the partial ordering of symmetric matrices given by Definition 4.1, the conditions (4.42) and (4.43) imply that the term proportional to  $1/r^3$  in (4.35) dominates the other term, that is proportional to  $1/r^5$ . Let us prove it. We can compute the derivatives of  $f(t)$  using Equations (1.10) to (1.12) and get

$$\ddot{f}(t) = -\frac{2e\sqrt{1-e^2}\sin(u(t))}{(1-e\cos(u(t)))^4},$$

where  $u$  is the eccentric anomaly. Using the maximum norm we see from (4.42) and (4.30) that  $1/(4\pi) > M \geq \|\mathcal{C}^{-1}F(t, \Theta^*(t))\|$ . Furthermore, from Lemma 4.2 we know that  $|\Theta_j^*(t)| \leq 2\pi^2 M$ , then, we can see graphically that

$$\cos \Theta_1^*(t) \geq \cos(2\pi^2 M) > 0,$$

therefore,

$$\begin{pmatrix} \frac{\Lambda_1}{\mathcal{C}_1} \cos \Theta_1^*(t) & 0 \\ 0 & \frac{\Lambda_2}{\mathcal{C}_2} \cos \Theta_2^*(t) \end{pmatrix} \geq \cos(2\pi^2 M) \min \left\{ \frac{\Lambda_1}{\mathcal{C}_1}, \frac{\Lambda_2}{\mathcal{C}_2} \right\} \mathbf{1}. \quad (4.44)$$

On the other hand, let us define

$$B = - \left( \frac{a}{r(t)} \right)^2 \sum_{(m_1, m_2) \in \Xi} \begin{pmatrix} \frac{m_1^2}{\mathcal{C}_1} & \frac{m_1 m_2}{\sqrt{\mathcal{C}_1 \mathcal{C}_2}} \\ \frac{m_1 m_2}{\sqrt{\mathcal{C}_1 \mathcal{C}_2}} & \frac{m_2^2}{\mathcal{C}_2} \end{pmatrix} \Lambda_{m_2}^{m_1} \cos(m_1 \Theta_1^*(t) + m_2 \Theta_2^*(t)).$$

As we did in the Proof of Theorem 4.1, we can take the maximum norm and obtain that

$$\max \left\{ \alpha_1 \frac{\Lambda_1}{\mathcal{C}_1}, \alpha_2 \frac{\Lambda_2}{\mathcal{C}_2} \right\} \geq \|B\| \geq \rho(B)$$

where  $\rho(B)$  is the spectral radius of  $B$ , then,

$$\max \left\{ \alpha_1 \frac{\Lambda_1}{\mathcal{C}_1}, \alpha_2 \frac{\Lambda_2}{\mathcal{C}_2} \right\} \mathbf{1} \geq B.$$

From this inequality, (4.44) and the definition (4.35) of  $\tilde{A}(t, \Theta)$ , we prove that  $\tilde{A}(t, \Theta^*(t)) \geq \gamma \mathbf{1}$  with

$$\gamma = \cos(2\pi^2 M) \min \left\{ \frac{\Lambda_1}{\mathcal{C}_1}, \frac{\Lambda_2}{\mathcal{C}_2} \right\} - \max \left\{ \alpha_1 \frac{\Lambda_1}{\mathcal{C}_1}, \alpha_2 \frac{\Lambda_2}{\mathcal{C}_2} \right\} > 0.$$

■

Now we see that Lemma 4.3 implies the first condition of (4.40) because  $\langle A(t)x, x \rangle \geq \gamma \|x\|^2 > 0$ .

### 4.3 The synchronous resonance in the dissipative regime

Recall from (1.22) that the *dissipative* spin-spin model takes the form of the system

$$\ddot{\Theta} + \text{diag}(\delta)D(t)\dot{\Theta} + \mathcal{C}^{-1}F(t, \Theta) = 0, \quad \delta = \begin{pmatrix} \delta_1 \\ \delta_2 \end{pmatrix}, \quad \delta_j \geq 0, \quad (4.45)$$

with  $D(t) = (a/r(t))^6$ . We know from Theorem 4.2 that, for  $\delta = 0$ , there exists an odd  $2\pi$ -periodic solution  $\Theta^*(t)$ , that is strongly linearly stable in the set of the parameters space satisfying the conditions given in Equations (4.41) to (4.43).

The main result of this section is Theorem 4.3. There we will see that the *conservative* periodic solution  $\Theta^*(t)$  can be continued in the presence of friction to an asymptotically stable periodic solution  $\Psi^*(t, \delta)$ . However, the odd symmetry of the solution is lost because (4.45) is not invariant under the change  $(t, \Theta) \rightarrow (-t, -\Theta)$  as in the *conservative* case. The proof of Theorem 4.3 is mainly based on Theorem 2 in [91] and on classical results on continuation of periodic solutions summarized in the next proposition.

**Proposition 4.3.** *Let  $\mathcal{F}$  be a real analytic function  $\mathcal{F} = \mathcal{F}(t, x, \zeta)$ , such that  $\mathcal{F}(t + T, x, \zeta) = \mathcal{F}(t, x, \zeta)$ , with  $t \in \mathbb{R}$ ,  $x \in \mathbb{R}^n$ ,  $\zeta \in \mathbb{R}^d$ . Assume that the equation  $\dot{x} = \mathcal{F}(t, x, 0)$  has a  $T$ -periodic solution  $x = p(t)$ .*

1. *Suppose that 1 is not a Floquet multiplier of the corresponding variational equation at  $x = p(t)$ ,*

$$\dot{y} = \partial_x \mathcal{F}(t, p(t), 0)y.$$

*Then, for  $\zeta \neq 0$ , with small enough norm  $\|\zeta\|$ , the equation  $\dot{x} = \mathcal{F}(t, x, \zeta)$  has a  $T$ -periodic solution  $x = p_c(t, \zeta)$  such that  $p_c(t, 0) = p(t)$ . Moreover,  $p_c(t, \zeta)$  is an analytic function and it is unique of each  $\zeta$ .*

2. *If additionally,  $p(t)$  is asymptotically stable, then this is also true for  $p_c(t, \zeta)$ .*

For the detailed proof of this proposition, see Theorems 1.1 and 1.2 in Chapter 14, [31]. Now we can state the main theorem.

**Theorem 4.3.** *Assume that the parameters of the system satisfy the conditions in Theorem 4.2. If  $|\delta_j|$  are small enough, then there exists a function  $\Psi^*(t, \delta)$ , analytic in both entries, satisfying*

i)  $\Psi^*(t, 0) = \Theta^*(t)$  for each  $t \in \mathbb{R}$ .

ii)  $\Psi^*(t, \delta)$  is a  $2\pi$ -periodic solution of (4.45). Moreover, if  $|\Lambda_{m_2}^{m_1}|$  are small enough, then,  $\Psi^*(t, \delta)$  is asymptotically stable.

**Proof.** Recall that the *conservative* periodic solution  $\Theta^*(t)$  is strongly linearly stable. Proposition 4.2 guarantees that 1 is not a Floquet multiplier of the variational equation at  $\Theta^*(t)$ . Then, we can apply the first item of Proposition 4.3 to make the analytic continuation of the periodic solution from the *conservative* ( $\delta_j = 0$ ) to the *dissipative* regime ( $\delta_j > 0$ ). We conclude that there exists a unique analytic  $2\pi$ -periodic solution  $\Psi^*(t, \delta)$  of (4.45) such that  $\Psi^*(t, 0) = \Theta^*(t)$  for small enough  $\delta_j$ .

Let us explain more in detail the proof that the continuation is asymptotically stable. If  $\Lambda_{m_2}^{m_1} = 0$  for all  $(m_1, m_2) \in \Xi$ , then (4.45) takes the form of two uncoupled *dissipative* spin-orbit equations

$$\ddot{\Theta}_j + \delta_j \left( \frac{a}{r(t)} \right)^6 \dot{\Theta}_j + \frac{\Lambda_j}{\mathcal{C}_j} \left( \frac{a}{r(t)} \right)^3 \sin \Theta_j = 0. \quad (4.46)$$

Besides, conditions in Equations (4.41) to (4.43) guarantee that, for  $\Lambda_{m_2}^{m_1} = 0$ , the *conservative* solution  $\Theta^*(t)$  is strongly linearly stable. We can see the solution  $\Theta^*(t)$  split in two components  $\Theta_j^*(t)$ , each of them is a solution of the *conservative* spin-orbit problem (4.46) with  $\delta_j = 0$ . Now we can apply Theorem 2 in [91] that guarantees that each equation in (4.46) has an asymptotically stable  $2\pi$ -periodic solution  $\Theta_{j, \delta_j}^*(t)$  provided that  $\delta_j \in (0, \bar{\delta}_j]$ . Here  $\bar{\delta}_j$  are small numbers quantified in [91]. Moreover,  $\Theta_{j, \delta_j}^*(t)$  is the unique continuation of  $\Theta_j^*(t) = \Theta_{j, 0}^*(t)$ .

Let us consider (4.46) as a system of two equations. This system has an asymptotically stable  $2\pi$ -periodic solution  $\Psi^*(t, \delta) = (\Theta_{1, \delta_1}^*(t), \Theta_{2, \delta_2}^*(t))^T$  such that  $\Psi^*(t, 0) = \Theta^*(t)$ . If  $|\Lambda_{m_2}^{m_1}|$  are small, we can see (4.45) as a perturbation of the system (4.46) and apply the second item of Proposition 4.3. In this way we guarantee that  $\Psi^*(t, \delta)$  has a  $2\pi$ -periodic continuation for  $\Lambda_{m_2}^{m_1} \neq 0$  that is asymptotically stable if  $|\Lambda_{m_2}^{m_1}|$  are small enough. ■

Note that for asymptotic stability we require not only that  $|\delta_j|$  should be small, but also  $|\Lambda_{m_2}^{m_1}|$ . We would like to erase this condition on the coupling parameters  $\Lambda_{m_2}^{m_1}$ . However, from a theoretical point of view, this is certainly difficult to address in general since we deal with systems of differential equations. Let us explain this point. The variational equation of (4.45) near  $\Psi^*(t, \delta)$  is

$$\ddot{\eta} + \text{diag}(\delta)D(t)\dot{\eta} + \mathcal{C}^{-1}\partial_{\Theta}F(t, \Psi^*(t, \delta))\eta = 0, \quad \delta = \begin{pmatrix} \delta_1 \\ \delta_2 \end{pmatrix}. \quad (4.47)$$

For  $e \neq 0$ , (4.47) is a linear  $2\pi$ -periodic system of two equations of second order. In [91], asymptotic stability was proved for the spin-orbit problem taking advantage of the following fact. Any second order periodic equation  $\ddot{x} + a_1(t)\dot{x} + a_0(t)x = 0$ ,  $x \in \mathbb{R}$ ,  $a_n(t) = a_n(t + T)$ , can be converted into a Hill's equation  $\ddot{\chi} + \alpha(t)\chi = 0$ ,  $\alpha(t) = a_0(t) - \frac{1}{4}a_1(t)^2 - \frac{1}{2}\dot{a}_1(t)$ , by the change of variables  $\chi(t) = x(t) \exp(\frac{1}{2} \int_0^t a_1(s) ds)$ . See [77]. We can see the *dissipative* problem ( $a_1(t) \neq 0$ ) as a perturbation of the *conservative* one ( $a_1(t) = 0$ ). Assume that  $\ddot{x} + a_0(t)x = 0$  is strongly stable, then  $\ddot{\chi} + \alpha(t)\chi = 0$  is stable. Since it is a Hill's equation (also a LPH system), the modulus of the Floquet multipliers of  $\ddot{\chi} + \alpha(t)\chi = 0$  is 1. Now we undo the change of variables and conclude that the modulus of the Floquet multipliers of  $\ddot{x} + a_1(t)\dot{x} + a_0(t)x = 0$  is smaller than 1, therefore, it is asymptotically stable. However, it is not clear how to perform an analogous procedure in (4.47). The main obstacle is the non-commutativity of matrices due to the asymmetric nature of the *dissipative* problem ( $\delta_1 \neq \delta_2$ ). Actually, if we follow the same steps, we end up with a system of equations that is no longer periodic for  $\delta_1 \neq \delta_2$ . The numbers  $\delta_j$  depend on several parameters of the bodies and we do not see any good physical reason to impose both dissipative parameters to be equal. In fact, if  $\delta_1 \neq \delta_2$ , in principle the *dissipative* spin-spin model cannot be considered conformally symplectic as the spin-orbit problem. See [20]. From this discussion, we conclude that this it is necessary a deeper theoretical study, but it is beyond the scope of this paper.

On the other hand, let us see that for  $e = 0$ , the solution of (4.47) is asymptotically stable. The solution given by Theorem 3.2 is  $\Psi^*(t, \delta) \equiv 0$ . Taking  $y = \mathcal{C}^{1/2}\eta$ , the corresponding variational equation is

$$\ddot{y} + \text{diag}(\delta)\dot{y} + Ay = 0, \quad (4.48)$$

where  $A$  is the symmetric constant matrix given by

$$A = \begin{pmatrix} \xi_1 & \sigma \\ \sigma & \xi_2 \end{pmatrix} = \begin{pmatrix} \frac{\Lambda_1}{c_1} & 0 \\ 0 & \frac{\Lambda_2}{c_2} \end{pmatrix} + \sum_{(m_1, m_2) \in \Xi} \begin{pmatrix} \frac{m_1^2}{c_1} & \frac{m_1 m_2}{\sqrt{c_1 c_2}} \\ \frac{m_1 m_2}{\sqrt{c_1 c_2}} & \frac{m_2^2}{c_2} \end{pmatrix} \Lambda_{m_2}.$$

Note that, by conditions (4.42) and (4.43),  $A$  is a positive definite matrix. See Lemma 4.3. The characteristic polynomial of equation (4.48) is

$$p(\omega) = \omega^4 + (\delta_1 + \delta_2)\omega^3 + (\xi_1 + \xi_2 + \delta_1\delta_2)\omega^2 + (\xi_1\delta_2 + \xi_2\delta_1)\omega + \det A.$$

Equation (4.48) is asymptotically stable if and only if all the roots of  $p(\omega)$  have negative real parts. This can be checked with the Routh-Hurwitz criterion, see [49]. According to it, all the roots of the polynomial have



#### 4.3. THE SYNCHRONOUS RESONANCE IN THE DISSIPATIVE REGIME 151

negative real parts if and only if the associated Hurwitz determinants of the polynomial are strictly positive, say,

$$D_1 = \delta_1 + \delta_2, \quad D_2 = \delta_1^2 \delta_2 + \delta_2^2 \delta_1 + \xi_1 \delta_1 + \xi_2 \delta_2,$$

$$D_3 = D_1^2 \sigma^2 + \delta_1 \delta_2 (D_1 (\xi_1 \delta_2 + \xi_2 \delta_1) + (\xi_1 - \xi_2)^2), \quad D_4 = D_3 \det A.$$

Since  $A$  is positive definite, we get asymptotic stability for all  $\delta_1$  and  $\delta_2$  such that both are non-negative and at least one is different from zero.

## 4.4 Applications

Recall from the end of Section 4.1 that our model depends on six independent physical parameters  $(e; \mathcal{C}_1, \lambda_1, \lambda_2, \hat{d}_1, \hat{q}_1)$ , where  $e$  is the orbital eccentricity,  $\mathcal{C}_j$  the moment of inertia of  $\mathcal{E}_j$  with respect to the  $\mathbf{c}_j$ -axis,  $\lambda_j = \Lambda_j/\mathcal{C}_j$  is the oblateness of  $\mathcal{E}_j$  in the plane of motion, and  $\hat{d}_j$  and  $\hat{q}_j$  are, respectively, the oblateness and the flatness of  $\mathcal{E}_j$  with respect to the size of the orbit.

We have two type of estimates. The first type in (4.36) guarantees uniqueness of the synchronous resonance in the *conservative* regime. The second one in Equations (4.41) to (4.43) guarantees linear stability of the same solution. Our estimates depend on certain values  $\alpha_j$  in (4.37). To write them in terms of the physical parameters, we use the definitions in Equations (4.23) to (4.26), then

$$\sum_{(m_1, m_2) \in \Xi} \frac{m_j^2}{\mathcal{C}_j} \Lambda_{m_2}^{m_1} = \lambda_j \left( \frac{25}{4} \hat{d}_j + \frac{25}{28} \hat{q}_j + \frac{19}{4} \hat{d}_{3-j} + \frac{5}{4} \hat{q}_{3-j} \right), \quad (4.49)$$

$$\sum_{(m_1, m_2) \in \Xi} \frac{|m_1 m_2|}{\sqrt{\mathcal{C}_1 \mathcal{C}_2}} \Lambda_{m_2}^{m_1} = \frac{19}{4} \sqrt{\frac{\mathcal{C}_1}{\mathcal{C}_2}} \lambda_1 \hat{d}_2 = \frac{19}{4} \sqrt{\frac{\mathcal{C}_2}{\mathcal{C}_1}} \lambda_2 \hat{d}_1, \quad (4.50)$$

$$\sum_{(m_1, m_2) \in \Xi} \frac{|m_j|}{\mathcal{C}_j} \Lambda_{m_2}^{m_1} = \lambda_j \left( \frac{25}{8} \hat{d}_j + \frac{25}{28} \hat{q}_j + \frac{19}{4} \hat{d}_{3-j} + \frac{5}{4} \hat{q}_{3-j} \right). \quad (4.51)$$

Now we are ready to apply our estimates to specific cases.

### 4.4.1 Real systems

In one hand, the Pluto-Charon binary is the largest known system that is in double synchronous resonance. The physical parameters of the system relevant for the spin-spin model are shown in Table 4.1. Pluto is almost twice the size of Charon, contains the 89% of the mass and the 97% of the body moment of inertia ( $\mathcal{C}_j$ ) of the system. Besides, the size of the orbit is quite large ( $a = 27.2$ ) compared to the sizes of the bodies. This results in very small values of  $\hat{d}_j$  of order  $10^{-7}$ , which means this is a certainly weak spin-spin coupling. The orbit has a very small eccentricity  $e = 0.0002$ . Recall that the double synchronous resonance of the circular case ( $e = 0$ ) is the trivial solution  $\Theta(t) \equiv 0$ , both for the *conservative* case (1.23) and the *dissipative* case (1.22). The asymptotic stability of the solution for any value of the dissipative parameters is easily guaranteed, as it was shown at the end of Section 3.3 using equation (4.48). For the real eccentricity, the solution  $\Theta^*(t)$  of (1.23) oscillates very close to zero and our estimates guarantee the

System	$M_j$	$a_j$	$\mathcal{C}_j$	$\lambda_j$	$\hat{d}_j$	$\hat{q}_j$	$a$	$e$
Pluto	0.89	1.65	0.97	$3.3 \cdot 10^{-5}$	$1.5 \cdot 10^{-7}$	$1.2 \cdot 10^{-6}$	27.2	$2.0 \cdot 10^{-4}$
Charon	0.11	0.84	0.03	$2.4 \cdot 10^{-3}$	$3.5 \cdot 10^{-7}$	$8.2 \cdot 10^{-7}$		
Patroclus	0.56	1.7	0.60	0.11	$2.6 \cdot 10^{-4}$	$1.2 \cdot 10^{-3}$	$18.2 \pm 0.5$	$0.02 \pm 0.02$
Menoetius	0.44	1.6	0.40	0.14	$2.2 \cdot 10^{-4}$	$9.9 \cdot 10^{-4}$		

Table 4.1: Real physical parameters for two binary systems. For Pluto and Charon, we take the largest values of  $\lambda_j$ ,  $\hat{d}_j$  and  $\hat{q}_j$  obtained from data in [61]. The parameters of Patroclus and Menoetius are obtained from data in [36] and the orbital parameters from [79].

uniqueness and linear stability of solution. Furthermore, Theorem 4.3 shows the existence of an asymptotically stable solution  $\Psi^*(t, \delta)$  of the *dissipative* model provided that  $\delta_j$ ,  $\hat{d}_j$  and  $\hat{q}_j$  are small enough. Unfortunately, this last result is not quantified in this paper for the real parameters.

On the other hand, the Trojan binary asteroid 617 Patroclus is a system whose components are of similar size, mass and moment of inertia. See the physical parameters of its components, Patroclus and Menoetius, in Table 4.1. Each body has a diameter of around one hundred kilometres, almost ten times smaller than Charon. Patroclus and Menoetius have a more oblate ellipsoidal shape than Pluto and Charon and the size of the orbit in this case ( $a = 18.2 \pm 0.5$ ) is smaller. In consequence, the corresponding dynamical parameters  $\lambda_j$ ,  $\hat{d}_j$  and  $\hat{q}_j$  are several orders of magnitude larger. The orbital eccentricity is not measured with enough precision,  $e = 0.02 \pm 0.02$ . With our estimates, we are able to guarantee the uniqueness of the solution  $\Theta^*(t)$  of (1.23) for eccentricities up to  $e = 0.04$ . However, we fail to guarantee linear stability even for  $e = 0$ . The main reason is that the stability test given by the conditions (4.40) is not fine enough for such large values of  $\lambda_j$ . In the following subsection we will explain what is the range of parameters that is covered by our study.

### 4.4.2 Stability diagrams in the space of parameters

Note that all the terms appearing in Equations (4.49) to (4.51) are positive. Since  $\hat{q} \geq \hat{d}$ , and, in order to reduce the parameters in the upper bounds for the expressions in Equations (4.49) to (4.51), we can take  $\hat{d}_j = \hat{q}_j$ . In this way, we reduce the independent parameters to five ( $e; \lambda_1, \lambda_2, \mathcal{C}_1, \hat{q}_1$ ). Note now that, to take  $\hat{q}_1 = 0$  is equivalent to break the coupling of the system, resulting in two independent spin-orbit problems.

We will consider two special cases with three free parameters. In one hand, the case of identical bodies, that we compare with the asteroid 617 Patroclus. Here the parameters are  $e$ ,  $\lambda_j = \lambda$  and  $\hat{q}_j = \hat{q}$ . On the other hand, the case when  $\mathcal{E}_1$  is twice the size of  $\mathcal{E}_2$ , that we compare with the Pluto-Charon system. Here we consider the same density and the free parameters are  $e$ ,  $\lambda_2$  and  $\hat{q}_1$ , whereas the dependent parameters are  $\lambda_1 = 2^{-3}\lambda_2$  and  $\hat{q}_2 = 2^{-5}\hat{q}_1$ .

Figure 4.2 shows regions in the space of parameters for which there is uniqueness and linear stability of the double synchronous resonance according to our theoretical estimates. We see that we cover the Patroclus-Menoetius system (top panels) only for the uniqueness of the solution but not for the linear stability. In contrast, the Pluto-Charon system (bottom panels) is covered for linear stability as well. We can compare the diagrams of  $\hat{q} = 0$  and  $\hat{q}_1 = 0$  with the theoretical estimates obtained in [91], shown in Figure 4.3. We see that, although the uniqueness region is similar, the stability region (in yellow) is considerably larger in Figure 4.3 than those in Figure 4.2. This shows that the mathematical techniques used in [91] are much finer than in this paper. In [91] we used generalized Lyapunov criteria using  $L^p$ -norms, with  $p \in [1, \infty]$ , see [128], and upper and lower solutions to bound the amplitude of the solution. Instead, in this paper we use the stability test given by (4.40), that is of type  $L^\infty$ , and a rougher bound for the amplitude of the solution in Lemma 4.2. Since the model is quite new, here we initiate the analysis with a simpler approach. Besides, the mathematical tools are not as well developed for systems of equations as for standard second order scalar equations.

We see in Figure 4.2 that an increase in the value of  $\hat{q}$  results in a global reduction of the regions that we estimated theoretically, both for stability and uniqueness regions. This behavior can be compared with the numerical plots in Figure 4.4. We focus only on the case of equal bodies. Here we see how the instability region changes when we increase  $\hat{q}$ . There are some interesting phenomena.

1. For  $\hat{q} = 0$  there is only one bifurcation point for the unstable solution in the  $\lambda$ -axis at  $(e, \lambda) = (0, 0.25)$ . However, for  $\hat{q} > 0$ , it becomes two

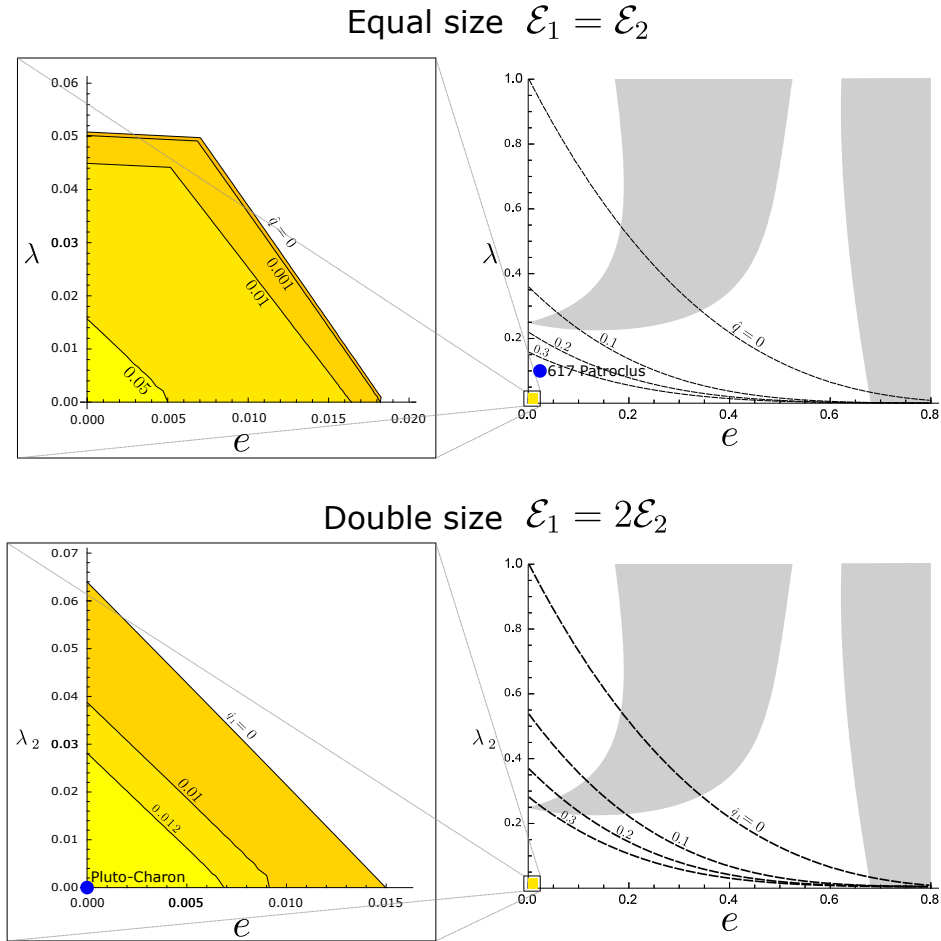


Figure 4.2: Stability diagrams in the  $(e, \lambda)$ -plane of the synchronous resonance of the spin-spin model. Top: both bodies are equal. Bottom: one body is double the size of the other. The double synchronous resonance is unique under the dashed lines (right) and linearly stable under the black lines (left) for the indicated value of  $\hat{q}$ . In the left we see zoomed views of the stable regions. The more yellow is the region indicates that stability is guaranteed for larger values of  $\hat{q}$ . The gray regions in the right are unstable for the uncoupled system (spin-orbit), i.e., with  $\hat{q} = 0$ .

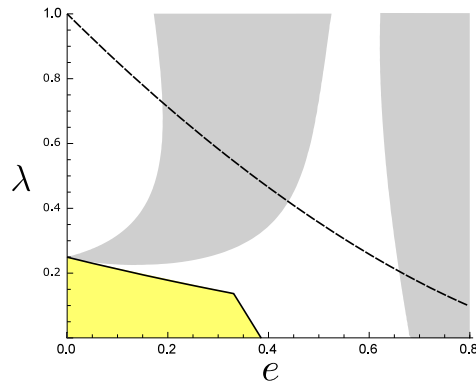


Figure 4.3: Stability diagram in the  $(e, \lambda)$ -plane of the spin-orbit in [91], Figure 3.

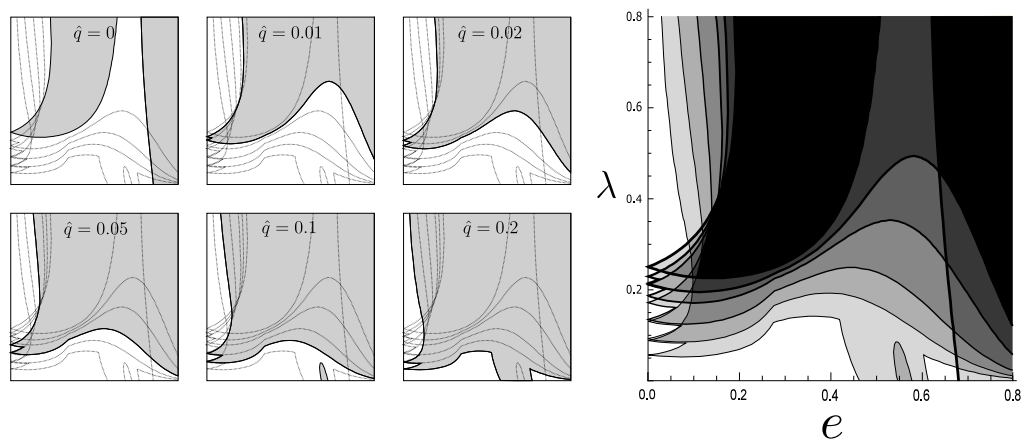


Figure 4.4: Stability diagrams in the  $(e, \lambda)$ -plane in the case of equal bodies. The six plots in the left show the unstable region in gray for different values of  $\hat{q}$ . The image in the right shows the six diagrams superimposed. Darker tones of gray indicate more overlapping between unstable regions.

bifurcation points at  $(0, \lambda_{(1)})$  and  $(0, \lambda_{(2)})$ , with  $0 < \lambda_{(1)} < \lambda_{(2)} < 0.25$ . This opens a small window of stability at the points  $(e, \lambda)$  with  $e$  close to 0 and  $\lambda \in (\lambda_{(1)}, \lambda_{(2)})$ .

2. For  $\hat{q} = 0$ , apart from the instability region bifurcating from the  $\lambda$ -axis, there is another one bifurcating from the  $e$ -axis at  $(e, \lambda) \approx (0.682, 0)$ . The existence of such bifurcation was studied in [91]. However, for  $\hat{q} > 0$ , it looks that the last bifurcation point moves to the right, at the same time that the two instability regions merge into a single one. This shows that turning on the coupling has a stabilizing effect of the synchronous resonance for large  $e$  and small  $\lambda$ . This holds up to a critical  $\hat{q} \in (0.05, 0.1)$  for which another unstable region bifurcates from the  $e$ -axis. This region merges with the large one at some  $\hat{q} \in (0.1, 0.2)$ . This leaves an island of stability for large  $e$  and small  $\lambda$ .
3. In the right panel of Figure 4.4 we see that there are some regions (the darkest ones), that remain unstable, not very affected by changes in  $\hat{q}$ . Instead, the lighter regions show more susceptibility to change their stability when  $\hat{q}$  changes.

In Figure 4.4 we have taken large values of  $\hat{q}$ , compared to the real values in Table 4.1. From its definition in (4.20) and (4.17) we see that  $\hat{q} \leq 1/a^2$  for equal bodies ( $M = 0.5, \mathcal{C} = 0.5$ ). In order to be consistent with the Keplerian orbit approximation,  $a$  should be quite larger than 1, that gives the scale of the objects. For example,  $a$  of order 10 would give an upper estimate of  $\hat{q}$  of order  $10^{-2}$ . In consequence, for more realistic parameters, we should not consider the appearance of the additional instability region bifurcating from the  $e$ -axis from large  $\hat{q}$ .





# Bibliography

- [1] E. Y. ALESHKINA, *Synchronous spin-orbital resonance locking of large planetary satellites*, *Solar System Research*, 43 (2009), pp. 71–78, <https://doi.org/10.1134/S0038094609010079>.
- [2] F. ANTOGNINI, L. BIASCO, AND L. CHIERCHIA, *The Spin-Orbit Resonances of the Solar System: A Mathematical Treatment Matching Physical Data*, *Journal of Nonlinear Science*, 24 (2014), pp. 473–492, <https://doi.org/10.1007/s00332-014-9196-7>.
- [3] T. M. APOSTOL, *Mathematical analysis*, Addison-Wesley Series in Mathematics, Addison-Wesley, Reading, MA, 2nd ed., 1974.
- [4] V. ARNOL'D, *Mathematical Methods of Classical Mechanics*, Graduate Texts in Mathematics, Springer, New York, NY, 2nd ed., 1989, <https://doi.org/10.1007/978-1-4757-2063-1>.
- [5] G. BALMINO, *Gravitational potential harmonics from the shape of an homogeneous body*, *Celestial Mechanics and Dynamical Astronomy*, 60 (1994), pp. 331–364, <https://doi.org/10.1007/BF00691901>.
- [6] K. BATYGIN AND A. MORBIDELLI, *Onset of secular chaos in planetary systems: Period doubling and strange attractors*, *Celestial Mechanics and Dynamical Astronomy*, 111 (2011), <https://doi.org/10.1007/s10569-011-9361-3>.
- [7] K. BATYGIN AND A. MORBIDELLI, *Spin-Spin coupling in the Solar System*, *The Astrophysical Journal*, 810 (2015), p. 110, <https://doi.org/10.1088/0004-637x/810/2/110>.
- [8] C. BEAUGÉ AND S. FERRAZ-MELLO, *Resonance Trapping in the Primordial Solar Nebula: The Case of a Stokes Drag Dissipation*, *Icarus*, 103 (1993), pp. 301 – 318, <https://doi.org/10.1006/icar.1993.1072>.

- [9] C. BEAUGÉ AND S. FERRAZ-MELLO, *Capture in Exterior Mean-Motion Resonances Due to Poynting-Robertson Drag*, *Icarus*, 110 (1994), pp. 239 – 260, <https://doi.org/10.1006/icar.1994.1119>.
- [10] V. V. BELETSKII, *Motion of an artificial satellite about its center of mass*, *Mechanics of Space Flight*, Israel Program for Scientific Translations; [available from the U.S. Dept. of Commerce, Clearinghouse for Federal Scientific and Technical Information, Springfield, Va.], Jerusalem, 1966, [https://archive.org/details/nasa\\_techdoc\\_19670006100](https://archive.org/details/nasa_techdoc_19670006100).
- [11] V. V. BELETSKII AND E. K. LAVROVSKII, *On the theory of the resonance rotation of Mercury*, *Astronomicheskii Zhurnal*, 52 (1975), pp. 1299–1308, <https://ui.adsabs.harvard.edu/abs/1975AZh...52.1299B>.
- [12] G. BOUÉ AND J. LASKAR, *Spin axis evolution of two interacting bodies*, *Icarus*, 201 (2009), pp. 750 – 767, <https://doi.org/10.1016/j.icarus.2009.02.001>.
- [13] G. BOUÉ, *The two rigid body interaction using angular momentum theory formulae*, *Celestial Mechanics and Dynamical Astronomy*, 128 (2017), pp. 261–273, <https://doi.org/10.1007/s10569-017-9751-2>.
- [14] S. BREITER AND A. JACKSON, *Unified analytical solutions to two-body problems with drag.*, *Mon. Not. R. Astron. Soc.*, 299 (1998), pp. 237–243, <https://doi.org/10.1046/j.1365-8711.1998.01768.x>.
- [15] D. BROUWER AND G. I. HORI, *Theoretical evaluation of atmospheric drag effects in the motion of an artificial satellite.*, *Astron. J.*, 66 (1961), pp. 193–225, <https://doi.org/10.1086/108070>.
- [16] A. D. BRUNO, *Families of Periodic Solutions to the Beletsky Equation*, *Cosmic Research*, 40 (2002), pp. 274–295, <https://doi.org/10.1023/A:1015981105366>.
- [17] J. BURNS, P. LAMY, AND S. SOTER, *Radiation Forces on Small Particles in the Solar System.*, *Icarus*, 40 (1979), pp. 1–48, [https://doi.org/10.1016/0019-1035\(79\)90050-2](https://doi.org/10.1016/0019-1035(79)90050-2).
- [18] A. CAÑADA AND S. VILLEGAS, *A Variational Approach to Lyapunov Type Inequalities. From ODEs to PDEs.*, Springer, Cham, 2015, <https://doi.org/10.1007/978-3-319-25289-6>.

- [19] R. CALLEJA AND A. CELLETTI, *Breakdown of invariant attractors for the dissipative standard map*, Chaos: An Interdisciplinary Journal of Nonlinear Science, 20 (2010), p. 013121, <https://doi.org/10.1063/1.3335408>.
- [20] R. C. CALLEJA, A. CELLETTI, AND R. DE LA LLAVE, *A KAM theory for conformally symplectic systems: Efficient algorithms and their validation*, Journal of Differential Equations, 255 (2013), pp. 978 – 1049, <https://doi.org/10.1016/j.jde.2013.05.001>.
- [21] A. CELLETTI, *Analysis of resonances in the spin-orbit problem in celestial mechanics: The synchronous resonance (Part I)*., Zeitschrift Angewandte Mathematik und Physik, 41 (1990), pp. 174–204, <https://doi.org/10.1007/BF00945107>.
- [22] A. CELLETTI, *Weakly dissipative systems in celestial mechanics*, in Topics in Gravitational Dynamics, D. Benest, C. Froeschle, and E. Lega, eds., vol. 729, Springer, Berlin, Heidelberg, 12 2007, pp. 67–90, [https://doi.org/10.1007/978-3-540-72984-6\\_3](https://doi.org/10.1007/978-3-540-72984-6_3).
- [23] A. CELLETTI, *Stability and Chaos in Celestial Mechanics*, Springer, Berlin, Heidelberg, 01 2010, <https://doi.org/10.1007/978-3-540-85146-2>.
- [24] A. CELLETTI AND L. CHIERCHIA, *Measures of basins of attraction in spin-orbit dynamics*, Celestial Mechanics and Dynamical Astronomy, 101 (2008), pp. 159–170, <https://doi.org/10.1007/s10569-008-9142-9>.
- [25] A. CELLETTI AND L. CHIERCHIA, *Quasi-Periodic Attractors in Celestial Mechanics*, Archive for Rational Mechanics and Analysis, 191 (2009), pp. 311–345, <https://doi.org/10.1007/s00205-008-0141-5>.
- [26] A. CELLETTI, S. DI RUZZA, C. LHOTKA, AND L. STEFANELLI, *Nearly-integrable dissipative systems and celestial mechanics*, European physical journal - Special topics, 186 (2010), pp. 33–66, <https://doi.org/10.1140/epjst/e2010-01259-2>.
- [27] A. CELLETTI, C. FROESCHLÉ, AND E. LEGA, *Dissipative and weakly-dissipative regimes in nearly-integrable mappings*, Discrete and Continuous Dynamical Systems - A, 16 (2006), p. 757, <https://doi.org/10.3934/dcds.2006.16.757>.

- [28] A. CELLETTI, L. STEFANELLI, E. LEGA, AND C. FROESCHLÉ, *Some results on the global dynamics of the regularized restricted three-body problem with dissipation*, *Celestial Mechanics and Dynamical Astronomy*, 109 (2011), pp. 265–284, <https://doi.org/10.1007/s10569-010-9326-y>.
- [29] B. V. CHIRIKOV, *A universal instability of many-dimensional oscillator systems*, *Physics Reports*, 52 (1979), pp. 263 – 379, [https://doi.org/10.1016/0370-1573\(79\)90023-1](https://doi.org/10.1016/0370-1573(79)90023-1).
- [30] A. CHONG, *Effect of tidal dissipation on the motion of celestial bodies.*, PhD thesis, Penn State University, 2012, <https://etda.libraries.psu.edu/catalog/16233>.
- [31] A. CODDINGTON AND N. LEVINSON, *Theory of ordinary differential equations*, International series in pure and applied mathematics, McGraw-Hill, 1955.
- [32] A. COMPÈRE AND A. LEMAÎTRE, *The two-body interaction potential in the stf tensor formalism: An application to binary asteroids*, *Celestial Mechanics and Dynamical Astronomy*, 119 (2014), pp. 313–330, <https://doi.org/10.1007/s10569-014-9568-1>.
- [33] J. L. CORNE AND N. ROUCHE, *Attractivity of closed sets proved by using a family of Lyapunov functions.*, *J. Differential Equations*, 13 (1973), pp. 231–246, [https://doi.org/10.1016/0022-0396\(73\)90016-8](https://doi.org/10.1016/0022-0396(73)90016-8).
- [34] A. C. M. CORREIA AND J. LASKAR, *Mercury’s capture into the 3/2 spin-orbit resonance as a result of its chaotic dynamics*, *Nature*, 429 (2004), pp. 848 – 850, <https://doi.org/10.1038/nature02609>.
- [35] J. M. A. DANBY, *Fundamentals of celestial mechanics.*, The Macmillan Company, New York, 1962.
- [36] A. B. DAVIS AND D. J. SCHEERES, *Doubly synchronous binary asteroid mass parameter observability*, *Icarus*, 341 (2020), p. 113439, <https://doi.org/10.1016/j.icarus.2019.113439>.
- [37] C. DE COSTER AND P. HABETS, *The lower and upper solutions method for boundary value problems*, in *Handbook of Differential Equations, Ordinary Differential Equations*, A. Cañada, P. Drábek, and A. Fonda, eds., vol. 1, Elsevier, Amsterdam, 2004, ch. 2, pp. 69–160, [https://doi.org/10.1016/S1874-5725\(00\)80004-8](https://doi.org/10.1016/S1874-5725(00)80004-8).

- [38] A. DEPRIT, *The Secular Accelerations in Gyldens Problem*, *Celestial Mechanics*, 31 (1983), pp. 1–22, <https://doi.org/10.1007/BF01272557>.
- [39] F. DIACU, *Two body problems with drag or thrust: qualitative results.*, *Celestial Mechanics and Dynamical Astronomy*, 75 (1999), pp. 1–15, <https://doi.org/10.1023/A:1008305723295>.
- [40] J. DIEUDONNÉ, *Chapter V Normed Spaces*, in *Foundations of Modern Analysis*, vol. 10 of *Pure and Applied Mathematics*, Elsevier, 1969, pp. 91 – 114, [https://doi.org/10.1016/S0079-8169\(08\)60167-1](https://doi.org/10.1016/S0079-8169(08)60167-1).
- [41] A. R. DOBROVOLSKIS, S. J. PEALE, AND A. W. HARRIS, *Dynamics of the Pluto-Charon binary*, in *Pluto and Charon*, A. Stern and D. Tholen, eds., *Space science series*, University of Arizona Press, 1997, <https://books.google.es/books?id=VcY7iYJwJZoC>.
- [42] M. EFROIMSKY AND V. V. MAKAROV, *Tidal friction and tidal lagging. applicability limitations of a popular formula for the tidal torque*, *The Astrophysical Journal*, 764 (2013), p. 26, <https://doi.org/10.1088/0004-637x/764/1/26>.
- [43] I. EKELAND, *Convexity Methods in Hamiltonian Mechanics*, vol. 19 of *Ergebnisse der Mathematik und ihrer Grenzgebiete : a series of modern surveys in mathematics. Folge 3*, Springer-Verlag, Berlin Heidelberg, 1990, <https://doi.org/10.1007/978-3-642-74331-3>.
- [44] L. EULER AND S. THOMAS, III. *Part of a letter from Leonard Euler, Prof. Math. At Berlin, and F. R. S. To the Rev. Mr. Caspar Wetstein, Chaplain to his Royal Highness the Prince of Wales, concerning the gradual approach of the Earth to the Sun.* Translated from the French, by S. T. M. D. F. R. S. *Phil. Trans. R. Soc.* 46, 1749-1750, <https://doi.org/10.1098/rstl.1749.0038>.
- [45] E. G. FAHNESTOCK AND D. J. SCHEERES, *Simulation of the full two rigid body problem using polyhedral mutual potential and potential derivatives approach*, *Celestial Mechanics and Dynamical Astronomy*, 96 (2006), pp. 317–339, <https://doi.org/10.1007/s10569-006-9045-6>.
- [46] S. FERRAZ-MELLO, *Tidal synchronization of close-in satellites and exoplanets. A rheophysical approach*, *Celestial Mechanics and Dynamical Astronomy*, 116 (2013), pp. 109–140, <https://doi.org/10.1007/s10569-013-9482-y>.

- [47] S. FERRAZ-MELLO, C. GROTTA-RAGAZZO, AND L. RUIZ DOS SANTOS, *Dissipative forces in celestial mechanics*, 30<sup>o</sup> Colóquio Brasileiro de Matemática. Publicações Matemáticas, IMPA, Rio de Janeiro, 2015, [https://impa.br/wp-content/uploads/2017/04/30CBM\\_03.pdf](https://impa.br/wp-content/uploads/2017/04/30CBM_03.pdf).
- [48] H. A. FOLONIER, S. FERRAZ-MELLO, AND E. ANDRADE-INES, *Tidal synchronization of close-in satellites and exoplanets. III. Tidal dissipation revisited and application to Enceladus*, *Celestial Mechanics and Dynamical Astronomy*, 130 (2018), <https://doi.org/10.1007/s10569-018-9872-2>.
- [49] F. GANTMACHER, *Applications of the Theory of Matrices*, Interscience Publishers, 1959.
- [50] I. GKOLIAS, C. EFTHYMIPOULOS, A. CELLETTI, AND G. PUCACCO, *Accurate modelling of the low-order secondary resonances in the spin-orbit problem*, *Communications in Nonlinear Science and Numerical Simulation*, 77 (2019), pp. 181 – 202, <https://doi.org/10.1016/j.cnsns.2019.04.015>.
- [51] P. GOLDREICH AND S. PEALE, *Spin orbit coupling in the Solar System*, *The Astronomical Journal*, 71 (1966), p. 425, <https://doi.org/10.1086/109947>.
- [52] R. GONCZI, C. FROESCHLE, AND C. FROESCHLE, *Poynting-Robertson drag and orbital resonance*, *Icarus*, 51 (1982), pp. 633 – 654, [https://doi.org/10.1016/0019-1035\(82\)90152-X](https://doi.org/10.1016/0019-1035(82)90152-X).
- [53] R. GREENBERG, *Orbital resonance in a dissipative medium*, *Icarus*, 33 (1978), pp. 62 – 73, [https://doi.org/10.1016/0019-1035\(78\)90024-6](https://doi.org/10.1016/0019-1035(78)90024-6).
- [54] R. J. GREENBERG, C. C. COUNSELMAN, AND I. I. SHAPIRO, *Orbit-orbit resonance capture in the solar system*, *Science*, 178 (1972), pp. 747–749, <https://doi.org/10.1126/science.178.4062.747>.
- [55] H. GYLDÉN, *Die bahnbewegungen in einem systeme von zwei körpern in dem falle, dass die massen veränderungen unterworfen sind*, *Astronomische Nachrichten*, 109 (1884), pp. 1–6, <https://doi.org/10.1002/asna.18841090102>.
- [56] J. HALE, *Ordinary Differential Equations*, Dover Books on Mathematics Series, Dover Publications, 2nd ed., 1980.

- [57] J. HALE, H. BUTTANRI, AND H. KOCAK, *Dynamics and Bifurcations*, Texts in Applied Mathematics, Springer-Verlag New York, 1991, <https://doi.org/10.1007/978-1-4612-4426-4>.
- [58] B. HAMILTON AND M. CRESCIMANNO, *Linear frictional forces cause orbits to neither circularize nor precess.*, J. Phys. A: Math. Theor., 41 (2008), pp. 235–205, <https://doi.org/10.1088%2F1751-8113%2F41%2F23%2F235205>.
- [59] C. G. J. JACOBI, *Jacobi's Lectures on Dynamics: Delivered at the University of Königsberg in the Winter Semester 1842-1843 and According to the Notes Prepared by C. W. Brockardt. Edited by A. Clebsch.*, Texts and Readings in Mathematics, Hindustan Book Agency, Gurgaon, 2009, <https://doi.org/10.1007/978-93-86279-62-0>.
- [60] M. JAFARI NADOUSHAN AND N. ASSADIAN, *Geography of the rotational resonances and their stability in the ellipsoidal full two body problem*, Icarus, 265 (2016), pp. 175 – 186, <https://doi.org/10.1016/j.icarus.2015.10.011>.
- [61] K. V. KHOLSHEVNIKOV, M. A. BORUKHA, B. B. ESKIN, AND D. V. MIKRYUKOV, *On the asphericity of the figures of Pluto and Charon*, Planetary and Space Science, 181 (2020), p. 104777, <https://doi.org/10.1016/j.pss.2019.104777>.
- [62] D. G. KING-HELE, *Theory of Satellite Orbits in an Atmosphere*, Butterworths mathematical texts, Butterworths, London, 1964, <https://books.google.es/books?id=gIVLAAAIAAJ>.
- [63] J. KLAČKA, M. KOCIFAJ, P. PÁSTOR, AND J. PETRŽALA, *Poynting-Robertson effect and perihelion motion.*, Astronomy & Astrophysics, 464 (2007), pp. 127–134, <https://doi.org/10.1051/0004-6361:20066132>.
- [64] Z. KOPAL, *Dynamics of Close Binary Systems*, Springer, Dordrecht, 1978, <https://doi.org/10.1007/978-94-009-9780-6>.
- [65] J. V. KOVALEVSKY, *Passage through resonance*, in Periodic Orbits, Stability and Resonances, G. Giacaglia, ed., Springer, Dordrecht, 1970.
- [66] J. V. KOVALEVSKY, *Non gravitational forces in the evolution of the solar system*, in The Big Bang and Georges Lemaître, A. Berger, ed., Springer, Dordrecht, 1984.

- [67] S. KRANTZ AND H. PARKS, *A Primer of Real Analytic Functions*, Birkhäuser, Boston, MA, 2002, <https://doi.org/10.1007/978-0-8176-8134-0>.
- [68] S. KRANTZ AND H. PARKS, *The Implicit Function Theorem: History, Theory, and Applications*, Birkhäuser, New York, NY, 2003, <https://doi.org/10.1007/978-1-4614-5981-1>.
- [69] J. A. KWIECINSKI, S. W. BIBER, AND R. A. VAN GORDER, *Chaotic rotations of a rigid ellipsoidal body exhibiting spin-orbit misalignment in a periodic orbit*, International Journal of Bifurcation and Chaos, 29 (2019), p. 1930018, <https://doi.org/10.1142/S0218127419300180>.
- [70] A. LEMAITRE AND P. DUBRU, *Secular resonances in the primitive solar nebula*, Celestial Mechanics and Dynamical Astronomy, 52 (1991), pp. 57–78, <https://doi.org/10.1007/BF00048587>.
- [71] C. LHOTKA AND A. CELLETTI, *The effect of Poynting-Robertson drag on the triangular Lagrangian points*, Icarus, 250 (2015), pp. 249–261, <https://doi.org/10.1016/j.icarus.2014.11.039>.
- [72] A. LICHTENBERG AND M. LIEBERMAN, *Regular and Chaotic Dynamics*, Applied Mathematical Sciences, Springer, New York, NY, 2nd ed., 1992, <https://doi.org/10.1007/978-1-4757-2184-3>.
- [73] J.-C. LIOU, H. A. ZOOK, AND A. JACKSON, *Radiation Pressure, Poynting-Robertson Drag, and Solar Wind Drag in the Restricted Three-Body Problem*, Icarus, 116 (1995), pp. 186 – 201, <https://doi.org/10.1006/icar.1995.1120>.
- [74] J. LITTLEWOOD, *Adiabatic invariance II. Elliptic motion about a slowly varying center of force*, Annals of Physics, 26 (1964), pp. 131 – 156, [https://doi.org/10.1016/0003-4916\(64\)90280-5](https://doi.org/10.1016/0003-4916(64)90280-5).
- [75] G. J. F. MACDONALD, *Tidal friction*, Reviews of Geophysics, 2 (1964), pp. 467–541, <https://doi.org/10.1029/RG002i003p00467>.
- [76] A. J. MACIEJEWSKI, *Reduction, relative equilibria and potential in the two rigid bodies problem*, Celestial Mechanics and Dynamical Astronomy, 63 (1995), pp. 1–28, <https://doi.org/10.1007/BF00691912>.
- [77] W. MAGNUS AND S. WINKLER, *Hill's Equation*, Dover, New York, 1979.



- [78] R. MALHOTRA, *Orbital resonances in the solar nebula: Strengths and weaknesses*, *Icarus*, 106 (1993), pp. 264 – 273, <https://doi.org/10.1006/icar.1993.1170>.
- [79] F. MARCHIS, D. HESTROFFER, P. DESCAMPS, J. BERTHIER, A. H. BOUCHEZ, R. D. CAMPBELL, J. C. Y. CHIN, M. A. VAN DAM, S. K. HARTMAN, E. M. JOHANSSON, R. E. LAFON, D. L. MIGNANT, I. DE PATER, P. J. STOMSKI, D. M. SUMMERS, F. VACHIER, P. L. WIZINOVICH, AND M. H. WONG, *A low density of  $0.8 \text{ g cm}^{-3}$  for the Trojan binary asteroid 617 Patroclus*, *Nature*, 439 (2006), pp. 565–567, <https://doi.org/10.1038/nature04350>.
- [80] A. MARGHERI, R. ORTEGA, AND C. REBELO, *Some analytical results about periodic orbits in the restricted three body problem with dissipation*, *Celestial Mechanics and Dynamical Astronomy*, 113 (2012), pp. 279–290, <https://doi.org/10.1007/s10569-012-9415-1>.
- [81] A. MARGHERI, R. ORTEGA, AND C. REBELO, *Dynamics of Kepler problem with linear drag.*, *Celestial Mechanics and Dynamical Astronomy*, 120 (2014), pp. 19–38, <https://doi.org/10.1007/s10569-014-9553-8>.
- [82] A. MARGHERI, R. ORTEGA, AND C. REBELO, *First integrals for the Kepler problem with linear drag.*, *Celestial Mechanics and Dynamical Astronomy*, 127 (2017), pp. 35–48, <https://doi.org/10.1007/s10569-016-9715-y>.
- [83] A. MARGHERI, R. ORTEGA, AND C. REBELO, *On a family of Kepler problems with linear dissipation.*, *Rend. Istit. Mat. Univ. Trieste*, 49 (2017), pp. 265–286, <https://doi.org/10.13137/2464-8728/16216>.
- [84] S. MATHIS AND C. LE PONCIN-LAFITTE, *Tidal dynamics of extended bodies in planetary systems and multiple stars*, *Astronomy & Astrophysics*, 497 (2009), pp. 889–910, <https://doi.org/10.1051/0004-6361/20079054>.
- [85] A. G. MAVRAGANIS AND D. G. MICHALAKIS, *The two-body problem with drag and radiation pressure.*, *Celestial Mechanics and Dynamical Astronomy*, 58 (1994), pp. 393–403, <https://doi.org/10.1007/BF00692013>.
- [86] J. MAWHIN, *Global Results for the Forced Pendulum Equation*, in *Handbook of Differential Equations: Ordinary Differential Equations*,

- A. Cañada, P. Drábek, and A. Fonda, eds., vol. 1, North-Holland, 2004, pp. 533 – 589, [https://doi.org/10.1016/S1874-5725\(00\)80008-5](https://doi.org/10.1016/S1874-5725(00)80008-5).
- [87] R. MCGEHEE, *Double collisions for a classical particle system with nongravitational interactions.*, Com. Math. Helvet., 56 (1981), pp. 524–557, <https://doi.org/10.1007/BF02566226>.
- [88] A. MELNIKOV AND I. SHEVCHENKO, *The rotation states predominant among the planetary satellites*, Icarus, 209 (2010), pp. 786–794, <https://doi.org/10.1016/j.icarus.2010.04.022>.
- [89] A. V. MELNIKOV, *Bifurcation Regime of a Synchronous Resonance in the Translational-Rotational Motion of Nonspherical Natural Satellites of Planets*, Cosmic Research, 39 (2001), pp. 68–77, <https://doi.org/10.1023/A:1002891929241>.
- [90] J. MESTSCHERSKY, *Ueber die integration der bewegungsgleichungen im probleme zweier körper von veränderlicher masse*, Astronomische Nachrichten, 159 (1902), pp. 229–242, <https://doi.org/10.1002/asna.19021591502>.
- [91] M. MISQUERO AND R. ORTEGA, *Some rigorous results on the 1:1 resonance of the spin-orbit problem*. In press. Preprint available at <https://www.ugr.es/%7Eecuadif/files/MisqueroOrtega.pdf>.
- [92] D. MITTLEMAN AND D. JEZEWSKI, *An analytic solution to the classical two body problem with drag.*, Celest. Mech., 28 (1982), pp. 401–413, <https://doi.org/10.1007/BF01372122>.
- [93] A. MOLCHANOV, *The resonant structure of the solar system: The law of planetary distances*, Icarus, 8 (1968), pp. 203 – 215, [https://doi.org/10.1016/0019-1035\(68\)90074-2](https://doi.org/10.1016/0019-1035(68)90074-2).
- [94] A. MORBIDELLI, *Modern Celestial Mechanics: Aspects of Solar System Dynamics*, vol. 5 of Advances in astronomy and astrophysics, Taylor & Francis, London ; New York, 2002.
- [95] J. MOSER AND E. ZEHNDER, *Notes on Dynamical Systems.*, American Mathematical Society, Courant Institute of Mathematical Sciences, New York, 2005.
- [96] F. MOULTON, *An Introduction to Celestial Mechanics*, Macmillan, 2nd revised ed., 1914.

- [97] J. A. MURDOCK, *Some mathematical aspects of spin-orbit resonance*, *Celestial mechanics*, 18 (1978), pp. 237–253, <https://doi.org/10.1007/BF01230164>.
- [98] C. D. MURRAY, *Dynamical Effects of Drag in the Circular Restricted Three-Body Problem: I. Location and Stability of the Lagrangian Equilibrium Points*, *Icarus*, 112 (1994), pp. 465 – 484, <https://doi.org/10.1006/icar.1994.1198>.
- [99] C. D. MURRAY AND S. F. DERMOTT, *Solar System Dynamics*, Cambridge University Press, Cambridge, 2000, <https://doi.org/10.1017/CB09781139174817>.
- [100] R. NAGLE, E. SAFF, AND A. SNIDER, *Fundamentals of Differential Equations and Boundary Value Problems*, Pearson Education, sixth ed., 2012.
- [101] D. NUÑEZ AND P. J. TORRES, *Stable odd solutions of some periodic equations modeling satellite motion*, *Journal of Mathematical Analysis and Applications*, 279 (2003), pp. 700 – 709, [https://doi.org/10.1016/S0022-247X\(03\)00057-X](https://doi.org/10.1016/S0022-247X(03)00057-X).
- [102] R. ORTEGA, *Linear motions in a periodically forced Kepler problem.*, *Port. Math.*, 68 (2011), pp. 149–176, <https://doi.org/10.4171/PM/1885>.
- [103] C. W. PATTERSON, *Resonance capture and the evolution of the planets*, *Icarus*, 70 (1987), pp. 319 – 333, [https://doi.org/10.1016/0019-1035\(87\)90138-2](https://doi.org/10.1016/0019-1035(87)90138-2).
- [104] D. PFENNIGER AND C. NORMAN, *Dissipation in barred galaxies - the growth of bulges and central mass concentrations*, *The Astrophysical Journal*, 363 (1990), pp. 391–410, <https://doi.org/10.1086/169352>.
- [105] H. C. PLUMMER, *On the Possible Effects of Radiation on the Motion of Comets, with special reference to Encke's Comet*, *Monthly Notices of the Royal Astronomical Society*, 65 (1905), pp. 229–238, <https://doi.org/10.1093/mnras/65.3.229>.
- [106] H. POINCARÉ, *Leçons sur les hypothèses cosmogoniques.*, Librairie Scientifique A. Hermann et fils, Paris, 1911, <https://archive.org/details/leonssurleshy00poin>.

- [107] H. POINCARÉ, *New methods of celestial mechanics (1892–1899)*; edited and introduced by Daniel L. Goroff, American Institute of Physics [Woodbury, NY], 1993.
- [108] J. H. POYNTING, *Radiation in the Solar System: Its Effect on Temperature and Its Pressure on Small Bodies*, Philosophical Transactions of the Royal Society of London. Series A, Containing Papers of a Mathematical or Physical Character, 202 (1904), pp. 525–552.
- [109] I. PRIGOGINE AND G. NICOLIS, *Self-organisation in nonequilibrium systems: Towards a dynamics of complexity*, in Bifurcation Analysis, M. Hazewinkel, R. Jurkovich, and J. Paelinck, eds., Springer, Dordrecht, 1985, [https://doi.org/10.1007/978-94-009-6239-2\\_1](https://doi.org/10.1007/978-94-009-6239-2_1).
- [110] H. P. ROBERTSON AND H. N. RUSSELL, *Dynamical Effects of Radiation in the Solar System*, Monthly Notices of the Royal Astronomical Society, 97 (1937), pp. 423–437, <https://doi.org/10.1093/mnras/97.6.423>.
- [111] C. ROBINSON AND J. A. MURDOCK, "some mathematical aspects of spin-orbit resonance. ii", *Celestial mechanics*, 24 (1981), pp. 83–107, <https://doi.org/10.1007/BF01228795>.
- [112] W. RUDIN, *Principles of mathematical analysis*, McGraw-Hill, New York, 3rd ed., 1976.
- [113] D. J. SCHEERES, *Stability in the Full Two-Body Problem*, *Celestial Mechanics and Dynamical Astronomy*, 83 (2002), pp. 155–169, <https://doi.org/10.1023/A:1020143116091>.
- [114] D. J. SCHEERES, *Stability of the planar full 2-body problem*, *Celestial Mechanics and Dynamical Astronomy*, 104 (2009), pp. 103–128, <https://doi.org/10.1007/s10569-009-9184-7>.
- [115] S. F. SINGER, *The Origin of the Moon and Geophysical Consequences*, *Geophysical Journal of the Royal Astronomical Society*, 15 (1968), pp. 205–226, <https://doi.org/10.1111/j.1365-246X.1968.tb05759.x>.
- [116] H. J. SPERLING, *The collision singularity in a perturbed two-body problem.*, *Celest. Mech.*, 1 (1969), pp. 213–221, <https://doi.org/10.1007/BF01228841>.

- [117] E. STEINBORN AND K. RUEDENBERG, *Rotation and translation of regular and irregular solid spherical harmonics*, vol. 7 of *Advances in Quantum Chemistry*, Academic Press, 1973, pp. 1 – 81, [https://doi.org/10.1016/S0065-3276\(08\)60558-4](https://doi.org/10.1016/S0065-3276(08)60558-4).
- [118] G. TALENTI, *Best Constant in Sobolev Inequality*, *Annali di Matematica Pura ed Applicata, Series 4*, 110 (1976), pp. 353–372, <https://doi.org/10.1007/BF02418013>.
- [119] P. TRICARICO, *Figure–figure interaction between bodies having arbitrary shapes and mass distributions: a power series expansion approach*, *Celestial Mechanics and Dynamical Astronomy*, 100 (2008), pp. 319–330, <https://doi.org/10.1007/s10569-008-9128-7>.
- [120] T. VAN HOOLST, N. RAMBAUX, O. KARATEKIN, V. DEHANT, AND A. RIVOLDINI, *The librations, shape, and icy shell of Europa*, *Icarus*, 195 (2008), pp. 386 – 399, <https://doi.org/10.1016/j.icarus.2007.12.011>.
- [121] R. VILHENA DE MORAES, *Non-gravitational disturbing forces*, *Advances in Space Research*, 14 (1994), pp. 45 – 68, [https://doi.org/10.1016/0273-1177\(94\)90097-3](https://doi.org/10.1016/0273-1177(94)90097-3).
- [122] R. C. WEBER, *Interior of the moon*, in *Encyclopedia of the Solar System (Third Edition)*, T. Spohn, D. Breuer, and T. V. Johnson, eds., Elsevier, Boston, third ed., 2014, ch. 24, pp. 539 – 554, <https://doi.org/https://doi.org/10.1016/B978-0-12-415845-0.00024-4>.
- [123] S. J. WEIDENSCHILLING, *Aerodynamics of solid bodies in the solar nebula*, *Monthly Notices of the Royal Astronomical Society*, 180 (1977), pp. 57–70, <https://doi.org/10.1093/mnras/180.2.57>.
- [124] J. WISDOM, *Rotational Dynamics of Irregularly Shaped Natural Satellites*, *Astronomical Journal*, 94 (1987), p. 1350, <https://doi.org/10.1086/114573>.
- [125] J. WISDOM, S. J. PEALE, AND F. MIGNARD, *The chaotic rotation of Hyperion*, *Icarus*, 58 (1984), pp. 137 – 152, [https://doi.org/10.1016/0019-1035\(84\)90032-0](https://doi.org/10.1016/0019-1035(84)90032-0).
- [126] V. A. YAKUBOVICH AND V. M. STARZHINSKII, *Linear Differential Equations with Periodic Coefficients*, Wiley, New York, 1975.

- [127] C. F. YODER, *Diagrammatic theory of transition of pendulum like systems*, *Celestial mechanics*, 19 (1979), pp. 3–29, <https://doi.org/10.1007/BF01230171>.
- [128] M. ZHANG AND W. LI, *A Lyapunov-Type Stability Criterion Using  $L^\alpha$  Norms*, *Proceedings of the American Mathematical Society*, 130 (2002), pp. 3325–3333, <http://www.jstor.org/stable/1194160>.
- [129] V. ZLATOUSTOV, D. OHOTZIMSKY, V. SARYCHEV, AND A. TORZHEVSKY, *Investigation of a satellite oscillations in the plane of an elliptic orbit*, in *Applied Mechanics. Proceedings of the Eleventh International Congress of Applied Mechanics Munich (Germany) 1964*, G. H., ed., Springer, Berlin, Heidelberg, 1966, pp. 436–439, [https://doi.org/10.1007/978-3-662-29364-5\\_59](https://doi.org/10.1007/978-3-662-29364-5_59).